Université de Montréal

LES VOIES DE SIGNALISATION UTÉRINES À L'ÉMERGENCE DE LA DIAPAUSE EMBRYONNAIRE CHEZ LE VISON AMÉRICAIN

par

Pavine L.C. Lefèvre

Département de biomédecine vétérinaire

Centre de recherche en reproduction animale

Faculté de médecine vétérinaire

Thèse présentée à la Faculté de médecine vétérinaire

en vue de l'obtention du grade de

Philosophiae Doctor (Ph.D.)

en sciences vétérinaires

option reproduction

Août, 2010

Université de Montréal

Faculté de médecine vétérinaire

Cette thèse intitulée

Les voies de signalisation utérines à l'émergence de la diapause embryonnaire chez le vison américain

présentée par

Pavine L.C. Lefèvre

a été évaluée par un jury composé des personnes suivantes

Alan K. Goff, président-rapporteur

Bruce D. Murphy, directeur de recherche

Marie-France Palin, membre du jury

Fuller W. Bazer, examinateur externe

Christopher A. Price, représentant du doyen

Résumé

La diapause embryonnaire se manifeste par un arrêt réversible du développement embryonnaire durant la période de préimplantation et induit un retard de l'implantation. Chez le vison américain, une diapause embryonnaire obligatoire caractérise chaque gestation. Si les mécanismes de contrôle de la diapause embryonnaire obligatoire chez cette espèce sont bien connus, le rôle utérin impliqué dans la réactivation de l'embryon demeure, quant à lui, encore inconnu.

Le sujet de ce doctorat a consisté dans un premier temps à explorer l'environnement utérin à la sortie de la diapause embryonnaire afin de caractériser, dans un deuxième temps, les principaux acteurs utérins qui provoquent la réactivation de l'embryon.

Nous avons effectué une analyse du transcriptome utérin à l'émergence de la diapause embryonnaire ce qui a permis de construire une librairie de 123 séquences d'ADNc utérines différentiellement exprimées à la réactivation de l'embryon et homologues à des séquences de gènes connues chez d'autres espèces. Ces gènes sont impliqués dans la régulation du métabolisme (25 %), de l'expression génique (21 %), de la transduction de signal (15 %), du cycle cellulaire (15 %), du transport (10 %) et de la structure cellulaire (9 %), reflétant ainsi d'importantes modifications utérines à la réactivation embryonnaire. Nous avons validé l'expression différentielle de dix gènes ainsi identifiés : *GDF3 (growth and differentiation 3)*, *ALCAM (activated leukocyte cell adhesion molecule)*, *ADIPOR1*

(adiponectin receptor 1), *HMGN1 (high mobility group N1)*, *TXNL1 (thioredoxin like 1)*, *TGM2 (tissue transglutaminase 2)*, *SPARC (secreted protein acidic rich in cystein)*, et trois gènes codant pour *AZIN1 (antizyme inhibitor 1)*, *ODC1* (*ornithine decarboxylase 1*) et *SAT1 (spermidine/spermine N1-acetyltransferase)*, des enzymes impliquées dans la biosynthèse des polyamines. Le patron de l'expression spatio-temporel de *SPARC* et d'*HMGN1* illustrent spécifiquement un remodelage tissulaire et de la chromatine au niveau utérin à la sortie de la diapause embryonnaire.

Ayant mesuré une augmentation des concentrations utérines en polyamines à la reprise du développement embryonnaire, nous avons émis l'hypothèse que les polyamines seraient impliquées dans les événements menant à la sortie de la diapause. L'inhibition de la biosynthèse des polyamines par un traitement à l' α-difluoromethylornithine (DFMO) a provoqué une diminution significative de la proliferation cellulaire dans les embryons à la réactivation, un retard du moment de l'implantation, mais n'a pas affecté le succès de la reproduction. De manière similaire, nous avons induit un état de dormance dans les cellules de trophoblaste de vison en présence DFMO dans le milieu de culture, et constaté que cet état était réversible.

En conclusion, cette étude a non seulement ouvert de nouveaux horizons quant à la compréhension du rôle utérin dans les événements menant à la sortie de la diapause embryonnaire, mais a démontré pour la première fois, l'existence de facteurs utérins indispensables à la réactivation de l'embryon: les polyamines.

Mots-clés : diapause, blastocyst, trophoblaste, uterus, implantation, hybridation suppressive soustractive (SSH), polyamines, vison.

Abstract

Embryonic diapause is characterized by a reversible arrest of blastocyst development prior to implantation and delay in implantation. In the American mink, embryonic diapause is a characteristic of each gestation. Although the mechanisms which control obligate embryonic diapause of this species are well known, the role of the uterus involved in blastocyst reactivation remains elusive.

The subject of this doctoral research consisted first in exploring the uterine environment at the emergence of embryonic diapause in order to subsequently determine, the main factors in the uterus that provoke reactivation of the embryo.

We have undertaken an analysis of the uterine transcriptome at the emergence of embryonic diapause which has enabled us to set up a library of 123 cDNA uterine sequences differentially expressed at blastocyst reactivation, and homologue gene sequences known in other species. Twenty-five percent of these genes are implicated in genetic expression, 15 % in cell signal transduction, 15 % in cell cycle, 10 % in transport and 9 % in cell structure. All of them reflect significant uterine modifications at blastocyst reactivation. We have validated differential expression of ten genes, identified as: *GDF3 (growth and differentiation 3)*, *ALCAM (activated leukocyte cell adhesion molecule)*, *ADIPOR1 (adiponectin receptor 1)*, *HMGN1 (high mobility group N1)*, *TXNL1 (thioredoxine like 1)*, *TGM2 (tissue transglutaminase 2)*, *SPARC (secreted protein acidic rich in cystein)*, and three genes encoding for *AZIN1 (antizyme inhibitor 1)*, *ODC1* (*ornithine decarboxylase 1*) and *SAT1 (spermidine/spermine N1-acetyltransferase)*, which are enzymes implicated in

polyamine biosynthesis. The spatio-temporal expression patterns of *SPARC* and *HMGN1* illustrate tissue and chromatin remodelling in the uterus at the termination of embryonic diapause.

Having measured an increase in concentration of polyamines in the uterus at the resumption of blastocyst development, we have hypothetized that polyamines are implicated in the emergence of blastocysts from diapause. We inhibited polyamine biosynthesis in pregnant mink females during early blastocyst reactivation. The inhibition of polyamine biosynthesis through treatment with α-difluoromehtylornithine (DFMO) provoked a major reduction in cell proliferation in blastocysts at reactivation and a delay in the timing of implantation, but did not affect the success of reproduction. Similarly, we induced a reversible dormant state in cultured mink trophoblast cells traited with DFMO.

To conclude, not only are results of this study a breakthrough in the understanding of the role of the uterus in stimulating at the emergence of blastocysts from embryonic diapause, but also, for the very first time, they indicate the existence of uterine factors, the polyamines, that are responsible for blastocysts reactivation.

Keywords : diapause, blastocyst, trophoblast, uterus, implantation, suppressive subtractive hybridization (SSH), polyamines, mink.

Table des matières

Liste des tableaux

Article 1: Differential gene expression in the uterus and blastocyst during the reactivation of blastocyst development in a model of delayed implantation

Article 2: Uterine signaling at the emergence of blastocysts from obligate diapause

Liste des figures

Recension de litterature

Article 1: Differential gene expression in the uterus and blastocyst during the reactivation of blastocyst development in a model of delayed implantation

Article 2: Uterine signaling at the emergence of blastocysts from obligate diapause

Article 3 : Polyamines in the reproductive lanscape

Article 4: Polyamines are implicated in the emergence of blastocysts from embryonic diapause

Liste des sigles et des abbréviations

ADIPOR1	Adiponectin receptor 1
ADN / DNA	Desoxyribonucleic acid
ADNc / cDNA	Complementary desoxyribonucleic acid
ARN / RNA	Acide ribonucléique / Ribonucleic acid
ALCAM	Activated leukocyte cell adhesion molecule
AZI	Antizyme
AZI	Antizyme inhibitor
BRCA1	Breast cancer 1
BTG1	B cell translocation 1
cAMP	Cyclic adenosine monophosphate
COX2	Cyclooxygenase 2
DFMO	α-difluoromethylornithine
dcSAM	decarboxylated S-adenosylmethionine
EGF	Epidermal growth factor
eIF5A	Eukaryotic initiation factor 5A
eIF4E	Eukaryotic initiation factor 4E
FSH	Follicle stimulating hormone
GAPDH	Glyceraldehyde phosphodeshydrogenase
GDF3	Growth and differentiation factor 3
GnRH	Gonadotropin releasing hormone
HB-EGF	Heparin-binding EGF

hCG	Human chorionic gonadotropin
HDAC-5	Histone deacetylase 5
HMGN1	High mobility group N1
ICM	Internal cell mass
IUGR	Intrauterine growth retardation
LH	Luteinizing hormone
LIF	Leukemia inhibitory factor
mARN	Messenger RNA
mTOR	Mammalian target of rapamycin
Na^+	Sodium
ODC1	Ornithine decarboxylase 1
PAO	Polyamine oxidase
PCNA	Proliferating cell nuclear antigen
PGE2	Prostaglandin E2
eCG	Equine chorionic gonadotropin
PPARγ	Peroxysome proliferating activated receptor γ
PPIA3	Peptidylprolyl isomerase A
Rhoa	Ras homolog gene family, member A
SAMDC	S-adenosylmethionine decarboxylase
SAM	S-adenosylmethionine
SAT1	Spermidine/Spermine N1-acetyltransferase
SLC3A2	Solute carrier family 3 member 2
SMO	Spermine oxidase

SPARC	Secreted protein, acidic rich in cystein
SSH	Suppressive subtractive hybridization
TGFβ	Transforming growth factor β
TGM2	Tissue tranglutaminase 2
TXNL1	Thioredoxine like 1
VEGF1	Vascular endothelial growth factor 1

A ma famille et mes amis

Remerciements

En premier lieu, je souhaite remercier mon directeur de recherche, Bruce Murphy, pour m'avoir ouvert les portes du CRRA et offert l'opportunité de réaliser ce projet de recherche si passionnant. Je lui suis profondément reconnaissante pour son soutien, ses précieux conseils et sa disponibilité, mais également pour m'avoir fait confiance et laissé une liberté de décision telle que la formation doctorale dont j'ai pu ainsi bénéficier fut, à mon sens, des plus instructives.

Je remercie infiniment Marie-France Palin pour son soutien, ses conseils constructifs et pour la formation technique qu'elle et son laboratoire m'ont offerte, en particulier son assistante de recherche Danièle Beaudry. Sans vous, mon projet n'aurait pas connu une telle avancée.

Je suis profondément reconnaissante envers Mira Dobias-Goff pour sa disponibilité, son aide et sa présence d'esprit qui ont apporté une richesse essentielle à mon travail.

A la « Mink-team » : Vickie Roussel, Deborah Salmeron, Brïte Pauchet, Evelyn Llerena, et les stagiaires de Technique de Santé Animale, Catherine, Laurence et Esther : votre implication, votre fiabilité et votre courage à affronter les visons ont contribué sans aucun doute au bon déroulement de mon projet. Un grand merci à vous toutes.

A tous les membres du CRRA, je vous remercie pour votre collaboration, en particulier Micheline Sicotte pour son aide administrative, Lawrence Smith, Alan Goff, Paul Carrière, Patrick Vincent et Christopher Price, pour leurs conseils avisés tout au long de mon doctorat.

A tous mes amis du laboratoire : Mon hermanita Adriana Verduzco avec qui j'ai pu partager au quotidien les hauts et les bas d'un doctorat, Joëlle Desmarais et Flavia Lopez qui m'ont « mise sur les rails », à Reza Kohan-Ghadr, Mario Binelli et Daniela Campos, pour leurs précieux conseils. A Erika Guerreiro, Kalyne Bertolin, Cong Zhang, Anne-Marie Bellefleur, Anne-Marie Cadutal, Catherine Dolbec et à tous

ceux que j'oublie au moment où j'écris ces lignes : merci pour votre belle présence quotidienne au laboratoire.

Je n'oublie pas l'écoute et les encouragements que mes parents, Philippe et Michelle, mon frère Grégory et sa petite famille, et Jack et Emma, m'ont apportés tout au long de mon doctorat. Merci de m'avoir poussée vers les bancs universitaires et de m'avoir ainsi permis de vivre cette magnifique expérience. Je tiens vivement à remercier ma mère, qui m'a soutenue et fourni une aide indéniable durant le dernier mois de la rédaction de ce manuscrit. A ma grande famille, -ma tribu-, merci pour l'intérêt que vous portez à mes études. Je souhaite également rendre un hommage particulier à Jean-François Lefèvre, mon oncle chercheur, qui m'a ouvert les portes du monde de la recherche et à qui j'ai toujours voué une profonde admiration, ainsi qu'à Florent Vernay, qui m'a vivement encouragée dans cette direction.

A mes amis d'ici, Audrey Simon, Brïte Pauchet, Benoit Rannou, Erin Reese, Isabelle Kling : merci pour votre écoute, merci pour tous ces merveilleux moments que nous avons partagés ensemble. Sans vous, cette aventure n'aurait pas été si enrichissante.

J'aimerais aussi remercier mes amis de « de l'autre côté de l'océan », Muriel Bossert, Caroline Gérard, Charlotte Trévidy, Fanny Bourjot, Delphine Beaudoin et Alain Espiller, dont la présence a sans aucun doute beaucoup compté durant mon doctorat.

I. INTRODUCTION

La diapause embryonnaire est un phénomène de la reproduction des mammifères qui fascine de nombreux chercheurs depuis quelques décennies : l'embryon, au stade de blastocyste, entre dans un état de dormance durant la période de préimplantation, induisant ainsi un retard de la nidation de l'embryon dans l'utérus maternel (revue par (Mead 1993)).

A ce jour, une période de diapause embryonnaire a été identifiée au cours de la gestation d'environ 70 espèces euthériennes et 30 espèces marsupiales reflétant ainsi une conservation de cette stratégie de reproduction au cours de l'évolution. Parmi les espèces euthériennes, la diapause embryonnaire concerne majoritairement les carnivores, incluant les mustélidés, phocidés, ursidés et les otaridés, ainsi que les rongeurs (revue par (Renfree and Shaw 2000)). D'un point de vue évolutif, la diapause embryonnaire permettrait de dissocier le processus de la fertilisation du moment de la mise bas, assurant ainsi un développement fœtal et / ou postnatal dans des conditions environnementales optimales (Sandell 1990; Ferguson, Virgl et al. 1996).

Les causes ultimes et mécanismes physiologiques contrôlant la diapause embryonnaire sont relativement bien identifiés à ce jour (revue par (Renfree and Shaw 2000; Lopes, Desmarais et al. 2004)). La diapause obligatoire se distingue de la diapause facultative par le fait qu'elle caractérise chaque période de gestation (revue par (Mead 1993)). Elle intervient principalement chez certaines espèces carnivores, tels que les mustélidés, soumis à un cycle de reproduction saisonnier et, est placée sous le contrôle de la photopériode. A l'inverse, la diapause facultative est

généralement induite par un stress nutritionnel, tel que la lactation, et concerne d'avantage des espèces qui présentent un œstrus *postpartum*, tels que les rongeurs.

De nombreuses études suggèrent que le maintien de l'embryon dans un état de dormance résulte de l'absence des facteurs ovariens et utérins essentiels à l'implantation de l'embryon. Qu'il s'agisse d'une diapause obligatoire ou facultative, la prolactine joue un rôle-clé dans le contrôle de la diapause embryonnaire et ce, grâce à son effet lutéotrope sur les ovaires (revue par (Mead 1993; Renfree and Shaw 2000)). Chez les rongeurs, un pic d'œstradiol 17β est nécessaire à la nidation (revue par (Dey, Lim et al. 2004)), mais ce dernier est inhibé par une hyperprolactinémie, associée à la lactation (McNeilly 1979; Tsukamura and Maeda 2001). A l'inverse, une augmentation de la prolactinémie est indispensable à l'implantation de l'embryon chez les carnivores (revue par (Mead 1993). Sous l'effet d'une courte photopériode et de la mélatonine, hormone du cycle circadien qui réprime la production de prolactine (revue par (Juszczak and Michalska 2006)), le développement embryonnaire est suspendu et ce, jusqu'à l'équinoxe vernal. Le taux de prolactine circulant est alors suffisant pour induire la lutéinisation des corps jaunes ovariens et la production de progestérone nécessaire à la nidation de l'embryon. En réponse aux changements ovariens, l'environnement utérin dans lequel « baigne » l'embryon en dormance est modifié, notamment au niveau de son activité de sécrétion dans la lumière utérine entrainant alors la réactivation du développement embryonnaire et son implantation dans l'endomètre maternel (revue par (Mead 1993)).

Si les mécanismes physiologiques sous-jacents la régulation de la diapause embryonnaire obligatoire et facultative ont été relativement bien décrits, il demeure que la nature des facteurs utérins et leur mode d'action moléculaire et cellulaire sur l'embryon en diapause sont encore vagues à ce jour.

L'objectif de ce projet de doctorat porte sur l'identification de (s) voie (s) de signalisation utérine provoquant la réactivation et l'implantation de l'embryon, chez le vison américain (*Mustela vison*). En tant que carnivore mustélidé, le vison présente une diapause embryonnaire obligatoire d'une durée moyenne de deux semaines (Hansson 1947), une des plus courte période répertoriée jusqu'alors (Pearson and Enders 1944) et le contrôle physiologique de la diapause embryonnaire chez cette espèce a été relativement bien décrit, d'où l'intérêt de ce modèle animal (revue par (Lopes, Desmarais et al. 2004)).

Dans un premier temps, nous avons effectué une analyse comparative du transcriptome utérin de visons en diapause et après la réactivation afin d'identifier les acteurs utérins responsables de l'émergence de la diapause embryonnaire. Une description de la méthodologie employée, la technique de l'hybridation suppressive soustractive (SSH) (Diatchenko, Lau et al. 1996), a fait l'objet d'un chapitre du livre *Human Embryogenesis, Method and Protocols* publié en 2009 qui est présenté en chapitre III du présent manuscrit. Les résultats de cette première étude sont exposés dans un article soumis à la revue *Biologie of Reproduction* en juin 2010 qui est présenté en chapitre IV de cet ouvrage.

Cette étude a permis la mise en évidence d'une éventuelle implication des polyamines dans la réactivation du développement embryonnaire. Afin de mieux

comprendre le rôle des polyamines dans la reproduction, nous avons recensé l'implication des polyamines dans divers processus de la reproduction dans une revue de littérature dont la présoumission a été acceptée dans *Endocrine Reviews*. Ce travail constitue le chapitre V de cette thèse. Pour finir, nous avons examiné le rôle des polyamines dans la réactivation du développement embryonnaire chez le vison dont résulte la publication présentée au chapitre VI et soumise à *Endocrinology*.

Le présent ouvrage se compose d'abord d'une recension de littérature décrivant le contexte du projet, des articles mentionnés ci-dessus, et finalement, d'une discussion et d'une conclusion générale.

II. RECENSION DES ÉCRITS

A. L'implantation

Chez les mammifères euthériens (placentaires), la gestation comprend différentes étapes essentielles au bon déroulement du développement embryonnaire, allant de la gamétogénèse à la parturition, en passant par la fécondation et, l'implantation de l'embryon dans la muqueuse utérine maternelle.

L'implantation est une étape cruciale pour la survie de l'embryon qui est alors rendu au stade de blastocyste (revue dans (Dey, Lim et al. 2004)). Le blastocyste se compose d'une membrane acellulaire, la zone pellucide, et de deux populations de cellules distinctes : les cellules de la masse interne (ICM) et les cellules du trophoblaste qui, respectivement, donneront naissance au fœtus en tant que tel et, au placenta et matrices extra embryonnaires (revue dans (Dey, Lim et al. 2004)). Durant l'implantation, s'effectue la placentation qui résulte de la formation d'une interaction entre la circulation sanguine maternelle et fœtale. Cette communication fœto-maternelle assure d'une part, un apport nutritionnel et d'oxygène au fœtus et d'autre part, l'évacuation des déchets fœtaux. Un échec de l'implantation constitue par conséquent une des causes majeures de la perte embryonnaire prénatale.

Sous l'effet d'une orchestration précise des hormones stéroïdiennes ovariennes (progestérone et œstrogènes), l'implantation se déroule sur une période limitée durant la gestation, appelée période de réceptivité, laquelle nécessite que le blastocyste soit compétent pour l'implantation et que l'utérus soit réceptif à ce dernier. L'implantation est initiée par l'apposition du trophectoderme sur

l'épithélium luminal utérin. Le développement du placenta s'effectue par l'invasion plus ou moins profonde du trophoblaste dans l'endomètre utérin. Il existe différents modèles d'implantation variables selon les espèces : les placentas indécidués, de type épithelio-chorial (porc, cheval) ou de type conjonctivo-chorial (ruminants) se distinguent des placentas décidués, de type endothélio-chorial (carnivores) ou hémo-chorial (rongeurs, primates) (revue dans (Dey, Lim et al. 2004)).

B. La diapause embryonnaire

1. Définitions

Selon les espèces, différentes stratégies visant à accroître le succès reproducteur ont été sélectionnées au cours de l'évolution. Celles-ci se basent principalement sur un compromis entre le nombre et la survie des embryons durant la gestation et le développement postnatal. Le retard du développement embryonnaire compte ainsi parmi ces adaptations et peut intervenir entre autre, au moment de l'implantation de l'embryon. Le moment de la fertilisation est ainsi dissocié du développement fœtale et de la mise bas, qui peuvent alors avoir lieu dans des conditions optimales pour la survie des nouveau-nés (Sandell 1990; Ferguson, Virgl et al. 1996 ; Thom, Johnson et al. 2004).

La diapause embryonnaire, ou l'implantation différée, consiste ainsi en un arrêt réversible du développement embryonnaire pendant la période de préimplantation durant laquelle l'embryon, au stade de blastocyste, entre dans un état de quiescence et « flotte » dans la lumière utérine maternelle (revue par (Mead 1993)). Concrètement, l'entrée et le maintien en diapause semble résulter de la

réduction ou de l'absence de facteurs ovariens, ou hormones stéroïdiennes, responsables de l'implantation de l'embryon.

Deux types de diapauses embryonnaires ont été décrits, à ce jour : la diapause embryonnaire facultative et obligatoire.

a. Diapause embryonnaire facultative

La diapause embryonnaire facultative se déclenche en réponse à un stress métabolique, tel que la lactation, qui pourrait compromettre la gestation en cours. Cette dernière est souvent observée chez les rongeurs (Bloch 1971) et les marsupiaux (Renfree 1981), espèces dont les femelles peuvent présenter un œstrus *postpartum*.

La diapause embryonnaire facultative peut être induite de manière expérimentale par une ovariectomie et maintenue par l'administration quotidienne de progestérone chez les rongeurs (Cochrane and Meyer 1957). Une injection unique d'œstradiol-17β, hormone stéroïdienne connue pour être le facteur déclenchant l'implantation chez les rongeurs (revue par (Dey, Lim et al. 2004)), induit la réactivation et l'implantation du blastocyste en 24 heures (Prasad, Dass et al. 1968; Dass, Mohla et al. 1969). Ce modèle expérimental a été fréquemment utilisé afin d'étudier les mécanismes moléculaires et cellulaires de l'implantation (Reese, Das et al. 2001).

b. Diapause embryonnaire obligatoire

La diapause embryonnaire obligatoire se distingue de la diapause embryonnaire facultative par le fait qu'elle intervient à chaque cycle de reproduction. Elle concerne davantage les espèces ayant un cycle de reproduction

saisonnier, tels que les carnivores et, est principalement contrôlée par la photopériode (Pearson and Enders 1944). Au cours de la gestation des mustélidés, tels que le vison américain ou la moufette tachetée, la réactivation du développement embryonnaire est ainsi corrélée à l'équinoxe vernal, lorsque la photopériode est supérieure à 12 heures (Mead 1971; Murphy and James 1974).

2. Caractéristiques du blastocyste en diapause

Durant la diapause embryonnaire, l'embryon est dit en dormance : outre une activité métabolique diminuée et maintenue à un état basal, se traduisant par de faibles taux de synthèse d'acide ribonucléique (ARN) (Gwatkin 1966), de protéines (Weitlauf and Greenwald 1965) et de consommation d'oxygène (Weitlauf 1974), les cellules ne se divisent pas, ou plus lentement (Given and Weitlauf 1981; Given and Weitlauf 1982). Le cycle cellulaire serait alors bloqué en phase G0/G1, une phase dite de quiescence (Sanyal and Meyer 1972; Sherman and Barlow 1972; Desmarais, Bordignon et al. 2004). Cette période serait associée avec la formation de cellules polyploïdes (Sherman and Barlow 1972).

La durée de la diapause embryonnaire et les caractéristiques morphologiques et cellulaires du blastocyste en dormance telles que le nombre de cellules, le taux de prolifération cellulaire dans l' ICM et du trophoblaste, le diamètre de l'embryon et l'expression génique sont spécifiques à chaque espèces (revue par (Lopes, Desmarais et al. 2004) et (Renfree and Shaw 2000)). Par exemple, chez le vison américain, le blastocyste en dormance est entouré d'une zone pellucide ainsi que d'une couche acellulaire de glycoprotéines et aucune activité mitotique, ni augmentation du diamètre de l'embryon ne sont détectées pendant la diapause

(Desmarais, Bordignon et al. 2004). A l'inverse, la perte de la zone pellucide chez la souris précède l'entrée en diapause (Spindler, Renfree et al. 1996) et une faible augmentation du diamètre de l'embryon ainsi que du nombre total de cellules ont été identifié chez la moufette tachetée et le blaireau (Mead 1993). Par ailleurs, la durée de la diapause dure de quelques jours à 60 jours, sous certaines conditions expérimentales chez le vison (Murphy and James 1974) tandis ce que la moufette est sujette à une période de diapause de 200 jours (Mead 1981).

3. Mécanismes de régulation de la diapause embryonnaire

a. Facteurs externes

i. Facteurs environnementaux

Tels que mentionnés précédemment, des facteurs environnementaux, généralement climatiques, tels que la photopériode mais également la température, sont à l'origine de la diapause embryonnaire obligatoire. Ainsi, une chute de la température maintiendrait la diapause embryonnaire obligatoire chez le blaireau européen (Canivenc and Bonnin 1979). Par ailleurs, un contrôle artificiel de la photopériode ou, la dénervation du nerf optique ont confirmé une corrélation positive entre l'accroissement de la photopériode et la sortie de la diapause embryonnaire chez le vison américain et la mouffette tachetée (Pearson and Enders 1944; Murphy and James 1974). Cependant, même si l'augmentation de la photopériode semble favoriser la réactivation de l'embryon, celle-ci n'est pas nécessaire et suffisante. En l'absence de source lumineuse, l'implantation de l'embryon est considérablement retardée mais finit par avoir lieu, probablement

sous l'effet de facteurs endogènes encore inconnus à ce jour (revue par (Lopes, Desmarais et al. 2004)).

ii. Stress nutritionnel

Une situation de stress nutritionnel peut également provoquer une diapause embryonnaire (revue par (Lopes, Desmarais et al. 2004)). Chez les espèces présentant un œstrus *postpartum*, la lactation induit une diapause embryonnaire facultative pouvant aller jusqu'à 14 jours, dépendamment de la taille de la portée en allaitement (Mantalenakis and Ketchel 1966; Bloch 1971; Maneckjee and Moudgal 1975; Graham and Daniel 1984). Une étude réalisée chez le rat démontre l'importance de la diapause embryonnaire facultative dans le développement fœtal (Oswald and McClure 1987). En effet, la réactivation forcée des embryons par une injection d'œstradiol 17β pendant la période de lactation a été corrélée à la mise-bas de nouveau-nés physiquement plus petits que la normale, reflétant ainsi un phénomène de retard de la croissance intra-utérine (intrauterine growth retardation, IUGR), fréquemment corrélée à une sous-nutrition ou malnutrition maternelle (Wu, Bazer et al. 2004; Ashworth, Toma et al. 2009). Le déclenchement de la diapause embryonnaire pourrait ainsi protéger les embryons d'une exposition à des conditions défavorables durant le développement fœtal, aux conséquences souvent néfastes sur le développement du fœtus et la survie postnatale.

b. Facteurs intrinsèques

i. Control maternel

Une étude de transfert d'embryons entre des visonnes et des furettes, une espèce fortement apparentée au vison américain qui ne présente pas de diapause au

cours de sa gestation, a montré que la diapause embryonnaire était placée sous un contrôle maternel (Chang 1968). En effet, un état de dormance est induit chez les blastocystes de furet transplantés dans la lumière utérine d'une femelle vison pendant la période de diapause, et la réactivation et l'implantation subséquente de blastocystes de visons en diapause est observée chez la femelle furet. Des résultats similaires ont été observés chez les rongeurs lors de transferts de blastocystes entre des femelles en période d'allaitement ou soumise à une diapause expérimentalement induite ou non (Weitlauf 1969).

ii. La prolactine, actrice principale de la diapause embryonnaire

Que se soit dans le cadre de la diapause embryonnaire induite par la lactation ou saisonnière, la prolactine, une hormone peptidique lutéotrope synthétisée par la glande pituitaire, joue un rôle majeur dans le contrôle de la diapause (revue (Renfree and Shaw 2000) et (Curlewis 1992)) (**Figure 1**(p 12) et **Figure 2** (p 14)). La prolactine est impliquée dans la lutéinisation des corps jaunes ovariens et la synthèse de progestérone nécessaire au maintien de la gestation, mais possède également un effet antigonadotropique qui réprime la production et sécrétion de l'hormone lutéinisante (LH) (Smith 1980).

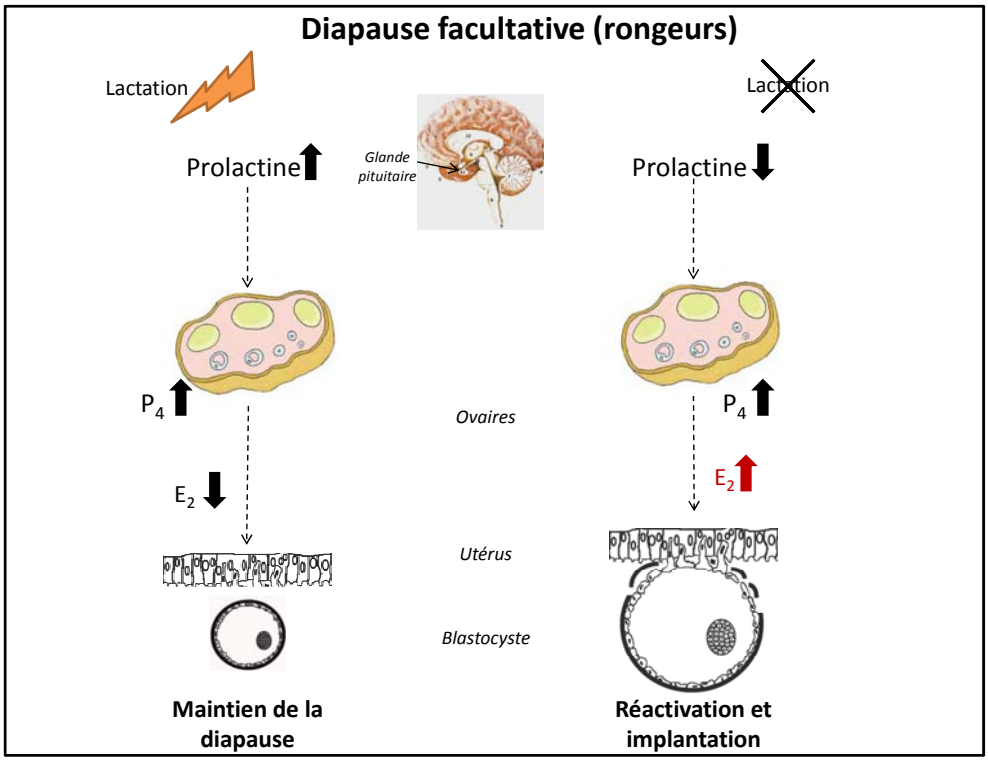

Figure 1. Contrôle de la diapause facultative chez les rongeurs.

La diapause facultative est provoquée par une hausse de la prolactinémie associée à la lactation chez des espèces qui présentent un œstrus *postpartum*. De part son effet antigonadotropique et lutéotrope, la prolactine empêche la synthèse et sécrétion ovarienne d'œstrogènes (E_2) essentielles à l'implantation du blastocyste dans l'endomètre utérin maternel. Ce dernier demeure alors dans un état de diapause, sa survie est maintenue sous l'effet de la progestérone (P_4) et ce, jusqu'à ce que les nouveaux nés soient sevrés et que la prolactinémie diminue. En fin de periode d'allaitement, la prolactinemie diminue et permet ainsi la sécrétion d'E_2 indispensable à la réactivation et l'implantation de l'embryon d'avoir lieu (Figure adaptée à partir de (Lopes, Desmarais et al. 2004) et http://www.colvir.net/prof/chantal.proulx/).

Il est bien établi que le processus de la lactation est associé à une prolactinémie élevée (McNeilly 1979; Tsukamura and Maeda 2001). Chez les rongeurs, la sécrétion ovarienne d'œstrogène essentiel à l'implantation est réprimée sous l'effet de taux de prolactine élevés pendant la lactation. Par conséquent, lors d'une fertilisation *post-partum*, les embryons se développent jusqu'au stade de blastocyste sous l'effet de la progestérone, mais ne peuvent s'implanter et sont maintenus en dormance jusqu'au moment où la prolactinémie est diminuée (revue par (Lopes, Desmarais et al. 2004)) (**Figure 1** (p 12))

Les espèces présentant un cycle de reproduction saisonnier sont soumises à une régulation par la photopériode via la mélatonine, hormone du cycle circadien produite par la glande pinéale, durant les périodes de noirceur et connue pour réprimer la synthèse de prolactine (revue par (Juszczak and Michalska 2006)) (**Figure 2** (p 14)). Chez les carnivores mustélidés, la prolactine est l'hormone-clé de la réactivation du développement embryonnaire et de l'implantation de l'embryon (Murphy, Concannon et al. 1981; Berria, Joseph et al. 1989). Suite à l'ovulation, le processus de lutéinisation ovarien est enclenché, se traduisant par la différenciation des cellules lutéales, l'augmentation du volume lutéale ainsi que la synthèse et sécrétion de progestérone (Mead 1981). Cependant, la concentration plasmatique de prolactine n'est pas suffisante pour induire une maturation complète des corps jaunes ; ceux-là demeurent dans un état d'involution jusqu'au moment où les taux de prolactine augmentent en réponse aux changements de la photopériode. Cette période correspond à la diapause

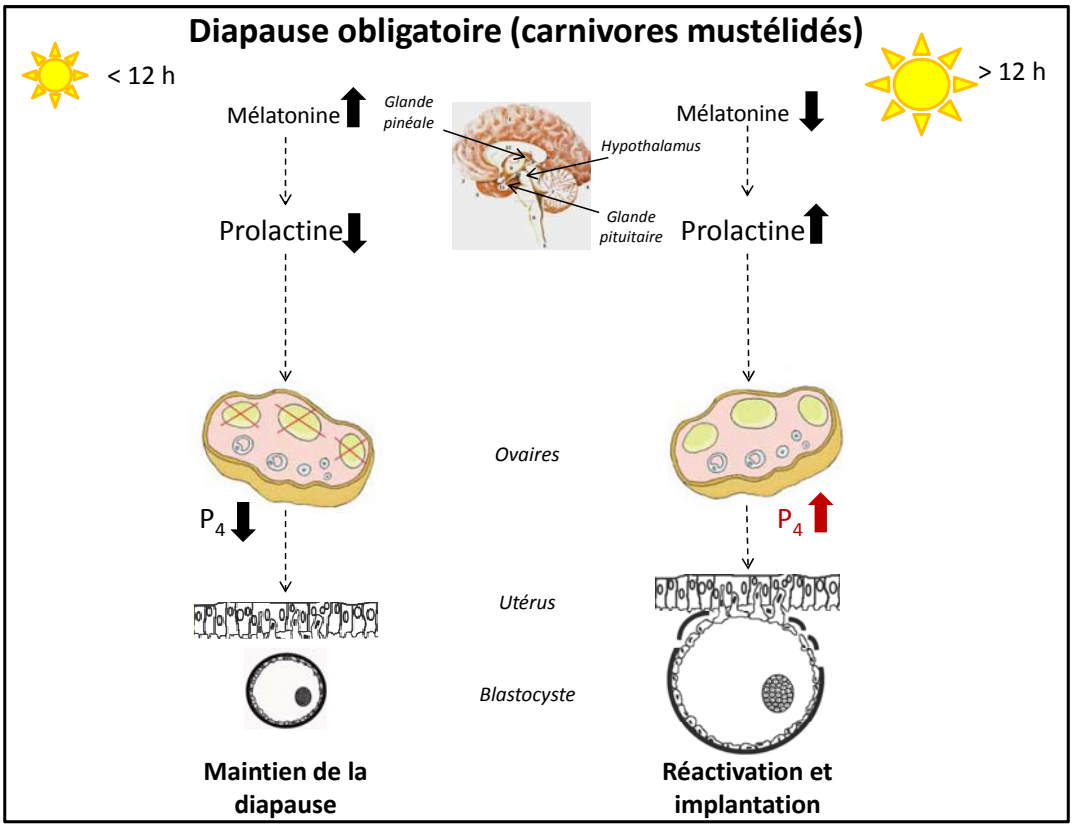

Figure 2. Contrôle de la diapause obligatoire chez les carnivores mustélidés.

La diapause obligatoire est placée sous le contrôle de la photopériode et de l'hormone circadienne, la mélatonine, qui réprime la production et sécrétion de la prolactine au niveau de la glande pituitaire. L'entrée et le maintien de la diapause est ainsi induit lorsque la prolactinémie n'est pas suffisante pour assurer la production et sécrétion ovarienne de progestérone (P_4), un facteur indispensable à l'implantation du blastocyste, chez les carnivores. En concordance avec l'augmentation de la photopériode, les taux de prolactine induisent la lutéinization des corps jaune et la production de progestérone. L'implantation peut alors s'effectuer. (Figure adaptée à partir de (Lopes, Desmarais et al. 2004) et http://www.colvir.net/prof/chantal. proulx/).

Chez le vison, la diapause embryonnaire est abolie et l'implantation provoquée par une simple injection de prolactine (Papke, Concannon et al. 1980), ou l'administration de pimozide, un antagoniste des voies dopaminergiques qui stimulent la production de prolactine (Murphy 1983). Chez des animaux hypophysectomisés ou traités à la mélatonine, la diapause embryonnaire est prolongée alors que l'administration de prolactine chez ces animaux induit la réactivation et l'implantation de l'embryon (Murphy, Concannon et al. 1981; Murphy, DiGregorio et al. 1990). Ces expériences ont également demontrées le rôle essentiel de la progestérone dans la réactivation et l'implantation de l'embryon chez ces espèces. Cependant, l'administration de progestérone à des femelles ovariectomisées en période de diapause n'abolit pas cette dernière, ce qui suggère qu'un ou plusieurs facteur (s) ovarien (s) supplémentaires sont indispensables à l'émergence de la diapause embryonnaire (Murphy 1983).

La prolactine occupe ainsi un rôle majeur dans la régulation de la diapause embryonnaire liée à la lactation ou saisonnière, et ce, en impliquant une régulation fine de l'axe gonado-hypophysaire.

iii. Control utérin de la diapause embryonnaire

Les expériences de transfert réciproque d'embryons mentionnées plus haut (Chang 1968; Weitlauf 1969) démontrent clairement une implication de l'environnement utérin dans lequel « baigne » l'embryon durant le contrôle de l'entrée, du maintien et de la sortie de la diapause embryonnaire. Le transfert de blastocystes de souris en diapause en un site ectopique tel que le rein (Kirby 1967) ou l'oviducte (Weitlauf 1971) a également été associé à une réactivation du

blastocyste. La mise en culture *in vitro* de blastocystes de souris ou de rat en diapause dans un milieu complet induit aussi la réactivation des embryons, se traduisant par une reprise de la croissance du trophoblaste (Gwatkin 1966).

Le traitement *in vitro* de blastocystes en diapause avec de l'œstradiol-17β ou de la progestérone n'a démontré aucun effet sur la réactivation du développement embryonnaire (Torbit and Weitlauf 1975), suggérant ainsi que le site d'action des hormones stéroïdiennes est bien l'endomètre et non, le blastocyste en diapause. L'expression différentielle de nombreux gènes utérins au moment de la sortie de la diapause, induite par une injection d'œstradiol-17β, démontre des changements moléculaires et cellulaires au niveau de l'utérus, indispensables à la préparation de l'implantation de l'embryon. Ces gènes sont principalement des facteurs de croissance, de prolifération, de remodelage tissulaire, de régulation de l'expression génique ou encore des facteurs vasoactifs (revue par (Dey, Lim et al. 2004; Lopes, Desmarais et al. 2004)). En tant que facteurs de croissance et de prolifération cellulaire, respectivement, les facteurs de croissance épidermique (epidermal growth factor, EGF) et d'inhibition de la leucémie (leukemia inhibitory factor, LIF) semblent jouer un rôle majeur dans la préparation à l'implantation. En effet, l'injection d'œstradiol-17β requise pour l'implantation chez les rongeurs peut être substituée par l'un ou l'autre de ces deux facteurs, chez les rongeurs (revue par (Lopes, Desmarais et al. 2004)).

Plusieurs études ont montré que la concentration en protéines dans les fluides utérins était significativement augmentée à la fin de la période de diapause facultative, expérimentalement induite (Surani 1975; Surani 1976; Aitken 1977;

Fishel 1979; Hoversland and Weitlauf 1981) ou obligatoire (Daniel and Krishnan 1969; Mead, Rourke et al. 1979). La réactivation du développement embryonnaire serait ainsi associée à un accroissement important de l'activité de sécrétion utérine. L'analyse des fluides utérins a montré la présence de protéines de hauts poids moléculaires uniquement dans les fluides utérins de femelles réactivées (Surani 1975). Des signes de réactivation de l'embryon en diapause, tels que la croissance et l'attachement du trophoblaste ainsi que la reprise de la synthèse d'ARN ont été observés *in vitro* en présence de fluide utérin prélevé sur des femelles non soumises à une diapause ou traitées à l'œstradiol 17β (Gwatkin 1969; Aitken 1977; Surani 1977; Weitlauf 1978; Weitlauf and Kiessling 1981). Inversement, le maintien des embryons dans un état de diapause a été rapporté lorsque ces derniers sont soumis à la présence de fluides utérins collectés sur des femelles en diapause (Aitken 1977; Surani 1977). De plus, la leucine et l'arginine apparaissent indispensables à la réactivation d'embryons, *in vitro* (Gwatkin 1966; Van Winkle, Tesch et al. 2006). Aucune corrélation entre la composition en acides aminés, vitamines, substrats énergétiques ou en ions du milieu de culture et la réactivation d'embryons en diapause n'a cependant été observée par rapport aux effets rapportés en présence d'un milieu de culture complet (Nieder and Weitlauf 1985). Aussi, le catéchol-œstrogène, produit du métabolisme des œstrogènes par l'endomètre, mais également la prostaglandine E_2 (PGE_2) et l'adénosine mono phosphate cyclique (cAMP) sont capables d'engendrer la réactivation *in vitro* des blastocystes en diapause (Paria, Lim et al. 1998), suggérant une implication de la voies de

signalisation des prostaglandines dans la réactivation de l'embryon, chez les rongeurs.

S'il est bien établi que la sortie de la diapause embryonnaire est contrôlée par un ou des facteur (s) utérin (s), la nature de ces facteurs ainsi que leurs mécanismes d'action sur le blastocyste en dormance demeure cependant encore vague.

c. Régulation de la diapause embryonnaire au niveau de l'embryon

i. Régulation du cycle cellulaire

La comparaison des transcriptomes d'embryons de souris en diapause versus réactivés par la technique des puces à ADN a révélé l'expression différentielle de gènes impliqués dans la régulation du cycle cellulaire, des voies de signalisations cellulaires et du métabolisme (Hamatani, Carter et al. 2004). L'expression des gènes codant pour *l'inhibiteur du cycle cellulaire p21* $^{cip1/WAF1}$, pour *la translocation des cellules B 1* (*B cell translocation 1*, *Btg1*), un inhibiteur de la phase GO/G1 ainsi que pour *l'histone deacetylase 5* (*Hdac5*), un condenseur de la chromatine, s'est avérée être élevée chez l'embryon en dormance. A l'inverse, les gènes codant pour *le cancer du sein 1* (*breast cancer 1*, *Brca1*), pour *l'EGF se liant à l'héparine* (*heparin-binding EGF*, *Hb-Egf*) et, pour *les récepteurs aux EGF*, ont une expression élevée chez les embryons réactivés (Hamatani, Carter et al. 2004). Principalement basé sur ces résultats, un modèle de régulation du cycle cellulaire pendant la diapause et à la réactivation a été proposé. Ce modèle implique différents facteurs moléculaires tels que le catéchol-estrogène, l'EGF mais aussi p21 $^{cip1/WAF1}$, BTG1, HDAC5, l'antigène

nucléaire de la prolifération cellulaire (proliferation nuclear antigen, PCNA) et les facteurs de transcription FOXO (Lopes, Desmarais et al. 2004).

A ce jour, les voies de signalisation en amont de la régulation de l'expression et/ou de l'activité de ces candidats potentiellement impliqués dans la régulation du cycle cellulaire au moment de la réactivation de l'embryon demeurent encore inconnues. Néanmoins, une voie de signalisation cellulaire régulant la diapause embryonnaire au niveau de l'embryon a été proposée : celle-ci fait intervenir les systèmes de transport d'acides aminés et la serine-thréonine kinase, cible mammifère de la rapamycine (mammalian target of rapamycine, mTOR) et les polyamines (Van Winkle, Tesch et al. 2006).

ii. Incorporation des acides aminés, voie de signalisation mTOR et les polyamines

La capacité d'incorporation d'acides aminés ou d'acides nucléiques présents dans le milieu de culture *in vitro* par le blastocyste en dormance apparait nettement amoindrie par rapport à des blastocystes activés (Weitlauf 1973). Ces travaux suggérent que l'activité de transport d'acides aminés intra-embryonnaires joue un rôle important dans la régulation de la diapause embryonnaire.

Les transporteurs d'acides aminés ont été classés selon leur spécificité pour les acides aminés cationiques, anioniques ou zwitterioniques (neutres) et selon que leur activation soit dépendante ou non d'un gradient sodique (Christensen 1990). Quatorze transporteurs d'acides aminés différents ont été identifiés au niveau du blastocyste de souris et leur activité semblerait augmenter pendant la période de réceptivité à l'implantation (Van Winkle 2001). Une augmentation de l'expression

du transporteur spécifique de la leucine, appelé système $B^{0,+}$, dont l'activité dépend d'un gradient de sodium (Na^+) et, d'au moins cinq différents transporteurs spécifique de l'arginine Na^+-indépendants, appelés système $b^{0,+}$, a été mesurée lors du développement de l'embryon entre le stade de morula et celui de blastocyste (Van Winkle 2001) de même qu' à la réactivation de l'embryon en dormance (Hamatani, Carter et al. 2004). De plus, les activités des systèmes $B^{0,+}$ et $b^{0,+}$ semblent être couplées: tandis que la leucine est importée dans le milieu intra embryonnaire par le système $B^{0,+}$ via un gradient de Na^+, le système $b^{0,+}$ effectue un hétéro-échange de l'arginine qui est importée dans le milieu intra embryonnaire contre la leucine qui est relarguée vers le milieu extra embryonnaire (Van Winkle 2001) (**Figure 3** (p 22)).

Chez des souris maintenues expérimentalement en diapause, une nette augmentation de la concentration en Na^+ dans les sécrétions utérines a été mesurée quelques heures seulement après une injection d'œstradiol-17β (Van Winkle, Campione et al. 1983; Nilsson and Ljung 1985). Par ailleurs, la réactivation *in vitro* d'embryons en diapause est inhibée lorsque le milieu de culture est dépourvu de Na^+ (Van Winkle 1981). Ces résultats pourraient par conséquent suggérer l'activation des systèmes de transport de la leucine et de l'arginine, les systèmes $B^{0,+}$ et $b^{0,+}$ dans le milieu intra embryonnaire, au moment de la réactivation du blastocyste.

Outre un rôle important dans la synthèse protéique, la leucine est capable d'activer la voie de signalisation mTOR (revue par (Martin, Sutherland et al. 2003)). Cette dernière induit une phosphorylation d'au moins deux protéines connues pour

leur implication dans l'initiation de la traduction, p70S6K et PHAS-I (revue par (Martin, Sutherland et al. 2003)). La phosphorylation de p70S6K induite par mTOR permet l'expression de composés importants de la machinerie traductionnelle (Meyuhas 2000). A l'inverse, PHAS-I est inactivée par la phosphorylation de mTOR dont résulte la libération du facteur eucaryotique de l'initiation 4E (eukaryotic initiation factor 4E, eIF4E), lequel est important pour l'initiation de la traduction (Raught, Gingras et al. 2000). *In vitro*, une inhibition totale de la croissance trophoblastique chez les blastocystes traités à la rapamycine, un inhibiteur spécifique de mTOR, a été observée (Martin and Sutherland 2001).

Par conséquent, la voie de signalisation mTOR pourrait être ainsi activée par la leucine et induire l'expression de gènes codant pour des facteurs importants pour la croissance du trophoblaste (Martin, Sutherland et al. 2003). L'expression du gène codant pour l'ornithine decarboxylase (*ODC1*), enzyme principale de la biosynthèse des polyamines à partir de l'arginine (revue par (Wallace, Fraser et al. 2003)), serait ainsi régulée par mTOR, sous l'action de la leucine (Kimball, Shantz et al. 1999) (**Figure 3** (p 22)). De plus, les polyamines se sont avérées être des molécules-clés du développement embryonnaire et de l'implantation chez les rongeurs (Fozard, Part et al. 1980; Van Winkle and Campione 1983).

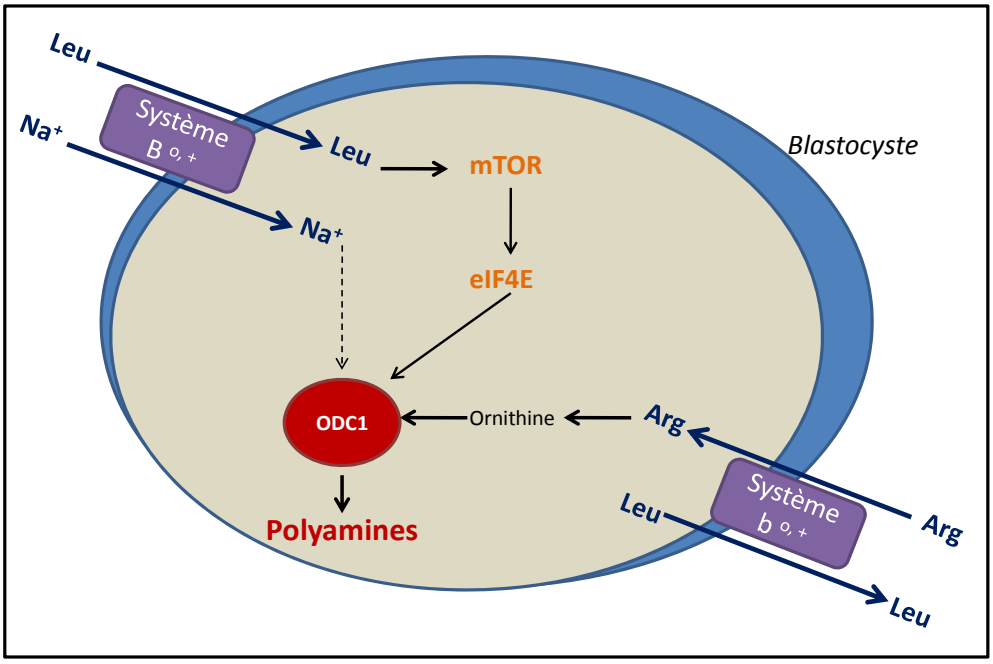

Figure 3. Activation de mTOR à l'émergence de la diapause embryonnaire.

La réactivation du développement embryonnaire a été associée à une augmentation de la concentration en ions sodium (Na^+) ainsi qu'en leucine (Leu) et en arginine (Arg) dans les fluides utérins et/ou *in vitro*, dans le milieu de culture du blastocyste. La leucine est incorporée via le système $B^{0,+}$, transporteur d'acides aminés Na^+-dépendant. Dans le milieu intraembryonnaire, la leucine est soit utilisée par le système $b^{0,+}$, Na^+ –indépendant qui assure l'importation de l'arginine, soit elle active la voie de signalisation mTOR, d'où résulte la libération du facteur d'initiation de la traduction 4E (eIF4E), responsable de la traduction du gène codant pour l'ornithine decarboxylase 1 (ODC1). Stimulée par une forte concentration sodique, ODC1 est l'enzyme principale de la biosynthèse des polyamines, et ce à partir de l'arginine (revue par (Martin, Sutherland et al. 2003)).

C. Les polyamines

Ayant fait l'objet d'une étude bibliographique présentée au chapitre V de cet ouvrage, la définition, les fonctions moléculaires et cellulaires et le rôle dans le développement embryonnaire en période de préimplantation ne seront que brièvement abordés dans cette partie.

1. Définition et fonctions moléculaires et cellulaires des polyamines

Les polyamines ou putrescine, spermidine et spermine, sont des molécules composées d'une longue chaine de carbone et d'un ou plusieurs groupe (s) aminé (s), chargé (s) positivement à pH physiologique. L'arginine est le principal précurseur de la biosynthèse des polyamines, via l'ODC1, l'enzyme limitante de la biosynthèse des polyamines (revue par (Wallace, Frazer et al. 2003)).

En tant que « supercations », les polyamines ont la capacité d'interagir avec les groupements phosphates des molécules d'ADN ou d'ARN et d'influer sur la structure chromatinienne, modulant ainsi la réplication, la prolifération cellulaire et l'expression génique au niveau de la transcription et de la traduction des gènes (revue par (Wallace, Frazer et al. 2003)).

2. Les polyamines et la diapause embryonnaire

Tel que présenté dans le modèle proposé à la **Figure 3** (p 22), l'émergence de la diapause embryonnaire pourrait dépendre d'un accroissement de la concentration sodique extra embryonnaire (Van Winkle 1977; Van Winkle, Campione et al. 1983) qui serait à l'origine de l'activation de mTOR, via la leucine, de l'expression de l'*ODC1* et de son activité de synthèse des polyamines (Van Winkle, Tesch et al. 2006). Les polyamines pourraient par conséquent jouer un rôle

important dans la réactivation du développement embryonnaire, suite à la diapause (Van Winkle and Campione 1983).

Pour tester cette hypothèse, des blastocystes de souris en diapause ont été placés dans un milieu de culture en présence d'α-difluoromethylornithine (DFMO), un inhibiteur irréversible de l'ODC1, afin de bloquer la biosynthèse des polyamines (Metcalf, Danzin et al. 1978). Aucune reprise de la croissance trophoblastique n'a été observée en présence de DFMO, comparativement à des blastocystes non soumis au traitement qui démontrent 100 % de croissance trophoblastique en quatre jours. En revanche, la réactivation des embryons traités au DFMO est induite à des taux similaires en moins de deux jours, lorsque ces mêmes embryons sont lavés et replacés dans des conditions de culture normale. En présence de polyamines exogènes, les effets associés au traitement du DFMO n'ont pas été observé, suggérant que l'ajout de polyamines compense la diminution des taux de polyamines induite par le DFMO. Par conséquent, l'inhibition de la biosynthèse des polyamines semble maintenir les embryons dans un état de diapause et réciproquement, la biosynthèse des polyamines semble être essentielle pour la réactivation des embryons *in vitro* chez la souris.

Le rôle des polyamines dans la réactivation du développement embryonnaire *in vivo* n'a cependant pas été démontré encore à ce jour, mais ces résultats préliminaires suggèrent fortement une implication essentielle des polyamines dans l'émergence de la diapause embryonnaire.

D. Biologie de la reproduction du vison américain

Le vison d'Amérique (*Mustela vison* ou *Neovison vison*), un mustélidé de la famille des carnivores, présente une période de diapause embryonnaire obligatoire. Étant l'espèce chez qui une des plus courte période de diapause embryonnaire ait été répertoriée - deux semaines en moyenne - (Pearson and Enders 1944), de nombreuses études ont utilisé ce modèle animal afin de comprendre les mécanismes physiologiques sous-jacents la diapause embryonnaire obligatoire.

1. Cycle de reproduction saisonnier

Chez le vison, la période de réceptivité sexuelle, ou période d'œstrus est observée une fois par an, et s'étend de la fin février au début du mois de mars, à la veille de l'équinoxe vernal (Enders 1952) (**Figure 4** (p 26)). Le restant de l'année, le cycle de reproduction du vison est en anoestrus, et est associé à une réduction considérable du poids des organes reproducteurs (ovaires et utérus), ainsi que des concentrations plasmatiques de progestérone et d'œstrogènes. La période de proestrus, en janvier-février, est caractérisée par un accroissement du poids ovarien ainsi qu'une augmentation maximale de la concentration plasmatique en œstrogène, associée à la réactivation des fonctions ovariennes, qui retourne ensuite à un niveau basal pendant la période d'œstrus (Travis, Pilbeam et al. 1978; Pilbeam, Concannon et al. 1979). Un accroissement de la concentration plasmatique en prolactine et progestérone caractérise la période d'œstrus, qui débute lorsque la photopériode commence à augmenter (**Figure 4**(p 26)).

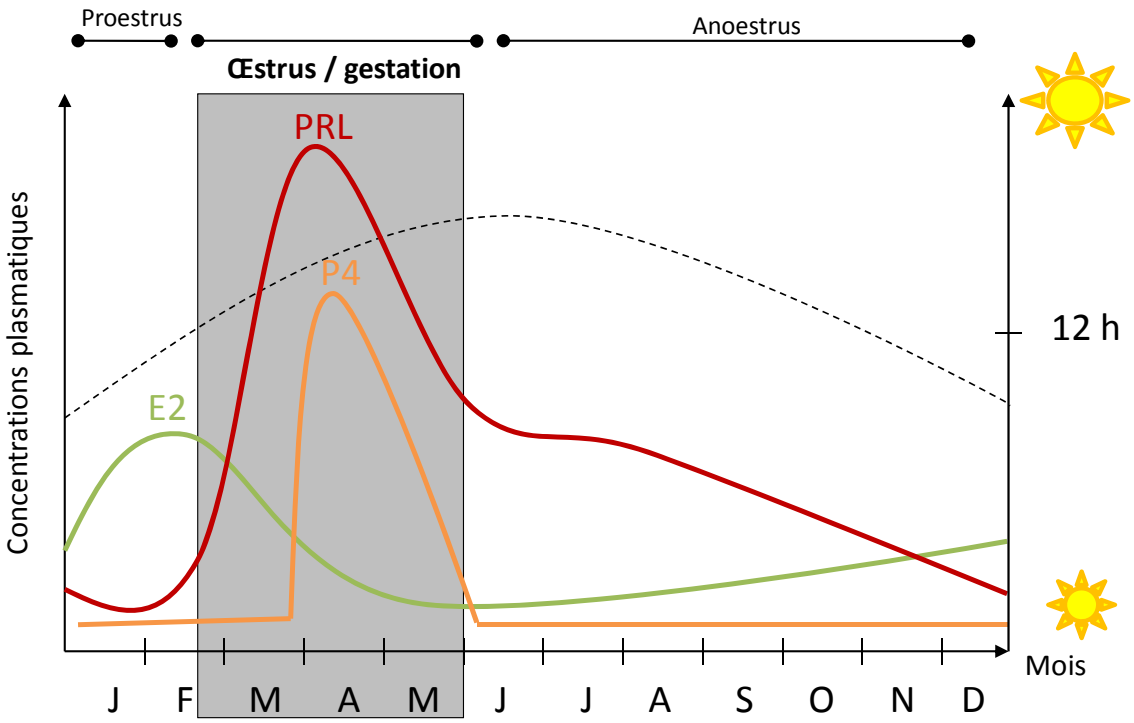

Figure 4. Cycle de reproduction saisonnier du vison américain.

La période de reproduction chez le vison a lieu une fois par an et s'étend de la fin février à la fin du mois de mai. Une élévation de la concentration plasmatique en œstrogènes (E_2) caractérise la période de proestrus, tandis que la période d'œstrus et de gestation sont corrélées à un accroissement des taux de prolactine (PRL) et de progestérone (P_4), induit par le rallongement de la photopériode. Le restant de l'année correspond à une période d'inactivité des fonctions de reproduction ou période d'anoestrus. (Figure adaptée de (Pilbeam, Concannon et al. 1979; Sundqvist, Amador et al. 1989)).

2. Ovulation induite et développement embryonnaire précoce

En période d'œstrus, l'ovulation est provoquée par un pic de LH induit par l'accouplement (Venge 1973) et s'effectue en moyenne 48 heures *post-coïtum* (Hansson 1947; Enders 1952). La fécondation des oocytes libérés au moment de l'ovulation peut résulter d'accouplements avec différents males durant cette courte période (superfécondation) (Hansson 1947). L'ovulation induite chez le vison s'accompagne d'une élévation de la concentration plasmatique en œstrogènes, qui chute rapidement après l'accouplement et demeure ainsi à un niveau basal durant toute la gestation, et le restant de l'année (revue par (Sundqvist, Amador et al. 1989)).

Six à sept jours suivant la fertilisation des oocytes dans l'oviducte, les embryons rendus au stade de blastocyste (300 à 400 cellules), pénètrent et demeurent groupés dans la région craniale de la corne utérine, ou ils entrent en diapause (Enders 1952) (**Figure 5** (p 29)). La proliferation cellulaire et la synthèse protéique sont suspendues et le métabolisme, est maintenu à un état basal dans le blastocyste en diapause (Desmarais, Bordignon et al. 2004).

Durant la phase précoce du développement embryonnaire, le processus de lutéinization est initié, induisant la formation des corps jaunes, mais ces derniers entrent cependant dans un état d'involution qui se traduit par une faible concentration plasmatique en progestérone pendant la diapause embryonnaire (Hansson 1947; Enders 1952). Parallèlement, la folliculogénèse et la production d'oocytes matures sont encore actives, sous l'action de l'hormone folliculo-stimulante (FSH) et de la LH, permettant ainsi, une seconde ovulation d'avoir lieu six

à sept jours plus tard (superfétation) (Douglas, Pierson et al. 1994). Un second accouplement peut par conséquent être à l'origine d'une deuxième « vague » d'embryons, qui suivront alors la même chronologie de développement embryonnaire que celle issue du premier accouplement (Hansson 1947) (**Figure 5** (p 29)). Suivant un processus similaire, jusqu'à quatre ovulations peuvent ainsi survenir durant la période d'œstrus et de diapause (revue par (Sundqvist, Amador et al. 1989)). Cependant, 80 à 90 % de la portée résultante de ces accouplements sera constituée des embryons provenant du deuxième ou du dernier accouplement, reflétant ainsi une importante mortalité embryonnaire durant la diapause (Adams 1981). Cette dernière résulterait de l'intromission lors de (s) accouplement (s) ultérieur (s) qui provoquerait une expulsion des blastocystes en diapause issus de (s) accouplement (s) précédent (s) (Adams 1981).

3. Diapause et réactivation du développement embryonnaire

La sortie de la diapause est initiée par le changement de photopériode à l'équinoxe vernal (Enders 1952; Murphy and James 1974) et suit une chronologie d'événements communs aux carnivores mustélidés présentant une diapause embryonnaire (**Figure 2** (p 14)). La durée de la diapause dépend de la date des accouplements : plus les accouplements ont lieu tôt dans la saison de reproduction, plus longtemps durera la diapause embryonnaire (Bowness 1968). La diapause peut néanmoins s'étendre jusqu'à 60 jours si les femelles gestantes en diapause sont maintenues dans la noirceur (Enders 1952).

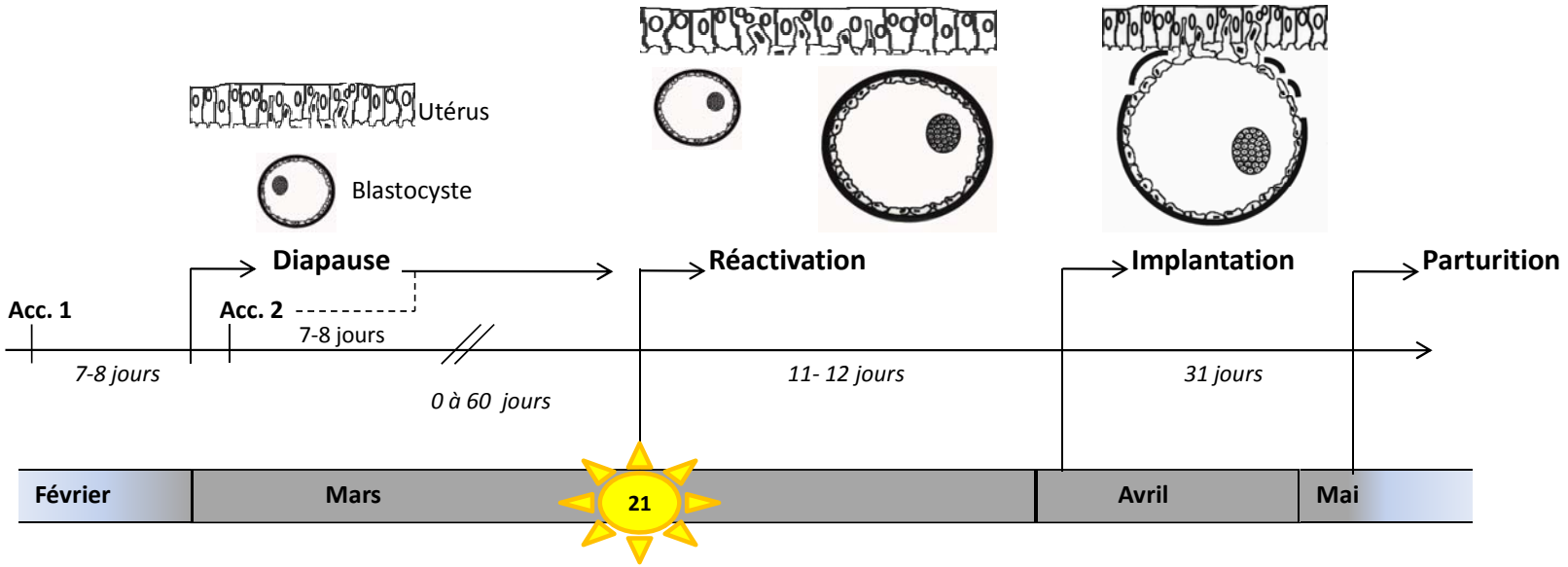

Figure 5. Chronologie du développement embryonnaire chez le vison.

Suite à un ou plusieurs accouplement (s) (Acc.), les embryons rendus au stade de blastocyste entrent en diapause dont la durée est variable, dépendamment de la date de(s) l'accouplement(s). La réactivation des blastocystes s'effectue à l'équinoxe vernal (21 mars), lorsque la photopériode passe à une durée supérieure à 12 heures par jour. Onze à 12 jours sont nécessaires avant que les blastocystes et l'utérus soient compétents pour que l'implantation puisse s'effectuer, au début du mois d'avril. Le développement fœtal dure en moyenne 31 jours et la parturition a lieu au début du mois de mai.

En réponse à l'accroissement de la photopériode, la synthèse de mélatonine au niveau de la glande pinéale est diminuée, levant ainsi l'inhibition qu'elle induit sur la production hypophysaire de prolactine (Martinet and Allain 1985; Murphy, DiGregorio et al. 1990). L'augmentation du taux de prolactine provoque alors la réactivation des corps jaunes, se traduisant par une hyperplasie et hypertrophie des corps jaunes, associées à une augmentation de l'activité de synthèse de la progestérone (Murphy and Moger 1977; Papke, Concannon et al. 1980; Murphy, Concannon et al. 1981). La prolactinémie s'élève ainsi progressivement de 10-15 ng/ml au début de la réactivation à plus de 30 ng/ml au moment de l'implantation de l'embryon, puis diminue progressivement (Douglas, Houde et al. 1998). Cette dernière est secondée par une élévation importante de la concentration plasmatique en progestérone qui passe de 8 ng/ml à plus de 30 ng/ml, dans les quelques jours précédent l'implantation au début du mois d'avril, puis diminue progressivement jusqu'à la parturition qui a lieu courant du mois de mai (Moller 1973; Murphy and Moger 1977; Allais and Martinet 1978) (**Figure 5** (p 29)).

En tant que facteur lutéal contrôlant la sortie de la diapause embryonnaire chez le vison, la progestérone est indispensable, mais non suffisante (Murphy, Mead et al. 1983). En référence aux rongeurs, les œstrogènes sont quasiment indétectables durant la réactivation et ont même été associés à des conséquences délétères sur l'implantation et la taille des portées, chez le vison (Cochrane and Shackelford 1962). Une élévation de l'activité de la glucose-6-phosphate isomerase, un facteur ovarien impliqué dans l'implantation de l'embryon chez le furet (Schulz and Bahr 2003), a été observé chez le vison au moment de la réactivation de

l'embryon (communication personnelle, B.D Murphy and R.D Bennett) et pourrait par conséquent être le facteur ovarien complémentaire de la progestérone, nécessaire à la réactivation de l'embryon.

Au niveau de l'endomètre utérin, la forte densité de granules de sécrétion ainsi que leur accroissement en taille au niveau des glandes utérines à la fin de la diapause suggèrent la préparation à une activité de sécrétion accrue durant la reprise du développement embryonnaire (Enders, Enders et al. 1963). Aussi, la réactivation *in vitro* de blastocystes de vison en diapause a été observée uniquement en présence d'une couche de cellules utérines de vison, démontrant que l'environnement utérin est indispensable à la sortie de la diapause embryonnaire (Moreau, Arslan et al. 1995). Cependant, les acteurs utérins qui provoquent la sortie de la diapause embryonnaire, sous l'effet de la progestérone, demeurent inconnus à ce jour.

Un délai de deux à trois jours de la réponse ovarienne à la prolactine a été observé à la réactivation des blastocystes (Enders 1952; Murphy, Concannon et al. 1981) . Durant ce laps de temps, il a été rapporté que les cornes utérines s'allongent et que les embryons commencent alors à migrer et à se distribuer le long de la lumière utérine au niveau de leur futur site d'implantation, puis cette motilité utérine serait réprimée sous l'effet de la progestérone (Enders 1952).

Durant la diapause et jusqu'à l'implantation, le blastocyste de vison est entouré d'une zone pellucide doublée d'une couche glycoprotéique acellulaire, une caractéristique commune aux carnivores (Desmarais, Bordignon et al. 2004). La réactivation du développement embryonnaire se caractérise par la reprise de la

prolifération cellulaire et de l'expression génique ainsi que par l'augmentation du diamètre de l'embryon à trois et à cinq jours suivant l'émergence de la diapause, respectivement (Desmarais, Bordignon et al. 2004). L'accroissement du diamètre de l'embryon résulterait de la reprise de la synthèse protéique mais témoignerait également d'une stimulation de l'activité d'incorporation des fluides utérins au sein de l'embryon. De plus, le développement de cultures de cellules embryonnaires de vison *in vitro* a suggéré que le trophoblaste était en premier lieu réactivé, suivi des cellules de la masse interne (Desmarais, Bordignon et al. 2004).

En se basant sur ces observations, le ou les facteur (s) utérin (s) provoquant la réactivation embryonnaire seraient directement ou indirectement impliqués dans la régulation de la prolifération cellulaire, de l'expression génique et de l'accumulation des fluides utérins au niveau du blastocyste.

4. Implantation et développement post-implantation

Onze à 12 jours suivant l'émergence de la diapause embryonnaire sont nécessaires pour la reprise du développement embryonnaire et pour la préparation de l'implantation, qui a lieu au début du mois d'avril (Enders 1952; Sundqvist, Amador et al. 1989) (**Figure 5** (p 29)). À la veille de l'implantation, le blastocyste a augmenté de dix fois son diamètre (2.0 mm) par rapport à la diapause (0.2 mm) (Desmarais, Bordignon et al. 2004).

L'implantation de l'embryon est de type eccentrique, s'effectuant au pôle antimesometrial de la chambre d'implantation (Kolpovskii 1976) (**Figure 6** (p 36)). Le développement du placenta est de type zonaire et endothelio-chorial (Hedlund, Nilsson et al. 1972; Pfarrer, Winther et al. 1999); Ce dernier implique l'invasion des

glandes utérines par le trophoblaste différencié en cytotrophoblaste et du mésenchyme chorionique, à l'origine des vaisseaux sanguins chorioniques. Au fur et à mesure que l'invasion progresse et que se développent les villis trophoblastiques, l'épithélium glandulaire est dégradé et repoussé à la base des glandes donnant lieu au symplasma maternel. Le cytotrophoblaste se différentie ensuite en syncythiotrophoblaste qui envahit et dégrade le stroma utérin pour atteindre et entourer les capillaires maternels. Il en résulte la formation d'un labyrinthe fœto-maternel s'effectuant durant la première semaine après le début de l'implantation (Song 1998). Le diamètre des sites d'implantation varie ainsi de 4.5 mm à 15 mm dans les dix jours suivants l'implantation (Stoufflet, Mondain-Monval et al. 1989; Song, Carriere et al. 1995).

Durant le développement fœtal, le placenta ne produit pas de progestérone et les corps jaunes représentent la seule source de progestérone nécessaire au développement du fœtus, sous l'effet de la prolactine et de la LH (Moller 1974; Murphy, Concannon et al. 1981; Murphy, Rajkumar et al. 1993; Douglas, Song et al. 1997). De plus, l'expression de gènes codant pour des marqueurs de l'implantation observés chez les rongeurs, tels que *la cyclooxygenase 2* (*COX2*) (Song, Sirois et al. 1998), *LIF* (Song, Houde et al. 1998), *le facteur de croissance de l'endothélium vasculaire* (*vascular endothelium growth factor 1*, *VEGF1*) (Lopes, Desmarais et al. 2006), *le récepteur au facteur activé par la prolifération des peroxysomes γ* (*peroxysome proliferator-activated receptor γ, PPAR γ*) (Desmarais, Lopes et al. 2007)et *la progranuline* (Desmarais, Cao et al. 2008) a été également décrite chez le vison.

Après l'implantation, le développement fœtal a une durée fixe de 31 jours (**Figure 5** (p 29)). La durée de la gestation est en moyenne de 51 jours mais peut varier de 42 à 79 jours, et ce, en raison de la période de diapause embryonnaire (Hansson 1947; Enders 1952).

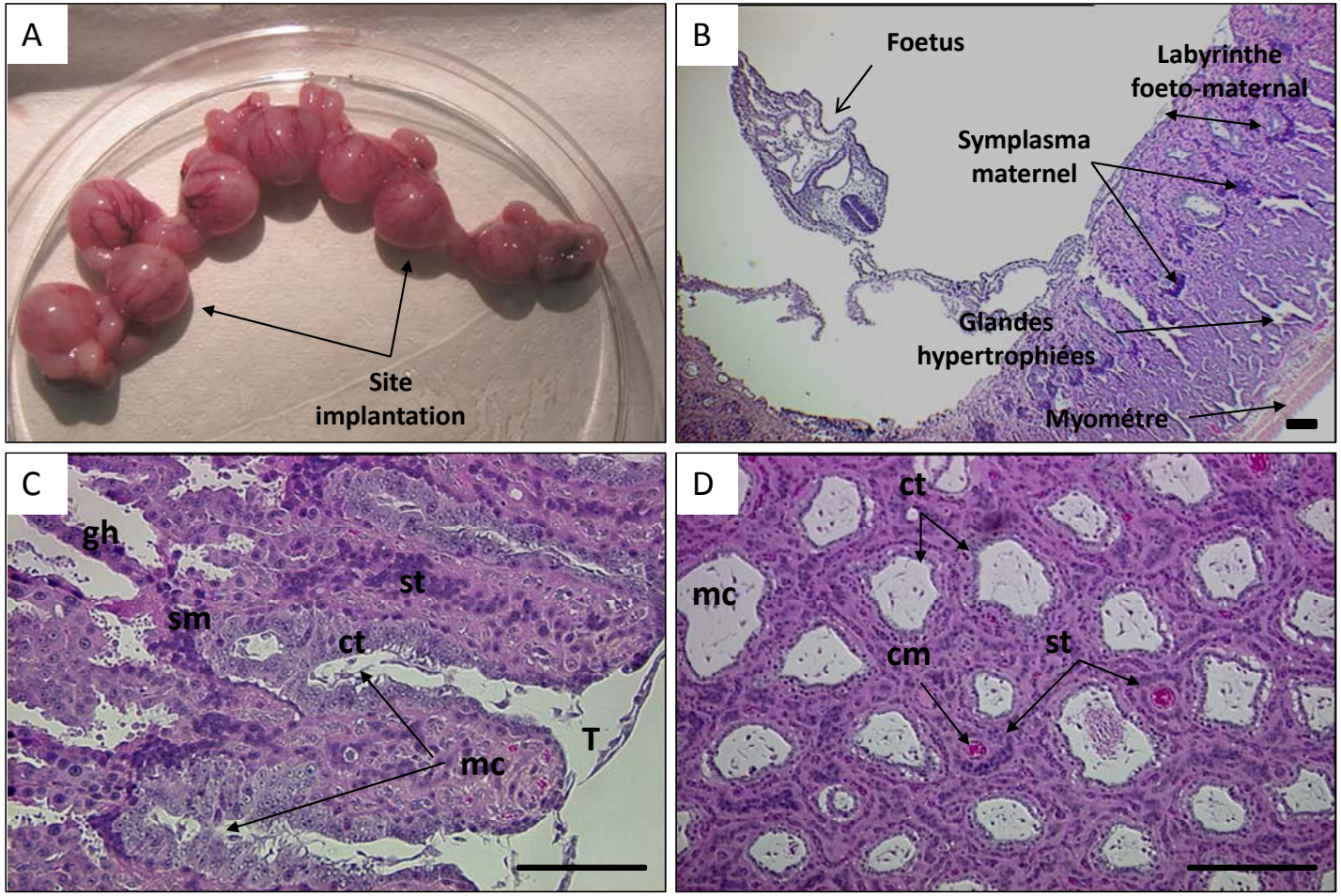
A
Site
implantation
B
Foetus
Labyrinthe
foeto-maternal
Symplasma
maternel
Glandes
hypertrophiées
Myométre
C
gh
st
sm
ct
T
mc
D
ct
mc
cm
st

Figure 6. Implantation de l'embryon chez le vison américain.

A). Uterus de femelles gestantes à 6 jours après l'implantation de l'embryon ou 18 jours après la réactivation du développement embryonnaire suite à la diapause. Huit sites d'implantation distincts sont observables. B) Coupe longitudinale d'un site d'implantation à 6 jours après l'implantation. L'implantation, dite endothelio-choriale, se caractérise par trois zones distincts au niveau du site d'implantation : le labyrinthe foeto-maternel, la zone de jonction contenant le symplasma maternel et la région glandulaire, sous jacente au myométre et composée de glandes maternelles hypertrophiées. . C) Grossissement de l'observation de la coupe longitudinale d'un site d'implantation à 6 jours après l'implantation. L'invasion des glandes utérines par le trophoblaste différencié en cytotrophoblaste et du mésenchyme chorionique est à l'origine des vaisseaux sanguins chorioniques. Au fur et à mesure que l'invasion progresse, l'épithélium glandulaire est dégradé et repoussé à la base des glandes formant le symplasma maternel qui represent la zone de jonction entre le labyrinthe foeto-maternel et les glandes maternelles hypertrophiées. Le cytotrophoblaste se différentie ensuite en syncythiotrophoblaste qui envahit et dégrade le stroma utérin pour atteindre et entourer les capillaires maternels. D) Observation transversale d'un site d'implantation à 6 jours après l'implantation. Les capillaires fœtaux sont séparés des capillaires maternels par le syncythiotrophoblaste et cytotrophoblaste. cm : capillaires maternels; ct : cytotrophoblaste, gh : glandes hypertrophiées; sm : symplasma maternel; st : syncythiotrophoblaste; T : trophoblaste. Echelle : les barres representent 200 μm. (Photographie Pavine Lefèvre, 2009, non publiées).

E. Objectifs de l'étude

Comme mentionné précédemment, le (s) mécanisme (s) moléculaire (s) et cellulaire (s) sous jacents aux voies de signalisation utérines provoquant la sortie de la diapause embryonnaire chez le vison demeurent inconnues à ce jour. L'objectif global de mon projet de doctorat était donc d'identifier les acteurs utérins et leur mode d'actions sur le blastocyste en diapause pour stimuler leur réactivation.

1. Analyse du transcriptome utérin du vison à l'émergence de la diapause embryonnaire

Notre premier objectif s'est porté sur l'analyse du transcriptome utérin au moment de la réactivation. Pour se faire, la technique de l'SSH (Diatchenko, Lau et al. 1996) a été employée. Cette technique a permis de générer une librairie d'ADNc différentiellement exprimés dans l'utérus de vison après la réactivation du développement embryonnaire versus durant la diapause. La méthodologie de la SSH appliquée au contexte de notre étude a été décrite en détails dans un chapitre du livre *Human Embryogenesis, Method and Protocols*, publié en 2009 et présenté au chapitre III de ce manuscrit. Les résultats de l'analyse de la librairie de gènes différentiellement exprimés à la réactivation au niveau utérin ont fait l'objet d'un article soumis au journal *Biology of Reproduction*, et présenté au chapitre IV de cet ouvrage.

2. Étude du rôle des polyamines à la sortie de la diapause embryonnaire

L'analyse du transcriptome utérin à la réactivation du développement embryonnaire nous a permis d'identifier l'augmentation de l'expression génique de trois gènes codant pour des enzymes impliqués dans la biosynthèse des polyamines dans l'utérus de vison à la sortie de la diapause embryonnaire. Nos recherches bibliographiques concernant le rôle des polyamines dans les fonctions de reproduction ont donné lieu à la rédaction d'une revue de littérature également vouée à la publication et présentée au chapitre V de cette thèse. Étant donné l'importance des polyamines dans la réactivation du développement embryonnaire d'embryons de souris en diapause, nous avons émis l'hypothèse que les polyamines étaient impliquées dans l'émergence de la diapause embryonnaire, chez le vison. Les résultats qui ont découlés des expériences de cette deuxième partie de mon doctorat sont regroupés dans un article également en voie d'être publié (chapitre VI).

III. ARTICLE 1: DIFFERENTIAL GENE EXPRESSION IN THE UTERUS AND BLASTOCYST DURING THE REACTIVATION OF EMBRYO DEVELOPMENT IN A MODEL OF DELAYED IMPLANTATION

Status: Published.

" Lefèvre, P. L. and B. D. Murphy (2009). Differential gene expression in the uterus and blastocyst during the reactivation of embryo development in a model of delayed implantation. Methods Mol. Biol. J. Lafond and C. Vaillancourt. Montreal, Humana Press. **550:** 11-61."

Differential gene expression in the uterus and blastocyst during the reactivation of blastocyst development in a model of delayed implantation

Pavine L.C. Lefèvre and Bruce D. Murphy.

Centre de recherche en reproduction animale, Faculté de médecine vétérinaire, Université de Montréal, Saint-Hyacinthe, Québec, Canada.

Running title: Gene expression in embryonic diapause

Corresponding author:

Bruce D. Murphy

Centre de recherche en reproduction animale

3200, rue Sicotte, Saint-Hyacinthe

QC, J2S 7C6, Canada

Tel: (001) (450) 773 8521 # 18627

Fax: (450) 778 8103

Abstract

Delayed implantation, a reversible arrest in embryo development while the embryo is at the blastocyst stage, provides an interesting window for observation of the preparation for implantation on both the embryonic and maternal sides. The American mink (*Mustela vison*) is a species in which delayed implantation is a normal aspect of embryo development as it consistently occurs at each breeding season. We used a transcriptome-wide approach to screen global gene expression and to identify new key genes expressed in the uterus and in the blastocyst at the resumption of the embryo development, after delayed implantation. By using the suppressive subtractive hybridization (SSH) technique, two libraries of differentially expressed cDNAs, one at the uterine level and a second one at the blastocyst level, were successfully generated. Candidate genes from those two libraries were selected and their differentially expressed pattern of expression between reactivation and delayed implantation was investigated by real time PCR and immunolocalization.

Key Words: Blastocyst; uterus; embryo implantation; delayed implantation; embryonic diapause; gene expression; suppressive subtraction hybridization (SSH).

A. Introduction

Embryo implantation represents a critical step in the human reproductive process when the blastocyst becomes intimately connected to the maternal endometrium and begins to form the placenta that will provide an interface between the growing fetus and the maternal circulation. Successful implantation requires a receptive endometrium, a normal and functional embryo at the blastocyst developmental stage, and a synchronized dialogue between maternal and embryonic tissues. Implantation failure is considered as a major cause of infertility in healthy women (Wang and Dey 2006). Investigations of human embryo implantation are constrained for practical and ethical reasons. Consequently, many animal models of implantation, such as primates, rodents (mice and rats), pigs, and ruminants (sheep and cows) and carnivores (minks and ferrets) have been used to investigate implantation (Lee and DeMayo 2004). Given the variation in placentation among species, each provides different insight into the nidatory process.

Delayed implantation consists in a reversible arrest in embryo development at the blastocyst stage during the preimplantation period. It therefore provides an interesting window for observation of molecular and cellular events associated with the preparation for implantation on both the embryonic and maternal sides. Mechanisms underlying delayed implantation in the mice and rats have been investigated. Ovariectomy on day 4 morning of pregnancy before ovarian estrogen

secretion initiates blastocyst dormancy which can last for many days if the animal is treated with progesterone (Yoshinaga and Adams 1966). An estrogen injection rapidly activates blastocysts and initiates their implantation. Although many studies adopted a "one by one" candidate approach to investigate gene expression in experimentally induced delayed implantation (Jha, Titus et al. 2006; Song and Lim 2006; Xiao, Yuan et al. 2006; Gao, Lei et al. 2007), a transcriptome-wide approach is nevertheless a powerful tool to screen global gene expression and to identify new key genes in the process. Hamatani *et al*. (Hamatani, Carter et al. 2004) and Reese *et al.* (Reese, Das et al. 2001) determined global gene expression by microarray analysis in mice during and after experimentally induced delayed implantation in embryo and uterus, respectively. Even though those studies generated valuable data on gene expression during preimplantation period in the embryo and in the uterus, they are subject to bias due to the experimental manipulation of embryo development. Further, restriction of investigation to a single species may not provide a global picture of the regulation of implantation. To address this issue, we used a carnivore animal model, the American mink (*Mustela vison*), a species in which delayed implantation, or embryonic diapause, is a normal aspect of embryo development, as it consistently occurs at each breeding season (Hansson 1947). An increased photoperiod at the vernal equinox is the principal environmental signal that reactivates embryos (Murphy and James 1974). Longer day photoperiod induces secretion of prolactin, which then activates the ovary, resulting in the secretion of progesterone and other factors that act on the uterus to reactivate the

embryo and initiate embryo implantation (Murphy, Concannon et al. 1981; Lopes, Desmarais et al. 2004). Embryo reactivation is associated with an increase in endometrial secretion into the uterine lumen (Mead 1989). Thus, our working hypothesis is that uterine factor(s) actively secreted by the endometrium into the uterine lumen acts on blastocysts in diapause to stimulate the resumption of development. The aim of our study was to identify key genes expressed in the uterus and embryo essential for termination of embryonic diapause. We therefore collected endometrium and embryos from mink females during diapause and 3, 5 and 7 days after reactivation. Using the SSH technique, we successfully generated two libraries of differentially expressed cDNAs between the diapause state and the state of reactivation of the blastocyst development: one from the blastocyst and a second from the uterus. The analysis of the two libraries allowed us to generate data on global gene expression analysis, and to identify potential key regulatory genes.

Of the different strategies available to study differential gene expression, SSH (Diatchenko, Lau et al. 1996) is an efficient and widely-used PCR-based method to obtain subtracted libraries and to isolate differentially expressed genes between two populations of mRNA: the tester, or cDNA that contains specific transcripts of interest and the driver, the reference cDNA. The protocol involves normalization and subtraction in a single procedure. The normalization step (hybridization) equalizes the abundance of cDNAs within the tester population and the subtraction step excludes the common sequences between the target and driver populations (**Figure 7** (p 107). Moreover, the SSH technique enriches for rare sequences over

1,000-fold in one round of subtractive hybridization. Because SSH can be initiated using PCR-amplified cDNAs, it seems particularly well-suited to the study of mammal preimplantation stage embryos which contain only a tens of picogram of mRNAs. Furthermore, because SSH does not require previous knowledge of gene sequences, it may also be suitable for species where only a small number of sequences are available in databases. The SSH technique has also the advantage of generating unknown cDNA fragments or previously unknown genes and expressed sequence tags (ESTs).

Following the SSH, expressed cDNA fragments are submitted to differential screening to remove cDNAs common to both the tester and driver samples from the subtracted sample ((Chan, Kan et al. 1997) and **Figure 7** (p 107)). The cDNA fragments are then sequenced and the sequences are classified according to their degree of homology with sequences listed in gene databases. The cDNAs sequences that exhibit a significant degree of homology to known sequences are classified according to their gene ontology, providing a global gene expression perspective. Frequency of copies of the known sequence in the library, its implication in the preimplantation period suggested in the literature for other species and its biological function are taken into account in selecting potential candidate genes. Finally, the spatio-temporal pattern expression of these selected genes is investigated by real time polymerase chain reaction (qPCR), *in situ* hybridization and immunolocalization. The last step allows validation of the SSH by identifying authentic targets of biological significance.

In this chapter, we describe the multiple steps of the method to approach a global gene expression analysis and to identify key regulatory genes (**Figure 8** (p 108)). We first list the material required (*see* **Section 2**) followed by a detailed description of the method itself (*see* **Section 3**).

B. Materials

1. Blastocyst and Uterine Sample Collection

1. Flushing medium: 500 mL TC-199 medium (Gibco, Burlington, ON, Canada) containing 10% of fetal bovine serum (FBS; Gibco) and 2.5 mL penicillin/streptomycin (Gibco). The solution is prepared under a sterile hood, aliquoted and stored at 4°C, and is stable at 4°C for 1 month.
2. 1X Phosphate buffered saline (PBS) stored at 4 °C.
3. Paraformaldehyde (PAF) 4 % (Sigma). Carcinogenic, corrosive. Safety glasses, gloves and effective ventilation are required while manipulating this solution.
4. Liquid nitrogen. Store in cryogenic containers and use with adequate ventilation. Use safety glasses and gloves.

2. Uterine Samples : Total RNA Extraction and mRNA Isolation

1. RNeasy® Mini kit (Cat. No 74104; Qiagen, Mississauga, ON, Canada): the manufacturer provides all required reagents except 14.3 *M* β-mercaptoethanol (β-ME) which has to be manipulated under a chemical hood, and ethanol (70% and 96–100%).

2. Oligotex® kit (Cat. No 70022; Qiagen): the manufacturer provides all the required reagents except 14.3 *M* β-ME which has to be manipulated under a chemical hood.

3. Total RNA Extraction from blastocysts

RNeasy® Micro kit (Cat. No 74004; Qiagen). All reagents are supplied in the kit except 14.3 *M* β-ME and ethanol (70% and 96–100%).

4. Suppressive Subtraction Hybridization

1. PCR-Select™ cDNA Subtraction Kit (Cat. No 637401; Clontech, Palo Alto, CA, USA). The following reagents are required, but not supplied in the kit:
   a. Hae III digest of bacteriophage fX174 (New England Biolabs DNA size markers (Cat. Nos. N3026S & N3026L)).
   b. 80% Ethanol and 96% Ethanol.
   c. Phenol:chloroform:isoamyl alcohol (25:24:1).
   d. Chloroform:isoamyl alcohol (24:1).
   e. AdvantageTM cDNA Polymerase Mix (Cat. No. 639105).
   f. dNTP Mix for PCR (10 mM each dATP, dCTP, dGTP, dTTP).
   g. 50X TAE electrophoresis buffer (242 g Tris base, 57.1 ml Glacial acetic acid, 37.2 g $Na_2EDTA•2H_2O$, Add H_2O to 1 L. For 1X TAE buffer, dilute 50X stock solution 1:49 with H_2O).

2. Super SMART™ PCR cDNA Synthesis Kit (Cat. No 635000; Clontech). The following reagents are required, but not supplied in the kit:
   a. SMART™ MMLV Reverse Transcriptase (Cat. No PT4045-2, Clontech)

b. Advantage® 2 PCR Kit (Cat. Nos. 639206 and 639207, Clontech)

c. NucleoSpin® RNA II Kit (Cat. No. 635990, Clontech)

d. β-mercaptoethanol (Sigma Cat. No. M6250)

e. RNase Inhibitor (20 U/µl) (Ambion's SUPERase, Cat. No. 2696)

f. DNA size markers (1 kb DNA ladder)

g. 50X TAE electrophoresis buffer

h. CHROMA SPIN+STE-10 Columns (Cat. No. 636055, Clontech)

5. Differential Screening

PCR-Select Differential Screening Kit (Cat. No 637403; Clontech). The following reagents are required, but not supplied:

1. Advantage® 2 Polymerase Mix (Cat. No. 639201)
2. dNTP mix for PCR (10 mM each dATP, dCTP, dGTP, dTTP)
3. T/A Cloning Kit Dual Promoter (Cat. No K2060-01; Invitrogen, Carlsbad, CA, USA).
4. Max Efficiency DH5α Competent Cells (Cat. No 18258-012; Invitrogen).
5. Luria Broth (LB) medium (10 g Bacto-tryptone, 5 g Bacto-yeast extract, 5 g NaCl: Add H2O to 900 ml. Adjust pH to 7.0 with 5 N NaOH, then bring up to a 1L volume with H_2O. Autoclave).
6. Ampicillin (50 mg/ml stock solution; store at –20°C).
7. Isopropyl β-D-1-thiogalactopyranoside (IPTG) (final concentration of 1 m*M*).

8. 5-bromo-4-chloro-3-indolyl-beta-D-galactopyranoside (X-Gal) (final concentration of 50 μg / ml).
9. 0.6 N NaOH
10. 0.5 *M* Tris-HCl (pH 7.5)
11. Denaturing solution (0.5 *M* NaOH, 1.5 *M* NaCl; make fresh each time)
12. Neutralizing solution (0.5 *M* Tris-HCl [pH 7.5], 1.5 *M* NaCl)
13. Nylon membrane
14. NucleoSpin® Extraction Kit (Cat. No. 635961, Clontech)
15. [α-32P]dCTP or [α-32P]dATP (3,000 Ci/mmol)
16. illustra™ MicroSpin Columns (Cat. No: S-200 27-5120-01 GE Health Care, Buckinghamshire, UK).
17. ExpressHybTM Hybridization Solution (Cat Nos. 636831, 636832, Clontech).
18. 20X SSC (175.3 g NaCl ; 88.2 g Na3Citrate•2H_2O. Adjust pH to 7.0 with 1 *M* HCl. Add H_2O to 1 L. Store at room temperature).
19. 20% SDS (200 g SDS ; Add H2O to 1 L. Heat to 65°C to dissolve. Store at room temperature).
20. Low-stringency washing solution (2X SSC, 0.5% SDS)
21. High-stringency washing solution (0.2X SSC, 0.5% SDS)
22. Ethanol
23. Sterile, deionized H_2O
24. 50X TAE electrophoresis buffer

C. Methods

1. Blastocyst and Uterine Sample Collection

All procedures involving live animals were approved by the *Comité de déontologie de la Faculté de Médecine Vétérinaire, Université de Montréal,* which is accredited by the Canadian Council on Animal Care.

1. Remove the uterine horns from the euthanized animal.
2. Rinse the uterus in PBS 1X in a 100 mm Petri dish.
3. Excise as much the adipose tissue as possible.
4. Transfer the uterus to a 50 mm Petri dish.
5. Flush each uterine horn with 2.5 mL flushing medium pre-warmed at 37°C using a syringe and a 21G1/2 in needle (**Figure 9** (p 109)).
6. Search for embryos under a microscope and collect by aspirating them with a mouth pipette.
7. Rinse the embryos in PBS 1X pre-warmed at 37°C in a fresh 50 mm Petri dish. Carefully use the mouth pipette to manipulate the embryos under the microscope.
8. Transfer the embryos into a 1.5 mL tube in as minimum amount (a drop or less) of PBS 1X.
9. Snap-freeze the 1.5 mL tube containing embryos in liquid nitrogen and store the samples at – 80°C until use.

10. Section the whole uterine horn, place each section of uterine horn piece in a 1.5 mL tube, snap-freeze the tube in liquid nitrogen and store sample at –80°C until use.

11. Place the other uterine horn in a 1.5 mL tube containing PAF 4%. Store the tube at 4°C for 24 h. Rinse the tissue in PBS 1X, three times and place the tissue in 70 % ethanol at -20°C until use (*see* **Note 1**).

2. Total RNA Extraction and mRNA Isolation.

a. Total RNA Extraction from Uterine Samples

1. Thaw uterine sample on dry ice (*see* **Note 2**) (**Figure 10** (p 110)).
2. Aliquot 350 µL of Buffer RLT (RNeasy® Mini kit) in 14 mL polypropylene tube.
3. Place the tissue in the tube with the Buffer RLT.
4. Disrupt and homogenize the tissue using a Rotor-Stator Homogenizer (Polytron): place the tip of the disposable probe into the tube containing the uterine sample. At room temperature, operate the polytron beginning at low speed and increase progressively the speed over 30 sec, until the lysate is homogenous (*see* **Note 3**).
5. Transfer the lysate to 2 mL tubes. Centrifuge the lysate for 3 min at maximum speed (14,000–18,000*g*). Carefully transfer the supernatant to a fresh 1.5 mL tube by pipetting.
6. Add 1 volume (350 µL) of 70% ethanol to the lysate, and mix well by pipetting.

7. Do not centrifuge (*see* **Note 4**).

8. Transfer the sample to an RNeasy MinElute (RNeasy® Mini kit) spin column placed in a 2 mL collection tube. Close the lid gently, and centrifuge for 15 sec at ≥ 8000*g*. Discard the flow-through (*see* **Note 5**).

9. Add 700 µL Buffer RW1 (RNeasy® Mini kit) to the RNeasy MinElute spin column. Close the lid gently, and centrifuge for 15 sec at ≥ 8000*g* to wash the spin column membrane. Discard the flow-through and the collection column.

10. Place the RNeasy MinElute spin column in a new 2 mL collection tube. Add 500 µL Buffer RPE (RNeasy® Mini kit) to the spin column. Close the lid gently, and centrifuge for 15 sec at ≥ 8000*g* to wash the spin column membrane. Discard the flow-through.

11. Add 500 µL of Buffer RPE to the RNeasy MinElute spin column. Close the lid gently, and centrifuge for 2 min at ≥ 8000*g* to wash the spin column membrane. Discard the flow-through and collection tube**.**

12. Place the RNeasy MinElute spin column in a new 2 mL collection tube. Close the lid gently, and centrifuge at maximum speed (14,000–18,000*g*) for 1 min.

13. Place the RNeasy MinElute spin column in a new 1.5 mL collection tube. Add 30–50 µL RNase-free water directly to the spin column membrane. Close the lid gently, and centrifuge for 1 min at ≥ 8000*g* to elute the RNA (*see* **Note 6**).

14. If the expected RNA yield is > 30 µg, repeat the elution step using another 30–50 µL RNase free water, or using the eluate from the first elution in case high RNA concentration is required.

b. Messenger RNA Isolation from Total RNA in Uterine Samples

Before starting (**Figure 11** (p 111)):

1. Heat Oligotex Suspension (Oligotex® kit) to 37°C in a water bath or heating block. Mix by vortexing, and then place at room temperature.
2. Heat a water bath or heating block to 70°C, and heat Buffer OEB (Oligotex® kit).

Procedure:

1. Determine the amount of starting RNA (*see* **Note 7**). Pipet total RNA into an Rnase free 1.5 mL microcentrifuge tube, and adjust the volume with RNase-free water (if necessary) to the volume indicated in **Table 1** (p 104) (*see* **Note 8**).
2. Add the appropriate volume of Buffer OBB and Oligotex Suspension (Oligotex® kit) (**Table 2** (p 104)). Mix the contents thoroughly by pipetting or flicking the tube. Incubate the sample for 3 min at 70°C in a water bath or heating block to disrupt the secondary structure of the RNA.
3. Remove sample from the water bath/heating block, and place at 20 to 30°C for 10 min. This step allows hybridization between the oligo dT30 of the Oligotex particle and the poly-A tail of the mRNA.
4. Pellet the Oligotex: mRNA complex by centrifugation for 2 min at maximum speed (14,000–18,000*g*), and carefully remove the supernatant by pipetting (*see* **Note 9**).

5. Resuspend the Oligotex: mRNA pellet in 400 µl Buffer OW2 (Oligotex® kit) by vortexing or pipetting, and pipet onto a spin column placed in a 1.5 mL microcentrifuge tube. Centrifuge for 1 min at maximum speed (14,000–18,000*g*).
6. Transfer the spin column to a new RNase-free 1.5 mL microcentrifuge tube, and apply 400 µL Buffer OW2 to the column. Centrifuge for 1 min at maximum speed (14,000–18,000*g*) and discard the flow-through.
7. Transfer spin column to a new RNase-free 1.5 mL microcentrifuge tube.
8. Pipet 20–100 µl hot Buffer OEB (Oligotex® kit) (70°C) onto the column, pipet up and down 3 or 4 times to resuspend the resin, and centrifuge for 1 min at maximum speed (14,000–18,000*g*) (*see* **Note 10**).
9. To ensure maximal yield, pipet another 20–100 µL hot Buffer OEB (70°C) onto the column. Pipet up and down 3 or 4 times to resuspend the resin, and centrifuge for 1 min at maximum speed (14,000–18,000*g*) (*see* **Note 11**).

c. Total RNA Extraction from Blastocysts

1. Carefully thaw embryos on dry ice (**Figure 10** (p 110)).
2. Add 150 µL of Buffer RLT (RNeasy® Micro kit) to disrupt the cells. Vortex or pipet to mix.
3. Homogenize by vortexing the tube for 1 min.
4. Add 1 volume of 70% ethanol to the lysate, and mix well by pipetting (*see* **Note 4**).

5. Transfer the sample, including any precipitate that may have formed, to an RNeasy MinElute (RNeasy® Micro kit) spin column placed in a 2 mL collection tube. Close the lid gently, and centrifuge for 15 sec at ≥ 8000*g*. Discard the flow-through (*see* **Note 5**).
6. Add 150 µL Buffer RW1 (RNeasy® Micro kit) to the RNeasy MinElute spin column. Close the lid gently, and centrifuge for 15 sec at ≥ 8000*g* to wash the spin column membrane. Discard the flow-through.
7. Add 700 µL Buffer RW1 instead, centrifuge for 15 sec at ≥ 8000*g*, and discard the flow-through and collection tube.
8. Place the RNeasy MinElute spin column in a new 2 mL collection tube.
9. Add 500 µL Buffer RPE (RNeasy® Micro kit) to the spin column. Close the lid gently, and centrifuge for 15 sec at ≥ 8000*g* to wash the spin column membrane. Discard the flow-through.
10. Add 500 µL of 80% ethanol to the RNeasy MinElute spin column. Close the lid gently, and centrifuge for 2 min at ≥ 8000*g* to wash the spin column membrane. Discard the flow-through and collection tube.
11. Place the RNeasy MinElute spin column in a new 2 mL collection tube. Open the lid of the spin column, and centrifuge at full speed for 5 min to insure that the entire ethanol residue is evaporated. Discard the flow-through and collection tube.
12. Place the RNeasy MinElute spin column in a new 1.5 mL collection tube. Add 14 µL RNase-free water directly to the center of the spin column membrane.

Close the lid gently, and centrifuge for 1 min at maximum speed (14,000–18,000*g*) to elute the RNA.

13. Quantify the amounts and purity of the extracted total RNA (*see* **Note 7**).

3. Suppressive Substraction Hybridization

The SSH is performed with the PCR-Select™ cDNA Subtraction Kit for both the uterine samples and embryos to generate differentially expressed cDNAs between diapause and blastocyst reactivation. **Figure 12** (p 112) details the molecular events that occur during PCR-Select cDNA subtraction. As the amount of total RNA extracted from blastocysts is too meager, an alternative is to introduce a cDNA preamplification step by means of the Super SMART™ PCR cDNA Synthesis Kit (*see* **Subheading 3.3.1**) With slight modifications to the standard protocol until the Rsa I digestion step, SuperSMART cDNA can be used directly for the adaptor ligation step of the PCR-Select cDNA subtraction (*see* **Subheading 3.3.4**).

Complementary DNA is synthesized from 0.5–2 µg of poly A+ RNA generated from the uterine samples in diapause and after reactivation (*see* **Subheading 3.3.3**). In the PCR-Select™ cDNA Subtraction Kit, cDNA that contains specific (differentially expressed) transcripts is referred as the tester, and the reference cDNA, as the driver. In the present study, samples collected when uterus or blastocysts are in diapause are considered as the driver while those collected after reactivation of blastocysts represent the tester. The tester and driver cDNAs are digested with Rsa I (*see* **Subheading 3.3.2 and 3.3.3**), a four-base-cutting restriction enzyme that yields blunt ends. The tester cDNA is then subdivided into two portions, and each is

ligated with a different cDNA adaptor (*see* **Subheading 3.3.4**). The two adaptors have stretches of identical sequence to allow annealing of the PCR primer once the recessed ends have been filled in (**Table 2** (p 104)).

Two hybridizations are then performed:

1. In the first (*see* **Subheading 3.3.5**), an excess of driver is added to each sample of tester. The samples are then heat denatured and allowed to anneal, generating the type '**a**', '**b**', '**c**', and '**d**' molecules in each sample. The concentration of high- and low-abundance sequences is equalized among the type '**a**' molecules because reannealing is faster for the more abundant molecules due to the second-order kinetics of hybridization. At the same time, type '**a**' molecules are significantly enriched for differentially expressed sequences while cDNAs that are not differentially expressed form type '**c**' molecules with the driver.
2. During the second hybridization (*see* **Subheading 3.3.6**), the two primary hybridization samples are mixed together without denaturing. Only the remaining equalized and subtracted single strand (ss) tester cDNAs can reassociate and form new type '**e**' hybrids. These new hybrids are double strand (ds) tester molecules with different ends, which correspond to the sequences of Adaptors 1 and 2R. Fresh denatured driver cDNA is added to further enrich fraction '**e**' for differentially expressed sequences.

After filling in the ends by DNA polymerase, the type '**e**' molecules - the differentially expressed tester sequences - have different annealing sites for the

nested primers on their 5' and 3' ends. The entire population of molecules is then subjected to PCR to amplify the desired differentially expressed sequences (*see* **Subheading 3.3.7**). During this PCR, type '**a**' and '**d**' molecules are missing primer annealing sites, and thus cannot be amplified. Due to the suppression PCR effect, most type '**b**' molecules form a pan-like structure that prevents their exponential amplification. Type '**c**' molecules have only one primer annealing site and amplify linearly. Only type '**e**' molecules - the equalized, differentially expressed sequences with two different adaptors - amplify exponentially. Next, a secondary PCR amplification is performed using nested primers to further reduce any background PCR products and enrich for differentially expressed sequences.

a. Complementary DNA Synthesis from Total Embryonic RNA and cDNA Preamplification

This protocol has been optimized for total RNA (*see* **Note 12**) (**Figure 13** (p 113)).

i. First-Strand cDNA Synthesis

1. For each sample and control human placenta RNA (provided within the kit), combine the following reagents in a sterile 0.5 mL reaction tube: 1–50 µL RNA sample (2–1,000 ng of total RNA) (*see* **Note 13**), 7 µL 3' SMART CDS Primer II A (Super SMART™ PCR cDNA Synthesis Kit) (12 µ*M*), 7 µL SMART II A Oligonucleotide (Super SMART™ PCR cDNA Synthesis Kit) (12 µ*M*), x µL deionized H_2O (total volume = 64 µL).
2. Mix contents and spin 5 s the tube in a microcentrifuge.

3. Incubate the tube at 65°C in a hot-lid thermal cycler for 2 min and then reduce the temperature to 42°C.
4. Add the following to each reaction tube (Super SMART™ PCR cDNA Synthesis Kit): 20 µL 5X First-Strand Buffer, 2 µL DTT (100 m*M*), 10 µL 50X dNTP (10 m*M*), 5 µL RNase Inhibitor (20 U/µL), 5 µL MMLV Reverse Transcriptase (42 mL total added per reaction)
5. Gently pipet up and down to mix, then spin the tubes briefly in a microcentrifuge.
6. Incubate the tubes at 42°C for 90 min in a hot-lid thermal cycler.
7. Add 2 µL of 0.5 *M* EDTA to stop the reaction (*see* **Note 14**).

ii. Column Chromatography

To purify the SMART cDNA from unincorporated nucleotides and small (< 0.1 kb) cDNA fragments, follow this procedure for each reaction tube:

1. Add 212 µL of Buffer NT (Super SMART™ PCR cDNA Synthesis Kit) to each cDNA synthesis reaction; mix well by pipetting.
2. Place a NucleoSpin Extract II Column (Super SMART™ PCR cDNA Synthesis Kit) into a 2 mL collection tube. Pipet the sample into the column. Centrifuge at 11,200*g* for 1 min. Discard the flow-through.
3. Add 600 mL of Wash Buffer NT3 (Super SMART™ PCR cDNA Synthesis Kit) to the column. Centrifuge at 11,200*g* for 1 min. Discard the flow-through.

4. Place the column back into the collection tube. Centrifuge at 11,200*g* for 2 min to remove any residual Wash Buffer NT3 (Super SMART™ PCR cDNA Synthesis Kit).
5. Transfer the NucleoSpin Columns into a fresh 1.5 mL microcentrifuge tube. Add 50 µL of sterile Milli-Q H_2O (Super SMART™ PCR cDNA Synthesis Kit) to the column. Allow the column to stand for 2 min with the caps open.
6. Close the tube and centrifuge at 11,200*g* for 1 min to elute the sample.
7. Repeat elution with 35 µL of sterile Milli-Q H_2O in the same 1.5 mL microcentrifuge tube. The total recovered elution volume should be 80–85 µl per sample. If necessary, add sterile Milli-Q H_2O to bring the total volume up to 80 µL (*see* **Note 15**) (**Table 3** p(105)).

iii. cDNA Amplification by Long Distance PCR (LD-PCR)

The complementary DNA amplification includes a step to determine optimal number of PCR cycles for the amplification (**Figure 14** (p 114)). Guidelines for optimizing the PCR, depending on the amount of total RNA used in the first-strand synthesis, are provided in **Table 3** (p 105).

1. Set up three 100 µL PCR reactions, labeled “A”, “B”, and “C”, for each tester and driver sample (**Figure 14** (p 114)).
2. Preheat the PCR thermal cycler to 95°C.
3. For each experimental sample, aliquot 80 µL ss cDNA into a labeled 1.5-mL reaction tube.

4. Prepare a Master Mix (Super SMART™ PCR cDNA Synthesis Kit) for all reaction tubes, plus one additional tube. Combine per reaction (220 µL total volume) : 172 µL Deionized H_2O, 30 µL 10X Advantage 2 PCR Buffer, 6 µL 50X dNTP (10 m*M*), 6 µL 5' PCR Primer II A (12 µ*M*), 6 µL 50X Advantage 2 Polymerase Mix
5. Mix well by vortexing and spin the tube for 5 sec in a microcentrifuge.
6. Aliquot 220 µL of the PCR Master Mix into each tube containing the 80 µL ss cDNA. Mix well.
7. Aliquot 100 µL of the resulting PCR reaction mix into three reaction tubes labeled “A”, “B”, and “C”.
8. Cap each tube, and place them in the preheated thermal cycler.
9. Commence thermal cycling (with an hot-lid thermal cycler) using : 95°C 1 min and 15 cycles: 95°C 5 sec, 65°C 5 sec, 68°C 6 min.
10. Subject each reaction tube to 15 cycles and then pause the program. Transfer 30 µL from Tube C to a second reaction tube labeled “Optimization”. Store Tubes A and B, and the “Experimental” tube containing the remaining 70 µL of Tube C, at 4°C.
11. Using the Optimization PCR tube, determine the optimal number of PCR cycles (**Figure 14** (p 114)):
12. Set up six 100 µL PCR tubes for each experimental sample, labeled 15, 18, 21, 24, 27 and 30.
13. Transfer 5 µL from the 15 cycles PCR to a clean microcentrifuge tube.

14. Return the Optimization tubes to the thermal cycler. Run three additional cycles (for a total of 18) with the remaining 25 µL of PCR mixture. Transfer 5 µL from the 18 cycles PCR to a clean microcentrifuge tube.
15. Run three additional cycles (for a total of 21) with the remaining 20 µL of PCR mixture. Transfer 5 µL from the 21 cycles PCR to a clean microcentrifuge tube.
16. Run three additional cycles (for a total of 24) with the remaining 15 µL of PCR mixture. Transfer 5 µL from the 24 cycles PCR to a clean microcentrifuge tube.
17. Run three additional cycles (for a total of 27) with the remaining 10 µL of PCR mixture. Transfer 5 µL from the 27 cycles PCR to a clean microcentrifuge tube.
18. Run three additional cycles (for a total of 30) with the remaining 5 µL of PCR mixture.
19. Electrophorese each 5 µL aliquot of the PCR reaction alongside 0.1 µg of 1 kb DNA size markers on a 1.2% agarose/ ethidium bromide (EtBr) gel in 1X TAE buffer (0.04 *M* Tris – Acetate; 0.001 *M* EDTA).Determine the optimal number of cycles required for each experimental and control sample (*see* **Note 16** and **Figure 15** (p 115)).
20. Retrieve the 15 cycles Experimental PCR tubes from 4°C, return them to the thermal cycler, and subject them to additional cycles, if necessary, until the optimal number is reached.

21. When the cycling is completed, analyze a 5 µL sample of each PCR product alongside 0.1 µg of 1 kb DNA size markers on a 1.2% agarose/EtBr gel in 1X TAE buffer (*see* **Note 16** and **Figure 15** (p 115)).

22. Add 2 µL of 0.5 *M* EDTA to each tube to terminate the reaction.

iv. Column Chromatography

1. For every experimental sample and control, combine the three reaction tubes (A, B, and Experimental) of PCR product into a 1.5 mL microcentrifuge tube.

2. Transfer 7 µL of the raw PCR product to a clean microcentrifuge tube and label this tube "Sample A". Store at –20°C. Sample A will be later used for analysis of column chromatography.

3. To each tube of combined PCR product, add an equal volume of phenol: choloroform: isoamyl alcohol (25:24:1). Vortex thoroughly.

4. Centrifuge the tubes at 11,200*g* for 10 min to separate the phases.

5. Remove the top (aqueous) layer and place it in a clean 1.5 mL tube.

6. Add 700 µL of n-butanol and vortex the mix thoroughly (*see* **Note 17**).

7. Centrifuge the solution at room temperature at 11,200*g* for 1 min.

8. Remove and discard the upper (n-butanol organic) phase (*see* **Note 18**).

9. Invert a CHROMA SPIN-1000 column several times to completely resuspend the gel matrix. Check for air bubbles in the column matrix. If bubbles are visible, resuspend the matrix in the column buffer by inverting the column again.

10. Remove the top cap from the column, and then remove the bottom cap.

11. Place the column into a 1.5 mL centrifuge tube.
12. Discard any column buffer that immediately collects in the tube and add 1.5 mL of 1X TNE buffer (For 10X TNE buffer: 100m*M* Tris; 2.0*M* NaCl; 10m*M* EDTA; pH 7.4) (Super SMART™ PCR cDNA Synthesis Kit).
13. Let the buffer drain through the column by gravity flow until the surface of the gel beads in the column matrix can be seen (*see* **Note 19**).
14. Discard the collected buffer and proceed with purification.
15. Carefully and slowly apply the sample to the center of the gel bed's flat surface. Do not allow any sample to flow along the inner wall of the column.
16. Apply 25 µL of 1X TNE buffer and allow the buffer to completely drain out of the column.
17. Apply 150 µL of 1X TNE buffer and allow the buffer to completely drain out of the column.
18. Transfer column to a clean 1.5 mL microcentrifuge tube.
19. Apply 320 µL of 1X TNE buffer and collect the eluate as the purified ds cDNA fraction. Transfer 10 µL of this fraction to a clean microcentrifuge tube and label this tube "Sample B". Store at –20°C. Use this aliquot for agarose/EtBr gel analysis.
20. Apply 75 µL of 1X TNE buffer and collect the eluate in a clean microcentrifuge tube. Label this tube "Sample C" and store at –20°C. Save this fraction until after agarose/EtBr gel analysis.

21. To confirm that the PCR product is present in the purified ds cDNA fraction, perform the agarose/EtBr gel analysis (*see* **Note 20**).

b. RSA I Digestion

This step generates shorter, blunt-ended ds cDNA fragments, which are necessary for both adaptor ligation and subtraction.

1. Before proceeding with RsaI digestion, set aside another 10 µL of purified ds cDNA for agarose/EtBr gel analysis to estimate the size range of the ds cDNA products Label this tube "Sample D".
2. Add the following reagents (provided in the Super SMART™ PCR cDNA Synthesis Kit) to the purified cDNA fraction collected from the CHROMA-SPIN column:

a. 36 µL 10X RsaI restriction buffer

b. 1.5 µL RsaI (10 U)

3. Mix by vortexing and spin briefly in a microcentrifuge.
4. Incubate at 37°C for 3 h.
5. To confirm that RsaI digestion was successful, electrophorese 10 µL of uncut ds cDNA (Sample D) and 10 µL of RsaI-digested cDNA on a 1.2% agarose/EtBr gel in 1X TAE buffer (*see* **Note 21** and **Figure 16** (p 116)).
6. Add 8 µL of 0.5 *M* EDTA to terminate the reaction.
7. Transfer 10 µL of the digested cDNA to a clean microcentrifuge tube, label this tube "Sample E", and store at –20°C. Compare this sample to the PCR product after final purification.

Purification of Digested cDNA (Clontech NucleoTrap Nucleic Acid Purification Kit and Accessories, provided in the Super SMART™ PCR cDNA Synthesis Kit):

1. Aliquot the RsaI-digested ds cDNA into two clean 1.5 mL microcentrifuge tubes (approximately 170 µL in each tube).
2. Vortex the NucleoTrap Suspension (NucleoTrap Nucleic Acid Purification Kit) thoroughly until the beads are completely resuspended.
3. Add 680 µL of Buffer NT2 and 17 µL of NucleoTrap Suspension to each tube of digestion mixture.
4. Incubate the sample at room temperature for 10 min. Mix gently every 2–3 min during the incubation period.
5. Centrifuge the sample at 10,000*g* for 1 min at room temperature. Discard the supernatant.
6. Add 680 µL of Buffer NT2 (NucleoTrap Nucleic Acid Purification Kit) to the pellet. Mix gently to resuspend. Centrifuge at 10,000*g* for 1 min at room temperature. Remove the supernatant completely and discard.
7. Add 680 µL of Buffer NT3 (NucleoTrap Nucleic Acid Purification Kit) to the pellet. Mix gently to resuspend. Centrifuge the sample at 10,000*g* for 1 min at room temperature. Remove the supernatant completely and discard.
8. Repeat the last step.
9. Centrifuge the pellet again at 10,000*g* for 1 min at room temperature. Air dry the pellet for 15 min at room temperature. Add 50 µL of TE buffer (10 m*M* Tris-Cl, pH 7.5; 1 m*M* EDTA) (NucleoTrap Nucleic Acid Purification Kit) to the

pellet. Resuspend the pellet by mixing gently. Combine the resuspended pellets into one tube. Mix gently.

10. Elute the cDNA by incubating the sample at 50°C for 5 min. Gently mix the suspension 2–3 times during the incubation step.
11. Centrifuge the sample at 10,000*g* for 30 sec at room temperature. Transfer the supernatant containing the pure cDNA to a clean 1.5 m that has been inserted into a 1.5 mL tube. Centrifuge for 5 min and discard the column.
12. Transfer 6 µL of the filtered cDNA solution to a clean 1.5 mL microcentrifuge tube containing 14 µL of deionized H_2O. Label this tube “Sample F” and store at –20°C. Use this sample to analyze the SMART cDNA after purification.
13. To precipitate the cDNA, add 50 µL of 4 *M* ammonium acetate and 375 µL of 95% ethanol to the remaining sample.
14. Vortex the mix thoroughly and centrifuge the tubes at 11,200*g* for 20 min at room temperature. Carefully remove and discard the supernatant.
15. Overlay the pellet with 500 µL of 80% ethanol. Centrifuge the tube at 11,200*g* for 10 min. Carefully remove the supernatant and discard.
16. Air dry the pellet for 5–10 min.
17. Dissolve the pellet in 6.7 µL of 1X TNE buffer.
18. Transfer 1.2 µL to a clean 1.5 mL microcentrifuge tube containing 11 µL of deionized H_2O, label this tube "Sample G," and store the remaining sample at –20°C.

19. Use 10 µL of the diluted cDNA to assess the yield of DNA by UV spectrophotometry (*see* **Note 22**). If DNA concentration is >300 ng/µL, dilute cDNA to a final concentration of 300 ng/µL in 1X TNE buffer, and follow the adaptor ligation step in accordance with the PCR-Select cDNA subtraction protocol.

c. Conventional cDNA synthesis and RSA I digestion

i. First-Strand cDNA Synthesis.

Perform this procedure with each experimental tester and driver poly A+ RNA, and with the Control Poly A+ RNA (from human skeletal muscle) provided with the PCR-Select™ cDNA Subtraction Kit. The skeletal muscle cDNA made in this section serves as control driver cDNA in later steps.

1. For each tester, driver, and the Control Poly A+ RNA (from human skeletal muscle), combine in a sterile 0.5-mL microcentrifuge tube: 2–4 µL poly A+ RNA (2 µg) (*see* **Note 23**), 1 µL cDNA Synthesis Primer (10 µ*M*) (PCR-Select™ cDNA Subtraction Kit). Add sterile H_2O to a final volume of 5 µL if needed. Mix and spin briefly in a microcentrifuge.
2. Incubate at 70°C for 2 min in a thermal cycler.
3. Cool on ice for 2 min and briefly centrifuge.
4. Add to each reaction (final volume 10 µL): 2 µL 5X First-Strand Buffer (PCR-Select™ cDNA Subtraction Kit), 1 µL dNTP Mix (10 m*M* each) (PCR-Select™ cDNA Subtraction Kit), 1 µL sterile H_2O, 1 µL AMV Reverse Transcriptase (20 units/µL) (PCR-Select™ cDNA Subtraction Kit).

5. Gently vortex and centrifuge the tubes for 5 sec
6. Incubate the tubes at 42°C for 1.5 h in an air incubator. Do not use a water bath or thermal cycler. Evaporation can reduce the reaction mixture volume, and therefore, reaction efficiency.
7. Place on ice to terminate first-strand cDNA synthesis.

ii. Second-Strand cDNA Synthesis

Perform the following procedure with each first-strand tester, driver, and the control skeletal muscle cDNA:

1. Add to the first-strand synthesis reaction tubes (final volume 80 µL): 48.4 µL sterile H_2O, 16.0 µL 5X Second-Strand Buffer (PCR-Select™ cDNA Subtraction Kit), 1.6 µL dNTP Mix (10 m*M*) (PCR-Select™ cDNA Subtraction Kit), 4.0 µL 20X Second-Strand Enzyme Cocktail (PCR-Select™ cDNA Subtraction Kit).
2. Mix contents and spin for 5 sec.
3. Incubate at 16°C for 2 h in water bath or thermal cycler.
4. Add 2 µL (6 U) of T4 DNA Polymerase (PCR-Select™ cDNA Subtraction Kit). Mix contents well.
5. Incubate at 16°C for 30 min in a water bath or thermal cycler.
6. Add 4 µL of 20X EDTA/glycogen Mix (PCR-Select™ cDNA Subtraction Kit) to terminate second-strand synthesis.
7. Add 100 µL of phenol: chloroform: isoamyl alcohol (25:24:1).
8. Vortex thoroughly, and centrifuge at 11,200*g* for 10 min at room temperature to separate phases.

9. Carefully collect the top aqueous layer and place in a fresh 0.5 mL microcentrifuge tube. Discard the inter- and lower- phases.
10. Add 100 µL of chloroform: isoamyl alcohol (24:1).
11. Vortex thoroughly, and centrifuge at 11,200*g* for 10 min at room temperature to separate phases.
12. Carefully collect the top aqueous layer and place in a fresh 0.5 mL microcentrifuge tube. Discard the inter- and lower- phases.
13. Add 40 µL of 4 *M* NH_4OAc and 300 µL of 95% ethanol.
14. Vortex thoroughly and centrifuge at 11,200*g* for 20 min at room temperature.
15. Carefully collect the supernatant.
16. Overlay the pellet with 500 µL of 80% ethanol. Centrifuge at 11,200*g* for 10 min.
17. Remove the supernatant.
18. Air dry the pellet for about 10 min to evaporate residual ethanol.
19. Dissolve precipitate in 50 µL of sterile H_2O.
20. Transfer 6 µL to a fresh microcentrifuge tube. Store this sample at –20°C until after Rsa I digestion (for agarose gel electrophoresis) to estimate yield and size range of ds cDNA products synthesized.

iii. RSA I Digestion

Perform the following procedure with each experimental ds tester and driver cDNA, as well as with the control skeletal muscle cDNA.

1. Add per reaction (final volume 94 µL): 43.5 µL ds cDNA, 5.0 µL 10X Rsa I Restriction Buffer, 1.5 µL Rsa I (10 U/µL).
2. Mix by vortexing and centrifuge for 5 s.
3. Incubate at 37°C for 1.5 h.
4. Set aside 5 µL of the digest mixture to analyze the efficiency of Rsa I digestion.
5. Add 2.5 µL of 20X EDTA/glycogen.
6. Mix to terminate the reaction.
7. Add 50 µL of phenol: chloroform: isoamyl alcohol (25:24:1).
8. Vortex thoroughly and centrifuge at 11,200*g* for 10 min at room temperature to separate phases.
9. Carefully collect the top aqueous layer and place in a fresh 0.5 mL tube.
10. Add 50 µL of chloroform: isoamyl alcohol (24:1).
11. Vortex thoroughly and centrifuge at 11,200*g* for 10 min at room temperature to separate phases.
12. Carefully collect the top aqueous layer and place in a fresh 0.5 mL tube.
13. Add 25 µL of 4 *M* NH4OAc and 187.5 µL of 95% ethanol.
14. Vortex thoroughly and centrifuge at 11,200*g* for 10 min at room temperature to separate phases.
15. Remove the supernatant.
16. Gently overlay the pellet with 200 µL of 80% ethanol.
17. Centrifuge at 11,200*g* for 5 min.

18. Carefully remove the supernatant.

19. Air dry the pellet for 5–10 min.

20. Dissolve the pellet in 5.5 µL of H_2O and store at –20°C (*see* **Note 38**).

21. Check Rsa I-digested cDNA using agarose/EtBr gel electrophoresis (*see* **Note 21**).

d. Adaptor ligation

Subtractions should be performed in both directions for each tester/driver cDNA pair (forward and reverse subtraction) (**Figure 17** (p 117)), in preparation of the differential screening step. To perform subtractions in both directions, tester cDNA corresponding to each of the poly A+ RNA samples are required. A control subtraction is also performed with the control skeletal muscle cDNA with φX174/Hae III DNA. As illustrated in **Figure 18** (p 118), three separate adaptor ligations must be performed for each experimental tester cDNA and the control skeletal muscle tester cDNA. Each cDNA (cDNA 1, cDNA 2 and cDNA 3 from the control) is aliquoted into two separate tubes: one aliquot is ligated with Adaptor 1 (Tester 1-1, 2-1, and 3-1), and the second is ligated with Adaptor 2R (Tester 1-2, 2-2, and 3-2). After the ligation reactions are set up, portions of each tester tube are combined so that the cDNA is ligated with both adaptors (unsubtracted tester control 1-c, 2-c, and 3-c). Each unsubtracted tester control cDNA serves as a positive control for ligation, and later serves as a negative control for subtraction.

1. Dilute 1 µL of each Rsa I-digested experimental cDNA (from conventional cDNA synthesis (*see* **Subheading** 3.3.3.3) and from the SuperSMART cDNA synthesis (*see* **Subheading** 3.3.2) with 5 µL of sterile H_2O.
2. Prepare the control skeletal muscle tester cDNA: dilute the φX174/Hae III Control DNA with sterile H_2O to a final concentration of 150 ng/mL, mix 1 µL of control skeletal muscle cDNA (PCR-Select™ cDNA Subtraction Kit) with 5µL of the diluted φX174/Hae III Control DNA (*see* **Note 25**).
3. Prepare the human placenta cDNA from the Super SMART™ PCR cDNA Synthesis Kit procedure by mixing it with φX174/Hae III Control DNA as for the control skeletal muscle tester cDNA (*see* **Note 26**).
4. Prepare a ligation Master Mix by combining in a 0.5 mL microcentrifuge tube: 3 µL sterile H_2O, 2 µL 5X Ligation Buffer (PCR-Select™ cDNA Subtraction Kit), 1 µL T4 DNA Ligase (400 U/µL) (PCR-Select™ cDNA Subtraction Kit) (*see* **Note 27**).
5. For each experimental tester cDNA and for the control skeletal muscle tester cDNA, combine the reagents in (**Table 4** (p 105)) in the order shown in 0.5 mL microcentrifuge tubes. Pipet mixture up and down to mix thoroughly.
6. In a fresh microcentrifuge tube, mix 2 µL of Tester 1-1 and 2 µL of Tester 1-2 (PCR-Select™ cDNA Subtraction Kit). After ligation is complete, this will be the unsubtracted tester control 1-c. Do the same for each additional experimental tester cDNA and the control skeletal muscle tester cDNA. After

ligation, approximately 1/3 of the cDNA molecules in each unsubtracted tester control tube will bear two different adaptors.

7. Centrifuge briefly, and incubate at 16°C overnight.
8. Add 1 µL of EDTA/glycogen (PCR-Select™ cDNA Subtraction Kit). Mix to stop ligation reaction.
9. Heat samples at 72°C for 5 min to inactivate the ligase.
10. Centrifuge the tubes for 5 sec.
11. Remove 1 µL from each unsubtracted tester control (1-c, 2-c, 3-c) and dilute into 1 mL of H_2O.
12. Store samples at –20°C.

i. Ligation Efficiency Analysis

The following PCR experiment allows verification that at least 25% of the cDNAs have adaptors on both ends. This experiment is designed to amplify fragments that span the adaptor/cDNA junctions of Testers 1-1 and 1-2, of second experimental tester cDNA (Tester 2-1 and 2-2) from the reverse subtraction, on the adaptor-ligated control skeletal muscle cDNA (Tester 3-1 and 3-2) and adaptor-ligated control human placenta cDNA (Tester 4-1 and 4-2).

1. Dilute 1 µL of each ligated cDNA (e.g., the Testers 1-1 and 1-2) into 200 µL of H_2O.
2. Combine the reagents in **Table 5** (p 105) in four separate tubes for each experimental cDNA samples and controls.

Prepare a Master Mix for all of the reaction tubes. For each reaction planned, combine the reagents in

3. **Table 6** (p 106) in the order shown.
4. Mix well by vortexing and centrifuging the tubes for 5 sec.
5. Aliquot 22 µL of Master Mix into each of the reactions.
6. Mix well by vortexing and centrifuging the tubes for 5 sec.
7. Overlay with 50 µL of mineral oil.
8. Incubate the reaction mix at 75°C for 5 min in a thermal cycler to extend the adaptors thus creating binding sites for the PCR primers. Do not remove the samples from the thermal cycler.
9. Immediately commence thermal cycling :

Thermal Cycler 480	PCR Systems 2400 or 9600
20 cycles:	94°C, 30 sec
94°C, 30 sec	**20 cycles:**
65°C, 30 sec	94°C, 10 sec
68°C, 2.5 min	65°C, 30 sec
	68°C, 2.5 min

10. Analyze 5 µL from each reaction on a 2.0% agarose/EtBr gel run in 1X TAE buffer (*see* **Note 28** and **Figure 19** (p 119)).

e. First Hybridization

1. Allow the 4X Hybridization buffer (PCR-Select™ cDNA Subtraction Kit) to warm up to room temperature for at least 15–20 min. Verify that there is no

visible pellet or precipitate before using the buffer. If necessary, heat the buffer at 37°C for ~10 min to dissolve any precipitate.

2. For each of the experimental and skeletal muscle subtractions, combine the reagents in **Table 7** (p 106) in 0.5 mL tubes in the order shown.
3. Overlay samples with one drop of mineral oil and centrifuge briefly.
4. Incubate samples at 98°C for 1.5 min in a thermal cycler.
5. Incubate samples at 68°C for 8 h. Samples may hybridize for 6–12 h. Do not let the incubation exceed 12 h.

f. Second Hybridization

Do not remove the hybridization samples from the thermal cycler for longer than is necessary to add fresh driver.

1. Add into a sterile tube for each experimental tester cDNA and for the control skeletal muscle cDNA (final volume 4 µL): 1 µL Driver cDNA, 1 µL 4X Hybridization Buffer (PCR-Select™ cDNA Subtraction Kit), 2 µL sterile H_2O.
2. Place 1 µL of this mixture in a 0.5 mL microcentrifuge tube and overlay it with 1 drop of mineral oil.
3. Incubate at 98 °C for 1.5 min in a thermal cycler.
4. Remove the tube of freshly denatured driver from the thermal cycler.
5. Use the following procedure to simultaneously mix the driver with hybridization samples 1 and 2 (**Table 7** (p 106)). This ensures that the two hybridization samples mix together only in the presence of freshly denatured driver:

a. Set a micropipettor at 15 µL.
b. Gently touch the pipette tip to the mineral oil/sample interface of the tube containing hybridization sample 2.
c. Carefully draw the entire sample partially into the pipette tip. Do not be concerned if a small amount of mineral oil is transferred with the sample.
d. Remove the pipette tip from the tube, and draw a small amount of air into the tip, creating a slight air space below the droplet of sample.
e. Gently touch the pipette tip to the mineral oil/sample interface of the tube containing the freshly denatured driver sample.
f. Carefully draw the entire sample partially into the pipette tip. Do not be concerned if a small amount of mineral oil is transferred with the sample. The pipette tip should now contain both samples (hybridization sample 2 and denatured driver) separated by a small air pocket.
g. Transfer the entire mixture to the tube containing hybridization sample 1.
h. Mix by pipetting up and down.
i. Incubate reaction at 68°C overnight.
j. Add 200 µL of dilution buffer (PCR-Select™ cDNA Subtraction Kit) and mix by pipetting.
k. Heat at 68°C for 7 min in a thermal cycler.
l. Store at –20°C.

g. PCR Amplification

Seven PCR reactions are recommended as described in **Figure 18** (p 118):

1. Forward-subtracted experimental cDNA.
2. Unsubtracted tester control (1-c),
3. Reverse-subtracted experimental cDNA,
4. Unsubtracted tester control for the reverse subtraction (2-c),
5. Subtracted control skeletal muscle cDNA,
6. Unsubtracted tester control for the control subtraction (3-c),
7. PCR control-subtracted cDNA. The PCR control subtracted cDNA provides a positive PCR control and contains a successfully subtracted mixture of Hae III-digested φX174 DNA.

i. Primary Amplification

Prepare the PCR templates:

1. Aliquot 1 µL of each diluted cDNA from subtracted experimental sample and the corresponding diluted unsubtracted sample into an appropriately labeled tube.
2. Aliquot 1 µL of the PCR control subtracted cDNA into an appropriately labeled tube.
3. Prepare a Master Mix for all of the primary PCR tubes. Combine in order (total volume 24 µL): 19.5 µL Sterile H_2O, 2.5 µL 10X PCR reaction buffer (PCR-Select™ cDNA Subtraction Kit), 0.5 µL dNTP Mix (10 m*M*) (PCR-Select™ cDNA Subtraction Kit), 1.0 µL PCR Primer 1 (10 µ*M*) (PCR-Select™ cDNA Subtraction Kit), 0.5 µL 50X Advantage cDNA Polymerase Mix.
4. Mix well by vortexing, and centrifuge the tube for 5 sec.

5. Aliquot 24 µL of Master Mix into each of the reaction tubes containing 1 µL of the diluted cDNA.
6. Overlay with 50 µL of mineral oil.
7. Incubate the reaction mix at 75°C for 5 min in a thermal cycler to extend the adaptors thus creating binding sites for the PCR primers.
8. Immediately commence thermal cycling:

Thermal Cycler 480	PCR Systems 2400 or 9600
27 cycles:	94°C, 25 sec
94°C, 30 sec	**27 cycles** :
66°C, 30 sec	94°C, 10 sec
72°C, 1.5 min	66°C, 30 sec
	72°C, 1.5 min

9. Set 8 µL aliquots aside from each tube for electrophoresis gel of PCR amplification.

ii. Secondary Amplification (Nested PCR)

1. Dilute 3 µL of each primary PCR mixture in 27 µL of H_2O.
2. Aliquot 1 µL of each diluted primary PCR product mixture into an appropriately labeled tube.
3. Prepare Master Mix for the secondary PCR reactions by combining in order (total volume 24 µL): 18.5 µL sterile H_2O, 2.5 µL 10X PCR reaction buffer (PCR-Select™ cDNA Subtraction Kit), 1.0 µL Nested PCR primer 1 (10 µ*M*) (PCR-Select™ cDNA Subtraction Kit), 1.0 µL Nested PCR primer 2R (10 µ*M*)

(PCR-Select™ cDNA Subtraction Kit), 0.5 µL dNTP Mix (10 m*M*) (PCR-Select™ cDNA Subtraction Kit), 0.5 µL 50X Advantage cDNA Polymerase Mix.

4. Mix well by vortexing, and centrifuge the tube for 5 sec.

5. Aliquot 24 µL of Master Mix into the tubes containing the diluted primary PCR product.

6. Overlay with 1 drop of mineral oil.

7. Immediately commence thermal cycling:

Thermal Cycler 480	PCR Systems 2400 or 9600
10 - 12 cycles:	**10 – 12 cycles**:
94°C, 30 sec	94°C, 10 sec
68°C, 30 sec	68°C, 30 sec
72°C, 1.5 min	72°C, 1.5 min

8. Analyze 8 µL from each reaction on a 2.0% agarose/EtBr gel run in 1X TAE buffer (*see* **Note 29** and **Figure 20** (p 120), **Figure 21** (p 121)).

9. Store reaction products at –20°C.

h. PCR Analysis of Subtraction Efficiency

Amplification by PCR can be used to estimate the efficiency of subtraction by comparing the abundance of known cDNAs before and after subtraction. Ideally this is done with both a non-differentially expressed gene (e.g. housekeeping gene), and with a gene known to be differentially expressed between the two RNA sources being compared. The test described below uses the G3PDH primers provided with the PCR-Select™ cDNA Subtraction Kit, and cyclophilin primers to confirm the

reduced relative abundance of G3PDH and cyclophilin following the PCR-Select procedure (*see* **Note 30** and **Figure 17** (p 119), **Figure 18** (p 118)).

1. Dilute the subtracted and unsubtracted (unsubtracted tester control 1-c and 2-c) secondary PCR products 10X in H_2O. The concentration of subtracted and unsubtracted product should be roughly equal.
2. Combine in 0.5 mL microcentrifuge tubes in order:
    a. For the skeletal muscle cDNA control (total volume 30 µL): 1 µL diluted subtracted cDNA or diluted unsubtracted tester control 1-c, 1.2 µL Cyclophiline 3' Primer (10 µ*M*), 1.2 µL Cyclophiline 5' Primer (10 µ*M*), 3.0 µL 10X PCR reaction buffer (PCR-Select™ cDNA Subtraction Kit), 22.4 µL sterile H_2O, 0.6 µL dNTP Mix (10 m*M*) (PCR-Select™ cDNA Subtraction Kit), 0.6 µL 50X Advantage cDNA Polymerase Mix.
    b. For the experimental cDNA samples (total volume 30 µL): 1 µL diluted subtracted cDNA or diluted unsubtracted tester control 1-c, 1.2 µl G3PDH 3' Primer (10 µ*M*), 1.2 µL G3PDH 5' Primer (10 µ*M*) (PCR-Select™ cDNA Subtraction Kit), 3.0 µL 10X PCR reaction buffer, 22.4 µL sterile H_2O, 0.6 µL dNTP Mix (10 m*M*), 0.6 µL 50X Advantage cDNA Polymerase Mix.
3. Mix by vortexing and briefly centrifuging.
4. Overlay with one drop of mineral oil.
5. Use the following thermal cycling program. 18 cycles: 94°C 30 sec, 60°C 30 sec, 68°C 2 min.

6. Remove 5 µL from each reaction and place it in a clean tube. Put the rest of the reaction back into the thermal cycler for 5 additional cycles.
7. Repeat the last step twice (i.e., remove 5 µL after 28 and 33 cycles).
8. Examine the 5 µL samples (i.e., the aliquots that were removed from each reaction after 18, 23, 28, and 33 cycles) on a 2.0% agarose/EtBr gel (*see* **Note 31** and **Figure 21** (p 121)).

4. Differential Screening

The PCR-Select Differential Screening Kit allows you to screen the PCR-Select subtracted library for differentially expressed cDNAs and to eliminate nondifferentially expressed transcripts. The procedure involves a first step of cloning cDNAs sequences into a cloning vector to isolate from each others and amplifiy subtracted cDNA fragments. Clones from the subtracted library are then arrayed on nylon membranes and hybridized with four different probes (**Figure 23** (p 123)): a probe made from the subtracted cDNA, another probe made from reverse-subtracted cDNA, and nonsubtracted probes synthesized directly from tester and driver cDNAs. Clones hybridizing to tester, but not to driver are differentially expressed; however, nonsubtracted probes are not sensitive enough to detect rare messages. Subtracted probes are greatly enriched for rare differentially expressed sequences and can detect rare transcripts, but they may give false positive results. Thus, using subtracted and nonsubtracted probes together provides the most effective way to identify potentially differentially expressed genes.

a. Secondary PCR of Subtracted cDNA

1. Label sterile 0.5 mL reaction tubes for PCR. Prepare two secondary PCR tubes for each subtracted and/or unsubtracted probe.
2. Prepare a PCR Master Mix in a 1.5 mL microcentrifuge tube. Combine in order (total volume 24 µL): 18.5 µL sterile H_2O, 2.5 µL 10X PCR reaction buffer (PCR-Select Differential Screening kit), 1.0 µL Nested PCR primer 1 (10 µ*M*) (PCR-Select Differential Screening kit), 1.0 µL Nested PCR primer 2R (10 µ*M*) (PCR-Select Differential Screening kit), 0.5 µL dNTP Mix (10 m*M*) (PCR-Select Differential Screening kit), 0.5 µL 50X Advantage cDNA Polymerase Mix.
3. Mix well by vortexing. Spin the tube for 5 sec in a microcentrifuge to collect contents at the bottom.
4. Aliquot 24 µL of Master Mix into each reaction tube labeled.
5. Into each tube, aliquot 1 µL of the appropriate template:
   a. For the forward- and reverse-subtracted probes, use the diluted products of *primary* PCR amplification from the PCR-Select cDNA subtraction.
   b. To amplify tester and driver cDNA to make unsubtracted probes: For the tester probe, use the primary PCR product of the unsubtracted tester control from the forward subtraction as the template. For the driver probe, use the primary PCR product of the unsubtracted tester control from the reverse subtraction as the template.
6. Immediately commence thermal cycling:

Thermal Cycler 480	PCR Systems 2400 or 9600
10 - 12 cycles:	**10 – 12 cycles:**
94°C, 30 sec	94°C, 10 sec
68°C, 30 sec	68°C, 30 sec
72°C, 1.5 min	72°C, 1.5 min
One additional cycle:	**One additional cycle:**
72°C, 5 min	72°C, 5 min

7. Electrophorese 8 µL from each reaction on a 2.0% agarose/EtBr gel in 1X TAE buffer (*see* **Note 29**).

8. Store reactions at –20°C. See part 3.4.4 for next step.

b. Subtracted cDNA Library Construction

i. T/A Cloning

The TA Cloning Kit Dual Promoter with pCRII provides a quick, one-step cloning strategy for the direct insertion of a PCR product into a plasmid vector. Taq polymerase has a nontemplate-dependent activity that adds a single deoxyadenosine (A) to the 3´ ends of PCR products. The linearized vector supplied in this kit has single 3´ deoxythymidine (T) residues. This allows PCR inserts to ligate efficiently with the vector.

1. Set up the 10 µL ligation reaction as follows (final volume 10 µL): 3µL fresh secondary PCR product from the forward subtraction (*see* **Note 32**), 1 µL 10X Ligation Buffer (T/A Cloning Kit Dual Promoter), 2 µL pCRII vector (25 ng/µL) (T/A Cloning Kit Dual Promoter), sterile water to a total volume of 9 µL, 1 µL T4 DNA Ligase (4.0 Weiss units) (T/A Cloning Kit Dual Promoter).

2. Incubate the ligation reaction at 14°C for a minimum of 4 h (preferably overnight).
3. Ligation reaction may be stored at -20°C until cell transformation.

ii. Transformation of MAX Efficiency DH5α Competent Cells

The φ80d*lac*ZΔM15 marker of those comptent cells provides α-complementation of the β-galactosidase gene from the pCRII vector and, therefore, can be used for blue/white screening of colonies on bacterial plates containing X-gal.

1. Thaw competent cells on wet ice.
2. Gently mix cells, then aliquot 100 µL of competent cells into chilled polypropylene tubes. Refreeze any unused cells in the dry ice/ethanol bath for 5 min before returning to the -70°C freezer.
3. For DNA from ligation reactions, dilute the reactions 5X TE buffer (10 m*M* Tris-HCl, pH 7.5; 1 m*M* EDTA) (Max Efficiency DH5α Competent Cells). Add 1 µL of the dilution to the cells (1 to 10 ng DNA), moving the pipette through the cells while dispensing. Gently tap tubes to mix.
4. Incubate cells on ice to 30 minutes.
5. Heat-shock cells 45 sec in a 42°C water bath; do not shake.
6. Place on ice for 2 min.
7. Add 0.9 mL room temperature of Super Optimal Catabolite repression medium (S.O.C.) (Max Efficiency DH5α Competent Cells).
8. Shake vigourously at 37°C for 1 h.

9. Dilute the experimental reactions 1/1000, 1/100, 1/10 or no dilutions, and spread 100 to 200 µL of this dilution on Luria Broth medium (LB) with 100 µg/mL ampicillin, and 40 µl of 0.1 *M* Isopropyl-beta-thio-galactoside (IPTG) and 40 µl of 5-bromo-4-chloro-3-indolyl-beta-D-galactopyranoside (X-Gal) 20 mg/ml.
10. Incubate overnight at 37°C.
11. Analyze the presence, the number and the color of the colonies grown on the plate for each different dilution.
12. Spread 100 µL of the optimal dilution per LB plates with 100 µg/mL ampicillin for the remaining experimental reactions.
13. Incubate overnight at 37°.

iii. Complementary DNA Amplification from Vector Inserts

After growth of individual bacterial colonies, the unique presence of the insert is verified by PCR using the nested primer 1 and the nested primer 2R which have binding site on the adaptors localized at the end of subtracted cDNA inserts. The amplified cDNA is then used to be arrayed on nylon membrane.

1. Randomly pick 1000 white bacterial colonies on LB plates.
2. Grow each colony in 100 µL of LB-amp medium 37°C overnight with vigourous shaking.
3. Prepare a Master Mix for the clones to be amplified. Combine in a clean microcentrifuge tube (total volume 19 µL): 2.0 µL 10X PCR reaction buffer, 0.6 µL Nested Primer 1 (PCR-Select Differential Screening kit), 0.6 µL Nested

Primer 2R (PCR-Select Differential Screening kit), 0.4 µL dNTP mix (10 m*M*), 15.2 µL H_2O, 0.2 µL 50X PCR enzyme mix.

4. Mix well by vortexing and spin the tube for 5 sec in a microcentrifuge.
5. Aliquot 19 µL of the Master Mix into each tube.
6. Transfer 1 µL of each bacterial culture to each tube.
7. Begin thermal cycling: 94°C 30 sec and 23 cycles: 95°C 10 sec, 68°C 3 min
8. Electrophorese 5 µL from each reaction on a 2.0% agarose/EtBr gel in 1X TAE buffer. Each PCR product should correspond to the cDNA insert (*see* **Note 33** and **Figure 24** (p 124)).

c. Preparation of cDNA Dot Blots of the PCR Products

1. For each PCR reaction, combine 5 µL of PCR product and 5 µL of 0.6 N NaOH (freshly made or at least freshly diluted from concentrated stock) in a 96-well plate. The NaOH will denature the DNA for hybridization.
2. Mix by briefly spinning the plate.
3. Using a micropipettor, transfer 1–2 µL of each mixture to a nylon membrane. Prepare four identical blots for hybridization with both subtracted and unsubtracted probes. For best results, array each cDNA in duplicate on each membrane.
4. Neutralize the blots for 2–4 min in 0.5 *M* Tris-HCl (pH 7.5) and wash in H_2O.
5. Cross-link the DNA to the membrane using a UV linking device under 120 mJ. Alternatively, bake the blots for 1–2 hours at 70°C in an oven (*see* **Note 34**).

d. Random Primer Labelling of cDNA Probes

i. Purification of Secondary PCR Products

1. Add 34 µL of Buffer NT to each cDNA synthesis reaction (obtained **Section 3.4.1**); mix well by pipetting.
2. Place a NucleoSpin Extract II Column (NucleoSpin Extract II Kit) into a 2 mL collection tube. Pipet the sample into the column. Centrifuge at 11,200*g* for 1 min.
3. Discard the flow-through.
4. Return the column to the collection tube.
5. Add 600 mL of Wash Buffer NT3 (NucleoSpin Extract II Kit) to the column. Centrifuge at 11,200*g* for 1 min.
6. Discard the flow-through.
7. Place the column back into the collection tube. Centrifuge at 11,200*g* for 2 min to remove any residual Wash Buffer NT3.
8. Transfer the NucleoSpin Columns into a fresh 1.5 mL microcentrifuge tube.
9. Add 20 µL of sterile Milli-Q H_2O to the column. Allow the column to stand for 2 min with the caps open.
10. Close the tube and centrifuge at 11,200 *g* for 1 min to elute the sample.

ii. Radiolabelling of cDNA Probes

1. In separate 0.5 mL microcentrifuge tubes, mix 3 µL (20–90 ng) of each of the purified forward- and reverse-subtracted cDNA and 3 µL of each of the unsubtracted tester and driver cDNAs with 6 µL of H_2O.

2. Denature by heating for 8 min at 95°C and then chill on ice.
3. Add to each tube (final volume 20 µL): 3 µL Reaction Buffer (–dCTP), 2 µL Random Primer Mix, 5 µL [α-^{32}P] dCTP (50 µCi, 3000Ci/mmol, aqueous solution), 1 µL Klenow Enzyme (exo-) (PCR-Select Differential Screening kit).
4. Incubate tubes at 37°C for 30 min.
5. Terminate each reaction by adding 5 µL of Stop Solution (PCR-Select Differential Screening kit).
6. Purify probe from unincorporated dNTPs using Illustra microspin columns (GE Health Care)
   a. Resuspend the resin in the column by vortexing. Use columns immediately after preparation to avoid drying out of the resin.
   b. Loosen the cap one-quarter turn and snap off the bottom closure.
   c. Place the column in a collection tube.
   d. Pre-spin the column for 1 min at 735*g.*
   e. Remove the top cap.
   f. Transfer the column to a new clean microcentrifuge tube.
   g. Slowly apply the sample to the centre of the resin bed. The resin will appear compacted and angled. Take care not to disturb the resin bed. Do not allow any of the samples to flow around the sides of the bed.
   h. Spin the column for 2 min at 735*g*. Purified sample is collected in the bottom of the microcentrifuge tube.
   i. Remove the spin column from the microcentrifuge tube and discard.

7. Determine the specific activity of each probe. More than 1 x 10^7 cpm per probe should be obtained.

e. Hybridization with the Subtracted cDNA

i. Membrane Preparation

1. Make hybridization solution for each membrane prepared arrayed with forward subtracted cDNA:
   a. Combine 50 µL of 20X SSC and 50 µL of Blocking Solution.
   b. Mix well.
   c. Boil for 5 min and chill on ice.
   d. Combine with 5 mL of hybridization solution.
2. Place each membrane in a hybridization container and add the hybridization solution.
3. Prehybridize for 40–60 min with continuous agitation at 72°C. Continuous agitation of the membranes in a hybridization incubator with rotating bottles is necessary during all prehybridization, hybridization, and washing steps.

ii. Preparation of the Hybridization Probes

1. Mix 50 µL of 20X SSC, 50 µl of Blocking Solution, and your purified probe (at least 1 x 10^7 cpm per 100 ng of subtracted cDNA). Be sure to add the same number of cpm for each pair of probes.
2. Boil for 5 min and then chill on ice.
3. To each hybridization container, add the probes. Avoid adding the probe directly to the membrane.

4. Hybridize at 72°C overnight with continuous agitation.
5. Warm low-stringency (2X SSC/0.5% SDS) and high-stringency (0.2X SSC/0.5% SDS) washing solutions to 68°C. Keep buffers at 68°C during washing.
6. Wash membranes with low-stringency washing solution (4 x 20 min) at 68°C.
7. Wash membranes with high-stringency washing solution (2 x 20 min) at 68°C.
8. Seal up each membrane in a plastic envelop.
9. Scan the membrane using a Phosphimager-Storm system to detect the radioactive signal and quantify each signal intensity using ImageQuant Software (Applied Biosystem) (**Figure 26** (p 126)).
10. Analyse data and remove false positive clones (**Figure 27** (p 158)).
11. The membranes can be stored at -20°C or be reused: remove the probes by stripping (100°C, 7 min in 0.5% SDS). Blots can typically be probed at least 5 times.

5. Differentially Expressed cDNA Sequences Analysis

a. Sequencing

Bacterial colonies from positive clones must be freshly grown on LB plates before the cDNA insert contained in the vector is extracted and then sent for sequencing. The primer used for the sequencing procedure can either be the nested primer 1 and nested primer 2R which are localised on the cDNA insert itself (on the

adaptors, **Table 2** (p 104), or primers like M13, Sp6 which have hybridization sites on the pCR II vector sequence in the cloning site.

b. Sequences Annotation

i. Comparison of Sequences with Sequences Listed in Genbank Database

The differentially expressed cDNA sequences are annotated by comparison with some sequences already listed in the Genbank database available on the internet network. A classification can be established to describe the proportion of sequences that have a high degree of homology with known and characterized or uncharacterized sequences already listed in the Genbank database, and the proportion of new sequences that have no significant degree of homology with already listed sequences. To characterize the degree of homology, the percentage of identity between two aligned sequences, the length of homologous sequences and the E-value which reflects the probability to find a given alignement among all the possible alignements with all the listed sequences of the Genbank are taken into account.

ii. Gene Ontology

Based on sequences that are homologous to known genes, a second classification of the gene ontology may be drawn up. Multiple sofwares are available on the internet network and provide free gene ontology analysis. This software may also identify signaling pathways involving some of the genes contained in the constructed library. That approach provides a global gene expression analysis.

c. Selection of Candidate Genes

Finally, a “one by one“ analysis of each known genes expected to be of significance based on expression patterns from the literature leads to the selection of candidate genes. Clones highly represented in the library, whether known or unknown sequences may also be selected.

d. Identification of Candidate Genes

Once a list of candidate genes have been selected, validation of the differential expression pattern of those genes must be undertaken. Informative techniques can be applied to define the expression pattern of any single gene. Among the most reliable are real time PCR or semi-quantitative PCR for gene expression quantification, and *in situ* hybridization of mRNA or immunocytochemical localization of protein gene products to establish the spatial gene expression pattern.

D. Notes

1. If embedding samples in paraffin in a few days following the tissue collection, they can be held in PBS 1X at 4 °C, after the three rinses.
2. It is essential to use the correct amount of starting material in order to obtain optimal RNA yield and purity. A maximum amount of 5 mg fresh or frozen tissue can generally be processed. Weighing tissue is the most accurate way to quantitate the amount of starting material. As a guide, a 1.5 mm cube (3.4 mm^3) of most animal tissues weighs 3.5–4.5 mg.

3. To avoid damage to the TissueRuptor and disposable probe during operation, make sure the tip of the probe remains submerged in the buffer. Foaming may occur during homogenization. If this happens, let the homogenate stand at room temperature for 2–3 min until the foam subsides before continuing with the procedure.
4. The volume of 70% ethanol to add may be less if some lysate was lost during homogenization. Precipitates may be visible after addition of ethanol, but this does not affect the procedure.
5. After centrifugation, carefully remove the RNeasy MinElute spin column from the collection tube so that the column does not contact the flow-through.
6. As little as 10 µL RNase-free water can be used for elution if a higher RNA concentration is required, but the yield will be reduced by approximately 20%.
7. The concentration of RNA should be determined by measuring the absorbance at 260 nm ($A260$) in a spectrophotometer. The ratio of the readings at 260 nm and 280 nm ($A260/A280$) provides an estimate of the purity of RNA with respect to contaminants that absorb in the UV, such as protein. Do not use more than 1 mg total RNA.
8. The initial volume of the RNA solution is not important as long as the volume can be brought up to the indicated amount with RNase-free water.
9. Loss of the Oligotex resin can be avoided if approximately 50 µL of the supernatant is left in the microcentrifuge tube. The remaining solution will not

affect the procedure. Save the supernatant until certain that satisfactory binding and elution of poly A+ mRNA has occurred.

10. The volume of Buffer OEB used depends on the expected or desired concentration of poly A+ mRNA. Ensure that Buffer OEB does not cool significantly during handling. With multiple samples, it may be necessary to place the entire microcentrifuge tube (with spin column, Oligotex, and sample) into a 70°C heating block to maintain the temperature while preparing the next samples.
11. To keep the elution volume low, the first eluate may be used for a second elution. Reheat the eluate to 70°C, and elute in the same microcentrifuge tube.
12. The minimum amount of starting material for standard cDNA synthesis is 2 ng of total RNA. However, if the RNA sample is not limiting, it is recommended to begin with 20–1,000 ng of total RNA for cDNA synthesis. Please note that if there is >100 ng of total RNA, dilute first strand cDNA product before proceeding with cDNA amplification.
13. For the control synthesis, add 10 ng of control human placenta total RNA.
14. If necessary, cDNA can be stored at -20°C until ready to proceed with column chromatography.
15. Samples can also be stored at –20°C for up to three months.
16. Choosing the optimal number of PCR cycles ensures that the ds cDNA will remain in the exponential phase of amplification. When the yield of PCR products stops increasing with more cycles, the reaction has reached its plateau.

The optimal number of cycles for an experiment is one cycle fewer than is needed to reach the plateau. **Figure 15** (p 115) shows a typical gel profile of ds cDNA synthesized using the Control Human Placenta Total RNA for SMART cDNA synthesis and amplification. The PCR reached its plateau after 24 cycles for the 5 ng experiment and 21 cycles for the 20 ng experiment; that is, the yield of PCR products stopped increasing. After 24 and 21 cycles, a smear appeared in the high-molecular-weight region of the gel, indicating that the reactions were overcycled. Therefore, the optimal number of cycles would be 23 for the 5 ng experiment and 20 for the 20 ng experiment. Note that the number and position of the bands, and the size of the smear observed will be different for each particular total RNA used.

17. Butanol extraction allows concentration of the PCR product to a volume of 40–70 µL. Addition of too much n-butanol may remove all the water and precipitate the nucleic acid. If this happens, add water to the tube and vortex until an aqueous phase reappears.
18. If volume is less than 40–70 µL, repeat the three last steps: Add 700 µL of n-butanol and vortex the mix thoroughly. Centrifuge the solution at room temperature at 11,200*g* for 1 min, and remove and discard the upper (n-butanol organic) phase. If final volume is < 40 µL after the second butanol concentration step, add H_2O to the aqueous phase to adjust volume to 40–70 µL.

19. The top of the column matrix should be at the 0.75 mL mark on the wall of the column. If the column contains much less matrix, discard it and use another column.
20. To analyze the ds cDNA after column chromatography, electrophorese 3 µL of the unpurified PCR product (Sample A) alongside 10 µL of the PCR product purified by column chromatography (Sample B) and 10 µL of the second fraction (Sample C) on a 1.2% agarose/EtBr gel. Compare the intensities of Sample A and Sample B, and estimate the percentage of PCR product that remains after column chromatography. The yield of cDNA after column chromatography is typically 50%. If the yield is < 30 %, check to see if it is present in the second fraction, Sample C. If this second fraction has a higher yield of cDNA than the first, combine the fractions. Otherwise if the cDNA is not present in Sample C, repeat the PCR and column chromatography steps.
21. Electrophorese 2.5 µL of undigested ds cDNA and 5 µL of Rsa I-digested cDNA on a 1% agarose/EtBr gel in 1X TAE buffer side-by-side. Double strand cDNA appears as a smear from 0.5–10 kb. Bright bands correspond to abundant mRNAs or rRNAs. After Rsa I digestion, the average cDNA size is smaller (0.1–2 kb compared to 0.5–10 kb). Typical results are shown in **Figure 16** (p 116).
22. For each reaction, 1–3 µg of SMART cDNA is obtained after purification. If the yield is lower than this, perform the agarose/EtBr gel analysis: electrophorese 10 µL of RsaI-digested cDNA before purification (Sample E) alongside 10 µL of purified diluted cDNA before ethanol precipitation (Sample F) and 1.8 µL of

purified diluted cDNA after ethanol precipitation (Sample G) on a 1.5% agarose/EtBr gel. Compare the intensities of the samples and estimate what percentage of RsaI-digested PCR product remains after purification and ethanol precipitation. The yield of cDNA after purification using the NucleoTrap PCR Kit and ethanol precipitation is typically 70 percent.

23. For the control synthesis, add 2 µL of the skeletal muscle control poly A+ RNA.
24. These 5.5-µL samples of Rsa I digested cDNA will serve as the experimental driver cDNA and the control skeletal muscle driver cDNA.
25. This is the control skeletal muscle tester cDNA. It contains 0.2% Hae III-digested φX174 DNA; each fragment corresponds to about 0.02% of the total cDNA. After subtraction of the skeletal muscle tester cDNA against the skeletal muscle driver cDNA, the primary bands produced in the final PCR should correspond to these control fragments.
26. For the rest of the PCR-Select protocol, the control human placenta cDNA should be analyzed in parallel with the control skeletal muscle cDNA.
27. The ATP required for ligation is a component of the T4 DNA Ligase mix (3 m*M* initial, 300 µ*M* final).
28. Typical results for the ligation efficiency test are shown in **Figure 19** (p 119). If no products are detected after 20 cycles, perform five additional cycles, and analyze by gel electrophoresis. The PCR product using one gene specific primer (G3PDH 3' Primer) and PCR Primer 1 should be about the same intensity as the PCR product amplified using two gene-specific primers (G3PDH 3' and 5'

Primers). If the band intensity for these PCR products differs by more than four-fold, the ligation was less than 25% complete and will significantly reduce subtraction efficiency. If working with mouse or rat cDNA, the PCR product amplified using the G3PDH 3' Primer and PCR Primer 1 will be ~1.2 kb instead of 0.75 kb for human cDNA.

29. Primary PCR: With the PCR control subtracted cDNA, the major bands appearing after 27 cycles should correspond to the φX174/Hae III fragments. This result should look similar to the performed skeletal muscle subtraction. The experimental primary PCR subtraction products usually appear as a smear from 0.2–2 kb, with or without some distinct bands (**Figure 20** (p 120)). Secondary PCR: The patterns of secondary PCR products from the PCR Control Subtracted cDNA and from the skeletal muscle subtraction should resemble lane 1, 4 and lane 7 in **Figure 21** (p. 121)), and lane 1 in **Figure 22** (p 122). A few additional bands may appear. The experimental subtracted samples usually appear as smears with or without a number of distinct bands (**Figure 20** (p 120)).
30. Not all housekeeping gene transcripts are subtracted evenly. In certain instances a particular housekeeping gene is present at different levels in tester and driver poly A^+ RNA. If the concentration of G3PDH message is even 2-fold higher in the tester sample, G3PDH will not be efficiently subtracted out. If subtraction is performed in both directions and there is unsubtracted tester control for both the subtraction and the reverse subtraction, the PCR analysis of subtraction efficiency will indicate if there is any difference in G3PDH abundance in the two

cDNA samples being compared. Moreover, G3PDH is not efficiently subtracted in skeletal muscle cDNA, which is the positive control of the subtraction. Therefore, we used cyclophiline as a housekeeping genes to validate the subtraction of the skeletal muscle cDNA. However, in the control skeletal muscle subtraction experiment, the agarose gel banding pattern of the φX174/Hae III digest has already indicated whether or not subtraction was successful (**Figure 17** (p 117) and **Figure 18** (p 118)).

31. **Figure 22** (p 122) shows an example of G3PDH and cyclophiline reduction in successfully subtracted mixtures of cDNA from positive control of the subtraction and from uterus with reactivated blastocysts versus uterus with blastocysts in diapause subtraction in the mink. The difference in the number of cycles required for equal amplification of the corresponding PCR product in subtracted and unsubtracted samples indicates the efficiency of the subtraction. For the unsubtracted cDNA, the housekeeping gene product is seen after 18–23 cycles, depending on its abundance in the particular cDNA. With the subtracted samples, a product should be detected at ~5–15 cycles later.

As a positive control for the enrichment of differentially expressed genes, repeat the procedure above using PCR primers for a gene known to be expressed in the tester RNA, but not in the driver RNA. This cDNA should become enriched during subtraction. The difference in the number of cycles required for equal amplification of the corresponding PCR product in subtracted and unsubtracted samples indicates the efficiency of the subtraction. 5 cycles corresponds roughly

to a 20-fold cDNA enrichment. Because of the equalization that occurs during subtraction, the level of enrichment will depend on the initial abundance of each differentially expressed gene, as well as the difference in abundance of each gene in tester and driver. Differentially expressed genes that are present in low abundance in the tester cDNA will be enriched more than differentially expressed genes that are present in high abundance.

32. For optimal ligation efficiencies, using fresh (less than 1 day old) PCR products is recommended. The single 3´ A-overhangs on the PCR products will be degraded over time, reducing ligation efficiency. Take care when handling the pCRII vector as loss of the 3´ T-overhangs will cause a blunt-end self-ligation of the vector and subsequent decrease in ligation efficiency.
33. **Figure 24** (p 124) shows an example of cDNA amplification of insert contained in vectors after MAX Efficiency DH5α Competent Cells transformation. While the amplification generate PCR product to be arrayed on membrane for the differential screening, it also provide an elimination step of false positive clones, i.e, bacteria colonies that may have either lost the vector, either may have been transformed by more than one vector.
34. Both techniques can proceed to insure an efficient cross-link of the cDNA on the membrane. First cross-link the DNA to the membrane using a UV linking device under 120 mJ and then bake the blots for 1–2 h at 70°C in an oven.

35. Yield of larger fragments (> 5-10 kb) can be increased by using prewarmed elution buffer (70°C): For elution, add prewarmed elution buffer and incubate at room temperature for 1 min before collecting.

E. Acknowledgments

The author would like to acknowledge Dr Marie–France Palin, Danièle Beaudry and Vickie Roussel for their invaluable assistance. This work was supported by a Discovery Grant from the Natural Sciences and Engineering Research Council of Canada to B.D. Murphy.

F. References

Chan, J., Y. W. Kan, et al. (1997). "Cloning differentially expressed genes from small amounts of total RNA with the ClontechPCR-Select cDNA Subtraction Kit." Clontechniques **XII**((1)): 25–26.

Diatchenko, L., Y. F. Lau, et al. (1996). "Suppression subtractive hybridization: a method for generating differentially regulated or tissue-specific cDNA probes and libraries." Proc Natl Acad Sci U S A **93**(12): 6025-6030.

Gao, F., W. Lei, et al. (2007). "Differential expression and regulation of prostaglandin transporter and metabolic enzymes in mouse uterus during blastocyst implantation." Fertil Steril **88**(4 Suppl): 1256-1265.

Hamatani, T., M. G. Carter, et al. (2004). "Dynamics of global gene expression changes during mouse preimplantation development." Dev Cell **6**(1): 117-131.

Hansson, A. (1947). "The physiology of reproduction in mink (Mustela vison) with special reference to delayed implantation." Acta Zoologica **28**: 1–136.

Jha, R. K., S. Titus, et al. (2006). "Profiling of E-cadherin, beta-catenin and Ca(2+) in embryo-uterine interactions at implantation." FEBS Lett **580**(24): 5653-5660.

Lee, K. Y. and F. J. DeMayo (2004). "Animal models of implantation." Reproduction **128**(6): 679-695.

Lopes, F. L., J. A. Desmarais, et al. (2004). "Embryonic diapause and its regulation." Reproduction **128**(6): 669-678.

Mead, R. A. (1989). "The physiology and evolution of delayed implantation in carnivores." In Carnivore behavior, ecology, and evolution **1**: 437–464.

Murphy, B. D., P. W. Concannon, et al. (1981). "Prolactin: the hypophyseal factor that terminates embryonic diapause in mink." Biol Reprod **25**(3): 487-491.

Murphy, B. D. and D. A. James (1974). "The effects of light and sympathetic innervation to the head on nidation in mink." J Exp Zool **187**(2): 267-276.

Reese, J., S. K. Das, et al. (2001). "Global gene expression analysis to identify molecular markers of uterine receptivity and embryo implantation." J Biol Chem **276**(47): 44137-44145.

Song, H. and H. Lim (2006). "Evidence for heterodimeric association of leukemia inhibitory factor (LIF) receptor and gp130 in the mouse uterus for LIF signaling during blastocyst implantation." Reproduction **131**(2): 341-349.

Wang, H. and S. K. Dey (2006). "Roadmap to embryo implantation: clues from mouse models." Nat Rev Genet **7**(3): 185-199.

Xiao, L. J., J. X. Yuan, et al. (2006). "Expression and regulation of stanniocalcin 1 and 2 in rat uterus during embryo implantation and decidualization." Reproduction **131**(6): 1137-1149.

Yoshinaga, K. and C. E. Adams (1966). "Delayed implantation in the spayed, progesterone treated adult mouse." J Reprod Fertil **12**(3): 593-595.

G. Figures and tables

Table 1. Buffer amounts for Oligotex mRNA Spin-Column Protocol.

Total RNA (mg)	Add Rnase-free water to: (µL)	Buffer OBB (µL)	Oligotex Suspension (µL)
≤0.25	250	250	15
0.25-0.50	500	500	30
0.50-0.75	500	500	45
0.75-1.00	500	500	55

Table 2. Sequences of the primers and adaptors used in the PCR-Select™ cDNA Subtraction and in the Super SMART™ PCR cDNA Synthesis Kits.

The sequence of the PCR primer 1 (in blue) is complementary to the 5' end sequence of adaptor 1 (in blue) and adaptor 2R (in blue) and, Nested primer 1 (in green) and Nested primer 2 (in orange) are respectively complementary to the 3' end sequence of adaptor 1 (in green) and adaptor 2R (in orange).

Sequence name	Sequences	Length
cDNA synthesis primer	5'-TTTTGTACAAGCTT$_{30}$N$_1$N-3'	45 nt
Adaptor 1	5'-CTAATACGACTCACTATAGGGCTCGAGCGGCCGCCCGGGCAGGT-3' 3'-GGGCCCGTCCA-5'	44 nt
Nested primer 1	5'-TCGAGCGGCCGCCCGGGCAGGT-3'	22 nt
Adaptor 2R	5 '-CTAATACGACTCACTATAGGGCAGCGTGGTCGCGGCCGAGGT-3' 3'-GCCGGCTCCA-5'	42 nt
Nested primer 2	5'-AGCGTGGTCGCGGCCGAGGT-3'	20 nt
PCR primer 1	5'-CTAATACGACTCACTATAGGGC-3'	22 nt
G3PDH 5' primer	5'-ACCACAGTCCATGCCATCAC-3'	20 nt
G3PDH 3' primer	5'-TCCACCACCCTGTTGCTGTA-3'	20 nt
SMART II A	5'-AAGCAGTGGTATCAACGCAGAGTACGCGGG-3'	30 nt
SMART CDS Primer II A	5'-AAGCAGTGGTATCAACGCAGAGTACT$_{(30)}$N-1N-3' (N = A, C, G, or T; N-1 = A, G, or C)	57 nt
5' PCR Primer II A	5'-AAGCAGTGGTATCAACGCAGAGT-3'	23 nt

Table 3. Guidelines for setting-up PCR.

Total RNA (ng)	Volume of ss cDNA (μL)	Volume of H_2O (μL)	Total volume (μL)	Typical optimal Number of PCR cycles
~ 2	80	-	80	24-28
~ 5	80	-	80	21-24
~ 25	80	-	80	17-20
~ 50	40	40	80	17-20
~ 100	25	55	80	17-20
~ 250	10	70	80	17-20
~ 500	5	75	80	17-20
~ 1,000	2.5	77.5	80	17-20

Table 4. Setting up the ligation reactions.

Component	Tester 1-1	Tester 1-2
Diluted tested cDNA	2 μL	2 μL
Adaptor 1 (10 μ*M*)	2 μL	-
Adaptor 2R (10 μ*M*)	-	2 μL
Master Mix	6 μL	6 μL
Final volume	**10 μL**	**10 μL**

Table 5. Setting up the ligation efficiency analysis.

Tube	1	2	3	4
Component(μL)				
Tester 1-1 (ligated to Adaptor 1)	1	1	-	-
Tester 1-2 (ligated to Adaptor 2R	-	-	1	1
G3PDH 3' Primer (10 μ*M*)	1	1	1	1
G3PDH 5' Primer (10 μ*M*)	-	1	-	1
PCR Primer 1 (10 μ*M*)	1	-	1	-
Total volume (μL)	**3**	**3**	**3**	**3**

Table 6. Preparation of the ligation efficiency analysis PCR Master Mix.

Component	Per Reaction
Sterile H_2O	18.5 µL
10 X PCR reaction buffer	2.5 µL
dNTP Mix (10 m*M*)	0.5 µL
50X Advantage cDNA Polymerase Mix	0.5 µL
Total volume	**22.0 µL**

Table 7. Setting up the first hybridization.

Hybridization Samples	**1**	**2**
	Tester 1 - 1	**Tester 1 - 2**
Component		
Rsa I-digested Driver cDNA	1.5 µL	1.5 µL
Adaptor 1-ligated Tester 1-1	1.5 µL	-
Adaptor 2R-ligated Tester 1-2	-	1.5 µL
4X Hybridization Buffer	1.0 µL	1.0 µL
Final volume	4.0 µL	4.0 µL

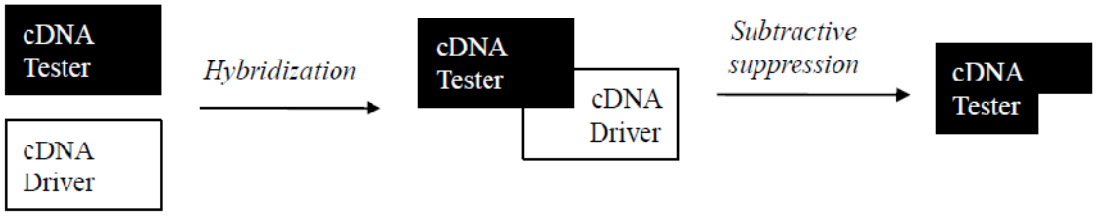

Figure 7. Flowchart summarizing the two major steps of the SSH technique.

First, both mRNA populations are converted into cDNA: Tester and driver cDNAs are hybridized, and the hybrid sequences are then removed. Consequently, the remaining unhybridized cDNAs represent sequences that are expressed in the tester yet absent from the driver mRNA population.

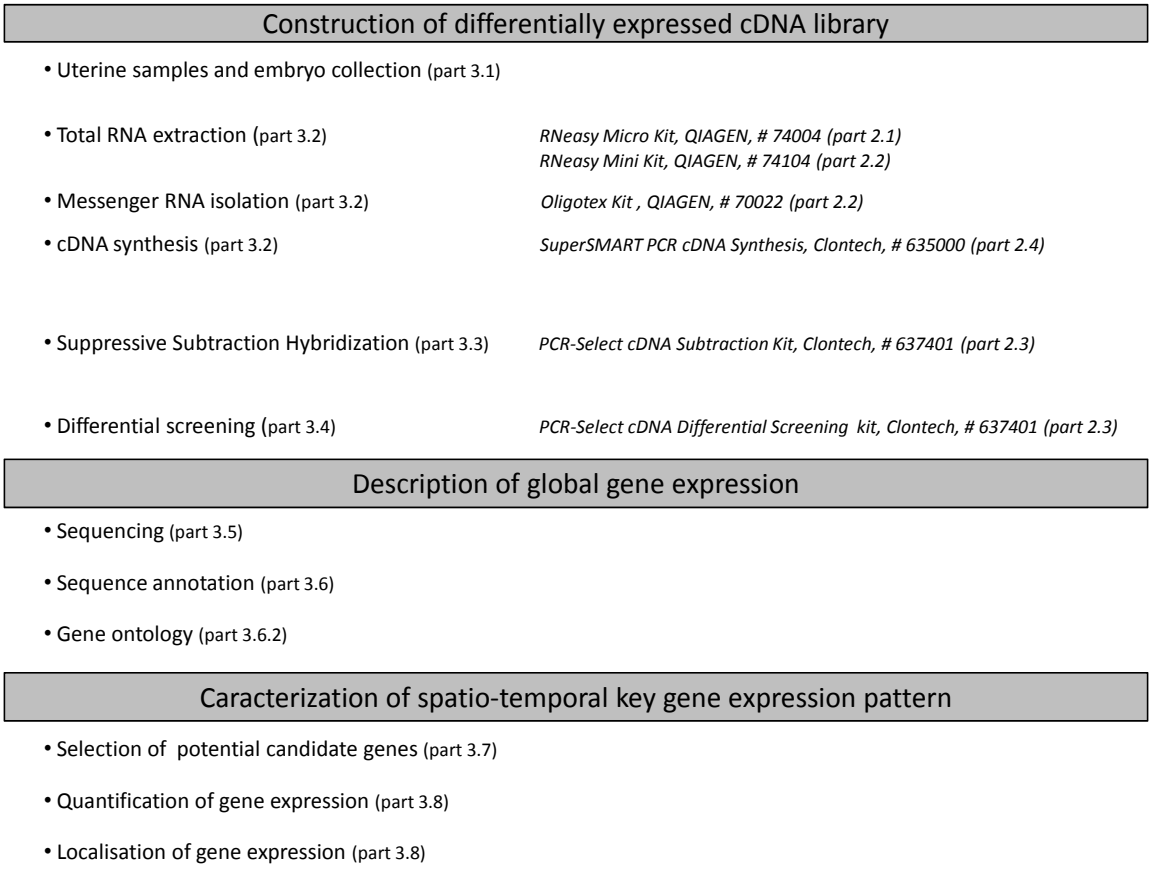

Figure 8. Methodological step to construct an SSH library.

Flowchart summarizing the steps of the methodology of global gene expression analysis and characterization of spatio-temporal key gene expression pattern following the use of the SSH technique to construct a differentially expressed cDNA library. The part number of manuscript refers to each mentioned step, as well as the company and catalog number of the required kits.

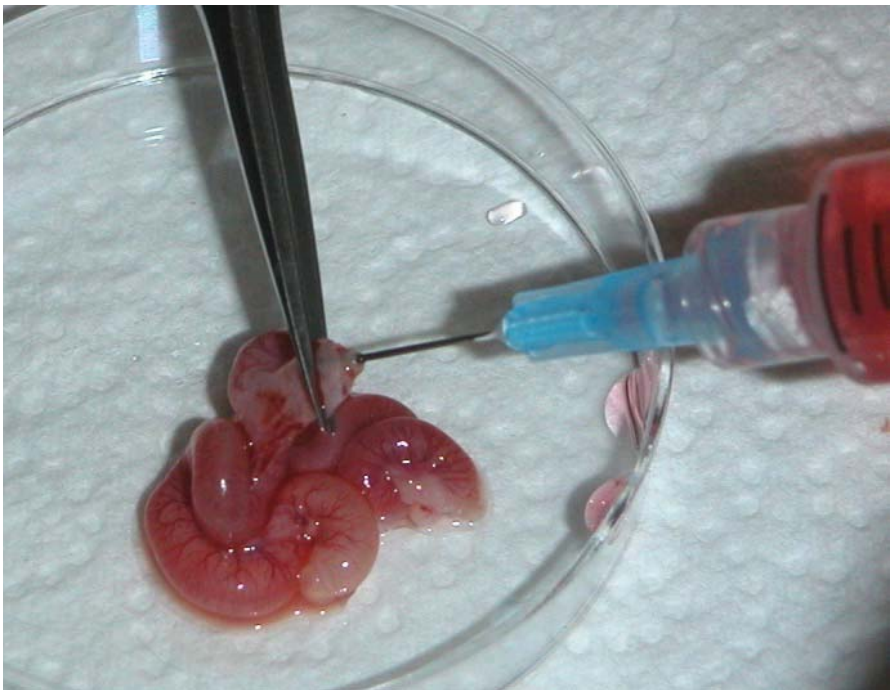

Figure 9. Photography of the procedure for flushing blastocysts from the uterine lumen.

The needle of the syringe is introduced through the cervix into one horn and flushing medium is injected to flush the embryos out the oviductal end of the uterine horn into the cultured dish (Lefèvre, 2006, Unpublished).

Figure 4: RNeasy principle and procedure about RNA isolation

The RNeasy procedure represents a well-established technology for RNA purification. This technology combines the selective binding properties of a silica-based membrane with the speed of microspin technology.
A specialized high-salt buffer system allows RNA longer than 200 bases to bind to the RNeasy silica membrane. Biological samples are first lysed and homogenized in the presence of a highly denaturing guanidine-thiocyanate containing buffer, which immediately inactivates Rnases to ensure purification of intact RNA (see figure on the left). Ethanol is added to provide appropriate binding conditions, and the sample is then applied to an RNeasy spin column, where the total RNA binds to the membrane and contaminants are efficiently washed away. High-quality RNA is then eluted. The table below summerizes specifications of the RNeasy Mini Kit and the RNeasy Micro kit. The latter allows purifying RNA from small amounts of tissue and is suitable for RNA extraction from embryo at blastocyst stage.

Specifications	RNeasy Mini Kit	RNeasy Micro Kit
Maximum binding capacity	100 µg	45 µg RNA
Maximum loading volume	700 µl	700 µl
RNA size distribution	RNA > 200 nucleotides	RNA > 200 nucleotides
Minimum elution volume	30 µl	10 µl

Summerization of specifications of RNeasy Micro column and RNeasy Mini column (Qiagen).

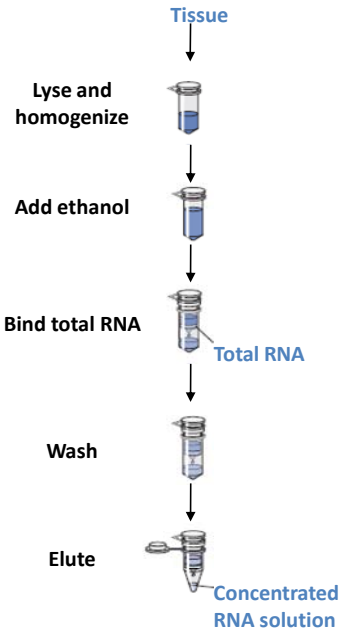

Summerization of total RNA extraction procedure using the RNeasy procedure.

(Adapted from RNeasy Micro Handbook and RNeasy Mini Handbook, Qiagen)

Figure 10. RNeasy principle and procedure for RNA isolation.

Figure 5: The Oligotex principle

Oligotex Suspension consists of polystyrene–latex particles of uniform size and a perfect spherical shape (see photography below). $dC_{10}T_{30}$ oligonucleotides are covalently linked to the surface of the polystyrene–latex particles via a condensation reaction. The particles form a stable suspension that provides a large surface area for rapid and efficient binding of polyadenylic acids. The Oligotex procedure for isolation, purification, and manipulation of poly A+ RNA takes advantage of the fact that most eukaryotic mRNA (and some viral RNAs) end in a poly-A tail of 20–250 adenosine nucleotides. In contrast, rRNAs and tRNAs, which account for over 95% of cellular RNAs, are not polyadenylated. Poly A+ mRNA can be purified by hybridizing the poly-A tail to a dT oligomer coupled to a solid-phase matrix. rRNA and tRNA species, without a poly-A tail, do not bind to the oligo-dT and are easily washed away. Since hybridization requires high-salt conditions, the poly A+ mRNA can then easily be released by lowering the ionic strength and destabilizing the dT:A hybrids (see figure on the left).

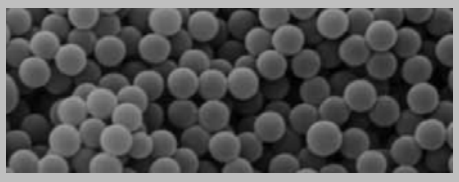

Scanning electron micrograph of Oligotex particules. Magnification 7500x

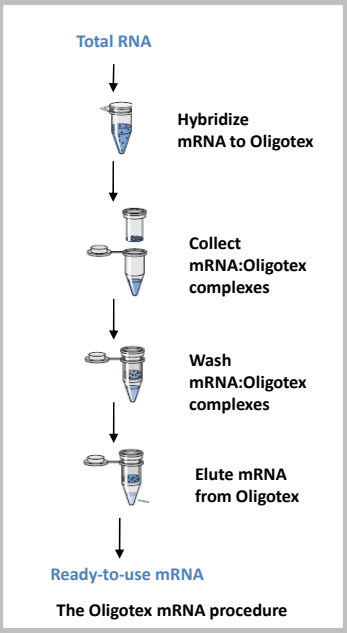

The Oligotex mRNA procedure

(Adapted from Oligotex Handbook, Qiagen)

Figure 11. The Oligotex principle.

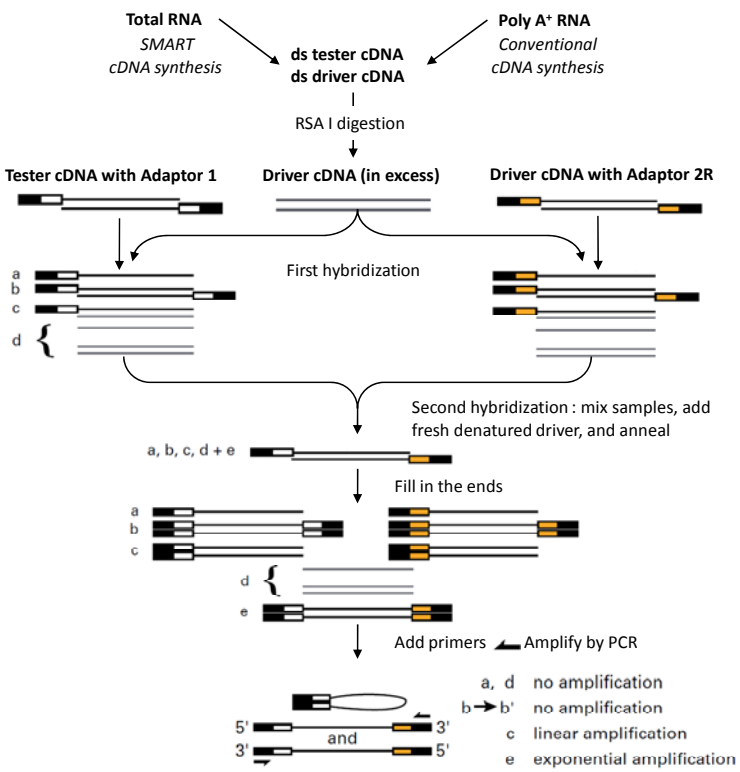

Prepare cDNA by either SMART or conventional synthesis (parts 3.3.1 & 3.3.2).

Separately digest tester and driver ds cDNA to obtain shorter, blunt – ended fragments (parts 3.3.1.5 & 3.3.2.3).

Divide tester cDNA into 2 portions and ligate each to a different adaptor (part 3.3.3)**. Driver cDNA has no adaptors.**

Hybridization kinetics lead to equalization and enrichment of differentially expressed sequences among tester molecules (part 3.3.4).

Generate templates for PCR amplification from differentially expressed sequences (part 3.3.5).

Differentially expressed sequences are amplified exponentially (part 3.3.6).

(Clontechniques, April 2004, Clontech)

Figure 12. The PCR Select cDNA subtraction technique.

Figure 7: SMART cDNA synthesis technology

All commonly used cDNA synthesis methods rely on the ability of reverse transcriptase (RT) to transcribe mRNA into single-stranded (ss) DNA in the first-strand reaction. However, because RT cannot always transcribe the entire mRNA sequence, the 5' ends of genes tend to be underrepresented in cDNA populations. With Clontech's patented SMART cDNA Technology, high yields of full-length and double-stranded cDNA from small amounts of RNA can be generated. SMART stands for **S**witching **M**echanism **A**t 5' end of **R**NA **T**emplate.

The SMART method SMART technology is based on two specific features of Moloney murine leukemia virus reverse transcriptase (MMLV RT):

1. The addition of non-template nucleotides to the 3' end of the newly synthesized cDNA strand, upon reaching the 5' end of the mRNA template (terminal transferase activity).
2. The ability to switch to a second template.

First-strand cDNA synthesis is primed by a modified oligo(dT) primer that contains additional sequence at the 3' end (the 3' SMART CDS Primer II A) (see figure on the left). When the MMLV RT reaches the 5' end of the mRNA, the enzyme's terminal transferase activity attaches several additional nucleotides, primarily deoxycytidine, onto the newly synthesized strand of cDNA.

The SMART Oligonucleotide (patent pending), which has an oligo(G) sequence at its 3' end, base-pairs with the deoxycytidine stretch, creating an extended template. RT then switches templates and continues replicating to the end of the oligonucleotide (17).

The SMART anchor sequence and the poly A sequence serve as universal priming sites for end-to-end cDNA amplification. In contrast, cDNA without these sequences such as prematurely terminated cDNAs, contaminating genomic DNA, or cDNA transcribed from poly A– RNA, will not be exponentially amplified.

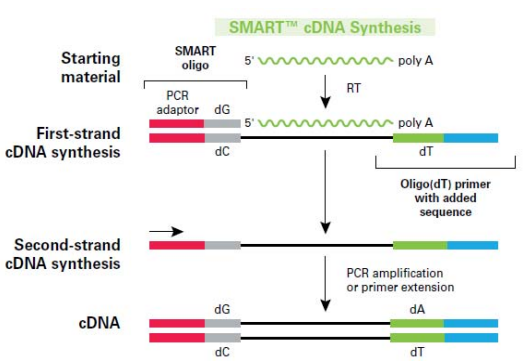

Overview of the SMART cDNA synthesis method.

(Adapted from the SuperSMART PCR cDNA synthesis Kit User Manual and the FL772387_SMARTcDNA Brochure, Clontech)

Figure 13. The SMART cDNA synthesis technology.

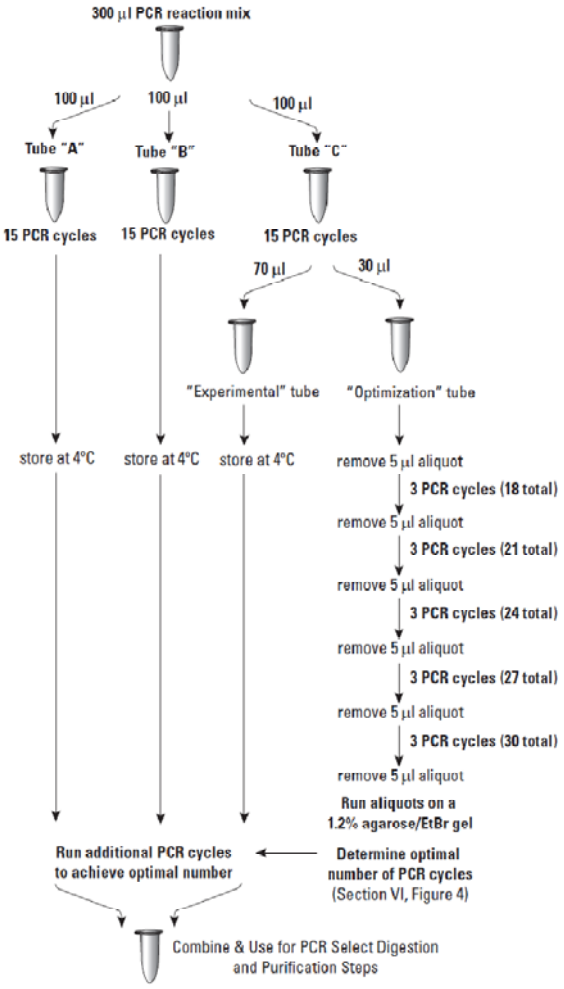

Figure 14. Optimizing PCR parameters for SMART cDNA synthesis.

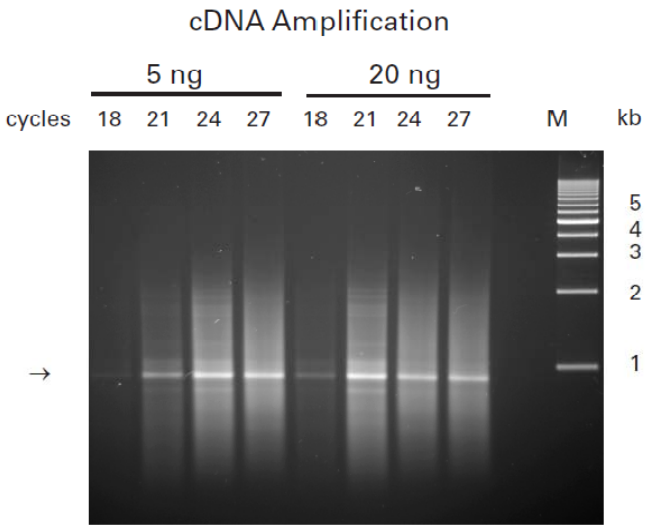

Figure 15. Analysis for optimizing PCR parameters.

Five or 20 ng of the control human placental total RNA was subjected to the first strand cDNA synthesis and purification as described in the protocol. 80 µL was used for PCR amplification. A range of PCR cycles were performed (18, 21, 24, and 27). 5 uL of each PCR product was electrophoresed on a 1.2% agarose/EtBr gel in 1X TAE buffer following the indicated number of PCR cycles. Lane M: 1 kb DNA ladder size markers. The arrow indicates the strong band at 900 bp typically seen for human placenta total RNA (Super SMART™ PCR cDNA Synthesis Kit User Manuel, Clontech).

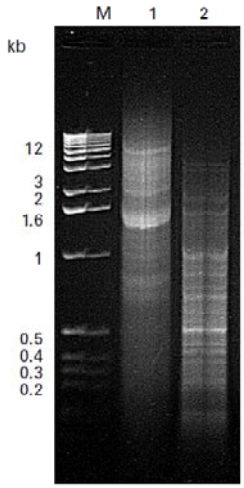

Figure 16. Positive control skeletal muscle ds cDNA before (Lane 1) and after (Lane 2) Rsa I digestion.

Complementary DNA was synthesized as described in the protocol (*see* Subheading 3.3.3) using the human skeletal muscle control poly A+ RNA included in the kit. Lane M: DNA size markers.

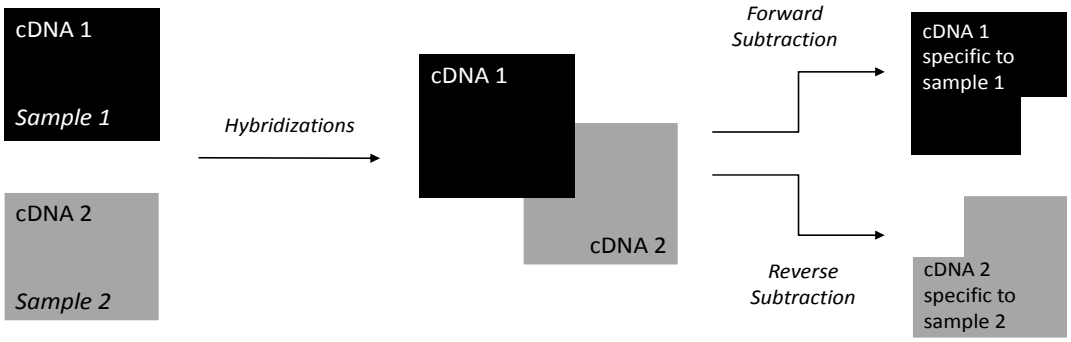

Figure 17. Forward and reverse subtraction hybridization

The forward subtraction experiment is designed to enrich for differentially expressed sequences present in poly A+ RNA sample 1 (cDNA 1, tester), but not poly A+ RNA sample 2 (cDNA 2, driver). However, in the reverse subtraction, cDNA 2 serves as tester and cDNA 1 serves as driver. The result is two subtracted cDNA populations: the forward-subtracted cDNA contains sequences that are specific to sample 1, and the reverse-subtracted cDNA contains sequences that are specific to sample 2.

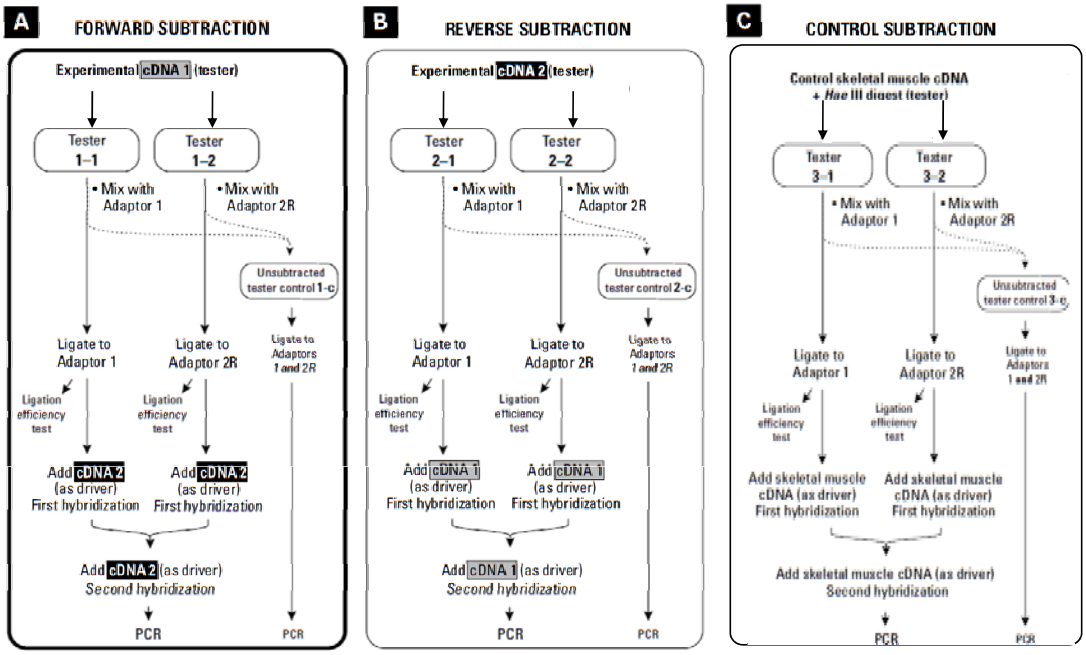

Figure 18. Preparing adaptor-ligated tester cDNAs for hybridization and PCR. Each tester cDNA (i.e. each different experimental cDNA and the control skeletal muscle tester cDNA) must be ligated to the appropriate adaptors, as shown above. Panel A. The forward subtraction is the intended experiment. Panel B. A second subtraction in reverse (i.e., tester as driver, driver as tester) is required for differential screening of the subtracted cDNA library. Panel C. Control subtraction with skeletal muscle cDNA. (Adapted from the PCR-Select cDNA Subtraction Kit User Manual, Clontech).

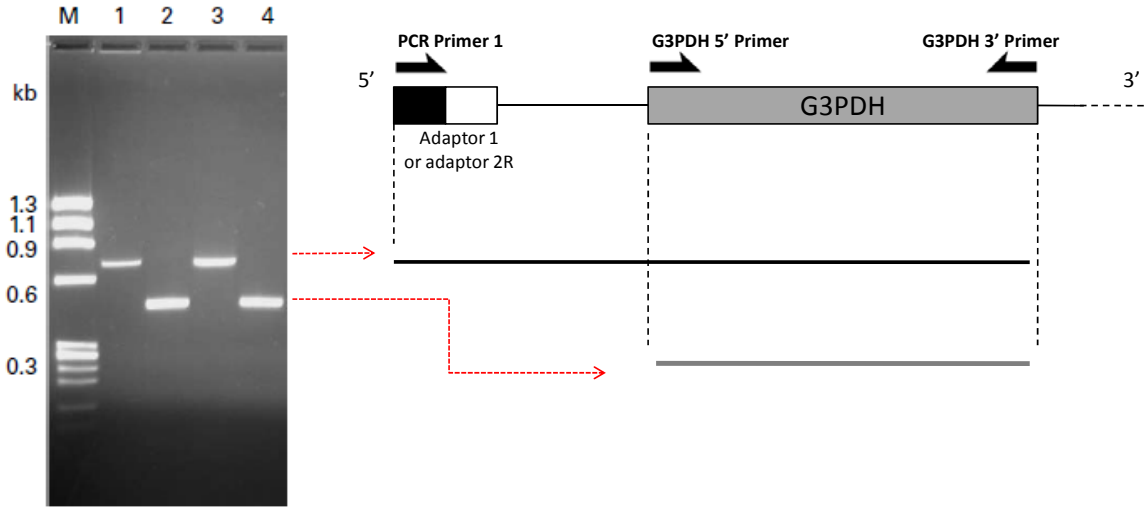

Figure 19. Typical results of ligation efficiency analysis.

The results shown here are for human placenta samples; Lane 1: PCR products using Tester 1-1 (Adaptor 1-ligated) as the template and the G3PDH 3' Primer and PCR Primer 1. Lane 2: PCR products using Tester 1-1 (Adaptor 1-ligated) as the template, and the G3PDH 3' and 5' Primers. Lane 3: PCR products using Tester 1-2 (Adaptor 2R-ligated) as the template, and the G3PDH 3' Primer and PCR Primer 1. Lane 4: PCR products using Tester 1-2 (Adaptor 2R-ligated) as the template, and the G3PDH 3' and 5' Primers. 2 % agarose/EtBr gel. Lane M: φX174 DNA/Hae III digest size markers (adapted from PCR-Select™ cDNA Subtraction Kit User Manual, Clontech).

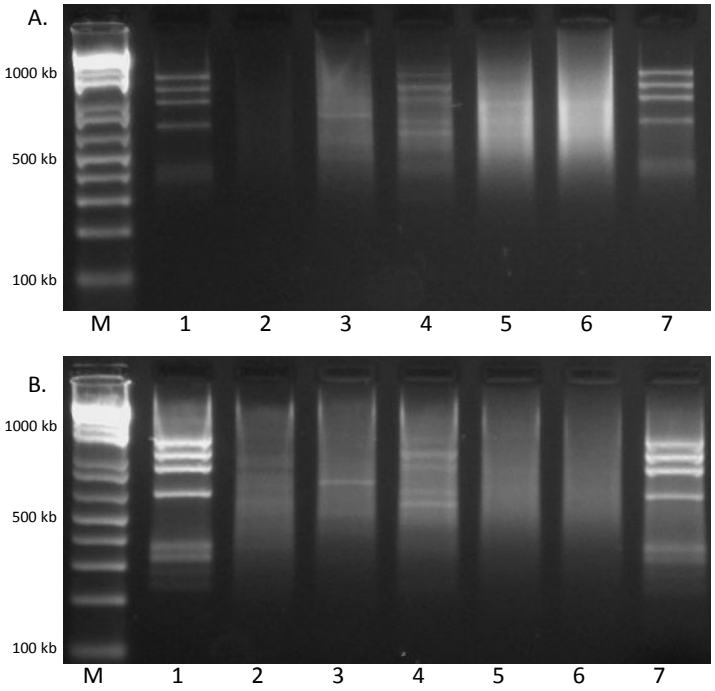

Figure 20. Amplification of results for uteri with reactivated blastocysts versus uteri with blastocysts in diapause by subtraction hybridization analysis.

Lane M: 100 bp size markers. Panel A: Primary PCR. Panel B: Secondary PCR. Lane 1: PCR products of subtracted skeletal muscle tester cDNA with 0.2% φX174/Hae III-digested DNA. Lane 2: PCR products of forward subtraction cDNA. Lane 3: PCR products of reverse subtraction cDNA. Lane 4: PCR products of unsubtracted skeletal muscle tester cDNA with 0.2% φX174/Hae III-digested DNA. Lane 5: PCR products of forward unsubtracted cDNA. Lane 6: PCR products of reverse unsubtracted cDNA. Lane 7: PCR control subtracted cDNA. Samples are electrophoresed on a 2% agarose/EtBr gel (Lefèvre, 2005, unpublished).

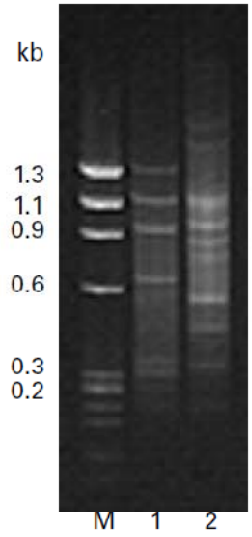

Figure 21. Typical results of control skeletal muscle subtraction hybridization analysis.

The secondary PCR product of the subtracted skeletal muscle sample contains mostly DNA fragments corresponding to the φX174/Hae III digest. The adaptor sequences on both ends of DNA fragments cause the mobility shift of these PCR products in comparison with original, digested φX174 DNA. Lane M: φX174 DNA/Hae III digest size markers. Lane 1: Secondary PCR products of subtracted skeletal muscle tester cDNA with 0.2% φX174/Hae III-digested DNA. Lane 2: Secondary PCR products of unsubtracted skeletal muscle tester cDNA ligated with both Adaptors 1 and 2R and containing 0.2% φX174/Hae III-digested DNA. Samples are electrophoresed on a 2% agarose/EtBr gel (from PCR-Select™ cDNA Subtraction Kit User Manual, Clontech).

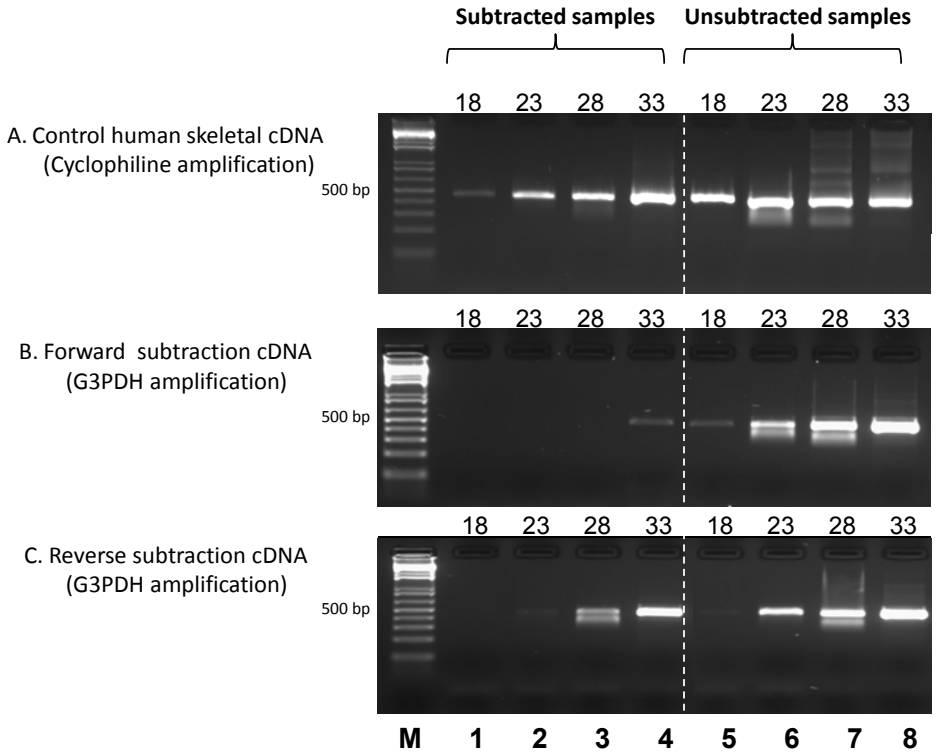

Figure 22. Efficiency of the subtraction hybridization between reactivated uterine cDNA versus cDNA of uterus during diapause, in the mink.

PCR was performed on the subtracted (Lanes 1–4) or unsubtracted (Lanes 5–8) secondary PCR product using housekeeping gene primers. Lanes 1 and 5: 18 cycles; Lanes 2 and 6: 23 cycles; Lanes 3 and 7: 28 cycles; Lanes 4 and 8: 33 cycles. Lane M: marker, 100 pb. Panel A: Cyclophilin reduction in control human skeletal cDNA subtraction. Panel B and C: G3PDH reduction in the forward subtraction cDNA and in the reverse subtraction cDNA, respectively. Housekeeping gene abundance is significantly reduced by PCR-Select subtraction. The three subtractions were successful. (Lefèvre, 2005, unpublished).

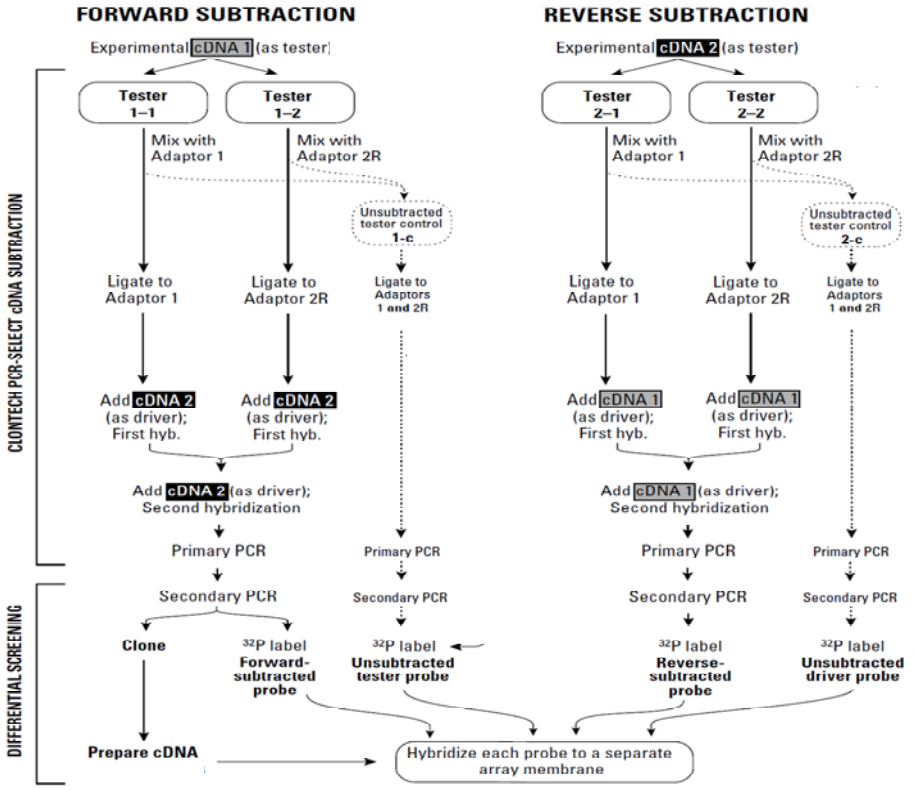

Figure 23. Experimental set-up for PCR-Select Differential Screening following the PCR-Select cDNA subtraction hybridization.

This flow chart indicates the procedure for preparing both subtracted and unsubtracted probes. Differential screening with subtracted probes is more sensitive. However, using both subtracted and unsubtracted probes is recommended. Secondary PCR products are cloned to construct the subtracted cDNA library. Complementaty DNA clones are hybridized on nylon membranes that are arrayed by four different probes: the forward and reverse subtracted probe, and the unsubtracted tester and driver probe.

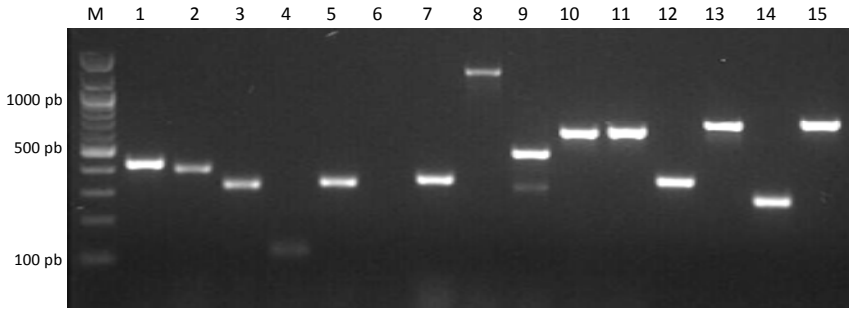

Figure 24. Amplification of 15 embryonic subtracted cDNA inserts in a cloning vector after transformation of MAX Efficiency DH5α Competent Cells using nested primer 1 and nester primer 2R.

Clone 6 is excluded from the analysis because no amplification product is detected as well as clone 9 because two different amplification products are detected. In the latter case, the original competent cell may have been transformed by two vectors containing an inserts at the same time. Electrophoresis in a 2.0% agarose/EtBr gel, 1X TAE buffer (Lefèvre, 2006, unpublished).

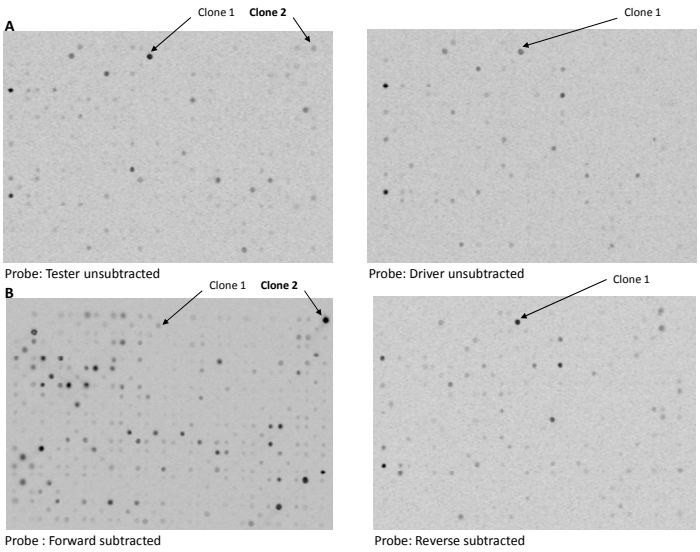

Figure 25. Sample of differential screening results.

Panel A. Dot blots hybridized with unsubtracted cDNA probes made from tester (mink uterus after reactivation of blastocyst) and driver (mink uterus with blastocysts in diapause) RNA. Panel B. Dot blots hybridized with cDNA probes made from forward-subtracted cDNA (mink uterus after reactivation as tester, mink uterus in diapause as driver) and reverse-subtracted cDNA (mink uterus in diapause as tester, mink uterus after reactivation as driver). As an example, a radioactive signal is detected for clone 2 only on the dot blots hybridized with unsubtracted cDNA probes made from tester and on dot blots hybridized with cDNA probes made from forward-subtracted cDNA. Consequently, clone 2 is a positive clone and is selected for the sequencing step. On the contrary, clone 1 is detected on the four dot blots hybridized with either both unsubtracted cDNA probes and both subtracted cDNA probes. As a false positive clone, clone 1 is removed from the library for the analysis (Lefèvre, 2006, unpublished).

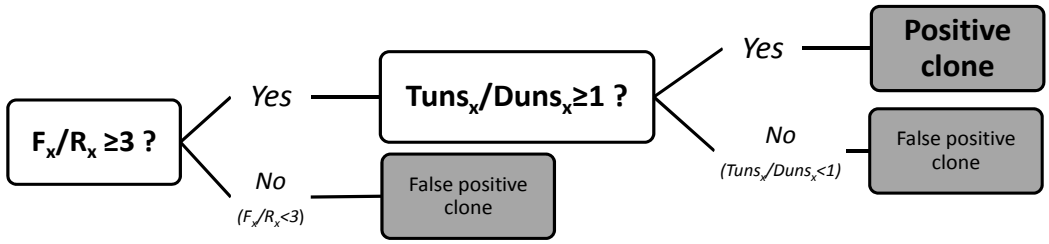

Figure 26. Analysis of the differential screening dot blots after quantification of the signal intensity for each blot by ImageQuant.

F_x, R_x, $Tuns_x$ and $Duns_x$ correspond to the radioactive signal's intensity measured with ImageQuant software (Applied Biosystem) for one clone x hybridized respectively with subtracted-forward cDNA probe (F_x), with subtracted-reverse cDNA probe (R_x), with unsubtracted tester cDNA probe ($Tuns_x$) and with unsubtracted driver cDNA probe ($Duns_x$). The procedure to determine whether a clone is positive or false positive is represented in the figure above, and is the one recommended by the manufacturer (PCR-Select Differential cDNA kit, Clontech). As the unsubtracted tester /driver cDNA probe do not hybridize with cDNA sequences that are less represented than 0.2 % in the whole population of cDNA, the ratio F_x/R_x is analyzed before the ratio $Tuns_x/Duns_x$.

IV. ARTICLE 2: UTERINE SIGNALING AT THE EMERGENCE OF THE BLASTOCYST FROM OBLIGATE DIAPAUSE

Status: Submitted for publication in *Biology of Reproduction*. Provisionally accepted, in revision.

Uterine Signaling at the Emergence of the Blastocysts from Obligate Diapause[1]

Pavine L.C. Lefèvre[2, 3], Marie-France Palin[4], Danièle Beaudry[4], Mira Dobias-Goff[3], Joëlle A. Desmarais[3], Evelyn M. Llerena V.[3] and Bruce D. Murphy [3]

[3]Centre de Recherche en Reproduction Animale, Faculté de Médecine Vétérinaire, Université de Montréal, 3200 rue Sicotte, St-Hyacinthe, Québec J2S 7C6, Canada.

[4]Dairy and Swine R & D Centre, Agriculture and Agri-Food Canada, 2000 College Street, PO Box 90 Stn Lennoxville, Sherbrooke, Québec J1M 1Z3, Canada.

Short Title: Uterine signaling at emergence from embryonic diapause.

Summary sentence: Uterine environment is modified at embryo reactivation, as illustrated by upregulation of gene expression for chromatin and tissue remodeling factors, *high mobility group nucleosome binding domain 1* (*HMGN1*) and the *secreted, protein acidic, cystein-rich* (*SPARC*), respectively, at blastocyst reactivation.

Keywords: embryonic diapause, delayed implantation, blastocyst, uterus, HMGN1, SPARC, endotheliochorial placenta, suppressive subtractive hybridization (SSH).

ABSTRACT

---

[1] Supported by a Discovery Grant from the Natural Sciences and Engineering Research Council of Canada to B.D.M.; The authors have no real or potential conflicts of interest to declare with entities related to the material being published. [2] Correspondence: Pavine L.C. Lefèvre, 3200 Sicotte, St-Hyacinthe, QC, Canada J2S 7C6. FAX: 450 778 8103;

Embryonic diapause is the reversible arrest of embryo development prior to implantation and is placed under a uterine control mechanism which remains elusive. Our objective was to explore uterine modifications associated with the emergence of embryonic diapause in the mink, a species in which embryonic diapause is a characteristic of every gestation. We investigated the mink uterine transcriptome at reactivation of blastocysts using the suppressive subtractive hybridization technique (SSH). A library of 123 differentially expressed uterine genes between diapause and reactivation of blastocysts was generated. Those genes are implicated in the regulation of metabolism (25%), gene expression (21%), signal transduction (15%), the cell cycle (15%) and intracellular transport (10%). This range of transcriptional change underlines the substantial modifications of the maternal uterine environment at the time of blastocyst reactivation. Two genes were chosen from the library, the *high mobility group nucleosome binding domain 1* (*HMGN1*), a chromatin remodeling factor which may be secreted and a second protein, known to be *secreted, acidic and cystein-rich* (*SPARC*), which is implicated in extracellular cell-cell interactions. Both *HMGN1* and *SPARC* uterine gene expression were significantly increased at blastocyst reactivation compared to diapause, principally in the endometrial epithelium and subepithelial stroma. Later in the process, HMGN1 protein was specifically localized in the invading trophoblast at the site of embryo implantation, while SPARC was more abundantly expressed in the maternal endometrium. These results provide new insight into the factors HMGN1 and SPARC as potential regulators of emergence of the mink embryo from obligate embryonic diapause and of subsequent blastocyst implantation.

A. Introduction

Embryonic diapause, the suspension of embryo development at the blastocyst stage during the preimplantation period, leads to a delay of implantation. In the American mink (*Mustela vison*), obligate embryonic diapause occurs each breeding season during the reproductive life (Hansson 1947; Enders 1952). It averages from 1-2 weeks, but can be extended to more than three months under specific experimental conditions (Murphy and James 1974). The chronology of the process is as follows. Six days after mating-induced ovulation and four days after fertilization in the oviduct the embryo reaches the uterus (Hansson 1947). There, the embryonic cells enter cell cycle arrest, presumably in G0/G1 phase, and undergo a reduction of their metabolism to a basal level, thus leading to the suspension of embryonic development (Desmarais, Bordignon et al. 2004). It is well established that termination of embryonic diapause in this species is induced by increasing secretion of prolactin from the pituitary gland (Murphy, Concannon et al. 1981), under the influence of the increasing photoperiod at the vernal equinox (Murphy and James 1974). Prolactin induces ovarian luteal cell activation and an increase in progesterone secretion which acts on the endometrium and is associated with embryo reactivation and implantation (Papke, Concannon et al. 1980). Implantation of blastocysts occurs 11 to 13 days following emergence from diapause and results in an endotheliochorial placentation where maternal blood vessels become surrounded by trophoblast after penetration of trophoblastic villi into maternal glands and degradation of the latter along with the associated endometrial stroma (Enders 1952; Krebs, Winther et al. 1997). Reciprocal embryo transfer experiments

between mink and ferret, a closely related species with no embryonic diapause, indicated that embryonic diapause is maternally controlled and dependent on the maternal uterine environment (Chang 1968). Nonetheless, uterine signaling responsible for emergence from embryonic diapause remains elusive. The aim of the present study was to explore uterine modifications concomitant with embryo reactivation and, subsequent implantation. A transcriptomic analysis was performed using SSH technique to construct a library of uterine genes expressed in the uterus specifically at the time of embryo reactivation.

B. Materials and methods

1. Tissue collection

All procedures involving live animals were approved by the *Comité de déontologie de la Faculté de Médecine Vétérinaire, Université de Montréal,* which is accredited by the Canadian Council on Animal Care. Investigations were carried out over four successive annual breeding seasons from 2005 to 2009 using ranch mink of the Dark and Pastel varieties purchased from A. Richard (St. Damase, QC, Canada). During this period, mink females were bred to two fertile males according to usual commercial farming procedures. Uterine horns from females during diapause were collected seven to nine days after the final mating and prior to March 21 (**Figure 27** A (p 158)). Embryo reactivation was synchronized among females by a daily injection of 1 mg/kg/day ovine prolactin (Sigma, Oakville, ON, Canada) starting on the 21st of March and for the seven following days (Murphy, Concannon et al. 1981). The first day of prolactin injection was designated Day 0 after embryo reactivation. The non-implanted embryos were flushed out from the uterine lumen using TC-199

medium (Gibco, Burlington, ON, Canada) containing 10% v/v fetal bovine serum (Gibco). The observation of expansion of embryos following prolactin treatment confirmed that reactivation had occurred as previously described (Desmarais, Bordignon et al. 2004). To perform the SSH technique, uterine horns from 24 females were collected during diapause (n=12) and on Days 3, 5 and 7 of prolactin-induced reactivation of blastocyst development (n=4 per stage) (**Figure 27A** (p 158)). For SSH validation and detailed spatiotemporal gene expression, uterine samples were collected during diapause and on Days 1, 3, 5, 7 and 9 after prolactin-induced embryo reactivation (n=3 per stage). Whole implantation sites, including blastocysts, and inter-implantation sites were dissected on Days 11 and 14 after prolactin-induced embryo reactivation (n=3 per stage), when blastocysts can no longer be flushed from the uterine lumen. Uterine tissue samples were snap-frozen and stored at – 80 °C for RNA extraction or fixed in paraformaldehyde (PAF) 4% w/v overnight and kept at 4 °C in phosphate buffered saline (PBS) 1X until paraffin embedding for immunohistochemical analysis.

2. Total RNA extraction and mRNA isolation from uterine samples

Total RNA was extracted from whole uterine samples using the Rneasy Mini kit (Qiagen, Mississauga, ON, Canada) according to the manufacturer's instructions. Messenger RNA was isolated from total RNA using the Oligotex kit (Qiagen) as described by the manufacturer.

3. Suppressive Subtraction Hybridization

The suppressive subtractive hybridization technique was performed with the PCR-Select cDNA Subtraction Kit (Clontech, Palo Alto, CA, USA) as detailed in

(Lefevre and Murphy 2009). This technique enables isolation of differentially expressed cDNA sequences between two different pools of cDNAs, the tester (specific cDNAs of interest) and the driver (cDNAs of reference) (Diatchenko, Lau et al. 1996). Messenger RNA from uterine samples collected at Days 3, 5 and 7 after reactivation of blastocysts were pooled and assigned to the tester group, while pooled mRNA from uterine samples collected during diapause was designed as the driver (**Figure 27** B (p 158)). In each group, 2 µg of mRNA was used for cDNA synthesis. Two subtractions were performed: 1) forward subtraction: uterine samples collected during blastocyst reactivation (tester) versus those collected during diapause (driver); 2) reverse subtraction: uterine samples collected during blastocyst diapause (tester) versus those collected at blastocyst reactivation (driver). The reverse subtraction is required to perform the differential screening validation (see below). Subtraction efficiency was assessed by determining the difference in cycle number required for detection of *peptidylpropyl isomerase A* (*PPIA*) amplification between subtracted cDNA and nonsubtracted cDNA by polymerase chain reaction (PCR). Primers used for *PPIA* amplification were: 5'-TAATGGCACTGGTGGCAAGTC-3' and 5'-CAGATGAAGAACTGGGAACCG-3' (Desmarais, Lopes et al. 2007).

4. Differential screening

Following SSH, subtracted cDNA fragments were submitted to differential screening to remove false positive cDNAs which would be common to both the tester and driver samples in the forward subtraction. The forward subtracted cDNA fragments generated by the SSH technique were cloned into the pCRII cloning vector

using the T/A Cloning Kit Dual Promoter (Invitrogen, Carlsbad, CA, USA) and transformed into Max Efficiency DH5α competent cells (Invitrogen) as described in (Lefevre and Murphy 2009). Briefly, one thousand clones were selected randomly and the presence of the insert was confirmed by PCR for each clone using primer 1 (5'TCGAGCGGCCGCCCGGGCAGGT-3') and primer 2R (5'-AGCGT GGTCGCGGCCGAGGT-3') (Clontech) according the manufacturer's instructions. Amplified cDNAs from positive insert containing clones were spotted on eight identical Hybond-N+ membranes (Amersham Pharmacia Biotech., Baie d'Urfé, QC, Canada). Subtracted cDNA fragments from the forward and reverse subtractions as well as nonsubtracted cDNAs from the tester and driver were used as probes to hybridize identical dot blot membranes containing the amplified cDNAs from positive clones of the forward subtraction. Probes were ^{33}P-labeled using [α-^{33}P]-dCTP (PerkinElmer, Boston, MA, USA). This procedure was performed in duplicate using the PCR-Select Subtraction Hybridization Screening kit (Clontech) following the manufacturer's instructions. Hybridization signals on the membranes were digitized using a Storm 840 PhosphoImager and densitometric quantification of the signals was carried out with the ImageQuant software (Pharmacia Biotech.). Clones selected for sequencing were those showing ≥ 3-fold differences in signal intensity between forward and reverse libraries.

5. Sequencing and sequence analysis

Plasmid DNA was extracted from the positive bacterial clones from the forward subtraction and sequenced using the SP6 universal primer with an Applied Biosystems 3730xl DNA analyzer (PE Applied Biosystems, Foster City, CA, USA).

This procedure was performed by McGill University and Genome Quebec Innovation Centre, Montreal, QC, Canada. Sequences were trimmed from vector and adaptor sequences using the National Centre for Biotechnology Information (NCBI) bl2seq program (http://blast.ncbi.nlm.nih.gov/bl2seq/wblast2.cgi). Sequences were then compared against the non-redundant GenBank database using the online computer Basic Local Alignment Search Tool (Blastn) software (Altschul, Gish et al. 1990). Aligned sequences were considered as homologous when the percentage of identities was > 89 %, the E-value < 1.0 e^{-11} and the length of similarity > 100 nucleotides. All cDNA sequences identified in the current study were submitted to GenBank (Accession nos. GH271800 to GH272100 and GH693995 to GH694029). Gene ontology was investigated for each known genes using the online GENATLAS and the Information Hyperlink Over Proteins (Hoffmann 2004) databases with emphasis concentrated on the biological process of products encoded by known genes. Identified gene products were compared against the Secretory Protein Database (Chen, Zhang et al. 2005) to identify potential secreted proteins. For convenience, differentially expressed cDNA sequences homologous to known genes will be designed by the name of the corresponding homologous known gene in other species.

6. Quantitative real-time PCR

One microgram of RNA was reverse transcribed with Superscript II Reverse Transcriptase (Invitrogen). The primers were designed based on the cloned cDNA sequences using the Primer Express software Version 3.0 (PE Applied Biosystem) (**Table 8** (p 157)). Primers used to amplify the reference gene (RG), glyceraldehyde

phosphodeshydrogenase (*GAPDH*) gene were designed based on the mink *GAPDH* mRNA sequence (Accession number AF076283) and were: 5'-TCCCCACCCCCAATGTG-3' and 5'-CCCTCTGATGCCTGCTTCA-3'. Primer concentrations were optimized according to the manufacturer's recommendations and specificity of amplified products was verified by dissociation curve analysis for each primer set. To evaluate PCR efficiency, standard curves were prepared for the studied genes and the RG using a pool of uterine cDNA from all samples collected during diapause and on Days 3, 5 and 7 after embryo reactivation. PCR efficiency for each gene was co-evaluated using LinRegPCR software (Ruijter, Ramakers et al. 2009). Triplicate real time PCR amplifications were performed in a 10 µl reaction volume consisting in 1 µl of the appropriate concentration of both sense and antisense primers, 5 µl of Power SYBRGreen PCR Master Mix (PE Applied Biosystems), 0.1 µl of Amperase Uracil N-glycosylase (UNG; PE Applied Biosystems) and 3 µl of cDNA diluted 1 in 15 in distilled water. Cycling conditions were 2 min at 50 °C and 10 min at 95 °C, followed by 40 cycles of 3 sec at 95 °C and 30 sec at 60 °C. Amplification, detection and data analysis were performed with a 7500 Fast Real-Time PCR System (PE Applied Biosystems) and using the Sequence Detection Software version 1.4 (PE Applied Biosystems). To measure the expression of the 10 selected genes between diapause and reactivation, quantification of gene expression was performed using the relative standard curve method as recommended by Applied BioSystems (PE Applied Biosystems). Relative quantitation using the comparative Ct method (delta-delta Ct) was employed to quantify gene expression of *HMGN1* and *SPARC* on Days 0, 3, 5, 7, 9 and 11 for implantation and inter-

implantation sites as previously described (Pfaffl 2001). Gene expression in three experimental samples for each stage was measured in triplicates.

7. Immunohistochemistry

Fixed and cross-sectioned uterine tissues were used to detect SPARC and HMGN1 proteins during diapause and thereafter during embryo reactivation and implantation as previously described with slight modifications (Desmarais, Lopes et al. 2007). Retrieval of antigens was performed on deparaffinized and hydrated sections by trypsin 0.075 % digestion at 37 °C for 20 min. After a blocking step using bovine serum albumin (BSA) 10 % w/v at room temperature for 6 h in a humid chamber at room temperature, tissues were then incubated overnight at 4 °C with 4 µg/ml of SPARC (H-14) or HMGN1 (HMG14 N-15) goat anti-human antibodies (Santa Cruz Biotechnology, Santa Cruz, CA, USA) in a dark and humid chamber. After washes in TPBS (PBS1X containing 0.1% v/v of Tween 20), sections were incubated with a biotinylated second antibody for 1 h at room temperature, and the Vectastain ABC kit (Vector Laboratories, Burlington, ON, CA) with 3,3'-diaminobenzidine (DAB), was used to detect the peroxidase activity. Negative control sections were submitted to the same procedures, except that the first antibody was replaced by 10 % v/v nonimmune goat serum.

8. Statistical analysis

Data from quantitative real-time PCR were analyzed using the JMP, Version 7(SAS Institute Inc., Cary, NC, USA) and STATISTICA 8.0 (StatSfoft, Inc., Tulsa, OK, USA). Wilcoxon rank sum test was employed to compare target gene expression during diapause and at reactivation and gene expression between implantation and

inter-implantation sites. Differences among HMGN1 and SPARC mRNA relative abundance measured during diapause and on days 3, 5, 7, 9 and 11 after reactivation was analyzed using the multiple comparison of mean rank. Statistical differences were considered significant when $P < 0.05$ and a tendency toward significance was considered at a $P < 0.1$.

C. Results

1. Analysis of the mink uterine transcriptome at reactivation versus diapause of blastocysts

The SSH was performed to enable construction of a uterine library comprising differentially expressed cDNA sequences between diapause and Days 3, 5 and 7 after reactivation of blastocysts. The subtraction efficiency of the SSH was assessed by measuring the difference in PCR cycle numbers required for detection of *PPIA* amplification between subtracted cDNA and nonsubtracted cDNA (**Figure 28** (p 159)). Fifteen and five additional amplification cycles, respectively were necessary in the forward and reverse subtracted compared with the nonsubtracted library to detect the *PPIA* amplicon, thus reflecting a reduction in *PPIA* mRNA abundance after both subtractions. Following subtraction, differentially expressed cDNAs from the forward subtraction were cloned in order to construct the SSH library. Among randomly selected SSH clones (n = 1000), 85.9% were single insert containing clones having an average length of 370 ± 82 (mean ± sd) base pairs. Screening was undertaken to confirm the differential expression of the cDNAs generated by the SSH resulting in identification of 45.6 % (392 out of 859) of the cDNA clones that had a difference in hybridization signals ≥ 3 between diapause and

reactivated samples. Of these differentially expressed cDNA sequences from the mink uterus, 337 were successfully sequenced and sequences were compared against the GenBank database. When considering the nonredundant list of differentially expressed genes, the uterine cDNA library comprised 211 unique sequences, among which 58 % are homologous to known gene sequences (supplementary data; **Table 9** (p 171)), 14 % to known, but uncharacterized sequences, such as expressed sequenced tags and 28 % correspond to novel sequences. A total of 10 sequences homologous to known genes were represented by more than 2 clones. The two most redundant clones were *beta defensin 139* (*DEFB139*, 56 clones) and *tumor rejection antigen 1* (*HSP90B1*, 7 clones) (supplementary data; **Table 9** (p 171)). Among the 123 identified genes, 41.5 % were listed in the Secretory Protein Database (supplementary data; **Table 9** (p 171)).

To gain further information on the biological importance of transcripts that were differentially expressed, the total list of non-redundant genes of apparent homology to known genes (n = 123) was subjected to functional annotation using the GENATLAS database. Some differentially expressed genes could be classified in more than one category. Ontology analysis indicated that 25 % of the genes identified are implicated in regulation of metabolism, 21% in gene expression, 15 % in signal transduction, 15 % in cell cycle, 10 % in regulation of transport and 9% in the regulation of cell structure (**Figure 29** (p 160)).

The differential expression pattern of 10 identified genes was investigated by quantitative real-time polymerase chain reaction (qPCR) (**Table 8** (p 157)) in order

to confirm the SSH. Comparison between mRNA abundance measured during diapause and mean mRNA abundance measured on Days 3, 5 and 7 after reactivation was undertaken for adiponectin receptor 1 (*ADIPOR1*), activated leukocyte cell adhesion molecule (*ALCAM*), growth and differentiation factor 3 (*GDF3*), high-mobility group nucleosome binding domain 1 (*HMGN1*), ornithine decarboxylase 1 (*ODC1*), AZI inhibitor 1 (*AZI1*), secreted protein, acidic, cysteine-rich (*SPARC*), spermidine/spermine N1-acetyltransferase (*SAT1*), thioredoxin-like 1 (*TXNL1*) and transglutaminase 2 (*TGM2*). The differential gene expression pattern of these 10 genes, as confirmed by mRNA abundance, increased ($P < 0.05$) between diapause and embryo reactivation (**Figure 30** (p 161)). These 10 genes were chosen because they were previously referenced in the literature as being implicated in preimplantation and implantation (*ADIPOR1* (Takemura, Osuga et al. 2006), *ALCAM* (Fujiwara, Tatsumi et al. 2003), *GDF3* (Jones, Stoikos et al. 2006; Levine and Brivanlou 2006), *ODC1*, *SAT1* and *AZI1* (Fozard, Part et al. 1980; Van Winkle and Campione 1983; Zhao, Chi et al. 2008), *TXNL1* (Lopata, Sibson et al. 2001), *TGM2* (Kabir-Salmani, Shiokawa et al. 2005) and *SPARC* (White, Robb et al. 2004)). As for factor of chromatin remodeling (Gerlitz 2010), *HMGN1* was potentially interesting for downstream gene expression and validation for its differential gene expression was also undertaken. *SPARC*, is a secreted glycoprotein known to be implicated in cell-cell adhesion (Sage, Johnson et al. 1984), cell proliferation (Murphy-Ullrich, Lane et al. 1995) and in mouse embryo implantation (White, Robb et al. 2004). Therefore, HMGN1 and SPARC may affect uterine

modifications associated with emergence of blastocysts from embryonic diapause, and further evaluation was performed.

2. *HMGN1* and *SPARC* are differentially expressed in the mink uterus at reactivation of blastocysts

The temporal expression pattern of these two selected candidate genes was analyzed by quantitative real-time PCR over a wider temporal scale, beginning from diapause through Day 9 after embryo reactivation in whole uterine samples (**Figure 31** A, B (p 163)). Both *HMGN1* and *SPARC* gene expression increased ($P < 0.05$) on Day 3, after embryo reactivation in comparison to diapause and tend to remain elevated thereafter, on Days 5, 7 and 9 after reactivation. In order to assess gene expression at the translational level and to evaluate cellular localization of HMGN1 and SPARC, protein immunolocalization in uterine cross-sections was undertaken during diapause and on Days 1, 3, 5, 7 and 9 after reactivation. As seen in **Figure 32** (p 165), signal intensity of HMGN1 and SPARC was strongly increased in mink uterine cross sections starting on Day 1 after embryo reactivation in comparison to diapause. Indeed, the HGMN1 signal was only slightly detectable in the luminal and glandular epithelia while more intensively present in the subepithelial stromal and glandular epithelial cells underlying the myometrium during diapause (**Figure 32** Aa, e (p 165)). Beginning at Day 1 after embryo reactivation, its expression was substantially increased in the cytoplasm of the luminal and glandular epithelial cells and of the subepithelial stromal cells throughout the endometrium (**Figure 32** Ab, f (p 165)). At higher magnification, HMGN1 appears to be more concentrated in the apical pole of luminal epithelial cells facing the uterine lumen at reactivation of

blastocysts (**Figure 32** Af (p 165)). A similar distribution pattern for HMGN1 was observed in uterus on Days 3, 5 and 7 in the uterus (data not shown) and was maintained until Day 9 after reactivation of blastocysts (**Figure 32** A c, g (p 165)). Immunolocalization of SPARC in the mink uterus at reactivation revealed increased abundance of SPARC protein (**Figure 32** B (p 165)). SPARC protein was substantially increased in the cytoplasm of luminal and glandular epithelial cells during diapause (**Figure 32** B a, e (p 165)). This distribution was increased and extended to the subepithelial stromal cells at Day 1 after embryo reactivation (**Figure 32** B b, f (p 165)). The presence of SPARC was also detected at the apical pole of luminal and glandular epithelial cells during diapause (**Figure 32** B, e (p 165)) and its concentration was locally elevated at reactivation (**Figure 32** B, f (p 165)). This specific distribution of SPARC could be observed on Days 3, 5 7 and 9 after reactivation of blastocysts (**Figure 32** B, c, g (p 165)) and data not shown).

3. HMGN1 and SPARC expression in mink embryo implantation sites

Given that HMGN1 and SPARC expression correlates with embryo activation, it was of interest to assess the potential role of HMGN1 and SPARC in embryo implantation. In the mink, embryo implantation results in endotheliochorial placentation, comprising an apposition phase during which the trophoblast becomes apposed to the uterine luminal epithelium all around the implantation chamber (Enders 1952; Song 1998). At the antimesometrial pole of the implantation chamber, the embryo attachment is induced by invasion of the trophoblastic plaques, mainly the syncytiotrophoblast, in the uterine glands, and

differentiation of the cytotrophoblast into fetal mesenchymal capillaries into the trophoblastic villi (Enders 1952; Song 1998). Thereafter, the endometrial epithelium and stroma are degraded to enable development of the placenta composed of a maternal-fetal labyrinth between syncytiotrophoblast and maternal capillaries, maternal symplasma formed by glandular epithelial cells which have been displaced ahead of the intruding trophoblast and, under the myometrium, a glandular zona comprising hypertrophied uterine glands (Enders 1952; Song 1998).

The HMGN1 and SPARC mRNAs and protein abundance were evaluated in both inter-implantation and implantation sites, at Days 11 and 14 after reactivation, which corresponds to the day of implantation and three days post-implantation, respectively. *HMGN1* gene expression was different between implantation and inter-implantation sites on Day 11 after embryo reactivation and was reduced at the same level observed in diapause (data not shown). HMGN1 protein at Day 11 after reactivation and on the day of implantation were not different in its distribution pattern in implantation and inter-implantation sites which was similar to that on Day 9 after reactivation (data not shown). However, on Day 14 after embryo reactivation or three days after implantation, HMGN1 protein exhibited a different distribution pattern between implantation (**Figure 33** a, b (p 167)) and inter-implantation sites (**Figure 33** c (p 167)). At the antimesometrial pole of the implantation site, its expression was clearly localized in the cytoplasmic and nuclear compartment of trophoblastic plates (**Figure 33** e (p 167)), in the cytoplasm of syncytiotrophoblast invading the maternal endometrium and in the nuclei of mesenchymal cells of the fetal capillaries (**Figure 33** f (p 167)). In cytotrophoblast

and maternal endothelial cells, HMGN1 protein was also present but at reduced levels relative to observations in other compartment tissues (**Figure 33** f (p 167)). The myometrium, glandular epithelium and stroma underlying the myometrium also expressed HMGN1 at implantation sites, but the signal was not present in the maternal symplasma (**Figure 33** b (p 167)). At mesometrial pole (data not shown) and inter-implantation sites (**Figure 33** c, g (p 167)), HMGN1 protein exhibited a cytoplasmic localization in the uterine epithelial cells, stromal cells and myometrium.

The relative abundance of *SPARC* mRNA increased ($p < 0.05$) two fold at inter-implantation sites in comparison to implantation sites at Day 11 after embryo reactivation, on the day of implantation (**Figure 34** (p 168)). At the protein level, SPARC was observed in both implantation and inter-implantation sites on the day of implantation (**Figure 35** a-h (p 170)) and on Day 14 after reactivation (**Figure 35** i-p (p 170)), but surprisingly, it did not exhibit the same local tissue distribution. In early implantation stages, when the trophoblastic plaques become apposed to the endometrium and when the luminal and glandular compartments as well as endometrial stroma are being degraded, SPARC was specifically detected at the antimesometrial pole with an unequivocal localization in the nucleus of endometrial epithelial and stromal cells and, in the nucleus of trophoblastic plaque cells (**Figure 35** a, b e (p 170)). Under the myometrium of antimesometrial pole, nuclei of cells from hypertrophied glands were also positive for SPARC (**Figure 35** f (p 170)). Conversely, SPARC was found in the cytoplasmic compartment of endometrial epithelia and stroma at the mesometrial pole of implantation (data not shown) and

at inter-implantation sites (**Figure 35** c, g (p 170)). As noted in tissues acquired before implantation, SPARC appeared to be highly concentrated in the apical pole facing the uterine lumen at the mesometrial pole of implantation (data not shown) and inter-implantation sites (**Figure 35** g (p 170)). It is of interest to note that this distribution pattern of SPARC was specific to the early stage of blastocyst implantation at implantation sites, since 3 days later, when the trophoblast invaded the endometrium and formed the maternal-fetal labyrinth, SPARC expression was limited to maternal symplasma and hypertrophied glands underlying the myometrium (**Figure 35** I, j (p 170)). Observations at higher magnification showed a nuclear localization of SPARC in maternal symplasma (**Figure 35** m (p 170)). Cells from trophoblastic plaques and mesenchymal cells of the fetal capillaries in trophoblastic villi also expressed SPARC in their nucleus (**Figure 35** m, n (p 170)). However, no staining was observed for SPARC in the cytotrophoblast and syncytiotrophoblast. Cytoplasmic subcellular localization of SPARC was present in hypertrophied glands underlying the myometrium at the antimesometrial pole (**Figure 35** o (p 170)). At the mesometrial pole (**Figure 35** k (p 170)) and inter-implantation sites (**Figure 35** l (p 170)), SPARC expression was unchanged from early stages of implantation and was found to be expressed in the cytoplasm of endometrial epithelium (**Figure 35** p (p 170)).

D. Discussion

The enigma of obligate embryonic diapause has fascinated researchers since the discovery of the phenomenon more than 100 years ago. The aim of the present study was to explore changes in the uterine environment associated with embryo

reactivation and consequent embryo implantation. We performed a transcriptomic analysis of the mink uterus using the SSH technique, which successfully enabled the construction of a library that includes a total of 211 non-redundant and differentially expressed uterine cDNA sequences between diapause and embryo reactivation. This technique does not require previous knowledge of gene sequences and was consequently suitable for analyzing the mink genome for which a limited number of sequences are available in databases. In addition, the upregulation of gene expression between diapause and reactivation, measured by quantitative real-time PCR for 10 selected genes, proved that the SSH was an efficient technique to generate differentially expressed cDNA sequences in the context of the present study. Among the known and characterized or uncharacterized sequences, 78 % were homologous to sequences found in the *Canis familiaris* database. This was expected since both *Mustela vison* and *Canis familiaris* belong to the Caniformia monophyletic group of the Carnivora and the dog genome is among the best characterized in this group (Bininda-Emonds, Gittleman et al. 1999). In addition, the SSH technique also generates unknown cDNA fragments or previously unknown genes, such as expressed sequence tags. Indeed, 31 % of the non-redundant differentially expressed cDNAs corresponded to known, but uncharacterized sequences and to unknown sequences. These unknown sequences were submitted to GenBank database and will therefore contribute to increase the number of the mink sequences available. They potentially correspond to novel genes that could be essential in the process of embryo reactivation and implantation

following obligate embryonic diapause. Further analysis is underway to assess the functions of these novel genes in the context of the present study.

With respect to the Gene Ontology biological process, the non-redundant genes identified were distributed in the metabolism, gene expression, signal transduction, cell cycle, transport and cell structure categories. We conclude that these processes are upregulated in the mink uterus after embryo reactivation when compared to diapause. This distribution is consistent with the one observed in estrogen-induced embryo reactivation in the uterus of a mouse model of delayed-implantation, where delayed implantation was terminated and embryo implantation initiated with estrogen injection (Reese, Das et al. 2001). In the present study, the highest representation of genes related with metabolism and gene expression suggests an increase in uterine protein synthesis during prolactin-induced reactivation. Consistent with this result, Shaw and Renfree (Shaw and Renfree 1986) reported an increase in uterine protein synthesis about one day before the reactivation of the blastocyst in the tammar wallaby. Moreover, it is not surprising to find a high percentage of genes in the cell cycle category as it is well known that an increase in ovarian progesterone secretion induces uterine stromal cell proliferation and consequent uterine swellings in mammals before the beginning of implantation (Dey, Lim et al. 2004). In the current study, genes in the transport activity category were also upregulated, thus suggesting an increase in the secretory activity of uterine proteins during the embryo reactivation. In addition, 41.5 % of the identified genes were listed in the Secreted Protein Database which suggests that they are encoding for products that may be subjected to extracellular secretion.

Increased uterine protein secretion into uterine lumen has been associated with resumption of embryo development in the skunk, which also presents embryonic diapause (Mead, Rourke et al. 1979). In addition, the *in vitro* model developed by Moreau et al. (Moreau, Arslan et al. 1995) provided evidence of embryo reactivation only when mink embryos in diapause were cocultured with mink uterine cell monolayers. Together, those results support the hypothesis that termination of embryonic diapause is triggered by the uterine environment and secretion of uterine factors into the uterine lumen. Overall, the gene ontology analysis indicated that there are substantial modifications of the mink maternal uterine environment presumably associated with increases uterine secretions at the resumption of embryo development after embryonic diapause. The 10 selected genes that were chosen to validate the SSH are potentially interesting in the context of the present study, namely *GDF3* and the three polyamine-related genes, *ODC1*, *SAT1* and *AZI1*. Both GDF3 and polyamines have been reported to be secreted and strongly implicated in the regulation of cell proliferation (Wallace, Fraser et al. 2003; Levine and Brivanlou 2006), and could therefore be potential uterine factors controlling emergence from embryonic diapause. Further investigations of these factors are now underway in *in vivo* pregnant mink females during diapause and reactivation, but also in *in vitro* mink embryos in diapause and in trophoblastic cell culture.

As chromatin and tissue remodeling factors, *HGMN1* and *SPARC* respectively, illustrate specific uterine modifications associated with exit from embryonic diapause and subsequent implantation, as confirmed by the detailed analysis of spatio-temporal gene expression in the mink uterus that was undertaken. *HMGN1*

was substantially elevated in the mink uterus during the early stages of embryo reactivation in mink, specifically in the cytoplasmic compartment of endometrial epithelial and stromal cells. *HMGN1* encodes for a non-histone nuclear protein which specifically binds to nucleosomes, promotes chromatin decondensation and induces transcriptional activation of downstream genes (reviewed by (Gerlitz 2010). Cytoplasmic distribution of HMGN1 was previously reported and associated with the mitosis phase while HMGN1 nucleic localization was correlated with interphase of the cell cycle (Louie, Gloor et al. 2000), thus suggesting that uterine cell proliferation at mink embryo reactivation may be in part a HMGN1-dependant process during emergence from embryonic diapause. Furthermore, we report, for the first time *HMGN1* expression during embryo implantation. In the mink implantation sites, HMGN1 was strongly detected in the extraembryonic part of the developing placenta. A similar expression pattern of the high mobility group I(Y) (HMGI(Y)) in human trophoblast suggested a potential role of HMGI(Y) in trophoblast invasion of maternal endometrium (Bamberger, Makrigiannakis et al. 2003). We also observed that HMGN1 exhibits a tissue-specific subcellular distribution in the mink uterus during implantation. HMGN1 was mainly found in the nucleus of the trophoblastic plaques and fetal capillaries of the trophoblastic villi. In contrast, a cytoplasmic HMGN1 distribution appears to be more specific to the invading syncytiotrophoblast and the maternal endometrial epithelial parts at the anti- and mesometrial poles of implantation site but also in inter-implantation sites. This HMGN1 tissue-specific subcellular expression may reflect specific functions of HMGN1 in the implantation of the mink blastocysts: Even though

further experiments are required to evaluate those functions in the mink embryo at reactivation and subsequent implantation, our results highlight a differential expression and potentially a role for HMGN1 in the uterus during the preimplantation and in the implantation process.

The present findings also revealed an increase in *SPARC* gene expression at the emergence from embryonic diapause in the mink uterus and thereafter, specifically in inter-implantation sites. Since *Sparc* encodes for a secreted glycoprotein belonging to the matricellular protein superfamily, modulators of cell-cell and cell-matrix interactions, it is involved in tissue remodeling (Sage, Johnson et al. 1984). Its gene expression has previously been reported to be progesterone-responsive in ovine uteri before embryo implantation (Gray, Abbey et al. 2006), but also in uteri from cycling humans (Dassen, Punyadeera et al. 2007) and cycling cattle (Mitko, Ulbrich et al. 2008) during the proliferative phase. Therefore, *SPARC* upregulation in the mink uterus at reactivation may be a product of the reactivation of the corpus luteum and increased progesterone secretion associated with embryo reactivation (Murphy, Mead et al. 1983). Since SPARC was described as an antiadhesive factor (Murphy-Ullrich, Lane et al. 1995), SPARC may serve as an important uterine factor which prevents precocious mink embryo implantation during the period of embryo reactivation. Alternatively, it could direct embryos to implantation sites in order to ensure embryo spacing. The fact that apical poles of uterine luminal epithelial cells facing the uterine lumen were strongly stained for SPARC at reactivation, in inter-implantation and the mesometrial pole of implantation site reinforces this hypothesis. We were nonetheless surprised to

observe a strong nuclear expression of SPARC specifically at the antimesometrial pole of implantation site, in the glandular epithelial and stromal cells on the day of implantation, and in the maternal symplasma and glandular epithelium underlying the myometrium at three days after implantation. The expression of *SPARC* was previously reported in mouse (Holland, Harper et al. 1987; White, Robb et al. 2004) and human deciduoma (Wewer, Albrechtsen et al. 1988) and, specifically in the cytoplasm of the endometrial decidualized stromal cells. In the mink, decidualization of stromal cells does not take place during placentation however, degradation of glandular epithelium occurs and results in the formation of the maternal symplasma at the fundi of the glands which are being invaded by trophoblast (Song 1998). Our results strongly support a potential role of SPARC in degradation of the mink maternal endometrium occurring at implantation to allow the maternal-fetal labyrinth to develop. This notwithstanding, SPARC was clearly specific to nuclei of endometrial cells at implantation sites in mink, contrary to its cytoplasmic localization in the mouse and human deciduoma (Wewer, Albrechtsen et al. 1988; White, Robb et al. 2004). The presence of SPARC in the nucleus was previously correlated with inhibition of cell proliferation of mink lung epithelial cells (Schiemann, Neil et al. 2003) and epithelial cells from human bladder (Kosman, Carmean et al. 2007). Therefore, the nucleic localization of SPARC at implantation sites may reflect its potential role in preventing endometrial cell proliferation during placental development in the mink. Furthermore, SPARC expression was observed in the mink fetal component of the placenta, mainly in the trophoblastic plaques and fetal capillaries. Similarly, *SPARC* mRNA was found to be increased in

the mouse embryo, principally in the extra-embryonic tissue invading the placenta (Mason, Murphy et al. 1986; Howe, Overton et al. 1988). Collectively, our results strongly suggest a role for SPARC during embryo reactivation and implantation in the mink. However, the fact that SPARC exhibits a differential subcellular distribution pattern during embryo implantation raises for the first time, the question whether SPARC could be involved in different processes during that window of pregnancy such as, the embryo spacing and / or endometrial degradation in response to placental development.

To conclude, the present findings successfully depicted a transcriptomic view of a carnivore endometrium during embryo reactivation, before embryo implantation occurs. The analysis of the uterine transcriptome demonstrates substantial modifications in the maternal uterine environment associated with embryo reactivation, such as chromatin remodeling, cell-cell and cell-matrix adhesion and cell proliferation as exhibited by increased in *HMGN1* and *SPARC* expression during that specific window of preimplantation embryo development. Furthermore, we have demonstrated that *HMGN1* and *SPARC* genes follow a specific expression pattern during the implantation process and thereafter during the post-implantation period. Even though molecular and cellular functions of HMGN1 and SPARC remain to be elucidated in the context of peri-implantation processes, our results open new avenues to get a better understanding of uterine modifications associated with mink embryo reactivation and consequent embryo implantation.

E. Acknowledgements

The authors acknowledge the participation of Benoit Labrecque, Vickie Roussel, Flavia Lopes, and Catherine Charron for technical support and sample collection and, Steeve Methot, Mario Binelli and Guy Beauchamp for help in statistical analysis.

F. References

Altschul, S. F., W. Gish, et al. (1990). "Basic local alignment search tool." J Mol Biol **215**(3): 403-410.

Bamberger, A. M., A. Makrigiannakis, et al. (2003). "Expression of the high-mobility group protein HMGI(Y) in human trophoblast: potential role in trophoblast invasion of maternal tissue." Virchows Arch **443**(5): 649-654.

Bininda-Emonds, O. R., J. L. Gittleman, et al. (1999). "Building large trees by combining phylogenetic information: a complete phylogeny of the extant Carnivora (Mammalia)." Biol Rev Camb Philos Soc **74**(2): 143-175.

Birger, Y., K. L. West, et al. (2003). "Chromosomal protein HMGN1 enhances the rate of DNA repair in chromatin." Embo J **22**(7): 1665-1675.

Chang, M. C. (1968). "Reciprocal insemination and egg transfer between ferrets and mink." J Exp Zool **168**(1): 49-59.

Chen, Y., Y. Zhang, et al. (2005). "SPD--a web-based secreted protein database." Nucleic Acids Res **33**(Database issue): D169-173.

Dassen, H., C. Punyadeera, et al. (2007). "Progesterone regulation of implantation-related genes: new insights into the role of oestrogen." Cell Mol Life Sci **64**(7-8): 1009-1032.

Desmarais, J. A., V. Bordignon, et al. (2004). "The escape of the mink embryo from obligate diapause." Biol Reprod **70**(3): 662-670.

Desmarais, J. A., F. L. Lopes, et al. (2007). "The peroxisome proliferator-activated receptor gamma regulates trophoblast cell differentiation in mink (Mustela vison)." Biol Reprod **77**(5): 829-839.

Dey, S. K., H. Lim, et al. (2004). "Molecular cues to implantation." Endocr Rev **25**(3): 341-373.

Diatchenko, L., Y. F. Lau, et al. (1996). "Suppression subtractive hybridization: a method for generating differentially regulated or tissue-specific cDNA probes and libraries." Proc Natl Acad Sci U S A **93**(12): 6025-6030.

Enders, R. (1952). "Reproduction in the mink (Mustela vison). ." Proc Am Philos Soc **96**: 691-755.

Fozard, J. R., M. L. Part, et al. (1980). "Inhibition of murine embryonic development by alpha-difluoromethylornithine, an irreversible inhibitor of ornithine decarboxylase." Eur J Pharmacol **65**(4): 379-391.

Fujiwara, H., K. Tatsumi, et al. (2003). "Human blastocysts and endometrial epithelial cells express activated leukocyte cell adhesion molecule (ALCAM/CD166)." J Clin Endocrinol Metab **88**(7): 3437-3443.

Gerlitz, G. (2010). "HMGNs, DNA repair and cancer." Biochim Biophys Acta **1799**(1-2): 80-85.

Gray, C. A., C. A. Abbey, et al. (2006). "Identification of endometrial genes regulated by early pregnancy, progesterone, and interferon tau in the ovine uterus." Biol Reprod **74**(2): 383-394.

Hansson, A. (1947). "The physiology of reproduction in mink (Mustela vison) with special reference to delayed implantation." Acta Zoologica **28**: 1–136.

Hock, R., T. Furusawa, et al. (2007). "HMG chromosomal proteins in development and disease." Trends Cell Biol **17**(2): 72-79.

Hoffmann, R., Valencia, A. (2004). "A Gene Network for Navigating the Literature." Nature Genetics **36**: 664.

Holland, P. W., S. J. Harper, et al. (1987). "In vivo expression of mRNA for the Ca++-binding protein SPARC (osteonectin) revealed by in situ hybridization." J Cell Biol **105**(1): 473-482.

Howe, C. C., G. C. Overton, et al. (1988). "Expression of SPARC/osteonectin transcript in murine embryos and gonads." Differentiation **37**(1): 20-25.

Jones, R. L., C. Stoikos, et al. (2006). "TGF-beta superfamily expression and actions in the endometrium and placenta." Reproduction **132**(2): 217-232.

Kabir-Salmani, M., S. Shiokawa, et al. (2005). "Tissue transglutaminase at embryo-maternal interface." J Clin Endocrinol Metab **90**(8): 4694-4702.

Krebs, C., H. Winther, et al. (1997). "Vascular interrelationships of near-term mink placenta: light microscopy combined with scanning electron microscopy of corrosion casts." Microsc Res Tech **38**(1-2): 125-136.

Lefevre, P. L. and B. D. Murphy (2009). Differential gene expression in the uterus and blastocyst during the reactivation of embryo development in a model of delayed implantation. Human Embryogenesis, Method and Protocols. J. Lafond and C. Vaillancourt. Montreal, Humana Press. **550:** 11-61.

Levine, A. J. and A. H. Brivanlou (2006). "GDF3, a BMP inhibitor, regulates cell fate in stem cells and early embryos." Development **133**(2): 209-216.

Lopata, A., M. C. Sibson, et al. (2001). "Expression and localization of thioredoxin during early implantation in the marmoset monkey." Mol Hum Reprod **7**(12): 1159-1165.

Louie, D. F., K. K. Gloor, et al. (2000). "Phosphorylation and subcellular redistribution of high mobility group proteins 14 and 17, analyzed by mass spectrometry." Protein Sci **9**(1): 170-179.

Mason, I. J., D. Murphy, et al. (1986). "Developmental and transformation-sensitive expression of the Sparc gene on mouse chromosome 11." Embo J **5**(8): 1831-1837.

Mead, R. A., A. W. Rourke, et al. (1979). "Changes in uterine protein synthesis during delayed implantation in the western spotted skunk and its regulation by hormones." Biol Reprod **21**(1): 39-46.

Mitko, K., S. E. Ulbrich, et al. (2008). "Dynamic changes in messenger RNA profiles of bovine endometrium during the oestrous cycle." Reproduction **135**(2): 225-240.

Mohamed, O. A., M. Bustin, et al. (2001). "High-mobility group proteins 14 and 17 maintain the timing of early embryonic development in the mouse." Dev Biol **229**(1): 237-249.

Moreau, G. M., A. Arslan, et al. (1995). "Development of immortalized endometrial epithelial and stromal cell lines from the mink (Mustela vison) uterus and their effects on the survival in vitro of mink blastocysts in obligate diapause." Biol Reprod **53**(3): 511-518.

Muller, S., P. Scaffidi, et al. (2001). "New EMBO members' review: the double life of HMGB1 chromatin protein: architectural factor and extracellular signal." Embo J **20**(16): 4337-4340.

Murphy-Ullrich, J. E., T. F. Lane, et al. (1995). "SPARC mediates focal adhesion disassembly in endothelial cells through a follistatin-like region and the Ca(2+)-binding EF-hand." J Cell Biochem **57**(2): 341-350.

Murphy, B. D., P. W. Concannon, et al. (1981). "Prolactin: the hypophyseal factor that terminates embryonic diapause in mink." Biol Reprod **25**(3): 487-491.

Murphy, B. D. and D. A. James (1974). "The effects of light and sympathetic innervation to the head on nidation in mink." J Exp Zool **187**(2): 267-276.

Murphy, B. D., R. A. Mead, et al. (1983). "Luteal contribution to the termination of preimplantation delay in mink." Biol Reprod **28**(2): 497-503.

Papke, R. L., P. W. Concannon, et al. (1980). "Control of luteal function and implantation in the mink by prolactin." J Anim Sci **50**(6): 1102-1107.

Pfaffl, M. W. (2001). "A new mathematical model for relative quantification in real-time RT-PCR." Nucleic Acids Res **29**(9): e45.

Reese, J., S. K. Das, et al. (2001). "Global gene expression analysis to identify molecular markers of uterine receptivity and embryo implantation." J Biol Chem **276**(47): 44137-44145.

Ruijter, J. M., C. Ramakers, et al. (2009). "Amplification efficiency: linking baseline and bias in the analysis of quantitative PCR data." Nucleic Acids Res **37**(6): e45.

Sage, H., C. Johnson, et al. (1984). "Characterization of a novel serum albumin-binding glycoprotein secreted by endothelial cells in culture." J Biol Chem **259**(6): 3993-4007.

Shaw, G. and M. B. Renfree (1986). "Uterine and embryonic metabolism after diapause in the tammar wallaby, Macropus eugenii." J Reprod Fertil **76**(1): 339-347.

Song, J. (1998). Implantation in the Mink (Mustela vison): Morphologic Progression of Trophoblast Invasion and Uterine Gene Expression. Faculté de Médecine Véterinaire. Montreal, CA, Université de Montreal.

Stros, M. (2010). "HMGB proteins: interactions with DNA and chromatin." Biochim Biophys Acta **1799**(1-2): 101-113.

Takemura, Y., Y. Osuga, et al. (2006). "Expression of adiponectin receptors and its possible implication in the human endometrium." Endocrinology **147**(7): 3203-3210.

Van Winkle, L. J. and A. L. Campione (1983). "Effect of inhibitors of polyamine synthesis on activation of diapausing mouse blastocysts in vitro." J Reprod Fertil **68**(2): 437-444.

Wallace, H. M., A. V. Fraser, et al. (2003). "A perspective of polyamine metabolism." Biochem J **376**(Pt 1): 1-14.

Wewer, U. M., R. Albrechtsen, et al. (1988). "Osteonectin/SPARC/BM-40 in human decidua and carcinoma, tissues characterized by de novo formation of basement membrane." Am J Pathol **132**(2): 345-355.

White, C. A., L. Robb, et al. (2004). "Uterine extracellular matrix components are altered during defective decidualization in interleukin-11 receptor alpha deficient mice." Reprod Biol Endocrinol **2**: 76.

Zhao, Y. C., Y. J. Chi, et al. (2008). "Polyamines are essential in embryo implantation: expression and function of polyamine-related genes in mouse uterus during peri-implantation period." Endocrinology **149**(5): 2325-2332.

Zicari, A., C. Centonze, et al. (2008). "Estradiol 17-beta and progesterone modulate inducible nitric oxide synthase and high mobility group box 1 expression in human endometrium." Reprod Sci **15**(6): 559-566.

G. Figures, tables and supplementary data

Table 8. Primers.

Primer sequences and concentrations used to validate the mink uterine differential expression pattern of ten selected cDNA sequences homologous to known genes using quantitative real-time-PCR analysis.

Genes[a]	Primer sequences	Concentrations (nM)
ADIPOR1	F 5' – CCATCCATTTTTGTAGCACACTTTT – 3'	300
	F 5' – AAGTTGGTGGCTTTGTTCTTCCT – 3'	300
ALCAM	F 5' – CACCAGTTTTCCTTTTCCTCCTAA– 3'	300
	F 5' – CTTTCAAGCAGAAGCCTGGTTT – 3'	900
AZI1	F 5' - GAGGTACTGAGCCAAACTAAACTTAAATG - 3'	900
	R 5' - CAGGCTAAAACTTTGGGAAAGG - 3'	900
GDF3	F 5' - TCTCGGGAGCCCCCATT - 3'	900
	R 5'- TCACCCCAGAAGTTCCAACCT - 3'	900
HMGN1	F 5' - GATGATGTTCCGCCCTTCTC - 3'	900
	R 5' - TCACCCCAGAAGTTCCAACCT - 3'	900
ODC1	F 5' – CTACAACGGATTCCAGATGATGAC – 3'	900
	F 5' – GGTGGCAATCCGCAAAAC – 3'	300
SAT1	F 5' – GCAGGTACTCCTTGTCGATCTTG – 3'	150
	F 5' – TGGAACGAACCATCTATCAACTTC – 3'	900
SPARC	F 5' - CATAACATGACTATCGATGCCTCTTG - 3'	900
	R 5' - CCACCCATACGCCACTAGGA - 3'	300
TGM2	F 5' - GTCAAGGTGAGGGTGGATCTG - 3'	300
	R 5' - AGGCGGGACCAATGATGA - 3'	900
TXNL1	F 5' – CCAACAATATATCAGCAACACCTACA – 3'	300
	F 5' – CCAACAGCATCTGCTCCTTGA – 3'	900

[a]*ADIPOR1:* adiponectin receptor 1*; ALCAM:* activated leukocyte cell adhesion molecule*; GDF3:* growth and differenciation factor 3*; HMGN1:* high-mobility group nucleosome binding domain 1*;ODC1:* ornithine decarboxylase*; AZI1:* AZI inhibitor 1*; SPARC:* secreted protein, acidic, cysteine-rich*; SAT1:* spermidine/spermine N1-acteyltransferase*; TXNL1:* thioredoxin-like 1*; TGM2:* transglutaminase 2.

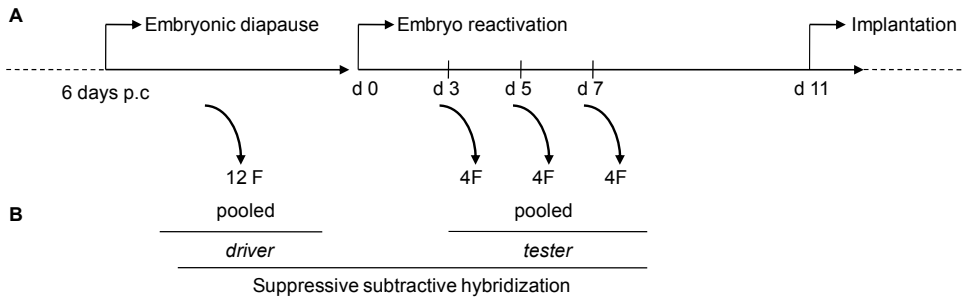

Figure 27. Experimental design for suppressive subtractive hybridization performed on mink uteri between diapause and reactivation of blastocyst.

A) Whole uterine samples were collected from 12 pregnant mink females during embryonic diapause and from four pregnant females in each of day (d) 3, d5 and d7 after the reactivation of embryonic development. B) Uterine samples collected at d3, d5 and d7 after reactivation were pooled and used as the tester to perform the suppressive subtraction hybridization against the driver, which consisted of pooled uterine samples collected during diapause. p.c, post coïtus; F, females; d, day.

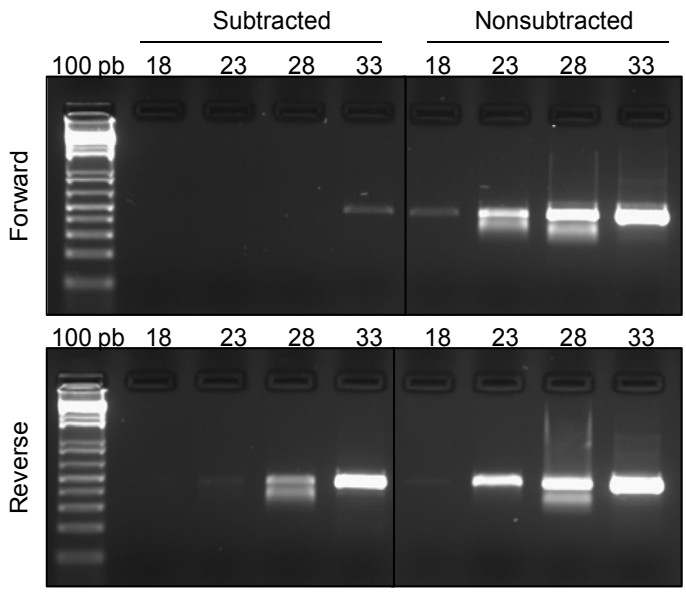

Figure 28. Efficiency of the forward and reverse subtraction hybridization.

The subtraction efficiency of the SSH was assessed by measuring the difference of PCR cycle numbers required for detection of *PPIA* amplification between subtracted cDNA and nonsubtracted cDNA from the forward (upper panel) and reverse subtraction (lower panel). Complementary DNA was collected after 18, 23, 28 and 33 cycles of PCR amplification. Fifteen and five additional amplification cycles were respectively necessary in the forward and reverse subtracted compared with the nonsubtracted library to detect *PPIA* amplicon, thus reflecting a reduction of *PPIA* mRNA abundance after the subtraction.

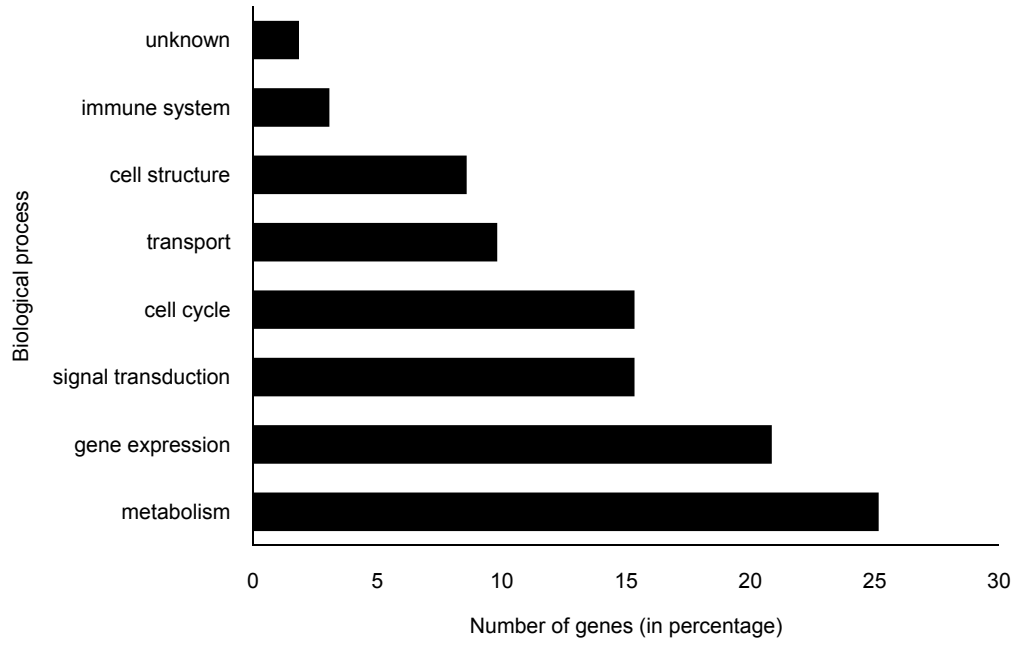

Figure 29. Gene ontology.

Distribution of biological process categories of the 123 nonredundant identified genes differentially expressed in the mink uterus at embryo reactivation, according to their biological functions annotations in the GENATLAS database. Identified genes were those having similarities >89% with sequences of known genes**.**

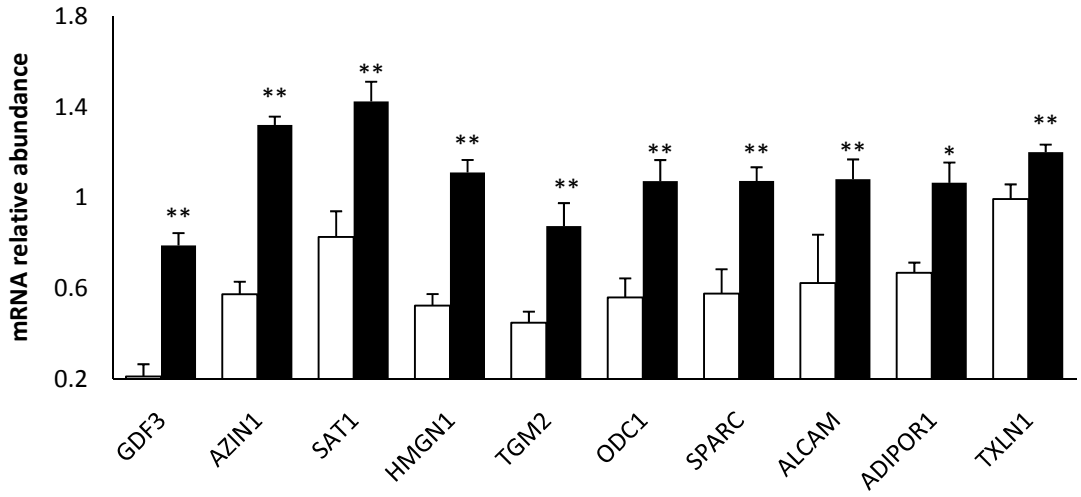

Figure 30. Validation of 10 differentially expressed genes in uteri with blastocysts in diapause and those in reactivation that were identified in the SSH library.

The differential gene expression patterns between uteri with embryos in diapause and reactivated embryos was determined for *adiponectin receptor 1* (*ADIPOR1*), *activated leukocyte cell adhesion mole*cule (*ALCAM*), *growth and differentiation factor 3* (*GDF3*), *high-mobility group nucleosome binding domain 1* (*HMGN1*), *ornithine decarboxylase 1* (*ODC1*), *antizyme inhibitor 1* (*AZI1*), *secreted protein, acidic cysteine-rich* (*SPARC*), *spermidine/spermine N_1-acetyltransferase* (*SAT1*), *thioredoxin-like 1* (*TXNL1*) *and transglutaminase 2* (*TGM2*) by quantitative real-time PCR. The relative abundance of mRNA was measured in triplicate for each gene in uterine samples collected from three individuals collected during diapause and in those from days (d) 3, d5 and d7 after embryo reactivation. Data represent the relative abundance (mean ± SEM) after embryo reactivation (black bars) and during embryonic diapause (open bars). Gene expression was increased ($P< 0.05$) at reactivation of embryos for the 10 analyzed genes.

A

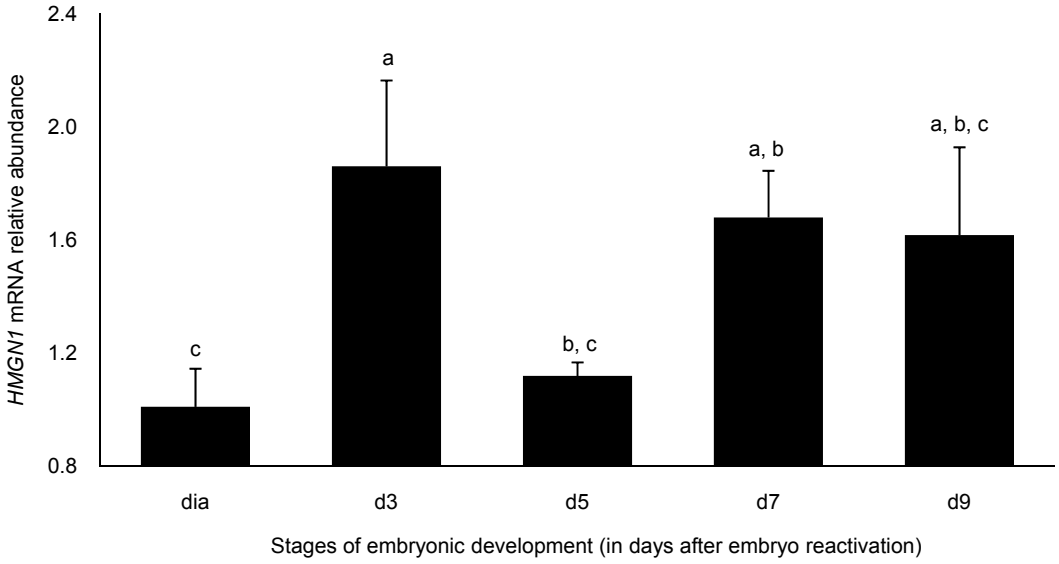
2.4
2.0
1.6
1.2
0.8
HMGN1 mRNA relative abundance
a
a, b
a, b, c
c
b, c
dia
d3
d5
d7
d9
Stages of embryonic development (in days after embryo reactivation)

B

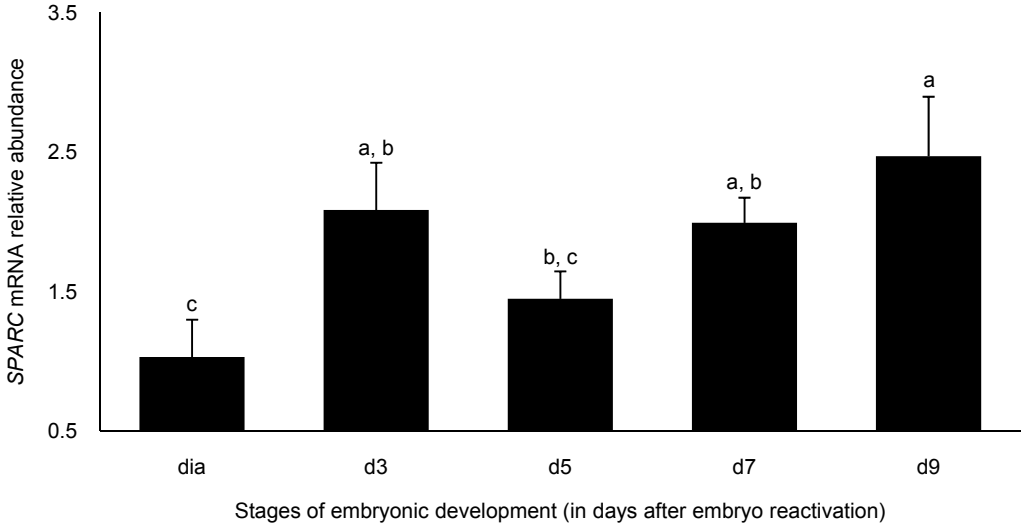
3.5
2.5
1.5
0.5
SPARC mRNA relative abundance
a
a, b
a, b
b, c
c
dia
d3
d5
d7
d9
Stages of embryonic development (in days after embryo reactivation)

Figure 31. Temporal gene expression of *HMGN1* and *SPARC* in mink uteri at blastocyst reactivation.

Temporal expression pattern for high mobility group nucleosomes binding domain 1 (*HMGN1*) (**A**) and secreted protein, acidic, cysteine-rich (*SPARC*) (**B**) genes in the mink uterus at reactivation of embryos. The abundance of *HMGN1* and *SPARC* mRNAs was measured by real time PCR (in triplicate) in whole uterine samples that were collected from three individuals during diapause (dia) and on each of days (d) 3, 5, 7 and 9 after embryo reactivation. Data represent mean ratios ± SEM relative to *GAPDH* and values for uteri with embryo in diapause. Means with different letters are different $P<0.05$.

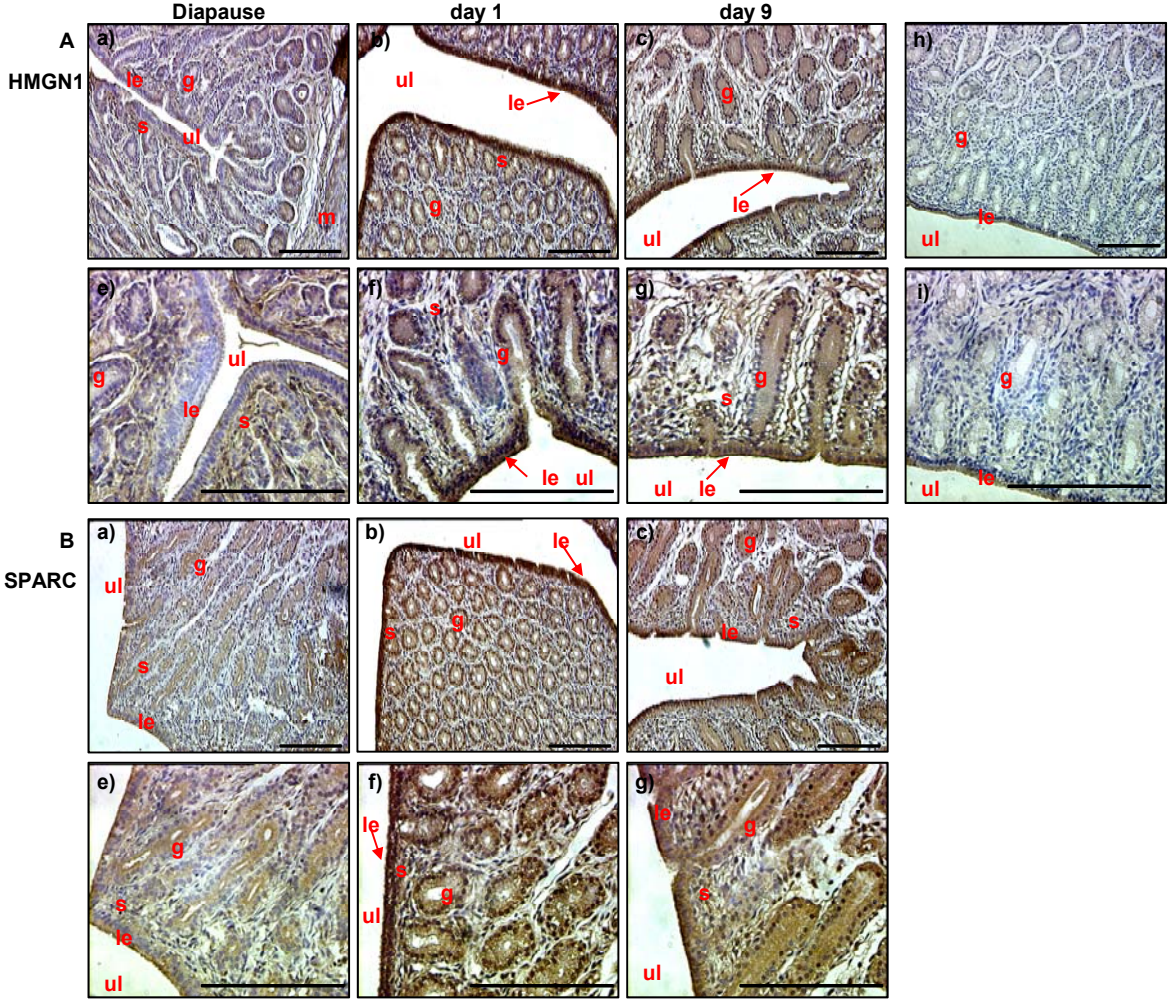
Diapause
day 1
day 9
A
HMGN1
a)
le
g
s
ul
m
b)
ul
le
s
g
c)
g
le
ul
h)
g
le
ul
e)
ul
g
le
s
f)
s
g
le ul
g)
g
s
ul le
i)
g
le
ul
B
SPARC
a)
g
ul
s
le
b)
ul
le
s
g
c)
g
le
s
ul
e)
g
s
le
ul
f)
le
s
g
ul
g)
le
g
s
ul

Figure 32. Immunolocalization of HMGN1 and SPARC in uteri of mink during diapause and blastocyst reactivation.

Immunolocalization of HMGN1 (**A**) and SPARC (**B**) was performed for mink uterine cross-sections during diapause (**a, e**), at day 1 (**b, f**) and day 9 (**c, g**) after prolactin-induced reactivation. **A**. High mobility group binding nucleosome N1 expression was increased between uteri with embryo in diapause (**a**) and with reactivated embryo (**b**), specifically in the cytoplasm of luminal and glandular epithelial cells and subepithelial stromal cells (**e, f**), and its distribution pattern remained the same until day 9 after prolactin-induced reactivation (**c**, **g**). **B**. The expression of SPARC increased between uteri with embryos in diapause (**a**) and with reactivated uteri (**b**), specifically in the cytoplasm of luminal and glandular epithelial cells (**e, f**), and its distribution pattern remained the same to day 9 after reactivation (**c**, **g**). Neither HMGN1 and SPARC were detectable in negative control uterine sections (**h, i)**. Bars correspond to 200μm. g: gland; le: luminal epithelium; m: myometrium; s:stroma; ul: uterine lumen.

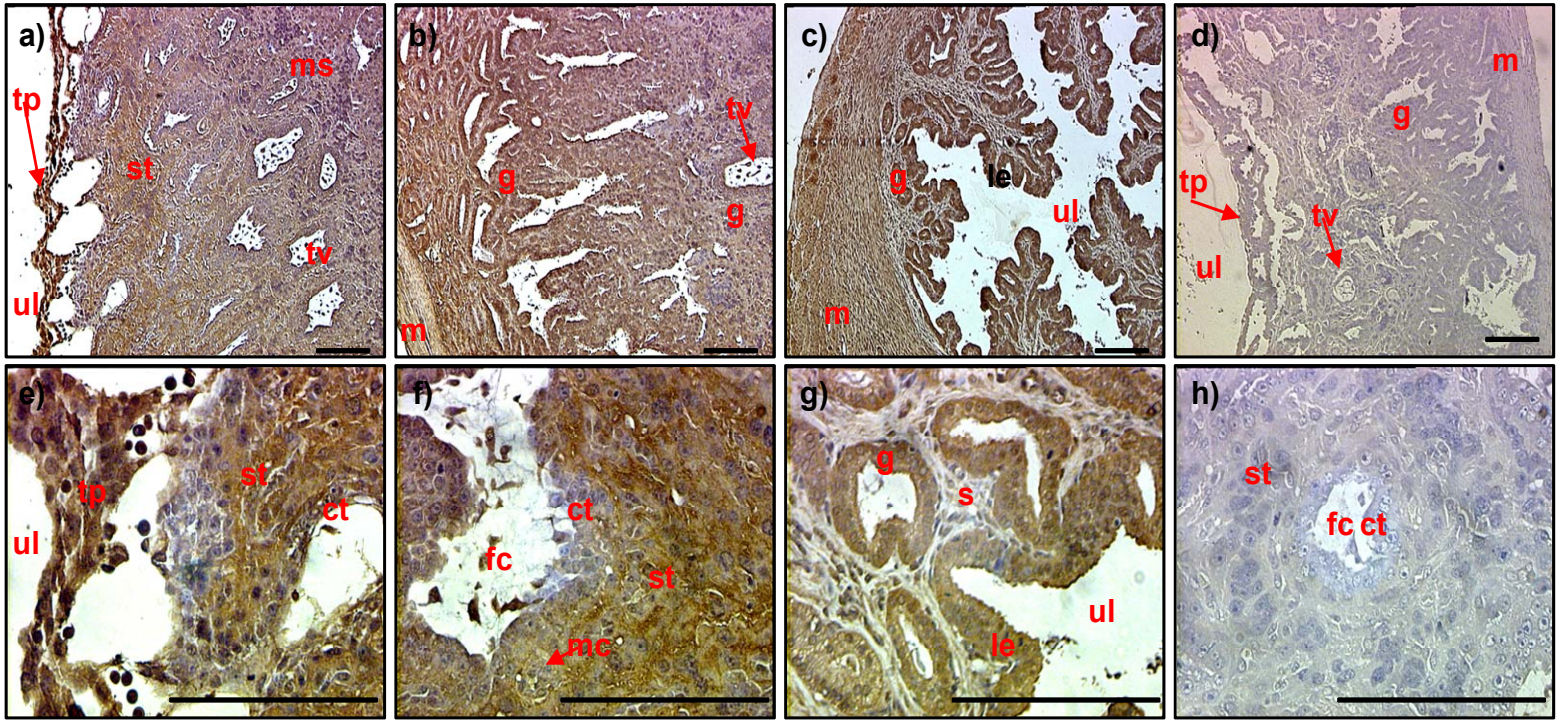
a)
ms
tp
st
tv
ul
b)
tv
g
g
m
c)
g
le
ul
m
d)
m
g
tp
tv
ul
e)
tp
st
ct
ul
f)
ct
fc
st
mc
g)
g
s
ul
le
h)
st
fc ct

Figure 33. Immunolocalization of HMGN1 in mink uteri after implantation.

Immunolocalization of HMGN1 in mink uterine cross-sections was determined at implantation and inter-implantation sites on day 14 after prolactin-induced blastocyst reactivation (3 days post-implantation). HMGN1 was strongly expressed at both implantation (**a, b**) and inter-implantation (**c**) sites. At higher magnification, HMGN1 was localized in the cytoplasm and nuclei of trophoblastic plaque cells (**e**), in nuclei of endothelial cells of fetal capillaries (**f**) and in the cytoplasm of syncytiotrophoblast cells (**e, f**) in the fetal maternal labyrinth at the antimesometrial pole of implantation site. Its expression was also detected in the glandular epithelium and stroma underlying the myometrium and, in the myometrium (**b**). In inter-implantation sites, HMGN1 was localized only in the cytoplasm of uterine epithelium (**g**) and myometrium (**c**). HMGN1 was not detectable in negative control tissues (**d, h**). The bars correspond to 200μm. ct: cytotrophoblast; fc: fetal capillary g: gland; le: luminal epithelium; m: myometrium; ms: maternal symplasma; s:stroma; tp: trophoblastic plaque; tv: trophoblastic villi; st: syncytiotrophoblast; ul: uterine lumen.

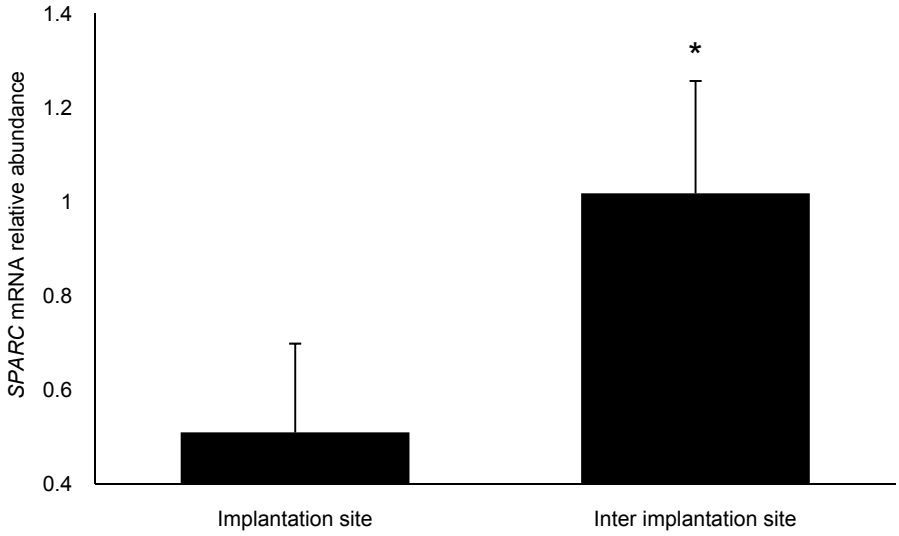

Figure 34. *SPARC* gene expression at implantation and inter-implantation sites of mink uteri.

SPARC mRNA abundance was quantified in triplicate by real time PCR analysis at implantation and inter-implantation sites isolated from whole uterine sample collected from three minks on day 11 after embryo reactivation. The data represent relative mRNA abundance (mean ± SEM) relative to *GAPDH*. The *SPARC* gene expression was higher ($P<0.05$) at inter-implantation than at implantation site.

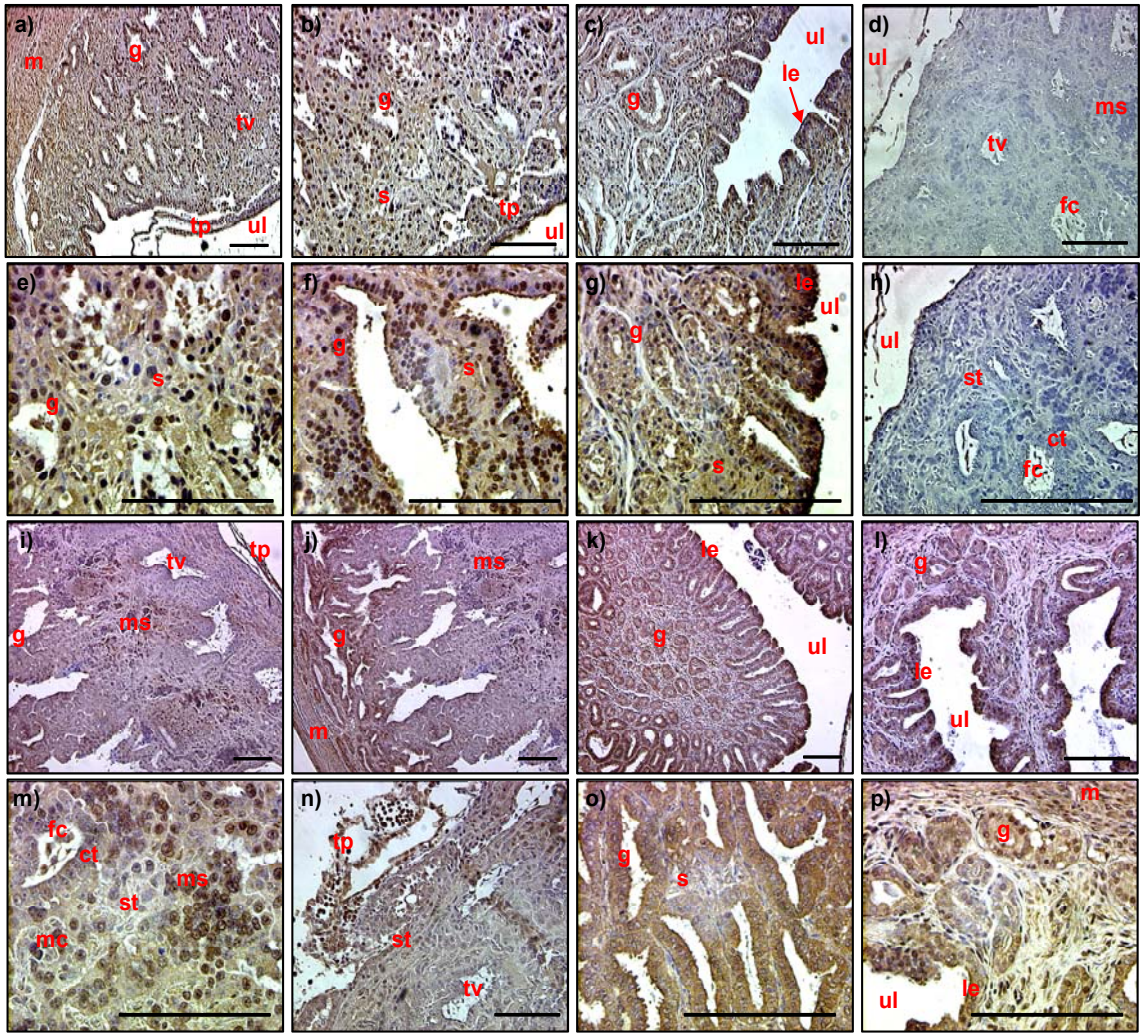
a)
m
g
tv
tp
ul
b)
g
s
tp
ul
c)
ul
le
g
d)
ul
ms
tv
fc
e)
s
g
f)
g
s
g)
le
ul
g
s
h)
ul
st
ct
fc
i)
tv
tp
g
ms
j)
ms
g
m
k)
le
g
ul
l)
g
le
ul
m)
fc
ct
ms
st
mc
n)
tp
st
tv
o)
g
s
p)
m
g
ul
le

Figure 35. Immunolocalization of SPARC at implantation and inter-implantation sites in mink uteri.

Immunolocalization of SPARC were determined in mink uterine cross-sections at implantation and inter-implantation sites on day 11 after reactivation (a-h), on the day of implantation, and at day 14 after reactivation of blastocysts or day 3 post-implantation (i-p). At early implantation, SPARC was detected at implantation (**a, b**) and inter-implantation (**c**) sites. At implantation sites, SPARC had a nuclear localization in the endometrial epithelial and stromal cells and in trophoblastic plaques (**b**, **e**). Hypertrophied uterine gland and stroma adjacent to the myometrium at implantation sites also had nuclear localization of SPARC (**f**). In inter-implantation sites, SPARC was observed in the cytoplasm of the stromal, glandular and luminal epithelial cells (**c, g**). SPARC was not detected in negative control tissues (**d, h**). At three days after implantation, SPARC was localized mainly in the maternal symplasma, in epithelial cells of hypertrophied uterine glands and in myometrium (**i, j**). Higher magnifications revealed nuclear localization of SPARC in the maternal symplasma, trophoblastic plaques and endothelial cells of fetal capillaries (**m, n**), and cytoplasmic localization of SPARC in epithelium of hypertrophied uterine glands (**o**). The mesometrial pole of implantation sites (**k**) and inter-implantation sites (**l**) were positive for SPARC, specifically in the cytoplasm of endometrial epithelial cells (**p**). Bars correspond to 200μm. ct: cytotrophoblast; fc: fetal capillary g: gland; le: luminal epithelium; m: myometrium; ms: maternal symplasma; s:stroma; tp: trophoblastic plaque; tv: trophoblastic villi; st: syncytiotrophoblast; ul: uterine lumen.

Table 9. Differentially expressed genes identified in the mink uterus between diapause and reactivation of blastocysts (Supplementary data).

GenBank accession No[a]	**Homologous genes**[b]	**Gene symbol**	**Nb of clones**
GH271897	*Cf beta-defensin 139*	*DEFB139*	56
GH271826	*Cf tumor rejection antigen 1*	*HSP90B1*	7
GH271918, GH271958, GH271985	*Cf dynein, cyplasmic, light peptide*	*DYNC1LI1*	4
GH272013, GH272015	Cf protein transport protein Sec24B	SEC24B	3
GH271812	Cf spermidine/spermine N1-acetyl transferase	SAT1	3
GH271832	Cf protein inhibitor of activated STAT protein 3	PIAS3	3
GH694000	Cf adiponectin receptor 1	ADIPOR1	3
GH271984	Cf RNA-binding region containing protein 2	RBM39	3
GH271916, GH694008	*Cf DnaJ homolog subfamily B member 1 (Heat shock 40 kDa protein 1)*	*DNAJB1*	3
GH271980	*Cf signal peptide, CUB domain, EGF-like 2*	*SCUBE2*	3
GH271808	Cf ATPase, H+ transporting,lysosomal 34kDa, V1 subunit D,	ATP6V1D	2
GH271989	Fc michondrial ATP synthase, H+ transporting F1 complex beta subunit	ATP5B	2
GH271800	Cf karyopherin beta 1	KPNB1	2
GH271869	Cf chromatin-modifying protein 7	CHMP7	2
GH693995	Cf nuclear RNA export factor 1	NXF1	2
GH271813	Cf ornithine decarboxylase	ODC1	2
GH271895	*Cf neighbor of breast cancer gene 1*	*NBR1*	2
GH27183&	*Cf programmed cell death 10*	*PDCD10*	2

Table 9. (Supplementary data). (Continued).

GenBank accession No[a]	Homologous genes[b]	Gene symbol	Nb of clones
GH271924	Cf cell growth regulatory gene 19 protein	CGRRF1	2
GH272049	Cf thioredoxin-like protein 1	TXNL1	2
GH272004	Hs kinesin-associated protein 3	KIFAP3	2
GH271967	*Cf leucine rich repeat (in FLII) interacting protein 2 isoform 2*	*LRRFIP2*	2
GH694001	Cf tousled-like kinase 1	TLK1	2
GH271846	Cf transcription initiation protein SPT4 homolog 2	SUPT4H2	2
GH271900	Cg 18S ribosomal RNA gene	RN18S1	2
GH272038	Cf 60S ribosomal protein L37a	RPL37A	2
GH271886	Cf SWI/SNF-related matrix-associated actin-dependent regular of chromatin a2	SMARCA2	2
GH272008	Cf thiopurine S-methyltransferase	TPMT	2
GH271819	Cf lysosomal protective protein precursor (Cathepsin A)	CTSA	2
GH271820	Cf glutamate dehydrogenase 1, michondrial precursor	GLUD1	2
GH272001	Bt isochorismatase domain containing 1	ISOC1	2
GH271803	*Mv NADH dehydrogenase subunit 4 (ND4)*	*MT-ND4*	2
GH272062, GH694010	Cf NADH dehydrogenase (ubiquinone) 1 beta subcomplex 8	NDUFB8	2
GH271803	*Mv NADH dehydrogenase subunit 4 (ND4)*	*MT-ND4*	2
GH272062, GH694010	Cf NADH dehydrogenase (ubiquinone) 1 beta subcomplex 8	NDUFB8	2
GH271896	Cf alcohol dehydrogenase [NADP+] (Aldehyde reductase)	AKR1A1	2
GH271962	Cf N-acylneuraminate cytidylyltransferase (CMP-N-acetylneuraminic acid synthetase)	CMAS	2
GH271937	Cf tsyrosine 3/trypphan 5 -monooxygenase activation protein, zeta	YWHAZI	2

Table 9. (Supplementary data). (Continued).

GenBank accession No[a]	Homologous genes[b]	Gene symbol	Nb of clones
GH272000	Cf S-adenosylhomocysteine hydrolase-like 1	AHCYL1	2
GH271974	*Cf secreted protein rich in cystein precursor*	*SPARC*	2
GH271933	Cf U2 small nuclear ribonucleoprotein A	SNRPA1	2
GH272064	Cf tubulin, beta 5	TUBB5	2
GH271941	*Cf G-rich RNA sequence binding factor 1*	*GRSF1*	2
GH271921	Cf ATP synthase michondrial F1 complex assembly factor 1	ATPAF1	1
GH271983	Cf ATP synthase, H+ transporting, michondrial F0 complex, subunit G	ATP5L	1
GH271834	Cf ATPase, H+ transporting, V1 subunit E isoform 1,	ATP6V1E1	1
GH271868	Cf michondrial H+ transporting ATP synthase F1	ATP5A1	1
GH271864	Cf importin-7	IPO7	1
GH271942	Cf zinc finger protein 638	ZNF638	1
GH271887	Hs sortilin 1	SORT1	1
GH271881	Cf adaptor-related protein complex 2, mu 1 subunit isoform b	AP2M1	1
GH271973	Bt clathrin heavy chain	CLTC	1
GH271954	*Cf destrin*	DSTN	1
GH271922	*Cf transmembrane emp24 protein transport domain containing 7*	*TMED7*	1
GH272014	Cf mitochondrial carnitine/acylcarnitine carrier protein	SLC25A20	1
GH272030	*Cf calcium-binding michondrial carrier protein Aralar2*	*SLC25A13*	1
GH271907	Cf LPS-responsive vesicle trafficking, beach and anchor containing	LRBA	1
GH693996	Cf E1B-55kDa-associated protein 5 isoform d	HNRPUL1	1

Table 9. (Supplementary data). (Continued).

GenBank accession No[a]	Homologous genes[b]	Gene symbol	Nb of clones
GH271811	Cf ornithine decarboxylase AZI inhibitor	AZI1	1
GH693997	Hs baculoviral IAP repeat-containing 4	XIAP	1
GH271892	Cf S-phase kinase-associated protein 1A isoform b (p45)	SKP2	1
GH271899	Cf abl-interacr 1 isoform c	ABI1	1
GH272009	*Cf protein disulfide-isomerase A6 precursor (Thioredoxin domain containing protein 7)*	*PDIA6*	1
GH272011	Ss growth arrest and DNA-damage-inducible protein alpha	GADD45A	1
GH271856	Cf ubiquitin-conjugating enzyme E2 D2	UBE2T	1
GH271979	*Cf growth differentiation facr 3 precursor*	*GDF3*	1
GH272023	Cf structural maintenance of chromosome 3 (Chondroitin sulfate proteoglycan 6)	SMC3	1
GH272035	Cf ubiquitin conjugation facr E4 A	UBE4A	1
GH271961	*Cf pleiotrophin precursor*	PTN	1
GH271882	Hs ring finger protein 130	RNF130	1
GH271815	Hs proline/serine-rich coiled-coil 2	ZFC3H1	1
GH271828	Cf transcription initiation factor TFIID subunit 10	TAF10	1
GH271840	Cf X-box binding protein 1	XBP1	1
GH271915	Mm mediar of RNA polymerase II transcription, subunit 31 homolog	MED31	1
GH271852	Mam transcription factor 7-like 2 (HMG box transcription factor 4)	TCF7L2	1
GH272005	Hs nuclear factor I/B (NFIB)	NFIB	1
GH694002	Hs heterogeneous nuclear ribonucleoprotein U (scaffold attachment facr A)	HNRNPU	1
GH272053	Cf MMS19 nucleotide excision repair homolog (S. cerevisiae)	MMS19	1

Table 9. (Supplementary data). (Continued).

GenBank accession No[a]	Homologous genes[b]	Gene symbol	Nb of clones
GH694003	Cf YTH domain family 3	YTHDF3	1
GH271928	Bt PRP38 pre-mRNA processing factor 38 (yeast) domain containing B	PRPF38B	1
GH271955	Cf methylosome protein 50	WDR77	1
GH271932	*Cf eukaryotic translation initiation factor 2-alpha kinase 4*	EIF2AK4	1
GH272027	Cf ribosomal protein P1 isoform 2	RPLP1	1
GH271910	Cf michondrial ribosomal protein L16	MRPL16	1
GH272055	Cf Lysyl-tRNA synthetase (Lysine--tRNA ligase) (LysRS)	KARS	1
GH271987	Cf nonhisne chromosomal protein HMG-14	HMGN1	1
GH271992	Cf H3 histone, family 3B	H3F3B	1
GH272066	Cf ring finger protein 20	RNF20	1
GH271939	Fc cysolic malate dehydrogenase	MDH1	1
GH271890	*Hs UDP-Gal:betaGlcNAc beta 1,4- galacsyltransferase*	B4GALT3	1
GH694005	Cf C-4 methylsterol oxidase (Methylsterol monooxygenase)	SC4MOL	1
GH271948	Cf choline/ethanolaminephosphotransferase	CEPT1	1
GH271904	*Cf protein-glutamine gamma-glutamyltransferase (Tissue transglutaminase)*	TGM2	1
GH271963	*Cf peptidyl-prolyl cis-trans isomerase B precursor*	PPIB	1
GH272043	*Mv cychrome oxidase subunit I (COX1)*	PTGS1	1
GH272084	Bt GDP-mannose pyrophosphorylase A	GMPPA	1
GH272085	Cf proteasome beta 5 subunit	PSMB5	1
GH272086	*Cf YME1-like 1 isoform 3*	YME1L1	1

Table 9. (Supplementary data). (Continued).

GenBank accession No[a]	Homologous genes[b]	Gene symbol	Nb of clones
GH272065	Cf signal peptide peptidase-like 2A	IMP3	1
GH694011	Mv michondrial gene for cychtorome b	MTCYB	1
GH271944	*Bt secreted modular calcium-binding protein 2*	SMOC2	1
GH271880	*Cf activated leukocyte cell adhesion molecule*	ALCAM	1
GH271903	Cf epithelial membrane protein-2	EMP2	1
GH694009	Cf ephrin receptor EphA7	EPHA7	1
GH271965	Mam ephrin B2	EFNB2	1
GH271970	Cf CD2 antigen (cyplasmic tail) binding protein 2	CD2BP2	1
GH271875	Mam protein tyrosine phosphatase, non-receptor type 11	PTPN11	1
GH271976	Cf acidic (leucine-rich) nuclear phosphoprotein 32 family, member E	ANP32E	1
GH271844	Cf protein C5orf5 (GAP-like protein N61)	FAM13B	1
GH271952	*Cf Rab12 protein*	RAB12	1
GH694012	*Cf RAN binding protein 9*	RANBP9	1
GH271908	*Cf tetratricopeptide repeat domain 14*	TTC14	1
GH271816	*Cf neurobeachin-like 1*	NBEAL1	1
GH271914	Mp basic H1 calponin	CNN1	1
GH271998	*Cf stromal cell-derived facr 2 precursor*	SDF2	1
GH694013	Fc caveolin 1	CAV1	1
GH272021	Cf M1-like 1 protein (Src activating and signaling molecule protein)	TOM1L1	1
GH272061	*Cf Src homology 2 domain containing adaptor protein B*	SHB	1

Table 9. (Supplementary data). (Continued).

GenBank accession No[a]	Homologous genes[b]	Gene symbol	Nb of clones
GH272088	Pt arrestin beta 1	ARRB1	1
GH694006	Mam sphingosine-1-phosphatase	SGPP1	1
GH271874	*Cf complement C1r subcomponent precursor*	C1R	1
GH272010	*Cf FERM, RhoGEF, and pleckstrin domain protein 1 isoform 1*	FARP1	1
GH694016	Cf myosin regulary light chain 2, nonsarcomeric	MYL12A	1
GH271945	*Hs ceroid-lipofuscinosis, neuronal 5*	CLN5	1
GH271809	*Cf coxsackie virus and adenovirus receptor*	CXADR	1

[a] GenBank accession numbers of differentially expressed cDNA sequences homologous to known and characterized genes from the current study.

[b] Known and characterized genes homologous to differentially expressed cDNA sequences with percentage of similarity was > 89 %, the E-value < 1.0 e^{-11} and the length of similarity > 100 nucleotides. Gene products listed in the Secretory Protein Database (SPD) are represented in italics. Cf, Canis familiaris; Fc, Felis catus; Hs, Homo sapiens; Bt, Bos taurus; Mv; Mustela vison ; Ss, Sus scorfa ; Mm, Mus musculus ; Mam, Macaca mulatta; Mp, Mustela putorius ; Pt, Pan troglodytes.

V. ARTICLE 3: THE POLYAMINES IN THE REPRODUCTIVE LANDSCAPE

Status: Presubmission accepted in *Endocrine Reviews.* In preparation.

Polyamines on the reproductive landscape

Lefèvre P.L.C [1], Palin M-F. [2] and Murphy B.D [1]

[1] Centre de Recherche en Reproduction Animale, Faculté de Médecine Vétérinaire, Université de Montréal, QC, Canada. [2] Dairy and Swine R & D Centre, Agriculture and Agri-Food Canada, QC, Canada.

ABSTRACT

Polyamines are essential regulators of cell growth and gene expression. Numerous studies demonstrating regulatory roles for polyamines in mammalian pregnancy have been published over the past 40 years. These studies elucidated mandatory involvement of the polyamines in gametogenesis, fertilization, early embryogenesis, implantation and post-implantation development. But, only one review of information on polyamines affecting the reproductive functions was undertaken 15 years ago. The present review is, therefore, an update of the current available knowledge of the roles of polyamines in reproductive biology.

A. Introduction

The polyamines, namely spermine and spermidine, were discovered in human semen (Wallace 2009; Bachrach 2010), and are involved in diverse mammalian reproductive functions. Besides their important role in spermatogenesis, polyamines are actively implicated in oogenesis, embryogenesis, implantation and placentation and to a great extent in parturition, lactation and postnatal development. Numerous studies on the occurrence and function of polyamines in mammalian pregnancy have been published over the past 40 years. To our knowledge, only one review dealing with the significance of polyamines in reproduction was written in 1977 (Sheth and Moodbidri 1977). Since then, extensive progress has been made in revealing an essential role for polyamines across the spectrum of reproductive biology. The purpose of this review is to highlight the involvement of the polyamines and to discuss the mechanisms by which polyamines regulate mammalian reproductive events. After a brief summary of general cellular and molecular functions of polyamines, this review will discuss effects of polyamines in gametogenesis, both spermatogenesis and oogenesis, in early embryonic development of the conceptus, as well as in a implantation and post-implantation development, and mechanisms of action of polyamines.

1. Definitions and variability in polyamines

Polyamines are low molecular weight aliphatic organic compounds composed of a carbon chain of variable length and 2 or more primary amino groups (Tabor and Tabor 1964). They are ubiquitous in all living species. In mammals, four different polyamine molecules have been identified: spermine, spermidine,

putrescine and cadaverine (Tabor and Tabor 1964; Kusano, Berberich et al. 2008). Their chemical structures are depicted in **Figure 36** (p 229). While spermine and spermidine were initially discovered in human semen as the volatile compounds responsible for the typical odor of semen, putrescine and cadaverine result from bacterial decomposition and emit the odor of putrefying flesh of cadavers (Kusano, Berberich et al. 2008). In mammalian cells, polyamines are either synthesized *de novo* from amino acids such as arginine, proline or methionine (Tabor and Tabor 1964; Tabor and Tabor 1984; Wu, Bazer et al. 2008), directly imported from the diet (Bardocz 1993; Larque, Sabater-Molina et al. 2007), or produced by the intestinal microflora (Hessels, Kingma et al. 1989). In the case of intestinal absorption, polyamines are released into blood circulation (Milovic 2001) and reach various tissues such as the intestine, thymus and liver (Bardocz 1993). In addition, *de novo* synthesized or imported putrescine, spermidine and spermine can be interconverted by interdependent enzyme reactions (**Figure 37** (p 231)).

2. Pathways and regulation of polyamine synthesis and the intracellular polyamine pool

When endogenously produced, polyamines are synthesized from the amino acids L-arginine or L-proline through L-ornithine (Wu and Morris 1998) and from /or L-methionine, via decarboxylated S-adenosylmethionine (dcSAM) (Tabor and Tabor 1984) (**Figure 37** (p 231)). Ornithine decarboxylase (ODC1), the rate limiting enzyme of polyamine biosynthesis, catalyzes the decarboxylation of L-ornithine, to yield putrescine. Putrescine combined with dcSAM, is then transformed into spermidine and spermine by spermidine synthase and spermine synthase,

respectively. Polyamine catabolism principally functions by back conversion mechanisms. Spermine can be back-converted into spermidine and, spermidine into putrescine by the combination of spermidine/spermine N_1-acetyltransferase (SAT1) and polyamine oxidase (Wallace 1987). This back conversion leads to intermediate acetylated polyamines, namely *N_1*-acetylspermidine and *N_1*-acetylspermine. Spermine oxidase induces a direct reconversion of spermine into spermidine (Vujcic, Liang et al. 2003).

Since polyamine levels have been associated with cell proliferation and tissue growth, intracellular polyamine homeostasis is expected to be tightly regulated (Kusano, Berberich et al. 2008). Its regulation can be achieved at two levels: either polyamine metabolism and catabolism or polyamine transport between intra- and extracellular environment (**Figure 37** (p 231)). Ornithine decarboxylase 1 abundance and therefore, its activity, is tightly controlled by the antizymes (AZIs) and the antizyme inhibitors (AZINs) (Kahana 2009). The antizyme family, which comprises 3 paralogs, the AZI1, AZI2 and AZI3, bind and direct ODC1 to degradation by the 26*S* proteasome without ubiquitination. While AZI1 and AZI2 are ubiquitously expressed, AZI3 expression is testis-specific (Ivanov, Rohrwasser et al. 2000; Kahana 2009). Antizyme inhibitors are ODC1-related proteins that lack decarboxylase activity. Theyinteract with AZIs with higher affinity than ODC1 and consequently rescues ODC1 from degradation (Kahana 2009). Two forms of AZINs were identified, AZIN1 and AZIN2, and bind indifferently to the three forms of AZIs, with the same affinity (Kahana 2009). Antizyme inhibitor 2 is specifically expressed in brain and testis (Lopez-Contreras, Ramos-Molina et al. 2010). The control of

ODC1 protein degradation by the complex AZIs-AZINs induces a rapid turnover and short half-life (10-30 min) of ODC1, thus characterizing ODC1 as the rate limiting enzyme for polyamine biosynthesis (Kahana 2009). Furthermore, negative feedback of polyamines on translation of polyamine-related enzymes such as ODC1, S-adenosylmethionine decarboxylase (SAMDC), spermine synthase, SAT1 and AZIN was reported, and polyamine stimulatory effects were also noted for AZI translation (Ivanov, Atkins et al. 2010). Upstream open-reading frames, which precede the initiator of the coding sequences in polyamine-related genes, are indeed polyamine-responsive (Ivanov, Atkins et al. 2010). .

Polyamine transport between the intra- and extracellular environments also enables maintenance of appropriate intracellular polyamine pools (Persson 2009). Polyamine uptake and release do not share common membrane transport systems (Seiler, Delcros et al. 1996). Two mechanisms have been proposed for importation, one is based on the binding proprieties of polyamines, specifically spermine, to heparan sulphate on glypican-1 molecules, which are subjected to endocytosis (Belting, Mani et al. 2003). The latter process involves a caveolar-dependent endocytic mechanism resulting in polyamine sequestration into secretory vesicles (Belting, Mani et al. 2003; Soulet, Gagnon et al. 2004). This process, is, time-, temperature- and concentration-dependent, requires energy, and is saturable (Palmer and Wallace 2010).The second mechanism proposed is based on the existence of a membrane transporter that requires an electronegative membrane potential (Soulet, Gagnon et al. 2004). Exportation of *N*1-acetylpolyamines and putrescine from the cell majoritably contributes to regulation of the intracellular

pool of free polyamines (Wallace and Mackarel 1998; Moinard, Cynober et al. 2005). To our knowledge, only one mechanism has been proposed, via the export solute carrier SLC3A2 that enables putrescine export (Uemura, Yerushalmi et al. 2008). Interestingly, regulation of polyamine transport has been reported to be dependent of the AZIs-AZINs equilibrium (Kahana 2009). AZIs decrease polyamine uptake (Mitchell, Judd et al. 1994), while AZINs stimulate polyamine uptake by counteracting the negative effects of AZIs (Kahana 2009; Lopez-Contreras, Ramos-Molina et al. 2010). Again, the mechanisms by which AZI-induced inhibition of polyamine uptake is achieved remain obscure. However, a recent study demonstrating the implication of AZIN2 in the regulation of intracellular trafficking of vesicle and the release of extracellular secretion (Kanerva, Makitie et al. 2010) suggests that AZIN2 may act through the endocytic absorption mechanism.

3. Molecular mechanisms of polyamine action on cellular processes

Since polyamines are fully protonated at physiologic pH, they are considered to be supercations" that have the capacity to strongly interact with polyanionic macromolecules such as nucleic acids, proteins and phospholipids (Wallace, Fraser et al. 2003). Through these molecular interactions, polyamines are known to stabilize DNA structure, induce chromatin remodeling to regulate gene expression (Wallace, Fraser et al. 2003; Igarashi and Kashiwagi 2009). Polyamines appear to play essential roles in cell proliferation (Alm and Oredsson 2009), in programmed cell death (Seiler and Raul 2005), in epigenetic modifications of chromatin (Heby 1995; Frostesjo, Holm et al. 1997; Bistulfi, Diegelman et al. 2009; Huang, Marton et al. 2009), in regulation of ion channels (Williams 1997) and in cell signaling

(Moruzzi, Marverti et al. 1993). Given these multiple and varied roles, tight regulation of intracellular polyamine homeostasis described above is essential. Indeed, increased metabolism and intracellular concentrations of polyamines in several cell types have been correlated unequivocally with development of various forms of cancer, and therefore targeting of polyamine metabolism has been proposed as a strategy for antiproliferative therapy (Seiler 2003; Casero and Pegg 2009; Casero and Woster 2009). In this context, the polyamine analogue α-difluoromethylornithine (DFMO), a potent irreversible inhibitor of ODC1 (Metcalf, Danzin et al. 1978), has been studied as a potential chemotherapeutic agent (Wallace and Niiranen 2007). DFMO has also been employed widely to evaluate the roles of polyamine in reproductive function.

B. Polyamines and gametogenesis

1. Polyamines in the male reproductive functions

a. Polyamines in somatic cells of the testis

During testicular maturation in the rat, polyamine concentrations undergo increase in Sertoli cells in the seminiferous tubules (Shubhada, Lin et al. 1989). The ODC1 protein is abundant in the proliferating Sertoli cells and interstitial Leydig cells from immature rats and and its activity is substantially higher than in adult rats (MacIndoe and Turkington 1973; Qian, Tsai et al. 1985). Additionally, ODC1 activity and *AZIN2* expression are greater in Leydig cells than in any other cells of the testes (Qian, Tsai et al. 1985; Makitie, Kanerva et al. 2009). Injections of FSH and LH increased testicular ODC1 activity in immature and hypophysectomized rats (MacIndoe and Turkington 1973; Osterman, Murono et al. 1983). Cultured Sertoli

cells from immature rat and bovine testes submitted to FSH treatment displayed increased ODC1 activity and, spermine and putrescine content (Francis, Triche et al. 1981; Swift and Dias 1987). Nonetheless, treatment with testosterone, alone or with FSH, decreased ODC1 activity and its expression in Sertoli cells (Swift and Dias 1988; Weiner, Pentecost et al. 1990).

b. Polyamines and spermatogenesis

ODC1 activity in the testis varies with the state of testicular development. Activity levels have been shown to be elevated in seminiferous tubules from three day old ratsbut rapidly repressed as testicular maturation took place (MacIndoe and Turkington 1973). In germ cells, ODC1 expression and activity follows a well-defined temporal and spatial pattern, suggesting specific involvement of polyamines in the process of spermatogenesis. Expression of *ODC1* is low in the mouse and the rat testis during the prepubertal period, but is still detectable and specifically in the spermatogonia (Alcivar, Hake et al. 1989; Blackshear, Manzella et al. 1989; Kaipia, Toppari et al. 1990). These authors show that it was substantially elevated during the first wave of spermatogenesis, namely in pachytene spermatocytes during meiotic prophase, in round spermatids and in residual bodies. ODC1 protein was also localized to the cytoplasm of freshly isolated epididymal spermatozoa and to the acrosomal region of round spermatids (Qian, Tsai et al. 1985). Together these findings indicate a role of polyamines in meiotic maturation of germ cells, in meiosis and in spermiogenesis. Reductions in nuclear spermine was reported to occur concomitant with maturation of primary spermatocytes to form elongated

spermatids, when histones are replaced by protamine and compaction of the chromatin occurs (Quemener, Blanchard et al. 1992).

Transgenic mice overexpressing the human *ODC1* gene displayed a 20- to 80-fold increase in testicular ODC1 activity and consequent increase in putrescine abundance (Halmekyto, Hyttinen et al. 1991; Hakovirta, Keiski et al. 1993). Males from the first generation had lower reproductive performance and exhibited an increase in spermatogonial DNA synthesis and a reduction in DNA synthesis in spermatocytes during spermatogenesis (Hakovirta, Keiski et al. 1993). In the second generation, male offspring were infertile and had an extremely high ODC1 activity in the testis, hypoplastic germinal epithelium and no spermatogenesis (Halmekyto, Hyttinen et al. 1991; Kilpelainen, Saarimies et al. 2001).

Temporal patterns of changes in testicular ODC1 activity and gene expression are inversely correlated: while ODC1 expression increased during spermatogenesis and reached its maximum during spermiogenesis and spermatidogenesis, maximal testicular ODC1 activity was restricted to the prepubertal period (Weiner and Dias 1992) (**Figure 38** (p 233)). Co-incubation of testicular cytosolic extracts from prepubertal and from mature males resulted in inhibition of ODC1 activity in the prepubertal cytosolic extract (Weiner and Dias 1992). Consistently, ODC1 activity remained stable and was enhanced by FSH supplementation to the culture medium in *in vitro* decapsulated testes from immature rats, while a decline in ODC1 activity and no responses to exogenous FSH was described for decapsulated testes of adult rats (Osterman, Murono et al. 1983).

The AZI3, which inactivates ODC1 activity and inhibits intracellular polyamine uptake, was reported to be specifically expressed in spermatids and spermatozoa, in the human and rodent testis from the early spermiogenesis until late spermatid phase (Ivanov, Rohrwasser et al. 2000; Tosaka, Tanaka et al. 2000). Since *AZI3* expression followed the *ODC1* gene expression pattern, it was hypothesized that AZI3 abolishes ODC1 activity to avoid detrimental effects of putrescine overproduction during spermiogenesis and spermatidogenesis (Lopez-Contreras, Ramos-Molina et al. 2010) (**Figure 38** (p 233)). Recently, *AZI3* knockout mice were found to have a disrupted spermatogenesis characterized by sperm with easily separable heads and tails and, subsequent loss of fertilizing capacity (Tokuhiro, Isotani et al. 2009). Furthermore, the testis-specific antizyme inhibitor 2 (AZIN2), which abrogates the inhibitory effects of the AZIs on ODC1 activity and polyamine uptake, was abundant in haploid germ cells in human and mouse testis and, similarly followed *AZI3* and *ODC1* with respect to temporal and spatial expression patterns during spermatogenesis (Pitkanen, Heiskala et al. 2001; Lopez-Contreras, Lopez-Garcia et al. 2006; Kanerva, Makitie et al. 2008; Lopez-Contreras, Ramos-Molina et al. 2008; Lopez-Contreras, Ramos-Molina et al. 2009). Even though the *ODC1* gene is expressed during spermio- and spermatidogenesis, its activity, along with polyamine transport and intracellular polyamine levels appear to be tightly regulated by the equilibrium between AZI3 and AZIN2 in haploid germ cells. An important role of AZIN2 in the process of intracellular vesicle trafficking underlying polyamine transport was recently reported, thus revealing a potential

involvement of AZIN2 in intracellular redistribution of polyamines during spermiogenesis as well (Kanerva, Makitie et al. 2010) (**Figure 38** (p 233)).

c. Polyamines, reproductive fluids, sperm motility and fertilization

Spermine and spermidine are the oldest known organic constituents of human prostatic secretions and human and rat seminal plasma contains higher levels of spermine than any other body fluid or tissue (van Leeuwenhoek 1678; Mann 1974). In the rat, castration-induced deprivation of testosterone induced a significant reduction in ODC1 and SAMDC activity and a decrease in concentrations of polyamines in the ventral prostate gland (Pegg, Lockwood et al. 1970; Danzin, Jung et al. 1979; Blackshear, Manzella et al. 1989), in the epididymis (de las Heras and Calandra 1987) and in the seminal vesicles (Danzin, Jung et al. 1979; Blackshear, Manzella et al. 1989). The repression of polyamine production in response to castration was correlated with a reduction in RNA and DNA synthesis in the seminal vesicle and the ventral prostate (Danzin, Jung et al. 1979). Testosterone injections abrogated the above-mentioned castration-induced inhibitory effects on ODC1 activity in the prostate, the epididymis and the seminal vesicles (Pegg, Lockwood et al. 1970; Danzin, Jung et al. 1979; de las Heras, Suescun et al. 1988; Blackshear, Manzella et al. 1989). The latter androgen effects in castrated rats were counteracted by DFMO in the ventral prostate and the seminal vesicles (Danzin, Jung et al. 1979; Kapyaho, Kallio et al. 1984), therefore revealing that polyamine biosynthesis is androgen-dependant in those reproductive organs in which semen is produced and stored until ejaculation.

In seminal plasma of infertile men, levels of spermidine and spermine are found to be strikingly low in comparison to normospermic men. Injections of S-adenosylmethionine into men who displayed low concentrations of spermatozoa in semen (oligospermia), increased polyamine content and enhanced sperm count and motility (Vanella, Pinturo et al. 1978). High levels of spermidine and spermine were correlated with high motility of ejaculated spermatozoa collected from rams (Melendrez, Ruttle et al. 1992). Addition of polyamines or L-arginine to human spermatozoa with reduced or no motility (asthenozoospermia) enhanced sperm motility (Morales, Rico et al. 2003). Motility of mouse, rat, guinea pig and rabbit spermatozoa from the vas deferens, which have not yet been in contact with polyamines from the prostatic fluid, can be induced by spermine (Tabor and Tabor 1964). The presence of spermidine, spermine or putrescine in the culture medium of mature spermatozoa collected from the epididymis enhanced glycolysis in the rat (Pulkkinen, Sinervirta et al. 1975), stimulated adenylate cyclase activity in bovine and human spermatozoa (Shah, Sheth et al. 1975; Casillas, Elder et al. 1980) and inhibited sperm phosphodiesterase activity, an inhibitor of cAMP signaling pathways in human spermatozoa (Shah, Sheth et al. 1975). Higher rates of *in vitro* fertilized ova were obtained when epididymal spermatozoa employed for fertilization were preincubated with spermine (Stanger and Quinn 1982). A correlation between spermine and spermidine concentrations in *in vitro* fertilization supernatants and the early embryo-associated immunosuppressive activity was associated with improvement in pregnancy success in the mouse (Porat and Clark 1990) and in the human (Lea, Porat et al. 1991). In the ram, spermine was localized

mainly in the acrosome part of the spermatozoa head (Rubinstein and Breitbart 1994) and spermine dissociation from spermatozoa was facilitated by heparin, a oviductal factor known to be implicated in sperm capacitation and the acrosome reaction, in the female reproductive tract (Rubinstein and Breitbart 1991). When submitted to low concentrations of spermine, the acrosome reaction occurred in capacitated bovine spermatozoa while higher concentrations of spermine inhibited those effects (Rubinstein, Lax et al. 1995). Thus, spermine was suggested to be a decapacitating factor in seminal fluid and to prevent premature capacitation and the acrosome reaction of sperm.

2. Polyamines in ovarian function

a. Polyamines, onset of puberty and folliculogenesis

Ornithine decarboxylase activity was reported to be high during the prepubertal period (YoungLai and Byskov 1983; Bastida, Cremades et al. 2005). Its activity was reported to be induced by gonadotropins like human chorionic gonadotropin (hCG), equine chorionic gonadotropin (eCG), follicle stimulating hormone (FSH) and/or luteinizing hormone (LH) in ovaries from immature rats (Johnson and Sashida 1977; Nureddin 1978; White and Ojeda 1981), hamsters (Sheela Rani and Moudgal 1979) and mice (Bastida, Cremades et al. 2005). Stimulation of ODC1 activity was cell-specific. In prepubertal rat ovary, the stimulation of ODC1 by hCG was specifically localized to the thecal layer of follicles as well as the interstitial glands (Persson, Rosengren et al. 1982). eCG-induced activity of ODC1 was associated with an increase in *ODC1* mRNA and protein expression specifically in granulosa cells and in ovarian weight in immature rat

ovaries (Lee and Dias 1988; Weiner and Dias 1993). Interestingly, *SAT1* overexpression in transgenic mice clearly resulted in an infertile phenotype which was associated with defects in folliculogenesis (Pietila, Alhonen et al. 1997), thus highlighting tight regulation of ovarian polyamine homeostasis required for folliculogenesis. In immature mice, the increase in ovarian ODC1 activity in response to eCG and hCG induced the development of antral follicles while only small pre-antral follicles and low ODC1 activity were observed in the control ovaries (Bastida, Cremades et al. 2005). The latter effects induced by eCG and hCG were counteracted by DFMO co-treatment, indicating an essential role for polyamines in the onset of puberty and folliculogenesis (Bastida, Cremades et al. 2005). However, results of previous studies in which rat females were subjected to DFMO treatment during the first 10 days of life demonstrated that polyamine deprivation impaired normal brain development resulting in prolonged high FSH serum levels and a delay in the onset of puberty, without affecting post-pubertal fertility (Thyssen, Hockl et al. 2002). Reversed effects, as exhibited by precocious somatic and behavioral development were induced by polyamine administration (Thyssen, Hockl et al. 2002). Therefore, the effects of DFMO-induced polyamine deprivation on folliculogenesis are disputable since it is not clear whether DFMO directly inhibits ovarian ODC1 or affects hypothalamic and pituitary production and release of gonadotropin-releasing hormone (GnRH) or gonadotropins respectively, which are responsible for stimulation of ovarian ODC1 activity and folliculogenesis.

b. Polyamines, ovulation and luteinization

In adult cycling mouse, hamster and rat females, ovarian ODC1 activity is elevated during late proestrus, when the preovulatory surge of LH takes place. The ODC1 protein was specifically localized to the theca intern of Graafian follicles and small follicles as well as in the interstitial tissue of the ovary (Kobayashi, Kupelian et al. 1971; Icekson, Kaye et al. 1974; Persson, Isaksson et al. 1986). Administration of LH or hCG to adult females induced an increase in ovarian ODC1 activity specifically in Graafian follicles in the mouse (Bastida, Tejada et al. 2002), hamster (Sheela Rani and Moudgal 1979) and rat (Kobayashi, Kupelian et al. 1971; Icekson, Kaye et al. 1974; Maudsley and Kobayashi 1974). Since LH administration was more effective in inducing ovarian ODC1 activity than FSH (Bastida, Cremades et al. 2005), it was hypothesized that polyamines are essential to folliculogenesis specifically at the time of ovulation of mature oocytes. In female rat, administration of DFMO just before proestrus was associated with a decrease in concentrations of LH and prolactin plasma, a reduction of polyamine content in the pituitary gland and, a decline in the number of ovulated oocytes and circulating concentrations of progesterone (Nicholson, Aslam et al. 1988; Nicholson and Wynne-Jones 1989). Since pituitary gonadotropin contents were not affected by DFMO treatment, it was suggested that polyamine deprivation was not disrupting gonadotropin production, but was rather affecting their release from the pituitary gland (Nicholson and Wynne-Jones 1989). Similar effects induced by DFMO were noted in ovariectomized rats treated with appropriate doses of progesterone and oestradiol, thus showing that the reduced concentration of LH in plasma was not a consequence of disrupted

ovarian feedback on the pituitary gland, but rather of pituitary polyamine deprivation (Nicholson and Wynne-Jones 1989). Consistently, inhibition of the preovulatory rise in ovarian ODC1 activity by DFMO treatment on the evening of proestrus in the mouse affected consequent steroidogenesis during luteinization (Bastida, Tejada et al. 2002; Bastida, Cremades et al. 2005). Plasma progesterone levels were significantly decreased at diestrus and this was associated with a strong reduction in vascularization of the corpus luteum as well as down-regulation of ovarian gene expression known to be essential for steroidogenesis, such as steroidogenic factor 1, cytochrome P450 cholesterol side chain cleavage enzyme, and steroidogenic acute regulatory protein (Bastida, Cremades et al. 2005). Nonetheless, another study revealed that inhibition of ODC1 activity by DFMO treatment on the day of proestrus in the rat did result in any deficiency in ovulation and surprisingly, was correlated with a 91 % increase in ovulated eggs (Carpenter and Fozard 1982). The discrepancy observed between the results of both these studies may be explained by a difference in doses and/or in timing of administration of DFMO in late proestrus, which has been shown to be critical (Nicholson and Wynne-Jones 1989).

In addition, ODC1 was specifically localized in the bovine corpus luteum during pregnancy (Lin and Rao 1980). Ovarian ODC1 activity was dependent on an intact placenta and estrogen from Days 12 to 21 of pregnancy in rats and was absent during pseudopregnancy, thus suggesting that ovarian ODC1 activity is induced by an unknown placental factor during pregnancy (Hickman-Smith, Bussmann et al. 1982). Recently, AZIN2, which prevents ODC1 degradation directed by AZI, was

localized in luteinized ovarian cells lining the corpus luteum cysts in humans (Makitie, Kanerva et al. 2009), thus suggesting that ovarian polyamine metabolism is tightly regulated during pregnancy, as well.

c. Polyamines, oögenesis and oocyte meiotic maturation

To our knowledge, no studies have been performed to assess polyamine functions during oögenesis during the prepubertal period, even though an increase in ODC1 activity in neonatal rat ovaries was associated with the onset of meiotic prophase, when germ cells enter the phase of premeiotic DNA synthesis (YoungLai and Byskov 1983), thus providing clues on a potential role of polyamine at that specific phase of oögenesis.

The ODC1 immunoreactivity was localized in the cytoplasm of oocytes of antral follicles and was increased after hCG induction of ODC1 activity in ovaries adult mice (Bastida, Cremades et al. 2005). The *ODC1* expression and variation in content of polyamines have been described for *xenopus* öocytes (Bassez, Paris et al. 1990; Osborne, Duval et al. 1991). When meiotic maturation of *xenopus* öocytes was induced *in vitro* with progesterone or hCG in mature follicles containing oocytes or follicle cell-free oocytes, an increase in ODC1 activity in the oocytes, prior to germinal breakdown and extrusion of the first polar body, was measured (Younglai, Godeau et al. 1980; Sunkara, Wright et al. 1981). The DFMO treatment resulted in the blockage of meiotic maturation of oocytes contained in mature follicles and, in *in vitro* cultures of ovarian fragments (Sunkara, Wright et al. 1981). In the latter case, exogenous putrescine counteracted DFMO inhibition and oocyte ovulation occurred. Nonetheless, germinal vesicle breakdown in follicle cell-free oocytes was not

disrupted when ODC1 was inhibited by DFMO (Younglai, Godeau et al. 1980), therefore suggesting that ODC1 activity and polyamine biosynthesis act upon follicles in supporting meiotic maturation of the oocytes rather than on the oocyte itself.

The physiological role of the increase in ODC1 in oocytes during maturation was recently investigated using antisense morpholino oligonucleotide (xODC1 mo) to inhibit *ODC1* translation in *xenopus* öocytes (Zhou, Ma et al. 2009). Even though xODC1 mo-injected oocytes appeared to undergo a complete meiotic maturation, metaphase II oocytes exhibited high levels of reactive oxygen species (ROS) and were apoptotic. When transferred to host frogs and subsequently ovulated, these eggs were fertilized, but exhibited embryo fragmentation and did not survive. Therefore, it was made clear that polyamines are essential for cytoplasmic maturation by protecting metaphase II oocytes from ROS-induced apoptosis and thus, promoting the production of healthy eggs.

C. Polyamines in embryogenesis

1. Polyamine production during early embryogenesis

Ornithine decarboxylase activity was reported to be increased in the embryo between the two-cell and early blastocyst stages in mice (Alexandre 1978; Alexandre 1979), pig (Cui and Kim 2005) and *xenopus* (Russell 1971; Osborne, Duval et al. 1991). In addition, uterine ODC1 activity also increased between day 2 and day 3 of pregnancy in rat and mouse uteri (Saunderson and Heald 1974; Fozard, Part et al. 1980).

2. Role of polyamines during early embryogenesis

a. Embryonic cell proliferation and survival

Genetic modifications of polyamine-related genes, the use of inhibitors of polyamine biosynthesis or addition of exogenous polyamines during early embryogenesis revealed that polyamines control cell proliferation and survival. *Odc1* deficient mouse embryos develop until the implantation stage, but not thereafter (Pendeville, Carpino et al. 2001). When isolated on day 3.5 post-coïtum and cultured *in vitro*, *Odc1* $^{-/-}$ embryos undergo cell degeneration and apoptosis in the inner cell mass, in contrast with trophoblastic giant cells, which were able to survive in long-term culture. *In vitro* development of two-cell stage mice embryos in the presence of DFMO was only affected after three days of culture as revealed by a decline in DNA synthesis (Zwierzchowski, Czlonkowska et al. 1986). Proliferation of mink trophoblast cells was reduced in presence of DFMO and removal of DMFO was associated with resumption of mitotic activity (Lefèvre, Palin, Chen, Turecki and Murphy, 2010; unpublished). In presence of putrescine, *in vitro* fertilized-oocytes showed a higher rate of development to embryos into blastocysts and likewise trophoblast outgrowth, compared to *in vivo* generated blastocysts (Muzikova and Clark 1995). Similarly, the exogenous supply of polyamines during *in vitro* development of two-cell pig embryos to blastocysts enhanced developmental rate and increased total cell numbers along with a substantial decrease in apoptosis (Cui and Kim 2005). These effects were abrogated by DFMO or cyclohexylamine, a spermidine synthase inhibitor. When an SAMDC inhibitor, methyl-glyoxal-bis(guanylhydrAZIone) (MGBG) was added to culture media, the rate of DNA

synthesis was inhibited when embryos reached the morula stage (Zwierzchowski, Czlonkowska et al. 1986). The latter entered a quiescence-like state at the eight-cell stage which induced a delay in embryo cavitation proportional to the duration of treatment (Alexandre 1978) and these effects were abrogated by an exogenous supply of spermidine and/or spermine (Zwierzchowski, Czlonkowska et al. 1986). Homozygous *Samdc* $^{-/-}$ mouse died between days 3.5 and 6.5 post-coitum (Nishimura, Nakatsu et al. 2002). When *in vitro* cultured, cell proliferation in 3.5 day old embryos was arrested, but no sign of apoptosis was observed (Nishimura, Nakatsu et al. 2002). Embryo cell proliferation resumed when spermidine was supplemented in the culture medium, thus suggesting that the embryos entered a quiescent state. Spermidine was reported to be required for the synthesis of hypusine, an amino-acid resulting in posttranslational modifications of eukaryotic initiation factor 5A (eIF5A) (Byers, Lakanen et al. 1994), a factor which regulates cell proliferation (Zanelli and Valentini 2007). Strikingly, *eIF5A* $^{-/-}$ embryos were not viable (Park, Nishimura et al. 2010), thus indicating the significance of spermine in *eIF5A* posttranscriptional modifications during embryogenesis.

b. Epigenetic modifications in embryonic cells

Epigenetic modifications, such as DNA methylation, are essential to zygotic gene activation and to determination of cell fate between ICM and trophectoderm during early embryogenesis (Corry, Tanasijevic et al. 2009; Shi and Wu 2009). Polyamine levels were associated with the state of DNA methylation and histone acetylation in different cell types (Huang, Marton et al. 2009), but no direct evidence of a correlation between epigenetic modifications and levels of polyamines during

embryogenesis have been highlighted. Nonetheless, SAMDC was proposed to be a significant regulator of both polyamine production and DNA methylation during early embryogenesis (Heby 1995). On the one hand, this enzyme transforms S-adenosylmethionine into dcSAM, which participates in putrescine transformation into spermidine and, spermidine into spermine (Tabor and Tabor 1984). On the other hand, it regulates the amount of S-adenosylmethionine, the substrate of DNA methyltransferase, an enzyme responsible for DNA methylation (Sistla and Rao 2004). Moreover, dcSAM has inhibitory effects on DNA methyltransferase and therefore, on DNA methylation (Heby, Persson et al. 1988; Heby 1995). Overexpression of the *SAMDC* gene in fertilized *Xenopus* eggs provoked cell dissociation and a developmental arrest that was induced by apoptosis in early blastula stage embryos (Shibata, Shinga et al. 1998; Shiokawa, Kai et al. 2000). Coinjections of S-adenosylmethionine, but not putrescine, in *xenopus* eggs overexpressing *SAMDC*, rescued embryonic development, thus suggesting that apoptosis was a consequence of DNA hypomethylation rather than putrescine depletion (Shibata, Shinga et al. 1998). Injection of 5-aza-2'-deoxycytidine, an inhibitor of DNA methylation also provoked apoptosis after the midblastula transition similar to what is observed when *SAMDC* is overexpressed in fertilized *xenopus* eggs (Kaito, Kai et al. 2001). Consequently, it appears that a well-balanced equilibrium between polyamine biosynthesis and DNA methylation is controlled by SAMDC and is required for early embryogenesis.

D. Polyamines in gestation

1. Polyamines and delayed implantation

Delayed implantation, or embryonic diapause, is a reversible arrest in embryonic development at the blastocyst stage during the preimplantation period (Dey, Lim et al. 2004; Lopes, Desmarais et al. 2004). In the mink, a species that exhibits delayed implantation as a normal aspect of its embryonic development, polyamine-related genes, such as *ODC1*, *SAT1* and *AZIN1*, and uterine polyamine contents are significantly upregulated in the uterus during the early stages of embryo reactivation (Lefèvre, Palin, Beaudry, Dobias-Goff, Llerena, Desmarais and Murphy, 2010 (unpublished); Lefèvre, Palin, Chen, Turecki and Murphy, 2010 (unpublished)). The ODC1 protein was also found to be upregulated in the uterine luminal and glandular epithelia at the time of embryo reactivation (Lefèvre, Palin, Chen, Turecki and Murphy, 2010 (unpublished)). Inhibition of polyamine biosynthesis by DFMO during blastocyst reactivation returned the mink blastocyst into a diapause-like state by repressing cell proliferation and delayed implantation, but was not detrimental to pregnancy (Lefèvre, Palin, Chen, Turecki and Murphy, 2010 (unpublished)).

Consistent with what was observed in the mink, polyamine-related genes namely *Odc1*, *Sat1*, *Samdc*, *Azi*, *spermidine synthase*, and *spermine oxidase* were substantially upregulated in the mouse uterine subluminal stroma at estrogen-induced reactivation, after delayed implantation (Zhao, Chi et al. 2008). No sign of reactivation, displayed by trophoblast outgrowths, in mouse-diapausing blastocysts was reported when the embryos were cultured in presence of DFMO and/or MGBG,

an inhibitor of SAMDC (Van Winkle and Campione 1983). Nonetheless, when blastocysts were washed and placed in an inhibitor-free medium, they were able to attach to the bottom of the culture dish and trophoblastic outgrowths were observed. It was reported that removal of arginine, the ornithine precursor, from culture medium prevented trophoblast outgrowths and attachment of mouse blastocysts (Gwatkin 1966). The latter remained arrested in free-floating conditions up to 5 days and reactivation was then observed once the embryos were transferred into a complete culture medium.

2. Polyamine production during implantation and post-implantation development

Embryo implantation and early post-implantation stages are crucial steps, during which the blastocyst achieves physical contact with the maternal endometrium and thereafter develops the placenta, through which a tightly regulated communication between the fetus and the maternal uterus is established. This foeto-maternal cross-talk is mandatory for successful intrauterine fetal development since it enables the exchange of nutrients, gases and waste between the mother and the developing fetus, until parturition (Dey, Lim et al. 2004). Polyamine biosynthesis was reported to occur during these steps in species with both noninvasive and invasive types of implantation, therefore suggesting a highly conserved role for polyamines during implantation and placentation across mammalian species.

a. Polyamines and non-invasive embryo implantation

Polyamines are widely reported to be produced by the uterus in mammalian with noninvasive implantation around the time of conceptus elongation and placentation, particulary in large domestic animals. In gilts, concentrations of spermidine, spermine and putrescine in uterine luminal fluids are at their maximal levels on day 12 of pregnancy, when pregnancy recognition is induced by conceptus estrogens (Rodriguez-Sallaberry, Simmen et al. 2001). Uterine *SAT1* gene expression was higher on that day when compared with cyclic endometrium and its expression was localized to the uterine luminal epithelium. The ODC1 activity and concentrations of ornithine and polyamines were also elevated in the porcine placenta between day 20 and day 40 of pregnancy, a critical period for porcine fetal growth and development (Wu, Pond et al. 1998), but decreased thereafter (Wu, Bazer et al. 2005). In allantoic fluid, concentrations of ornithine and polyamine increase between day 40 and day 60 of gestation, when placental development is maximal (Wu, Bazer et al. 1995; Wu, Pond et al. 1998). Similar observations were made in the ewe. During the preimplantation period, *ODC1* gene and protein expression were shown to be elevated in the ovine uterine luminal and superficial glandular epithelia but also in the trophectoderm when compared with the extraembryonic endoderm of the conceptus (Gao, Wu et al. 2009). Between day 30 to day 60 of gestation, during rapid growth of the ovine placenta, ornithine, arginine and polyamine concentrations, and ODC1 and arginase activities peaked at day 40 of gestation in whole placentomes, intercotyledonary placenta, intercarunculary endometrium and, in amniotic and allantoic fluids (Kwon, Wu et al. 2003).

b. Polyamines and invasive implantation

Elevated uterine ODC1 and SAMDC activities were measured on the day of embryo implantation (day 5) in the rat (Guha and Janne 1976). Increased activity of ODC1 and polyamine content were measured specifically at implantation sites, right after implantation, as placentation and decidualization take place, in the mouse (Fozard, Part et al. 1980), in the rat (Saunderson and Heald 1974; Heald 1979; Fozard, Part et al. 1980; Hoshiai, Lin et al. 1981), in the rabbit (Fozard, Part et al. 1980) and in the hamster (Luzzani, Colombo et al. 1982; Galliani, Colombo et al. 1983). Polyamine biosynthesis appears to take place in both the maternal and fetal compartment during the early stages of implantation. On day 5 of pregnancy, expression of polyamine-related genes such as *Odc1*, *Sat1*, *Samdc*, *Azi*, *spermidine synthase* and *spermine oxidase* were upregulated in the mouse uterine subluminal stroma at implantation sites (Zhao, Chi et al. 2008). In the mouse conceptus (including the decidua and the embryo), the amount of ODC1 protein and its enzymatic activity are maximal on day 8 of gestation (Lopez-Garcia, Lopez-Contreras et al. 2008). No difference in the level of ODC1 activity was detected between the embryo and the uterine decidua. Nevertheless, ODC1 activity and putrescine concentration were higher in the fetal part than in the maternal compartment of placental tissue after day 15 of pregnancy in the rat and in the mouse (Guha and Janne 1976; Lopez-Garcia, Lopez-Contreras et al. 2009). Consistently, ODC1 protein was specifically localized to the labyrinthine zone of the placenta (Lopez-Garcia, Lopez-Contreras et al. 2008). Although low ODC1 activity was detected in the mouse fetus and yolk sac when compared with the placenta,

polyamine content was higher in the fetus and yolk sac than in the placental compartment (Lopez-Garcia, Lopez-Contreras et al. 2009). Thus, it was suggested that the placenta may produce polyamines to sustain fetal development during the post-implantation period.

Spermidine and polyamine oxidase (PAO) concentrations are elevated on day 8 of pregnancy in the mouse uterus (Mehrotra, Kitchlu et al. 1998), when high trophoblast proliferation takes place to develop the ectoplacenta cone, a preplacental structure (Oda, Shiota et al. 2006). While serum PAO concentrations increase in humans during pregnancy (Illei and Morgan 1979), low levels of serum PAO were measured in women who experienced spontaneous abortion (Rijke and Ballieux 1978).

3. Role of polyamines during gestation

a. Polyamines and post-implantation embryo development

Specific inhibitors of polyamine biosynthesis have been widely employed to investigate biological functions of polyamines during pregnancy. In this way, polyamine biosynthesis was shown to be mandatory for post-implantation embryonic development. Administration of DFMO in drinking water, by gavage or subcutaneous, intrauterine or intraperitoneal injections during the peri-implantation period, unequivocally provoked embryonic development arrest, right after implantation in mice (Fozard, Part et al. 1980), rats (Reddy and Rukmini 1981; Mendez, Diaz-Flores et al. 1983), rabbits (Fozard, Part et al. 1980), hamsters (Galliani, Colombo et al. 1983) and mink (Lefèvre 2009 (personal communication)). This detrimental effect was specific to the post-implantation period, since

polyamine deprivation induced by DFMO before and after that critical period was not correlated with abnormal pregnancy in the mouse (Fozard, Part et al. 1980; Reddy and Rukmini 1981; Galliani, Colombo et al. 1983; Lopez-Garcia, Lopez-Contreras et al. 2008). Strikingly, DFMO-induced arrest of post-implantation embryonic development was counteracted by putrescine administration in the hamster and in the rat (Galliani, Colombo et al. 1983; Mendez, Diaz-Flores et al. 1983). Administration of two putrescine analogues, 1, 3-diaminopropane and 1, 6-diaminohexane, to pregnant female mice during the time of maximal fetal ODC1 activity (days 10-14 of gestation) inhibited fetal ODC1 activity and caused a reduction in fetal weight on day 18 of gestation (Manen, Hood et al. 1983). An adequate level of polyamines consequently appears to be essential for the post-implantation development of the fetus.

Detailed studies were undertaken to evaluate the developmental effects of an increasing range of orally-administered DFMO during the post-implantation period in rodents (Galliani, Colombo et al. 1983; O'Toole, Huffman et al. 1989; Kirchner, Mercieca et al. 1999; Ishida, Hiramatsu et al. 2002). The severity of maternal and fetal detrimental effects in response to DFMO treatment was dose-dependent. Low doses provoked an increase in post-implantation losses due to embryo resorptions, a reduction in fetal and placental weight and a decrease of the rate of DNA synthesis in the placenta. Nonetheless, viable fetuses did not show any external, visceral or skeletal abnormalities at any doses of the treatment (O'Toole, Huffman et al. 1989; Kirchner, Mercieca et al. 1999). Since polyamine deprivation-induced defects in fetal development that were comparable to those observed in a case of intrauterine

growth retardation (IUGR) in the rat (Ishida, Hiramatsu et al. 2002), it may reflect that the maternal uterine environment is not optimal to sustain fetal development when subjected to low doses of DFMO. More drastic effects on fetal survival and maternal health were provoked when higher doses of DFMO treatment were administered. While preterm deliveries became more frequent, maternal food and water consumption was diminished, resulting in decreases in body and uterine weights (Kirchner, Mercieca et al. 1999) and thus revealing that severe polyamine deprivation is toxic for the pregnant female.

b. Polyamines and placentation

Recently, histological analysis revealed that polyamine deprivation induced by DFMO was specifically associated with abnormal development of extraembryonic structures, such as the yolk sac and placenta (Lopez-Garcia, Lopez-Contreras et al. 2008). In the yolk sac, where blood exchanges between the maternal and fetal compartment take place (Ferkowicz and Yoder 2005), the number of blood islands was reduced and the expression of genes encoding for embryonic globins was decreased in DFMO-treated mice, thus suggesting that polyamines are essential in fetal vasculogenesis. Moreover, chorioallantoic attachment and development of the labyrinthine zone were abnormal and the spongiotrophoblast layer was absent in arrested embryonic development induced by polyamine deprivation. The expression of genes encoding for *embryonic hemoglobins* and for markers of trophoblastic lineage, such as *trophoblast specific protein α*, *placental specific protein 1*, *reproductive homeobox 6*, *Cbp/p300-interacting transactivator*, *integrin α4* and *eomesodermin* were down-regulated in response to polyamine deprivation (Lopez-

Garcia, Lopez-Contreras et al. 2008). In addition, concentration of progesterone in plasma was reduced in DFMO-treated females and the expression of genes encoding for steroidogenic enzymes namely, steroidogenic acute regulatory protein, 3β-hydroxysteroid dehydrogenase IV and 17-α-steroid hydrolase in the placenta was decreased. Since expression of ovarian steroidogenesis markers was not affected by DFMO treatment, it was suggested that alteration in plasma progesterone concentrations resulted from placental rather than an ovarian steroidogenic deficiency (Lopez-Garcia, Lopez-Contreras et al. 2008). Altogether, available results indicate that polyamines are essential for the development of extraembryonic structures, such as the placenta.

In pregnant mice and hamsters, administration of the inhibitor of polyamine oxidase, MDL-725227DA, right after implantation, induced embryonic losses in a dose-dependent manner (Mehrotra, Kitchlu et al. 1998). Histological analysis revealed a high occurrence of fetal resorptions and complete absence of any sign of uterine decidualization in the treated females. Moreover, mouse trophoblastic cells displayed consistent dose-dependent responses to the presence of MDL-725227DA in culture media, ranging from a reduction in trophoblastic cell proliferation to their degeneration (Mehrotra, Kitchlu et al. 1998).

c. Polyamines and uterine decidualization

High doses of DFMO administered on the day of implantation induced detrimental effects on uterine decidualization, such as a strong reduction in uterine weight, which resulted in a compromised pregnancy in the hamster (Galliani, Colombo et al. 1983; Kirchner, Mercieca et al. 1999). Uterine ODC1 activity

increases in parallel to uterine synthesis of RNA and DNA in implantation sites (Heald 1979), thus the increase in uterine polyamine content may be related to uterine swelling at implantation sites. Spermidine and spermine in culture medium of nuclei isolated from rat decidual tissue stimulate the rate of RNA synthesis (Hoshiai, Lin et al. 1981). In cultures of porcine uterine glandular epithelium and stroma cells, exogenous of putrescine and spermidine increased the rate of DNA synthesis, while spermine stimulated DNA synthesis only in stromal cell lines (Rodriguez-Sallaberry, Simmen et al. 2001).

Nonetheless, low doses of DFMO had no effect on uterine decidualization since deciduomal weight, and the rate of RNA, DNA and protein synthesis at implantation sites were normal in treated mouse and rat females (Fozard, Part et al. 1980; Fozard, Part et al. 1980; Mendez, Diaz-Flores et al. 1983; Rorke, Kendra et al. 1984). Histological analyses of mouse implantation sites after polyamine deprivation indicated that implantation occurs normally without an apparent deficiency in the deciduoma (Fozard, Part et al. 1980). Uteri of mice on day 18 of pregnancy after DFMO-treatment during post-implantation embryonic development were histologically and functionally normal, since the treated females produced litters of standard size when mated at the first estrus after treatment (Fozard, Part et al. 1980).

d. Polyamines and organogenesis

Although polyamine deprivation during embryo implantation was associated with a reduction in fetal weight, the fetus did not show any external, skeletal or visceral abnormalities as a consequence of DFMO administration, even at high doses

(O'Toole, Huffman et al. 1989; Kirchner, Mercieca et al. 1999). Nevertheless, mouse embryos overexpressing *Sat1* were viable, but infertile (Pietila, Alhonen et al. 1997; Min, Simmen et al. 2002). Histological analysis revealed a hypoplastic uterine morphology as displayed by a thin myometrium and underdeveloped uterine stroma and glands. Furthermore, *Odc1* and *Azi* gene and protein expression were reported to be developmentally-regulated during early embryogenesis with respect to axonogenesis, epithelial-mesenchymal interactions and apoptosis (Gritli-Linde, Nilsson et al. 2001).

4. Regulation of polyamine homeostasis at implantation sites

Since polyamines are unequivocally required for post-implantation embryonic development, it is essential that the intracellular polyamine pool be maintained to optimal levels, therefore implying tight regulation of polyamine metabolism and catabolism and polyamine transport in both fetal and maternal compartment of implantation sites.

a. Compensatory mechanisms in polyamine biosynthesis

Mouse females subjected to DFMO treatment during the post-implantation period displayed a decline in uterine ODC1 activity, but an increase in *Samdc* gene expression and activity and, in spermine concentrations at implantation sites (Fozard, Part et al. 1980; Zhao, Chi et al. 2008). The addition of DFMO to culture medium of mouse uterine stromal or epithelial cells inhibited ODC1 activity, but stimulated *SAMDC* gene expression (Zhao, Chi et al. 2008). Conversely, *Odc1* gene overexpression in those cells resulted in the downregulation of *Samdc* expression (Zhao, Chi et al. 2008). Expression of the *Sat1* gene was upregulated in response to

exogenous supplementation of spermidine and spermine to culture medium of porcine and mouse uterine stromal and epithelial cells (Rodriguez-Sallaberry, Simmen et al. 2001; Zhao, Chi et al. 2008). These results support the presence of compensatory mechanisms involving polyamine-related gene expression, triggered when the rate of polyamine biosynthesis is experimentally up- or down-regulated in order to maintain optimal levels of the intracellular polyamine pool during pregnancy.

Furthermore, expression of *Azi1* and *Azin2* genes are elevated at implantation sites in the mouse (Lopez-Garcia, Lopez-Contreras et al. 2008; Zhao, Chi et al. 2008; Lopez-Garcia, Lopez-Contreras et al. 2009). In the mouse conceptus, *Azin2* was significantly upregulated in response to DFMO treatment (Lopez-Garcia, Lopez-Contreras et al. 2008). The *Odc1* gene overexpression in mouse uterine stromal and epithelial cells induced an increase in *Azi1* gene expression (Zhao, Chi et al. 2008). Modulation of polyamine transport by the AZI1 and AZIN2, in response to inhibition or stimulation of ODC1 activity, may therefore be another compensatory mechanism which ensures the maintenance of homeostasis of intracellular pools of polyamines. This autoregulatory circuit of polyamine biosynthesis, implicating the AZI- AZIN tandem, also plays an important role during organogenesis, since both ODC1 and AZI proteins follow a precise spatio-temporal pattern of expression during the critical period of fetal development (Gritli-Linde, Nilsson et al. 2001). Moreover, the *Azi1* knockout mouse is not viable after parturition (Tang, Ariki et al. 2009) as they exhibit abnormal liver morphology, a high rate of ODC1 degradation and, reduced putrescine and spermidine production,

thus confirming that this autoregulatory circuit of polyamine biosynthesis is critical for organogenesis during fetal development.

b. Control of polyamine biosynthesis by steroid hormones

In pregnant rat uterus, ODC1 activity is stimulated when compared with the non-pregnant uterine horn unilaterally in ovariectomized females (Heald 1979). Uterine ODC1 and SAMDC activities were significantly elevated within a few hours in response to estradiol-17β injection in adult or immature rat females (Kaye, Icekson et al. 1971; Lavia, Stohs et al. 1983; Rorke, Kendra et al. 1984) and in pseudopregnant females subjected to artificially-induced decidualization (Barkai and Kraicer 1978; Hoshiai, Lin et al. 1981; Hoshiai, Uehara et al. 1982; Wing 1988). Co-administration of cycloheximide, an inhibitor of protein synthesis, inhibited the increase in uterine ODC1 activity induced by estradiol-17β, indicating that ODC1 expression, rather than ODC1 activity, is stimulated by estradiol-17β (Kaye, Icekson et al. 1971). Uterine *Odc1* gene expression is up-regulated in mouse implantation sites after estrogen induced-reactivation, following delayed implantation (Zhao, Chi et al. 2008). In ovariectomized mice, estrogen, rather than progesterone administration, stimulates uterine *Odc1* and *Azi* gene expression (Zhao, Chi et al. 2008). ODC1 enzymatic activity was higher in human endometrium during the estrogen-dominated follicular phase than in secretory endometrium of the menstrual cycle when the corpus luteum is secreting progesterone (Holinka and Gurpide 1985). Administration of estrogen antagonists, such as tamoxifen, CDRI-85/287 or ICI, inhibited *Odc1* gene expression and its activity in the mouse and the rat uterus (Bulger and Kupfer 1976; Dwivedi, Gupta et al. 1999; Zhao, Chi et al.

2008). In the hamster, pregnancy was arrested by ovariectomy, associated with a decline in uterine ODC1 activity (Luzzani, Colombo et al. 1982). The detrimental effects were abrogated by exogenous administration of progesterone which restored uterine ODC1 activity to its normal level. Porcine uterine *SAT1* gene expression was more responsive to progesterone than estrogen during conceptus elongation (Green, Blaeser et al. 1996). Altogether the above results indicate that polyamine-related gene expression is responsive to steroid hormones during implantation and post-implantation development in a species-specific manner.

c. Contribution of maternal diet to polyamine content

Since polyamines are synthesized from arginine, proline, methionine and/or ornithine (Tabor and Tabor 1964; Wu, Bazer et al. 2005), or imported from the diet (Bardocz 1993; Larque, Sabater-Molina et al. 2007), their production is strongly related to maternal nutrition.

The link between maternal nutrition, polyamine biosynthesis, placentation and/or embryonic/fetal development has, therefore, been widely investigated in large animals (Wu, Bazer et al. 2004; Wu, Bazer et al. 2006). In pigs, a deficiency in maternal dietary protein is associated with IUGR, which is characterized by a decrease in placental and fetal growth and lower birth weight (Pond, Maurer et al. 1991; Osgerby, Wathes et al. 2002). In the latter case, IUGR was associated with a decrease in ODC1 activity and concentrations of arginine, ornithine and polyamines in the endometrium and placenta between day 40 and day 60 of gestation, corresponding to the period of placental development (Wu and Morris 1998; Wu, Pond et al. 1998; Wu, Pond et al. 1998). In sheep, IUGR also occurs in response to

maternal undernutrition (Osgerby, Wathes et al. 2002). A 50 % decrease of nutrient requirement markedly-reduced arginine and polyamine concentrations in maternal and fetal plasma, but also in allantoic and amniotic fluids during mid- and late-gestation (Kwon, Ford et al. 2004). Surprisingly, realimentation of nutrient-restricted ewes with 100 % of nutrient requirements increased all concentrations of all aminoacids and polyamines in all of the measured compartments of the conceptus and prevented IUGR (Kwon, Ford et al. 2004). In the rat, dietary arginine supplementation to pregnant females, throughout gestation or during the first 7 days of gestation, increased circulating ornithine and arginine concentrations and resulted in an improved reproductive performance, as litter size was increased 30 % at term (Zeng, Wang et al. 2008). Similarly, plasma concentrations of ornithine and arginine were increased in arginine-supplemented pregnant gilts between day 30 and day 114 of gestation (Mateo, Wu et al. 2007). In the latter case, litter size at birth was 22 % greater and litter weight of live born piglets, 24 % heavier (Mateo, Wu et al. 2007).

Moreover, low birth weigh, delayed embryonic development, and fetal or maternal death are observed in pregnant females affected by diabetes mellitus (Buchanan and Kitzmiller 1994). Delayed embryonic development in diabetic female rats was associated with a reduction in embryonic ODC1 activity on day 11 of gestation and with a decline in embryonic DNA and polyamine content (Bengtsson, Wiberg et al. 1994). Administration of arginine or polyamines on day 5 of pregnancy in diabetic females was recently reported to prevent embryo toxicity and delayed development (Chirino-Galindo, Baiza-Gutman et al. 2009).

E. Concluding remarks

When van Leeuwenhoek in 1678 depicted the presence of the "three-sided crystals" in human semen (van Leeuwenhoek 1678), he was probably far from suspecting that he was opening such huge avenues on the significance of what we call today, polyamines, in reproductive functions. As demonstrated in the present review, polyamines are implicated in gametogenesis during which they clearly appear to be essential for both meiotic maturation of male and female haploid germ cells, but also somatic cells, like Sertoli and follicle cells, for their role in sustaining gametogenesis. Apart from a significant role in ovarian steroidogenesis during the estrous cycle and pregnancy, polyamines are also indispensable for early embryogenesis, blastocyst implantation and post-implantation conceptus development. Results of several studies tend to support the hypothesis that polyamines are definitely required for development of the placenta, a critical step in pregnancy since it allows foeto-maternal communications to sustain fetal development. Moreover, polyamines are implicated in both invasive and non-invasive types of implantation which suggest that the role of polyamines in pregnancy has been highly conserved among mammalian species and may reflect their great value in reproductive functions.

Nonetheless, a question concerning the molecular mechanisms of polyamines to ensure their biological effects in the reproductive tissues remains to be elucidated. Since *Odc1* knockout embryos do not survive beyond the blastocyst stage, inhibitors of polyamine-related enzymes were widely used to induce polyamine deprivation and to reveal major defects during gametogenesis and

embryogenesis. However, it remains unclear whether the detrimental effects of polyamine deprivation are really induced by local polyamine deprivation in reproductive tissues, or are consequences of disruptions in other crucial biological processes linked to reproductive functions, such as in the hypothalamic-pituitary axis. Therefore, other experimental tools are needed to target inhibition of polyamine synthesis specifically in reproductive tissues. For instance, gene ablation using a cre-lox system in mice (Sauer 1998) would enable suppression of specific polyamine-related gene expression in reproductive organs and would help to discriminate local effects from global effects of polyamine deprivation on reproductive functions. In addition, the significance of polyamines in reproductive functions was mainly revealed by a cause-and -effect chain resulting from inhibitors of polyamine synthesis; nonetheless, the molecular mechanisms underlying polyamine functions in the above processes remain uncharacterized.

As a conclusion, the present review provides strong clues for the *sine qua non* requirement of polyamines in reproductive functions which generate a major breakthrough in our understanding of both various aspects of the reproductive process and the role of polyamines in the reproductive landscape.

F. References

Alcivar, A. A., L. E. Hake, et al. (1989). "Developmental and differential expression of the ornithine decarboxylase gene in rodent testis." Biol Reprod **41**(6): 1133-1142.

Alexandre, H. (1978). "[Effect of inhibitors of polyamine biosynthesis on primary differentiation of mouse egg]." C R Acad Sci Hebd Seances Acad Sci D **286**(16): 1215-1217.

Alexandre, H. (1979). "The utilization of an inhibitor of spermidine and spermine synthesis as a tool for the study of the determination of cavitation in the preimplantation mouse embryo." J Embryol Exp Morphol **53**: 145-162.

Alm, K. and S. Oredsson (2009). "Cells and polyamines do it cyclically." Essays Biochem **46**: 63-76.

Bachrach, U. (2010). "The early history of polyamine research." Plant Physiol Biochem.

Bardocz, S. (1993). "The role of dietary polyamines." Eur J Clin Nutr **47**(10): 683-690.

Barkai, U. and P. F. Kraicer (1978). "Definition of period of induction of deciduoma in the rat using ornithine decarboxylase as a marker of growth onset." Int J Fertil **23**(2): 106-111.

Bassez, T., J. Paris, et al. (1990). "Post-transcriptional regulation of ornithine decarboxylase in Xenopus laevis oocytes." Development **110**(3): 955-962.

Bastida, C. M., A. Cremades, et al. (2005). "Influence of ovarian ornithine decarboxylase in folliculogenesis and luteinization." Endocrinology **146**(2): 666-674.

Bastida, C. M., F. Tejada, et al. (2002). "The preovulatory rise of ovarian ornithine decarboxylase is required for progesterone secretion by the corpus luteum." Biochem Biophys Res Commun **293**(1): 106-111.

Belting, M., K. Mani, et al. (2003). "Glypican-1 is a vehicle for polyamine uptake in mammalian cells: a pivital role for nitrosothiol-derived nitric oxide." J Biol Chem **278**(47): 47181-47189.

Bengtsson, B. O., K. Wiberg, et al. (1994). "Ornithine decarboxylase activity and concentrations of polyamines in embryos of diabetic rats." Biol Neonate **66**(4): 230-237.

Bistulfi, G., P. Diegelman, et al. (2009). "Polyamine biosynthesis impacts cellular folate requirements necessary to maintain S-adenosylmethionine and nucleotide pools." Faseb J.

Blackshear, P. J., J. M. Manzella, et al. (1989). "High level, cell-specific expression of ornithine decarboxylase transcripts in rat genitourinary tissues." Mol Endocrinol **3**(1): 68-78.

Bolkenius, F. N. and N. Seiler (1981). "Acetylderivatives as intermediates in polyamine catabolism." Int J Biochem **13**(3): 287-292.

Buchanan, T. A. and J. L. Kitzmiller (1994). "Metabolic interactions of diabetes and pregnancy." Annu Rev Med **45**: 245-260.

Bulger, W. H. and D. Kupfer (1976). "Induction of uterine ornithine decarboxylase (ODC) by antiestrogens. Inhibition of estradiol-mediated induction of ODC: a possible mechanism of action of antiestrogens." Endocr Res Commun **3**(3-4): 209-218.

Byers, T. L., J. R. Lakanen, et al. (1994). "The role of hypusine depletion in cytostasis induced by S-adenosyl-L-methionine decarboxylase inhibition: new evidence

provided by 1-methylspermidine and 1,12-dimethylspermine." Biochem J **303 (Pt 2)**: 363-368.

Carpenter, J. R. and J. R. Fozard (1982). "Enhancement of ovulation in the rat by DL-alpha-difluoromethylornithine, an irreversible inhibitor of ornithine decarboxylase." Eur J Pharmacol **80**(2-3): 263-266.

Casero, R. A. and A. E. Pegg (2009). "Polyamine catabolism and disease." Biochem J **421**(3): 323-338.

Casero, R. A. and P. M. Woster (2009). "Recent Advances in the Development of Polyamine Analogues as Antitumor Agents (section sign)." J Med Chem.

Casillas, E. R., C. M. Elder, et al. (1980). "Adenylate cyclase activity of bovine spermatozoa during maturation in the epididymis and the activation of sperm particulate adenylate cyclase by GTP and polyamines." J Reprod Fertil **59**(2): 297-302.

Chirino-Galindo, G., L. A. Baiza-Gutman, et al. (2009). "Polyamines protect rat embryo in vitro from high glucose-induced developmental delay and dysmorphogenesis." Birth Defects Res B Dev Reprod Toxicol **86**(1): 58-64.

Corry, G. N., B. Tanasijevic, et al. (2009). "Epigenetic regulatory mechanisms during preimplantation development." Birth Defects Res C Embryo Today **87**(4): 297-313.

Cui, X. S. and N. H. Kim (2005). "Polyamines inhibit apoptosis in porcine parthenotes developing in vitro." Mol Reprod Dev **70**(4): 471-477.

Danzin, C., M. J. Jung, et al. (1979). "Effects of alpha-difluoromethylornithine, an enzyme-activated irreversible inhibitor or ornithine decarboxylase, on testosterone-induced regeneration of prostate and seminal vesicle in castrated rats." Biochem J **180**(3): 507-513.

de las Heras, M. A. and R. S. Calandra (1987). "Androgen-dependence of ornithine decarboxylase in the rat epididymis." J Reprod Fertil **79**(1): 9-14.

de las Heras, M. A., M. O. Suescun, et al. (1988). "Ornithine decarboxylase activity as a marker of androgen and antiandrogen action in the rat epididymis." J Reprod Fertil **83**(1): 177-183.

Dey, S. K., H. Lim, et al. (2004). "Molecular cues to implantation." Endocr Rev **25**(3): 341-373.

Dwivedi, A., G. Gupta, et al. (1999). "Changes in uterine ornithine decarboxylase activity and steroid receptor levels during decidualization in the rat induced by CDRI-85/287." Eur J Endocrinol **141**(4): 426-430.

Ferkowicz, M. J. and M. C. Yoder (2005). "Blood island formation: longstanding observations and modern interpretations." Exp Hematol **33**(9): 1041-1047.

Fozard, J. R., M. L. Part, et al. (1980). "Inhibition of murine embryonic development by alpha-difluoromethylornithine, an irreversible inhibitor of ornithine decarboxylase." Eur J Pharmacol **65**(4): 379-391.

Fozard, J. R., M. L. Part, et al. (1980). "L-Ornithine decarboxylase:an essential role in early mammalian embryogenesis." Science **208**(4443): 505-508.

Francis, G. L., T. J. Triche, et al. (1981). "In Vitro Gonadotropin Stimulation of Bovine Sertoli

Cell Ornithine Decarboxylase Activity." J Androl **2**: 312-320.

Frostesjo, L., I. Holm, et al. (1997). "Interference with DNA methyltransferase activity and genome methylation during F9 teratocarcinoma stem cell differentiation induced by polyamine depletion." J Biol Chem **272**(7): 4359-4366.

Galliani, G., G. Colombo, et al. (1983). "Contragestational effects of DL-alpha-difluoro-methylornithine, an irreversible inhibitor of ornithine decarboxylase, in the hamster." Contraception **28**(2): 159-170.

Gao, H., G. Wu, et al. (2009). "Select Nutrients in the Ovine Uterine Lumen. V. Nitric Oxide Synthase, GTP Cyclohydrolase, and Ornithine Decarboxylase in Ovine Uteri and Periimplantation Conceptuses." Biol Reprod.

Green, M. L., L. L. Blaeser, et al. (1996). "Molecular cloning of spermidine/spermine N1-acetyltransferase from the periimplantation porcine uterus by messenger ribonucleic acid differential display: temporal and conceptus-modulated gene expression." Endocrinology **137**(12): 5447-5455.

Gritli-Linde, A., J. Nilsson, et al. (2001). "Nuclear translocation of antizyme and expression of ornithine decarboxylase and antizyme are developmentally regulated." Dev Dyn **220**(3): 259-275.

Guha, S. K. and J. Janne (1976). "The synthesis and accumulation of polyamines in reproductive organs of the rat during pregnancy." Biochim Biophys Acta **437**(1): 244-252.

Gwatkin, R. B. (1966). "Defined media and development of mammalian eggs in vitro." Ann N Y Acad Sci **139**(1): 79-90.

Hakovirta, H., A. Keiski, et al. (1993). "Polyamines and regulation of spermatogenesis: selective stimulation of late spermatogonia in transgenic mice overexpressing the human ornithine decarboxylase gene." Mol Endocrinol **7**(11): 1430-1436.

Halmekyto, M., J. M. Hyttinen, et al. (1991). "Transgenic mice aberrantly expressing human ornithine decarboxylase gene." J Biol Chem **266**(29): 19746-19751.

Heald, P. J. (1979). "Changes in ornithine decarboxylase during early implantation in the rat." Biol Reprod **20**(5): 1195-1199.

Heby, O. (1995). "DNA methylation and polyamines in embryonic development and cancer." Int J Dev Biol **39**(5): 737-757.

Heby, O., L. Persson, et al. (1988). "Polyamines, DNA methylation and cell differentiation." Adv Exp Med Biol **250**: 291-299.

Hessels, J., A. W. Kingma, et al. (1989). "Microbial flora in the gastrointestinal tract abolishes cytostatic effects of alpha-difluoromethylornithine in vivo." Int J Cancer **43**(6): 1155-1164.

Hickman-Smith, D., L. E. Bussmann, et al. (1982). "Ornithine decarboxylase as a monitor for luteal stimuli in the pregnant rat." J Reprod Fertil **66**(1): 265-272.

Holinka, C. F. and E. Gurpide (1985). "Ornithine decarboxylase activity in human endometrium and endometrial cancer cells." In Vitro Cell Dev Biol **21**(12): 697-706.

Hoshiai, H., Y. C. Lin, et al. (1981). "Ornithine decarboxylase activity and polyamine content of the placenta and decidual tissue in the rat." Placenta **2**(2): 105-116.

Hoshiai, H., S. Uehara, et al. (1982). "The variations of estrogen receptor, progesterone receptor, cAMP, ODC activity and RNA synthesis of deciduomata in pseudopregnant rats." Tohoku J Exp Med **137**(4): 349-360.

Huang, Y., L. J. Marton, et al. (2009). "Polyamine analogues targeting epigenetic gene regulation." Essays Biochem **46**: 95-110.

Icekson, I., A. M. Kaye, et al. (1974). "Stimulation by luteinizing hormone of ornithine decarboxylase in rat ovary: preferential response by follicular tissue." J Endocrinol **63**(2): 417-418.

Igarashi, K. and K. Kashiwagi (2009). "Modulation of cellular function by polyamines." Int J Biochem Cell Biol.

Illei, G. and D. M. Morgan (1979). "Polyamine oxidase activity in human pregnancy serum." Br J Obstet Gynaecol **86**(11): 878-881.

Ishida, M., Y. Hiramatsu, et al. (2002). "Inhibition of placental ornithine decarboxylase by DL-alpha-difluoro-methyl ornithine causes fetal growth restriction in rat." Life Sci **70**(12): 1395-1405.

Ivanov, I. P., J. F. Atkins, et al. (2010). "A profusion of upstream open reading frame mechanisms in polyamine-responsive translational regulation." Nucleic Acids Res **38**(2): 353-359.

Ivanov, I. P., A. Rohrwasser, et al. (2000). "Discovery of a spermatogenesis stage-specific ornithine decarboxylase antizyme: antizyme 3." Proc Natl Acad Sci U S A **97**(9): 4808-4813.

Johnson, D. C. and T. Sashida (1977). "Temporal changes in ovarian ornithine decarboxylase and cyclic AMP in immature rats stimulated by exogenous or endogenous gonadotrophins." J Endocrinol **73**(3): 463-471.

Kahana, C. (2009). "Antizyme and antizyme inhibitor, a regulatory tango." Cell Mol Life Sci **66**(15): 2479-2488.

Kaipia, A., J. Toppari, et al. (1990). "Stage- and cell-specific expression of the ornithine decarboxylase gene during rat and mouse spermatogenesis." Mol Cell Endocrinol **73**(1): 45-52.

Kaito, C., M. Kai, et al. (2001). "Activation of the maternally preset program of apoptosis by microinjection of 5-aza-2'-deoxycytidine and 5-methyl-2'-deoxycytidine-5'-triphosphate in Xenopus laevis embryos." Dev Growth Differ **43**(4): 383-390.

Kanerva, K., L. T. Makitie, et al. (2010). "Ornithine decarboxylase antizyme inhibitor 2 regulates intracellular vesicle trafficking." Exp Cell Res.

Kanerva, K., L. T. Makitie, et al. (2008). "Human ornithine decarboxylase paralogue (ODCp) is an antizyme inhibitor but not an arginine decarboxylase." Biochem J **409**(1): 187-192.

Kapyaho, K., A. Kallio, et al. (1984). "Differential effects of 2-difluoromethylornithine and methylglyoxal bis(guanylhydrazone) on the testosterone-induced growth of ventral prostate and seminal vesicles of castrated rats." Biochem J **219**(3): 811-817.

Kaye, A. M., I. Icekson, et al. (1971). "Stimulation by estrogens of ornithine and S-adenosylmethionine decarboxylases in the immature rat uterus." Biochim Biophys Acta **252**(1): 150-159.

Kilpelainen, P. T., J. Saarimies, et al. (2001). "Abnormal ornithine decarboxylase activity in transgenic mice increases tumor formation and infertility." Int J Biochem Cell Biol **33**(5): 507-520.

Kirchner, D. L., M. D. Mercieca, et al. (1999). "Developmental toxicity studies of 2-(difluoromethyl)-dl-ornithine (DFMO) in rats and rabbits." Toxicol Sci **50**(1): 127-135.

Kobayashi, Y., J. Kupelian, et al. (1971). "Ornithine decarboxylase stimulation in rat ovary by luteinizing hormone." Science **172**(981): 379-380.

Kusano, T., T. Berberich, et al. (2008). "Polyamines: essential factors for growth and survival." Planta **228**(3): 367-381.

Kwon, H., S. P. Ford, et al. (2004). "Maternal nutrient restriction reduces concentrations of amino acids and polyamines in ovine maternal and fetal plasma and fetal fluids." Biol Reprod **71**(3): 901-908.

Kwon, H., G. Wu, et al. (2003). "Developmental changes in polyamine levels and synthesis in the ovine conceptus." Biol Reprod **69**(5): 1626-1634.

Larque, E., M. Sabater-Molina, et al. (2007). "Biological significance of dietary polyamines." Nutrition **23**(1): 87-95.

Lavia, L. A., S. J. Stohs, et al. (1983). "Polyamine biosynthetic decarboxylase activities following estradiol-17 beta or estriol stimulation of the immature rat uterus." Steroids **42**(6): 609-618.

Lea, R. G., O. Porat, et al. (1991). "The detection of spermine and spermidine in human in vitro fertilization supernatants and their relation to early embryo-associated suppressor activity." Fertil Steril **56**(4): 771-775.

Lee, C. Y. and J. A. Dias (1988). "Cellular origin of prolonged induction of ornithine decarboxylase in the rat ovary." Proc Soc Exp Biol Med **187**(3): 350-354.

Lin, M. T. and C. V. Rao (1980). "Ornithine decarboxylase in bovine corpora lutea." J Endocrinol Invest **3**(2): 131-136.

Lopes, F. L., J. A. Desmarais, et al. (2004). "Embryonic diapause and its regulation." Reproduction **128**(6): 669-678.

Lopez-Contreras, A. J., C. Lopez-Garcia, et al. (2006). "Mouse ornithine decarboxylase-like gene encodes an antizyme inhibitor devoid of ornithine and arginine decarboxylating activity." J Biol Chem **281**(41): 30896-30906.

Lopez-Contreras, A. J., B. Ramos-Molina, et al. (2008). "Antizyme inhibitor 2 (AZIN2/ODCp) stimulates polyamine uptake in mammalian cells." J Biol Chem **283**(30): 20761-20769.

Lopez-Contreras, A. J., B. Ramos-Molina, et al. (2010). "Antizyme inhibitor 2: molecular, cellular and physiological aspects." Amino Acids **38**(2): 603-611.

Lopez-Contreras, A. J., B. Ramos-Molina, et al. (2009). "Expression of antizyme inhibitor 2 in male haploid germinal cells suggests a role in spermiogenesis." Int J Biochem Cell Biol **41**(5): 1070-1078.

Lopez-Garcia, C., A. J. Lopez-Contreras, et al. (2008). "Molecular and morphological changes in placenta and embryo development associated to the inhibition of polyamine synthesis during midpregnancy in mice." Endocrinology.

Lopez-Garcia, C., A. J. Lopez-Contreras, et al. (2008). "Molecular and morphological changes in placenta and embryo development associated with the inhibition of polyamine synthesis during midpregnancy in mice." Endocrinology **149**(10): 5012-5023.

Lopez-Garcia, C., A. J. Lopez-Contreras, et al. (2009). "Transcriptomic analysis of polyamine-related genes and polyamine levels in placenta, yolk sac and fetus during the second half of mouse pregnancy." Placenta **30**(3): 241-249.

Luzzani, F., G. Colombo, et al. (1982). "Evidence for a role of progesterone in the control of uterine ornithine decarboxylase in the pregnant hamster." Life Sci **31**(15): 1553-1558.

MacIndoe, J. H. and R. W. Turkington (1973). "Hormonal regulation of spermidine formation during spermatogenesis in the rat." Endocrinology **92**(2): 595-605.

Makitie, L. T., K. Kanerva, et al. (2009). "High expression of antizyme inhibitor 2, an activator of ornithine decarboxylase in steroidogenic cells of human gonads." Histochem Cell Biol.

Manen, C. A., R. D. Hood, et al. (1983). "Ornithine decarboxylase inhibitors and fetal growth retardation in mice." Teratology **28**(2): 237-242.

Mann, T. (1974). "Secretory function of the prostate, seminal vesicle and other male accessory organs of reproduction." J Reprod Fertil **37**(1): 179-188.

Mateo, R. D., G. Wu, et al. (2007). "Dietary L-arginine supplementation enhances the reproductive performance of gilts." J Nutr **137**(3): 652-656.

Maudsley, D. V. and Y. Kobayashi (1974). "Induction of ornithine decarboxylase in rat ovary after administration of luteinizing hormone or human chorionic gonadotrophin." Biochem Pharmacol **23**(19): 2697-2703.

Mehrotra, P. K., S. Kitchlu, et al. (1998). "Effect of inhibitors of enzymes involved in polyamine biosynthesis pathway on pregnancy in mouse and hamster." Contraception **57**(1): 55-60.

Melendrez, C. S., J. L. Ruttle, et al. (1992). "Polyamines in ejaculated ram spermatozoa and their relationship with sperm motility." J Androl **13**(4): 293-296.

Mendez, J. D., M. Diaz-Flores, et al. (1983). "Inhibition of rat embryonic development by the intrauterine administration of alpha-difluoromethylornithine." Contraception **28**(1): 93-98.

Metcalf, B. W., C. Danzin, et al. (1978). "Catalytic irreversible inhibition of mammalian ornithine decarboxylase (E.C. 4.1.1.17) by substrate and product analogs." J Am Chem Soc **100**: 2551–2553

Milovic, V. (2001). "Polyamines in the gut lumen: bioavailability and biodistribution." Eur J Gastroenterol Hepatol **13**(9): 1021-1025.

Milovic, V., D. Faust, et al. (2001). "Permeability characteristics of polyamines across intestinal epithelium using the Caco-2 monolayer system: comparison between transepithelial flux and mitogen-stimulated uptake into epithelial cells." Nutrition **17**(6): 462-466.

Min, S. H., R. C. Simmen, et al. (2002). "Altered levels of growth-related and novel gene transcripts in reproductive and other tissues of female mice overexpressing spermidine/spermine N1-acetyltransferase (SSAT)." J Biol Chem **277**(5): 3647-3657.

Mitchell, J. L., G. G. Judd, et al. (1994). "Feedback repression of polyamine transport is mediated by antizyme in mammalian tissue-culture cells." Biochem J **299 (Pt 1)**: 19-22.

Moinard, C., L. Cynober, et al. (2005). "Polyamines: metabolism and implications in human diseases." Clin Nutr **24**(2): 184-197.

Morales, M. E., G. Rico, et al. (2003). "[Progressive motility increase caused by L-arginine and polyamines in sperm from patients with idiopathic and diabetic asthenozoospermia]." Ginecol Obstet Mex **71**: 297-303.

Moruzzi, M. S., G. Marverti, et al. (1993). "Effect of spermine on membrane-associated and membrane-inserted forms of protein kinase C." Mol Cell Biochem **124**(1): 1-9.

Muzikova, E. and D. A. Clark (1995). "Polyamines may increase the percentage of in-vitro fertilized murine oocytes that develop into blastocysts." Hum Reprod **10**(5): 1172-1177.

Nicholson, S. A., M. Aslam, et al. (1988). "Effect of difluoromethylornithine on the LH surge and subsequent ovulation in the rat." J Endocrinol **117**(3): 447-453.

Nicholson, S. A. and G. A. Wynne-Jones (1989). "Differential effect of difluoromethylornithine on the increases in plasma concentrations of reproductive hormones on the afternoon of pro-oestrus in the rat." J Endocrinol **121**(3): 495-499.

Nishimura, K., F. Nakatsu, et al. (2002). "Essential role of S-adenosylmethionine decarboxylase in mouse embryonic development." Genes Cells **7**(1): 41-47.

Nureddin, A. (1978). "Ovarian ornithine decarboxylase regulation in the immature, the pubescent, and the pseudopregnant rat." Proc Natl Acad Sci U S A **75**(5): 2530-2534.

O'Toole, B. A., K. W. Huffman, et al. (1989). "Effects of eflornithine hydrochloride (DFMO) on fetal development in rats and rabbits." Teratology **39**(2): 103-113.

Oda, M., K. Shiota, et al. (2006). "Trophoblast stem cells." Methods Enzymol **419**: 387-400.

Osborne, H. B., C. Duval, et al. (1991). "Expression and post-transcriptional regulation of ornithine decarboxylase during early Xenopus development." Eur J Biochem **202**(2): 575-581.

Osgerby, J. C., D. C. Wathes, et al. (2002). "The effect of maternal undernutrition on ovine fetal growth." J Endocrinol **173**(1): 131-141.

Osterman, J., E. P. Murono, et al. (1983). "Regulation of testicular ornithine decarboxylase in vitro. Effect of age, follicle-stimulating hormone, and luteinizing hormone." J Androl **4**(3): 175-182.

Palmer, A. J. and H. M. Wallace (2010). "The polyamine transport system as a target for anticancer drug development." Amino Acids **38**(2): 415-422.

Park, M. H., K. Nishimura, et al. (2010). "Functional significance of eIF5A and its hypusine modification in eukaryotes." Amino Acids **38**(2): 491-500.

Pegg, A. E., D. H. Lockwood, et al. (1970). "Concentrations of putrescine and polyamines and their enzymic synthesis during androgen-induced prostatic growth." Biochem J **117**(1): 17-31.

Pendeville, H., N. Carpino, et al. (2001). "The ornithine decarboxylase gene is essential for cell survival during early murine development." Mol Cell Biol **21**(19): 6549-6558.

Persson, L. (2009). "Polyamine homoeostasis." Essays Biochem **46**: 11-24.

Persson, L., K. Isaksson, et al. (1986). "Distribution of ornithine decarboxylase in ovaries of rat and hamster during pro-oestrus." Acta Endocrinol (Copenh) **113**(3): 403-409.

Persson, L., E. Rosengren, et al. (1982). "Immunohistochemical localization of ornithine decarboxylase in the rat ovary." Histochemistry **75**(2): 163-167.

Pietila, M., L. Alhonen, et al. (1997). "Activation of polyamine catabolism profoundly alters tissue polyamine pools and affects hair growth and female fertility in transgenic mice overexpressing spermidine/spermine N1-acetyltransferase." J Biol Chem **272**(30): 18746-18751.

Pitkanen, L. T., M. Heiskala, et al. (2001). "Expression of a novel human ornithine decarboxylase-like protein in the central nervous system and testes." Biochem Biophys Res Commun **287**(5): 1051-1057.

Pond, W. G., R. R. Maurer, et al. (1991). "Fetal organ response to maternal protein deprivation during pregnancy in swine." J Nutr **121**(4): 504-509.

Porat, O. and D. A. Clark (1990). "Analysis of immunosuppressive molecules associated with murine in vitro fertilized embryos." Fertil Steril **54**(6): 1154-1161.

Pulkkinen, P., R. Sinervirta, et al. (1975). "Modification of the metabolism of rat epididymal spermatozoa by spermine." Biochem Biophys Res Commun **67**(2): 714-722.

Qian, Z. U., Y. H. Tsai, et al. (1985). "Localization of ornithine decarboxylase in rat testicular cells and epididymal spermatozoa." Biol Reprod **33**(5): 1189-1195.

Quemener, V., Y. Blanchard, et al. (1992). "Depletion in nuclear spermine during human spermatogenesis, a natural process of cell differentiation." Am J Physiol **263**(2 Pt 1): C343-347.

Reddy, P. R. and V. Rukmini (1981). "Alpha-difluoromethylornithine as a postcoitally effective antifertility agent in female rats." Contraception **24**(2): 215-221.

Rijke, E. O. and R. E. Ballieux (1978). "Is thymus-derived lymphocyte inhibitor a polyamine?" Nature **274**(5673): 804-805.

Rodriguez-Sallaberry, C., F. A. Simmen, et al. (2001). "Polyamine- and insulin-like growth factor-I-mediated proliferation of porcine uterine endometrial cells: a potential role for spermidine/spermine N(1)-acetyltransferase during peri-implantation." Biol Reprod **65**(2): 587-594.

Rorke, E. A., K. L. Kendra, et al. (1984). "Relationships among uterine growth, ornithine decarboxylase activity and polyamine levels: studies with estradiol and antiestrogens." Mol Cell Endocrinol **38**(1): 31-38.

Rubinstein, S. and H. Breitbart (1991). "Role of spermine in mammalian sperm capacitation and acrosome reaction." Biochem J **278 (Pt 1)**: 25-28.

Rubinstein, S. and H. Breitbart (1994). "Cellular localization of polyamines: cytochemical and ultrastructural methods providing new clues to polyamine function in ram spermatozoa." Biol Cell **81**(2): 177-183.

Rubinstein, S., Y. Lax, et al. (1995). "Dual effect of spermine on acrosomal exocytosis in capacitated bovine spermatozoa." Biochim Biophys Acta **1266**(2): 196-200.

Russell, D. H. (1971). "Putrescine and spermidine biosynthesis in the development of normal and anucleolate mutants of Xenopus laevis." Proc Natl Acad Sci U S A **68**(3): 523-527.

Saunderson, R. and P. J. Heald (1974). "Ornithine decarboxylase activity in the uterus of the rat during early pregnancy." J Reprod Fertil **39**(1): 141-143.

Seiler, N. (2003). "Thirty years of polyamine-related approaches to cancer therapy. Retrospect and prospect. Part 2. Structural analogues and derivatives." Curr Drug Targets **4**(7): 565-585.

Seiler, N., J. G. Delcros, et al. (1996). "Polyamine transport in mammalian cells. An update." Int J Biochem Cell Biol **28**(8): 843-861.

Seiler, N. and F. Raul (2005). "Polyamines and apoptosis." J Cell Mol Med **9**(3): 623-642.

Shah, G. V., A. R. Sheth, et al. (1975). "Effect of spermine on adenyl cyclase activity of spermatozoa." Experientia **31**(6): 631-632.

Sheela Rani, C. S. and N. R. Moudgal (1979). "Effect of follicle-stimulating hormone and its antiserum on the activity of ornithine decarboxylase in the ovary of rat and hamster." Endocrinology **104**(5): 1480-1483.

Sheth, A. R. and S. B. Moodbidri (1977). "Significance of polyamines in reproduction." Adv Sex Horm Res **3**: 51-74.

Shi, L. and J. Wu (2009). "Epigenetic regulation in mammalian preimplantation embryo development." Reprod Biol Endocrinol **7**: 59.

Shibata, M., J. Shinga, et al. (1998). "Overexpression of S-adenosylmethionine decarboxylase (SAMDC) in early Xenopus embryos induces cell dissociation and inhibits transition from the blastula to gastrula stage." Int J Dev Biol **42**(5): 675-686.

Shin, M., L. I. Larsson, et al. (2007). "Polyamines in spermatocytes and residual bodies of rat testis." Histochem Cell Biol **127**(6): 649-655.

Shiokawa, K., M. Kai, et al. (2000). "Maternal program of apoptosis activated shortly after midblastula transition by overexpression of S-adenosylmethionine decarboxylase in Xenopus early embryos." Comp Biochem Physiol B Biochem Mol Biol **126**(2): 149-155.

Shubhada, S., S. N. Lin, et al. (1989). "Polyamine profiles in rat testis, germ cells and Sertoli cells during testicular maturation." J Androl **10**(2): 145-151.

Soulet, D., L. Covassin, et al. (2002). "Role of endocytosis in the internalization of spermidine-C(2)-BODIPY, a highly fluorescent probe of polyamine transport." Biochem J **367**(Pt 2): 347-357.

Soulet, D., B. Gagnon, et al. (2004). "A fluorescent probe of polyamine transport accumulates into intracellular acidic vesicles via a two-step mechanism." J Biol Chem **279**(47): 49355-49366.

Stanger, J. D. and P. Quinn (1982). "Effect of polyamines on fertilization of mouse ova in vitro." J Exp Zool **220**(3): 377-380.

Sunkara, P. S., D. A. Wright, et al. (1981). "An essential role for putrescine biosynthesis during meiotic maturation of amphibian oocytes." Dev Biol **87**(2): 351-355.

Swift, T. A. and J. A. Dias (1987). "Stimulation of polyamine biosynthesis by follicle-stimulating hormone in serum-free cultures of rat Sertoli cells." Endocrinology **120**(1): 394-400.

Swift, T. A. and J. A. Dias (1988). "Testosterone suppression of ornithine decarboxylase activity in rat Sertoli cells." Endocrinology **123**(2): 687-693.

Tabor, C. W. and H. Tabor (1984). "Methionine adenosyltransferase (S-adenosylmethionine synthetase) and S-adenosylmethionine decarboxylase." Adv Enzymol Relat Areas Mol Biol **56**: 251-282.

Tabor, C. W. and H. Tabor (1984). "Polyamines." Annu Rev Biochem **53**: 749-790.

Tabor, H. and C. W. Tabor (1964). "SPERMIDINE, SPERMINE, AND RELATED AMINES." Pharmacol Rev **16**: 245-300.

Tang, H., K. Ariki, et al. (2009). "Role of ornithine decarboxylase antizyme inhibitor in vivo." Genes Cells **14**(1): 79-87.

Thyssen, S. M., P. F. Hockl, et al. (2002). "Effects of polyamines on the release of gonadotropin-releasing hormone and gonadotropins in developing female rats." Exp Biol Med (Maywood) **227**(4): 276-281.

Tokuhiro, K., A. Isotani, et al. (2009). "OAZ-t/OAZ3 is essential for rigid connection of sperm tails to heads in mouse." PLoS Genet **5**(11): e1000712.

Tosaka, Y., H. Tanaka, et al. (2000). "Identification and characterization of testis specific ornithine decarboxylase antizyme (OAZ-t) gene: expression in haploid germ cells and polyamine-induced frameshifting." Genes Cells **5**(4): 265-276.

Uemura, T., H. F. Yerushalmi, et al. (2008). "Identification and characterization of a diamine exporter in colon epithelial cells." J Biol Chem **283**(39): 26428-26435.

van Leeuwenhoek, A. (1678). "Observationes D. Anthonii Leeuwenhoek, de Natis e semine genitali Animalculis." Philos. Trans. R. Soc. London **12**: 1040–1043.

Van Winkle, L. J. and A. L. Campione (1983). "Effect of inhibitors of polyamine synthesis on activation of diapausing mouse blastocysts in vitro." J Reprod Fertil **68**(2): 437-444.

Vanella, A., R. Pinturo, et al. (1978). "Polyamine levels in human semen of unfertile patients: effect of S-adenosylmethionine." Acta Eur Fertil **9**(2): 99-103.

Vujcic, S., P. Liang, et al. (2003). "Genomic identification and biochemical characterization of the mammalian polyamine oxidase involved in polyamine back-conversion." Biochem J **370**(Pt 1): 19-28.

Wallace, H. M. (1987). "Polyamine catabolism in mammalian cells: excretion and acetylation." Med. Sci. Res. **15**: 1437–1440.

Wallace, H. M. (2009). "The polyamines: past, present and future." Essays Biochem **46**: 1-9.

Wallace, H. M., A. V. Fraser, et al. (2003). "A perspective of polyamine metabolism." Biochem J **376**(Pt 1): 1-14.

Wallace, H. M. and A. J. Mackarel (1998). "Regulation of polyamine acetylation and efflux in human cancer cells." Biochem Soc Trans **26**(4): 571-575.

Wallace, H. M. and K. Niiranen (2007). "Polyamine analogues - an update." Amino Acids **33**(2): 261-265.

Weiner, K. X. and J. A. Dias (1992). "Developmental regulation of ornithine decarboxylase (ODC) in rat testis: comparison of changes in ODC activity with changes in ODC mRNA levels during testicular maturation." Biol Reprod **46**(4): 617-622.

Weiner, K. X. and J. A. Dias (1993). "Regulation of ovarian ornithine decarboxylase activity and its mRNA by gonadotropins in the immature rat." Mol Cell Endocrinol **92**(2): 195-199.

Weiner, K. X., B. T. Pentecost, et al. (1990). "Testosterone decreases ornithine decarboxylase messenger RNA levels in primary cultures of rat Sertoli cells." Mol Endocrinol **4**(8): 1249-1256.

White, S. S. and S. R. Ojeda (1981). "Changes in ovarian luteinizing hormone and follicle-stimulating hormone receptor content and in gonadotropin-induced ornithine decarboxylase activity during prepubertal and pubertal development of the female rat." Endocrinology **109**(1): 152-161.

Williams, K. (1997). "Interactions of polyamines with ion channels." Biochem J **325 (Pt 2)**: 289-297.

Wing, L. Y. (1988). "Effect of estradiol on the activities of ornithine decarboxylase and S-adenosyl-methionine decarboxylase in tissues of ovariectomized rats." Chin J Physiol **31**(2): 95-103.

Wu, G., F. W. Bazer, et al. (2004). "Maternal nutrition and fetal development." J Nutr **134**(9): 2169-2172.

Wu, G., F. W. Bazer, et al. (2008). "Proline metabolism in the conceptus: implications for fetal growth and development." Amino Acids **35**(4): 691-702.

Wu, G., F. W. Bazer, et al. (2005). "Polyamine synthesis from proline in the developing porcine placenta." Biol Reprod **72**(4): 842-850.

Wu, G., F. W. Bazer, et al. (1995). "Developmental changes of free amino acid concentrations in fetal fluids of pigs." J Nutr **125**(11): 2859-2868.

Wu, G., F. W. Bazer, et al. (2006). "Board-invited review: intrauterine growth retardation: implications for the animal sciences." J Anim Sci **84**(9): 2316-2337.

Wu, G. and S. M. Morris, Jr. (1998). "Arginine metabolism: nitric oxide and beyond." Biochem J **336 (Pt 1)**: 1-17.

Wu, G., W. G. Pond, et al. (1998). "Maternal dietary protein deficiency decreases nitric oxide synthase and ornithine decarboxylase activities in placenta and endometrium of pigs during early gestation." J Nutr **128**(12): 2395-2402.

Wu, G., W. G. Pond, et al. (1998). "Maternal dietary protein deficiency decreases amino acid concentrations in fetal plasma and allantoic fluid of pigs." J Nutr **128**(5): 894-902.

YoungLai, E. V. and A. G. Byskov (1983). "Relationship of meiotic prophase and ornithine decarboxylase in the neonatal rabbit ovary." Cell Tissue Res **231**(3): 565-570.

Younglai, E. V., F. Godeau, et al. (1980). "Increased ornithine decarboxylase activity during meiotic maturation in Xenopus laevis oocytes." Biochem Biophys Res Commun **96**(3): 1274-1281.

Zanelli, C. F. and S. R. Valentini (2007). "Is there a role for eIF5A in translation?" Amino Acids **33**(2): 351-358.

Zeng, X., F. Wang, et al. (2008). "Dietary arginine supplementation during early pregnancy enhances embryonic survival in rats." J Nutr **138**(8): 1421-1425.

Zhao, Y. C., Y. J. Chi, et al. (2008). "Polyamines are essential in embryo implantation: expression and function of polyamine-related genes in mouse uterus during peri-implantation period." Endocrinology **149**(5): 2325-2332.

Zhou, Y., C. Ma, et al. (2009). "Antiapoptotic role for ornithine decarboxylase during oocyte maturation." Mol Cell Biol **29**(7): 1786-1795.

Zwierzchowski, L., M. Czlonkowska, et al. (1986). "Effect of polyamine limitation on DNA synthesis and development of mouse preimplantation embryos in vitro." J Reprod Fertil **76**(1): 115-121.

G. Figures

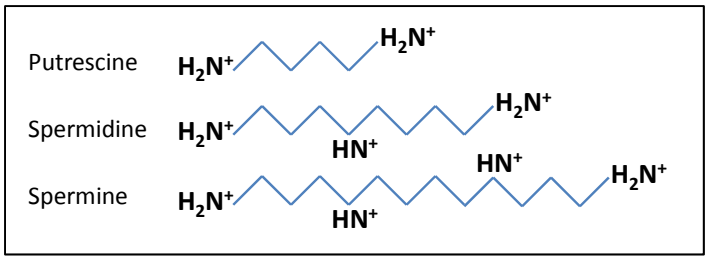

Figure 36: Chemical structures of polyamines.

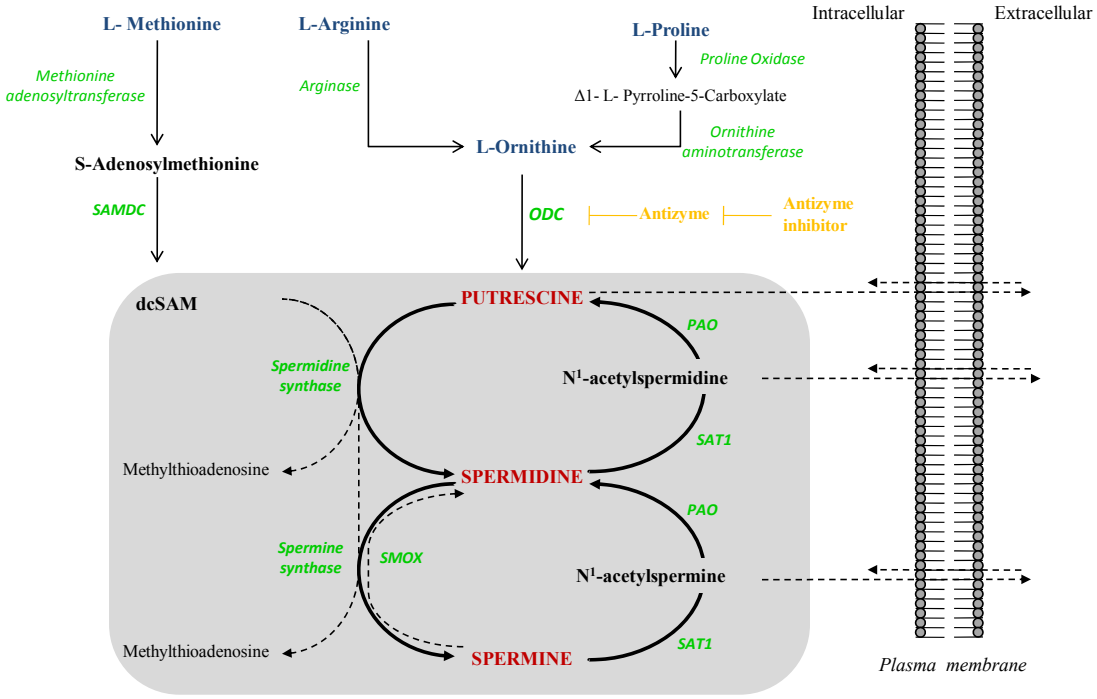
L- Methionine
L-Arginine
L-Proline
Intracellular
Extracellular
Methionine adenosyltransferase
Arginase
Proline Oxidase
Δ1- L- Pyrroline-5-Carboxylate
Ornithine aminotransferase
S-Adenosylmethionine
L-Ornithine
SAMDC
ODC
Antizyme
Antizyme inhibitor
dcSAM
PUTRESCINE
PAO
Spermidine synthase
N¹-acetylspermidine
SAT1
Methylthioadenosine
SPERMIDINE
PAO
Spermine synthase
SMOX
N¹-acetylspermine
Methylthioadenosine
SPERMINE
SAT1
Plasma membrane

Figure 37. *De novo* polyamine biosynthesis and regulation of intracellular polyamine content.

Polyamines are synthesized from L-arginine or L-proline through L-ornithine (Wu and Morris 1998) and L-methionine, via decarboxylated S-Adenosylmethionine (dcSAM), the decarboxylated product formed by *S*-adenosylmethionine decarboxylase (SAMDC) (Tabor and Tabor 1984). Ornithine decarboxylase (ODC1) catalyzes the decarboxylation of L-ornithine to yield putrescine. Putrescine combined with dcSAM, is then transformed into spermidine and spermine via spermidine synthase and spermine synthase, respectively. Spermidine can be converted back into putrescine and, spermine into spermidine by the combination of spermidine/spermine N_1-acetyltransferase (SAT1) and polyamine oxidase (PAO) (Wallace 1987). This back conversion leads to intermediate acetylated polyamines, namely N_1-acetylspermidine and N_1-acetylspermine (N_1-acetylpolyamines). Spermine oxidase (SMOX) induces direct reconversion of spermine into spermidine (Vujcic, Liang et al. 2003)). Polyamines can also be transported in and out of the cells (Seiler, Delcros et al. 1996; Milovic, Faust et al. 2001; Soulet, Covassin et al. 2002). *N*1-acetylpolyamines and putrescine are the main polyamines exported from the cell (Bolkenius and Seiler 1981; Wallace and Mackarel 1998). ODC1 protein is regulated by an antizyme (AZI) which binds and directs ODC to degradation, and the antizyme inhibitor (AZIN), which negates AZI effects (Kahana 2009).

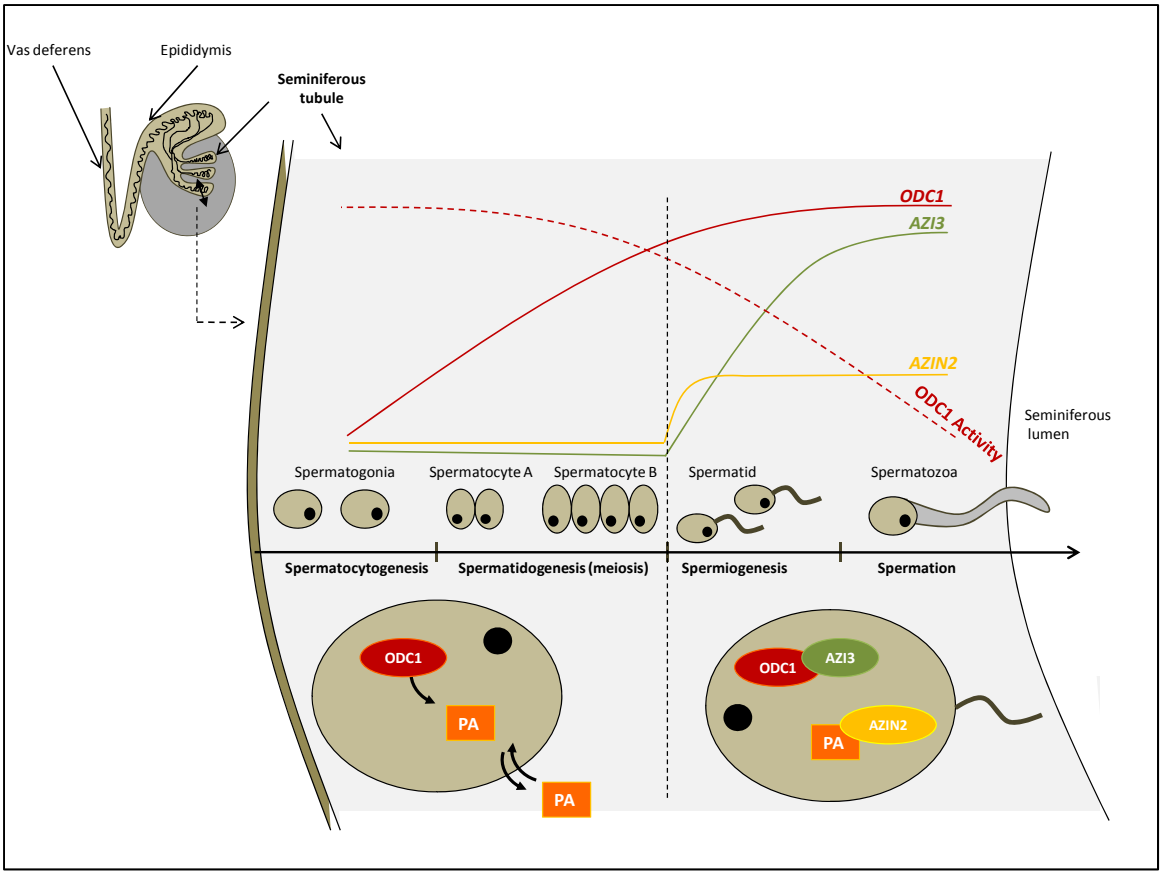
Vas deferens
Epididymis
Seminiferous tubule
ODC1
AZI3
AZIN2
ODC1 Activity
Seminiferous lumen
Spermatogonia
Spermatocyte A
Spermatocyte B
Spermatid
Spermatozoa
Spermatocytogenesis
Spermatidogenesis (meiosis)
Spermiogenesis
Spermation
ODC1
PA
PA
ODC1
AZI3
AZIN2
PA

Figure 38. Regulation of biosynthesis and intracellular distribution of polyamines by the tandem antizyme 3 and the antizyme inhibitor 2 during spermatogenesis.

Mature spermatozoa are produced in the seminiferous epithelium of the seminiferous tubules in the testis. Briefly, male primary germ cells, spermatogonia, undergo active division to ensure a constant supply of spermatogonia for spermatogenesis. Some of those will become haploid spermatocytes A and B by a meiotic division (spermatocytogenesis) and will lead to the formation of spermatids (spermatidogenesis). Spermatids are then transformed into mature spermatozoa (spermiogenesis) which are released into the lumen of the seminiferous tubules (spermation). While *ornithine decarboxylase 1* gene expression (*ODC1*) steadily increases during spermatogenesis, its activity is conversely reduced after meiotic maturation and formation of haploid germ cells (spermiogenesis and spermation) (Weiner and Dias 1992). The antizyme 3 (AZI3) and antizyme inhibitor 2 (AZIN2), which respectively inhibit ODC1 activity and polyamine uptake, and regulate the intracellular distribution of polyamines are elevated in a similar temporal and spatial pattern during spermiogenesis and spermation, in the outer part of the seminiferous epithelium, therefore controlling intracellular polyamine biosynthesis and distribution (Ivanov, Rohrwasser et al. 2000; Tosaka, Tanaka et al. 2000; Lopez-Contreras, Ramos-Molina et al. 2009; Kanerva, Makitie et al. 2010; Lopez-Contreras, Ramos-Molina et al. 2010).

VI. ARTICLE 4: POLYAMINES ARE IMPLICATED IN THE EMERGENCE OF THE BLASTOCYST FROM OBLIGATE DIAPAUSE

Status : Submitted for publication in *Endocrinology.* Provisionally accepted, in revision.

Polyamines are implicated in the emergence of the blastocyst from obligate diapause

Pavine L.C. Lefèvre[1], Marie-France Palin[2], Gary Chen[3], Gustavo Turecki[3] and Bruce D. Murphy[1]

[1] Centre de Recherche en Reproduction Animale, Faculté de Médecine Vétérinaire, Université de Montréal, QC, Canada. [2] Dairy and Swine R & D Centre, Agriculture and Agri-Food Canada, QC, Canada. [3] Department of psychiatry, McGill Group for Suicide Studies, Douglas Hospital, QC, Canada.

Short title: Polyamines and obligate embryonic diapause

Key words: polyamines, ornithine decarboxylase 1, embryonic diapause, implantation, trophoblast.

[1] Corresponding Author (to whom reprint requests should be addressed): Centre de Recherche en Reproduction Animale, Faculté de Médecine Vétérinaire, Université de Montréal, 3200 rue Sicotte, St-Hyacinthe, J2S 7C6, QC, Canada. Tel: 001-450-773-8521 ext. 8627; fax: 001-450-778-8103;

This work was supported by the Discovery Grant from the Natural Sciences and Engineering Research Council of Canada to Bruce D. Murphy. The authors have no real or potential conflicts of interest to declare with entities related to the material being published.

ABSTRACT

Embryonic diapause is a poorly understood phenomenon of reversible arrest of embryo development prior to implantation. In many carnivores, such as mink (*Neovison vison*), obligate diapause is a characteristic of each gestation. Reactivation of the blastocyst is controlled by the uterus by mechanisms that remain elusive. As polyamines are essential regulators of cell proliferation and growth, it was hypothesized that they trigger blastocyst reactivation. To test this, mated mink females were treated with α–difluoromethylornithine (DFMO), an inhibitor of ornithine decarboxylase 1 (ODC1), the rate limiting enzyme in polyamine biosynthesis, or saline as a control, during the first five days of blastocyst reactivation. This treatment induced polyamine deprivation with the consequence of rearrest in proliferation of embryonic cell. A mink trophoblast cell line maintained in an *in vitro* culture system and subjected to DFMO treatment likewise displayed an arrest in cell proliferation, morphological changes and intracellular translocation of ODC1 protein. The arrest in embryonic development deferred implantation for a period consistent with the length of treatment after which successful implantation and parturition ensued. We conclude that polyamine deprivation brought about a reversible rearrest of embryonic development which returned the mink embryo to diapause, and induced a second delay in implantation of the blastocysts. These results are the first to demonstrate a factor essential to reactivation of embryos in obligate diapause.

A. Introduction

Putrescine, spermidine and spermine are polyamine molecules found in all mammalian cells (Wallace, Fraser et al. 2003). At physiological pH, the positively charged polyamines bind DNA and RNA molecules (Wallace, Fraser et al. 2003), thereby modifying chromatin structure, regulating the rate of DNA synthesis and influencing cell proliferation (Alm and Oredsson 2009), as well as controlling gene expression at both the transcriptional and translational levels (reviewed in (Igarashi and Kashiwagi 2009)). Polyamines can be either directly imported from the diet (Bardocz 1993), or synthesized *de novo* from amino acids, such as L-arginine and L-methionine (Tabor and Tabor 1964; Tabor and Tabor 1984). Ornithine decarboxylase 1 (ODC1), the rate limiting enzyme in polyamine biosynthesis, converts L-ornithine derived from L-arginine into putrescine (Tabor and Tabor 1964). Polyamines are essential to gametogenesis (Kaipia, Toppari et al. 1990; Hakovirta, Keiski et al. 1993; Bastida, Cremades et al. 2005) and fertilization (Fleming and Armstrong 1985), and are indispensable for early embryonic development (Alexandre 1978). Null mutation of the *Odc1* gene in mice interdicts survival beyond the blastocyst stage (Pendeville, Carpino et al. 2001). Polyamine deprivation, induced by administration of a polyamine biosynthesis inhibitor, such as α-difluoromethylornithine (DFMO) on the day of implantation, causes an arrest of embryonic development in the mouse, rat and hamster (Fozard, Part et al. 1980; Fozard, Part et al. 1980; Reddy and Rukmini 1981; Galliani, Colombo et al. 1983; Lopez-Garcia, Lopez-Contreras et al. 2008).

Embryonic diapause is the reversible arrest of embryonic development at the blastocyst stage, resulting in implantation (Lopes, Desmarais et al. 2004). Interestingly, *in vitro* reactivation of mouse embryos in diapause was delayed in the presence of DFMO, while trophoblast outgrowth, reflecting reactivation, was induced when DFMO was removed and/or replaced by polyamines (Van Winkle and Campione 1983). In the mink, obligate embryonic diapause occurs during each pregnancy during its reproductive life (Hansson 1947; Enders 1952). Termination of embryonic diapause in this species is induced by increasing secretion of prolactin from the pituitary gland (Murphy, Concannon et al. 1981), under the influence of increasing photoperiod at the vernal equinox (Murphy and James 1974). Prolactin induces ovarian luteal cell activation and an increase in progesterone secretion associated with reactivation and implantation of blastocysts (Papke, Concannon et al. 1980). It has been suggested that the mink embryo in diapause is maintained in the quiescent G0/G1 phase of the cell cycle (Desmarais, Bordignon et al. 2004). Following initiation of reactivation, a marked increase in embryo diameter and DNA and protein synthesis occurs within 72 hours (h) (Desmarais, Bordignon et al. 2004). To better understand mink embryo reactivation, we recently performed a transcriptomic analysis of the mink uteri, comparing those with reactivated blastocysts and with blastocyst in diapause, using suppressive subtractive hybridization (SSH) (Lefèvre PLC, Palin M-F, Beaudry D, Dobias-Goff M, Desmarais JA, Vargas EML and Murphy BD, 2010, unpublished). We found upregulation of uterine expression of three genes at emergence from embryonic diapause of mink embryos. These three genes encode for enzymes implicated in polyamine metabolism, *ODC1*,

antizyme inhibitor 1 (AZIN1) and *spermidine/spermine N1-acetyltransferase 1 (SAT1)*.

The aim of the present study was to assess whether polyamines are essential to blastocyst reactivation and consequent development of blastocysts, using an animal model that naturally exhibits embryonic diapause, i.e. the mink. After establishing that uterine production of polyamines increases concomitantly with embryonic reactivation, we investigated the consequences of polyamine deprivation induced by DFMO treatment during early embryo reactivation on: 1) embryonic development, 2) on subsequent implantation and post-implantation development of blastocysts and 3) the success of gestation. We confirmed our results using an *in vitro* mink trophoblast cell culture experimental model.

B. Material and methods

1. Tissue collection and treatment

All procedures involving live animals were approved by the *Comité de déontologie de la Faculté de Médecine Vétérinaire, Université de Montréal,* which is accredited by the Canadian Council on Animal Care. Investigations were carried out during two consecutive annual breeding seasons in 2009 to 2010 using ranch mink of the Pastel variety purchased from A. Richard (St. Damase, QC, Canada). During this period, each mink female was bred to two fertile males according to usual farm mating practices. Embryo reactivation was synchronized among females by daily injection of 1 mg/kg/day ovine prolactin (Sigma-Aldrich, Oakville, ON, Canada) beginning on the March 21st and for the following 10 days as we have previously described (Murphy, Concannon et al. 1981). The first day of prolactin injection was

designated day (d) 0 of embryo reactivation. Uterine horns from mated females were collected during diapause (n = 3), seven to nine days after the final mating and prior to March 21st and on days (d) 1, 3, 5 and 7 after prolactin-induced reactivation of blastocyst development (n=3 per stage). Embryos activated, but not yet implanted, were flushed from the uterus using TC-199 medium (Gibco, Burlington, ON, Canada) containing 10% v/v fetal bovine serum (Gibco). Diameters of recovered embryos were measured using an ocular micrometer to assess blastocyst expansion following prolactin treatment (Desmarais, Lopes et al. 2007) and confirm that reactivation had occurred. Uterine samples were fixed in paraformaldehyde (PAF) 4% w/v overnight and kept at 4 C in phosphate buffered saline (PBS) 1X until they were paraffin embedded for immunohistochemical analysis.

To investigate the role of polyamines during embryo reactivation, 12 mated mink females were subcutaneously injected twice daily at 0800 h and 1600 h, during the first five days of prolactin-induced embryo reactivation (**Figure 39** (p 285)), with 500 mg/kg of α-difluoromethylornithine (DFMO) (Lopez-Garcia, Lopez-Contreras et al. 2008; Zhao, Chi et al. 2008) . DFMO was kindly provided by Dr. Patrick Woster, Wayne State University, MI, USA. Control groups comprised 19 mated females that were either sacrificed during diapause (n = 3) or injected with saline following the same schedule as DFMO injections (n = 16). Thereafter, individuals were randomly divided in three experimental groups (n = 8 per group comprising DFMO (n = 4) and saline (n = 4) treated individuals. Among those groups, mated mink females were euthanized: either one day after the end of the five day of DFMO or saline injection regime (d6 after embryo reactivation) or on day

18 after embryo reactivation (6 days after implantation). Four saline-injected individuals were sacrificed on day 14 after embryo reactivation or two days after blastocyst implantation. Entire uteri, whether with or without implantation swellings, were weighed. Implantation sites, including blastocysts/conceptuses, were isolated and individually weighed and measured. Ovaries were also collected for each individual female. Embryos activated, but not yet implanted, were flushed from the uterus using TC-199 medium (Gibco) containing 10 % v/v fetal bovine serum (Gibco) and cultured at 37 C in M16 medium (Sigma-Aldrich) for cell proliferation assays. Uterine tissue samples, implantation sites and ovaries were snap-frozen and maintained at -80 C for quantification of uterine polyamine content or fixed in 4% PAF as described above for histological and immunochemical analyses. The third experimental group was left to complete gestation and parturition (day 41).

2. Quantification of uterine polyamine content

Polyamine levels were quantified in 100 mg of uterine samples collected from mated females during diapause (n = 3), and from DFMO- and saline-treated mated females (n = 4 per group) on d6 after embryo reactivation using a gas chromatography-mass spectrometry (GC-MS) method recently developed for extraction and quantification of polyamines in post-mortem human brain tissue (Chen, Turecki et al. 2009). The method is based on a dual derivatization process with ethoxycarbonyl (EOC) reaction with functional amino groups with ethyl chloroformate (ECF) in aqueous phase followed by trifluoroacetic acid anhydride (TFAA) derivatization of the N-ethoxylcarbonyl (N-EOC) derivatives in ethyl acetate

solvent to yield the full N-EOC-N-TFA polyamine derivatives. Briefly, internal standards, [2,2,3,3-^{2}H4]-1,4-diaminobutane (putrescine-D_4) and 1,7-diaminoheptane were added at 10 ng/mg wet tissue followed by homogenization in 10 volumes of 5 % NaCl in 0.2 N HCl. Polyamines contained in the supernatant were extracted with diethyl ether. The ether layer that contains lipids and other potential contaminants was discarded. The aqueous extract layer was adjusted to pH 10 ± 1 to carry out the N-ethoxycarbonylation of the amines with ethyl chloroformate (ECF), then trifluoroacetylation reaction with trifluoroacetic acid anhydride (TFAA). GC-MS measurement of polyamines in each sample was performed in triplicate using an Agilent bench-top HP6890/MSD5973N system (Agilent Technologies, Santa Clara, CA) by electron ionization with selected ion monitoring (SIM) techniques. The GC-MS data analysis was carried out using the Chemstation software (Agilent Technologies). Calibration curves for each target analyte were plotted against measurements from authentic polyamines as calibration standards.

3. Measurement of ovarian progesterone by radioimmunoassay

Briefly, the ovaries were weighed, homogenized and extracted three times with diethyl-ether, with an extraction efficiency of 88.7 %. The progesterone concentration was analyzed by radioimmunoassay as previously described (Douglas, Houde et al. 1998). The progesterone tracer was purchased from PerkinElmer (NET 381250UC) and the progesterone antibody was kindly provided by Dr. Gordon Niswender, Colorado State University. The intra-assay coefficient of variation varied between 4-10 % and the inter-assay coefficient of variation was 7.76 %.

4. Immunoblotting

Total protein extracts from whole uterine tissue samples were obtained by sonification in buffer (20 mM Tris-HCl pH 8.0, 0.05 mM EDTA, 0.1 mM diethyldithiocarbamic acid (DEDTC) and Mini Complete EDTA-free protease inhibitor cocktail (1 tablet / 10 ml) (Roche, Mannheim, GE)). An aliquot of 40 µg of protein extract was separated by electrophoresis in 10 % polyacrylamide sodium dodecyl sulfate gel (SDS-PAGE) after which protein were transferred to Amsersham Hybond-P hydrophobic polyvinyl difluoride (PVDF) membranes (GE Healthcare, Buckinghamshire, UK) according to the manufacturer's instructions. The blots were blocked with 5 % nonfat dry milk in PBS 1X for 1 h at room temperature and probed with 0.2 µg/ml of a goat anti-human ODC1 antibody (ODC (N-15): sc-21515, Santa Cruz Biotechnology) for 1h at room temperature. After washing in PBS 1X 0.1 % Tween, membranes were incubated with horseradish peroxidase (HRP)-labeled goat secondary antibody (Santa Cruz Biotechnology, Santa Cruz, CA, USA) for 1 h at room temperature. Membranes were incubated with 2 ng/ml of β-actin HRP-conjugated antibody (β-Actin (C4): sc-47778, Santa Cruz Biotechnology) for 30 min at room temperature as a loading control. Immunoreactive bands were detected by Immobilon Western Chemioluminescent HRP Substrate (Millipore, Billerica, MA, USA) and visualized on Amersham Hyperfilm ECL (GE Healthcare, Buckinghamshire, UK).

5. Immunohistochemistry

Paraffin embedded cross-sections of uterine tissues were used to localize ODC1 protein expression during diapause and thereafter, according to a previously

described protocol (Desmarais, Lopes et al. 2007). Briefly, retrieval of antigens was performed on deparaffinized and hydrated sections by boiling the slides in 0.01 M citrate buffer, pH 6.0, at 95 C for 5 min. After a blocking step using 10 % w/v of bovine serum albumin (BSA) at room temperature for 6 h, tissues were incubated overnight at 4 C with 4 μg/ml of ODC (N-15) goat anti-human antibody (Santa Cruz Biotechnology, Santa Cruz, CA, USA) in a humid chamber. After three washes in PBS 1X, sections were incubated with a biotinylated rabbit anti-goat IgG antibody for 1 h at room temperature with the Vectastain ABC kit (Vector Laboratories, Burlington, ON, CA) and 3,3'-diaminobenzidine (DAB) was used to detect peroxidase activity. Negative control sections were submitted to the same procedures, except that the first antibody was replaced by diluted goat serum.

6. Mink trophoblast cell culture and treatment

Mink trophoblast cells, previously derived from mink blastocysts collected at d5 after embryo reactivation have been characterized in detail (Desmarais, Bordignon et al. 2004; Desmarais, Lopes et al. 2007). Cells were thawed and plated in mouse trophoblast stem cell medium (TS) along with 20 % fetal bovine serum, 25 ng/ml of fibroblast growth factor 4 (FGF4) (Sigma-Aldrich) and 1 μg/ml of heparin (Sigma-Aldrich). Culture medium was changed every two days. The cultures were divided at confluence (around six days of culture), by collecting and manually disrupting floating trophoblast vesicles with gentle pipetting before transferring them into a new Petri dish. For the experiments, an equal volume of homogenized trophoblast cells was plated into six well-plates of 2 ml each. Based on previous studies (Van Winkle and Campione 1983; Zhao, Chi et al. 2008), 10 mM DFMO

and/or 1 mM putrescine (1, 4-diaminobutane 99 %, Sigma-Aldrich) was administered to trophoblast cell cultures at each time the culture medium was replaced. Each experiment was performed in triplicate and replicated at least three times.

7. Cell proliferation assays

Evaluation of cell proliferation in non-implanted blastocysts and trophoblast cell culture was carried out using the Click-iT EdU Imaging Kit (Invitrogen, Carlsbad, CA, USA), according to manufacturer's instructions. Briefly, blastocysts and trophoblast cells were incubated overnight at 37 C with 100 μM of EdU diluted in M16 medium (Sigma - Aldrich) or TS medium, respectively. After fixation and permeabilization of the samples in 3.7 % formaldehyde and 0.5 % Triton X-100, EdU was detected by incubation of the samples in the Click-iT reaction cocktail including the $CuSO_4$ and Alexa Fluor 595 azide, required for the click-it reaction. Nuclei were counterstained by Hoechst 33342 before mounting the slides using Permafluor (Thermo Fisher Scientific Inc., Fremont, CA, USA) as a mounting medium. The signals were visualized using fluorescence microscopy with a Leica AS LMD microscope (Leica Microsystems Inc. Leica, Cambridge, UK).

8. Immunocytofluorescence in trophoblast cell culture

Immunocytolocalization of ODC1 by fluorescence in trophoblast cell cultures was carried out as an additional step in the cell proliferation assay protocol, following the manufacturer's instructions (Invitrogen, Carlsbad, CA, USA). After EdU detection in the Click-iT reaction cocktail and before Hoechst nuclei counterstaining, nonspecific sites in trophoblast cells were blocked by 3 % BSA for 3h. Cells were

then incubated overnight at 4 °C with 4 µg/ml goat anti-human ODC1 antibody ((N-15) Santa Cruz Biotechnology, Santa Cruz, CA, USA). After three washes in TPBS (PBS1X containing 0.1 % Tween 20), incubation with an anti-goat Alexa 488-labeled antibody took place for 45 min to localize positive staining. Negative controls were submitted to the same procedures, except that the first antibody was replaced by diluted goat serum. Nuclei were counterstained with Hoechst 33342 and slides were mounted as described above.

9. Quantification of gene expression by quantitative real-time PCR

Total RNA was extracted from whole uterine samples and trophoblast cells using the RNeasy Micro and RNeasy Mini kits (Qiagen, Mississauga, ON, Canada) respectively, according to the manufacturer's instructions. One microgram of RNA was reverse transcribed into complementary DNA (cDNA) with Superscript II Reverse Transcriptase (Invitrogen, Carlsbad, CA, USA). The primers sequences for the reference gene *glyceraldehyde-3-phosphate dehydrogenase* (*GAPDH*, GenBank AF076283) and *ODC1* (GenBank GH271813) were as follow: 5'-TCCCCACCCCCAATGTG-3' and 5'-CC CTCTGATGCCTGCTTCA-3' for *GAPDH* and 5'-CTACAACGGATTCCAGATGATGAC-3' and 5'-GGTGGCAATCCGCAAAAC-3' for *ODC1*. The specificity of amplified products was verified by dissociation curve analysis for each primer set. To evaluate PCR efficiency, standard curves were prepared for the studied genes using a pool of either uterine cDNA or trophoblast cDNA, from all samples. PCR efficiency for each gene was co-evaluated using the LinRegPCR software (Ruijter, Ramakers et al. 2009). Triplicate real-time PCR amplifications were performed in 20 µl reaction volume consisting of 1 µl each of the sense and

antisense primers (20 μM), 10 μl of Power SYBRGreen PCR Master Mix (PE Applied Biosystems) and 6 μl of cDNA diluted 1:15 and 2 μl of distilled water. Cycling conditions were 2 min at 50 C and 10 min at 95 C, followed by 40 cycles of 15 sec at 95 C and 1 min at 60 C. Amplification, detection and data analyses were performed using a 7300 Real-Time PCR System (PE Applied Biosystems) and the Sequence Detection Software version 1.4 (PE Applied Biosystems). Relative quantitation using the comparative Ct method (delta-delta Ct) was employed to quantify gene expression as previously described (Pfaffl 2001). Gene expression in three experimental samples for each stage of gestation was measured in triplicate.

10. Statistical analysis

Data were analyzed using the JMP, Version 7 (SAS Institute Inc., Cary, NC, USA) and STATISTICA 8.0 (StatSfoft, Inc., Tulsa, OK, USA). Differences in *ODC1* gene expression in uterine samples between diapause and days 3, 5 and 7 after blastocyt reactivation, polyamine quantification in uterine samples collected from DFMO-treated or control group during diapause and on day 5 after reactivation, in percentage of proliferating cell in blastocysts collected from females subjected to DFMO or control females and in diameter and weight of implantation sites from DFMO or control females at day 14 or 18 after blastocyst reactivation.were undertaken using the multiple comparison of mean rank. When two sample means were compared, the Wilcoxon rank sum test was employed. Data obtained from ODC1 immunoblottings were submitted to ANOVA and Tukey's test for multiple mean comparisons. Statistical difference was recognized when $P < 0.05$.

C. Results

1. Polyamine biosynthesis at embryo reactivation in the mink uterus

Expression of the *ODC1* gene increased between diapause and days 3 after blastocyst reactivation (P = 0.004) (**Figure 40** A (p 287)). The result was further confirmed by immunoblots that showed increases in ODC1 protein abundance in uterine tissue between diapause and day 5 after activation (P= 0.041) (**Figure 40** B (p 287)). Immunolocalization of ODC1 in the mink endometrium also revealed a strong increase in ODC1 protein level in the endometrial luminal and glandular epithelia and, subepithelial stroma at day 1 after embryo reactivation (**Figure 40** C b (p 287)) in comparison to diapause where the intensity of staining for ODC1 was weaker and limited to luminal epithelium and subepithelial stroma (**Figure 40** C a (p 287)). At higher magnification, ODC1 protein could be observed in the cytoplasm of endometrial cells (**Figure 40** C c, d (p 287)).

Since *ODC1* encodes for the rate-limiting enzyme for polyamine biosynthesis, we quantified polyamines, namely putrescine, spermidine and spermine in uterus samples during diapause and after blastocyst reactivation by GC-MS (**Figure 41** A (p 289)). The amounts of putrescine, spermidine and spermidine tends to increase on d6 after embryo reactivation in comparison to diapause, but was only significant for the concentrations of putrescine (P = 0.049).

2. Validation of the *in vivo* experimental model based on DFMO treatment during early embryo reactivation

To evaluate the potential role of polyamines in emergence of the embryo from diapause, mated females were treated for the first five days of embryo reactivation with DFMO, an inhibitor of ODC1, the rate-limiting enzyme for polyamine biosynthesis (**Figure 39** (p 285)). To confirm the effectiveness of DFMO treatment, concentrations of polyamines were quantified in uterine samples from DFMO- and non-treated pregnant females at d6 after embryo reactivation (**Figure 41** B (p 289)). Uterine concentrations of putrescine, spermine and spermidine were reduced after five days of DFMO treatment, in comparison to polyamine content of control uteriand this decrease was significant for putrescine (P = 0.034) and spermidine (P = 0.034). These results indicate that polyamine content is strongly reduced in the uterus after five days of treatment with DFMO during early embryo reactivation.

An earlier study found that DFMO treatment could affect ovarian production of progesterone (Bastida, Tejada et al. 2002). To assess whether the effect of polyamine deprivation observed on blastocyst reactivation is due to disrupted corpus luteum formation and secretion of progesterone during blastocyst reactivation, progesterone was measured in ovaries collected from DFMO- and non-treated mated females on day 6 after blastocyst reactivation. Levels of ovarian progesterone in the control group (26.82 ± 4.93 ng/mg (mean ± SEM)) and DFMO-treated group (22.00 ± 1.64 ng / mg (mean ± SEM)) were not different, thus confirming that polyamine deprivation induced by DFMO treatment of mated mink

females does not disrupt ovarian luteinization and progesterone production during early reactivation of blastocysts.

3. Effects of polyamine deprivation on embryo reactivation

We investigated the effect of polyamine deprivation during the first 5 days of blastocyst reactivation at day 6 after reactivation (**Figure 39** (p 285)). Since viable embryos were found in medium obtained from uterine flushings for all mated females whether treated or not with DFMO (n=4 per group), no pregnancy loss appeared to be associated with uterine polyamine deprivation. The mean number of embryos recovered in uterine flushings per female was higher (*P=0.027*) in the DFMO-treated group (9.25 ± 1.44 (mean ± SEM)) than in the control group collected during diapause (4.00 ± 0.00 (mean ± SEM)), but was similar to the saline control group at d6 after reactivation (6.25 ± 0.56 (mean ± SEM)). Evaluation of uterine morphology and histology revealed no macroscopical or microscopical abnormalities associated with polyamine deprivation (data not shown). In addition, the DFMO treatment had no effect on uterine weight in these samples taken prior to implantation (data not shown).

Characteristics of embryo reactivation, such as increases in diameter of blastocysts and resumption of embryonic cell proliferation, were evaluated for blastocysts recovered in uterine flushings from DFMO-treated and -saline control groups at day 6 after embryo reactivation. Mean diameters of embryos collected in the DFMO-treated group (0.47 ± 0.02 (mean ± SEM)) and in the control group (0.45 ± 0.01 (mean ± SEM)) were comparable and both were increased ($P < 0.002$) in comparison to mean diameter of blastocysts collected during diapause (0.31 ± 0.01

(mean ± SEM)), indicating that embryo expansion was not affected by DFMO treatment.

We also assessed whether DFMO treatment influenced the rate of cell proliferation during early reactivation of blastocysts (**Figure 42** (p 291)). In blastocysts flushed from uteri of the control group at 6 days after embryo reactivation, nearly all trophoblast cells and cells from the internal cell mass (ICM) were positive for EdU (**Figure 42** a, b, c (p 291)). This suggests a high rate of cell proliferation in the whole blastocyst. In contrast, the number of proliferating cells was sharply reduced in embryos from the DFMO-treated females (**Figure 42** d (p 291)) compared to embryos from the control group (**Figure 42** a (p 291)). In addition, cell distribution was not expanded as observed in blastocysts from the control group (**Figure 42** c, f (p 291)). Cell proliferation was only detectable in ICM cells (**Figure 42** f (p 291)) in blastocysts recovered from the DFMO-treated group. That observation was confirmed by counts of proliferating and total cells in blastocysts collected from DFMO-treated group (n = 7) and blastocysts from the control group (n = 4) at six days after embryo reactivation. The mean percentage of proliferating cells in blastocysts flushed from DFMO-treated females (8.80 ± 1.99 % (mean ± SEM)) was substantially lower (P=0.008) than in the control group (67.10 ± 6.47 % (mean ± SEM)). These results suggest that polyamine deprivation maintained or induced a state of diapause, primarily in the trophoblast.

4. Effects of polyamine deprivation or putrescine administration on mink trophoblast cells *in vitro*

Since trophectoderm cell proliferation arrest in blastocysts appeared to be associated with polyamine deprivation during early embryo reactivation, we next focused on evaluating direct effects of polyamine deprivation and/or putrescine supplementation on *in vitro* mink trophoblast cell cultures

Figure 43 a (p 293)). Trophoblast cells were treated for two weeks with PBS, as a control, with putrescine or with DFMO to investigate long-term effects of putrescine and DFMO treatment on trophoblast cell cultures *in vitro*. In the control group, trophoblast cells grew normally in compact colonies of small cells that became confluent after six days of culture (**Figure 43** A (p 293), upper panel). After 10 days of culture, trophoblast outgrowth in the form of vesicles floating at the surface of the colonies was detected. Similar observations were made for trophoblast cells treated with putrescine (**Figure 43** A (p 293), middle panel). For both control and putrescine treated cells, the number of proliferating trophoblast cells was substantially increased after 13 days of culture (**Figure 43** B a, c (p 293)) and nuclear staining confirmed the presence of high density of trophoblast cells (**Figure 43** B b, d (p 293)). In contrast, when DFMO was administered to trophoblast cells, changes in colony and cell morphology occurred (**Figure 43** A (p 292), lower panel). Well-defined colonies were not observed at day 3 of culture as were present in the control or putrescine-treated cell cultures. Cell density decreased, resulting in dispersed trophoblast cells with expanded cytoplasm, and that effect was increased with the duration of DFMO treatment. No outgrowth of trophoblast vesicles were

seen in DFMO-treated cells. Furthermore, no cell proliferation among trophoblast cells could be detected after the 13 days of culture in presence of DFMO (**Figure 43** B e (p 293)) and the density of Hoechst-stained nuclei was dramatically reduced in comparison to the control and putrescine-treated groups (**Figure 43** B f (p 293)). Interestingly, enlarged nuclei and binucleate trophoblast cells were detected in DFMO-treated group (**Figure 43** B f (p 293)), suggesting differentiation.

We then assessed whether DFMO treatment of trophoblast cells was reversible. DFMO was administered for the first week to trophoblast cell culture and, replaced by either PBS (**Figure 44** A (p 295), middle panel) or putrescine (**Figure 44** A (p 295), lower panel). During the first week of treatment, growth of well-defined colonies was arrested, trophoblast cell density was reduced and enlargement of the cytoplasmic compartment occurred, as previously observed (**Figure 44** A (p 295), lower panel or **Figure 44** A (p 295), upper panel)). Surprisingly, DFMO removal and replacement by either PBS or putrescine was followed by a rapid resumption of trophoblast cell proliferation, as exhibited by the formation of compact colonies with small cells observed three days after the removal of DFMO **Figure 44** A (p 295), middle and lower panel). The latter observation was confirmed by an increase in the rate of cell proliferation (**Figure 44** B c, e (p 295)) and higher cell density (**Figure 44** B d, f (p 295)) one week after removal of DFMO treatment. Co-treatment for two weeks with DFMO and putrescine repressed DFMO-induced morphological changes and the consequent trophoblast cell colonies displayed normal growth and formation of trophoblastic vesicles, as observed in the control group (data not shown).

ODC1 immunocytolocalization in DFMO- and putrescine-treated trophoblast cells and control cells was carried out after two weeks of treatment (**Figure 45** (p 297)). In the control group, ODC1 was strongly expressed in all trophoblast cells, including proliferating and non-proliferating cells (**Figure 45** a, b (p 297)). At higher magnification, ODC1 consistently displayed a clear perinuclear distribution seemingly contained in small vesicles surrounding the nucleus in all cells (**Figure 45** c, d (p 297)). In putrescine-treated cells, a similar pattern for ODC1 immunocytochemical localization was observed (data not shown). In contrast, ODC1 was detected in DFMO-treated trophoblastic cells (**Figure 45** g-j (p 297)), but surprisingly, its subcellular distribution differed. Besides a minor signal for ODC1 in the cytoplasm and plasma membrane, ODC1 was strongly localized within nuclei of mono- and multinucleate cells (**Figure 45** h, I (p 297)). The ODC1 staining in DFMO-treated trophoblast cells confirmed DFMO-induced morphological changes with extensive expansion of the cytoplasm and enlarged nuclei in contrast to the smaller cells observed in the control group.

5. Effect of polyamine deprivation on post-implantation embryo development

To assess whether polyamine deprivation during early embryo reactivation affects consequent implantation, mated females treated with DFMO (n = 4) or saline (n = 4) during the first five days following embryo reactivation were sacrificed 18 days after embryo reactivation (six days after implantation). A second control group was constituted of mated females (n = 4), sacrificed on d14 after reactivation (two days post-implantation). Uteri of females from both the DFMO and control

groups, contained similar numbers of either implantation sites or non-implanted embryos. There was an average of 10.67 ± 2.31 (mean ± SEM) and 7.00 ± 1.32 (mean ± SEM) implantation sites per female in DFMO- and saline-treated groups respectively at day 18 post reactivation, or day 6 after expected implantation. The morphology and histology of implantation sites in the DFMO-treated group revealed no apparent abnormalities. Implantation sites were equally spaced along the two uterine horns in the DFMO-treated group, consistent with the observations in the control group. Microscopic observation revealed embryo attachment and invasion which had occurred at the antimesometrial pole of the implantation sites in both the DFMO-treated and control groups. The typical endotheliochorial placenta with its fetal-maternal labyrinth, maternal symplasma and glandular zona at implantation site could be readily identified in the DFMO and control groups at day 18 postreactivation. Pregnancy was confirmed by the presence of the fetus in the implantation chambers collected from mink in both DFMO and control groups. Both the mean diameter and weight of implantation sites from the DFMO-treated group were lower than those measured in the control group at day 6 post-implantation ($P < 0.001$ for both parameters) (**Figure 46** (p 299)). Interestingly, mean diameter and weight of implantation sites from the DFMO-treated group at day 6 post-implantation were comparable to those found at implantation sites collected from the control group at day 2 post-implantation (**Figure 46** (p 299)), demonstrating that a five day treatment with DFMO delayed the process of embryo implantation by an equivalent interval.

To further validate fetal viability of the DFMO-induced retarded embryos, we investigated litter size at parturition in control (n=4) and mated females (n=4) treated with DFMO during the first five days of embryo reactivation. In the control group, all of the females gave birth with an average of 3.75 ± 1.60 (mean ± SEM) pups per female at 55.0 ± 2.03 (mean ± SEM) days of gestation, while DFMO-treated females gave birth with a mean litter size of 4.5 ± 1.50 (mean ± SEM) pups per female at 58.50 ± 7.52 (mean ± SEM) days of gestation.

D. Discussion

The polyamines, putrescine, spermidine and spermine play multiple roles in cell survival and in cell proliferation. Obligate embryonic diapause is characterized by mitotic arrest (Lopes, Desmarais et al. 2004), and global gene expression analysis has demonstrated the upregulation of genes regulating polyamine synthesis associated with the reactivation of the embryo in diapause (Lefèvre PLC, Palin M-F, Beaudry D, Dobias-Goff M, Desmarais JA, Vargas EML and Murphy BD. 2010, unpublished). We therefore hypothesized that these compounds are involved in the escape of the mink embryo from diapause. To verify the latter hypothesis, we reactivated embryonic development *in vivo* in embryos in diapause by means of exogenous prolactin treatment, a method that we have previously demonstrated to be effective (Murphy, Concannon et al. 1981), and which has resulted in cell proliferation in control animals. We blocked polyamine biosynthesis during the early stages of emergence of blastocysts from diapause using DFMO, as specific inhibitor of ODC1. Globally, the lack of polyamines during resumption of embryo development was not detrimental to pregnancy, as shown by normal fetuses at

implantation sites and subsequent normal litters in DFMO-treated females. Nonetheless, the timing of implantation was retarded in females that were subjected to polyamine deprivation, as reflected by reduced diameter and weight of implantation sites. The length of this artificially-induced delay was comparable to the duration of DFMO treatment during early reactivation, thus demonstrating that a lack of polyamines at reactivation of blastocysts postponed implantation. These results concur with results from studies to evaluate the effects of polyamine deprivation at different stages of mouse embryonic development where fetal viability at one day before parturition was not affected by DFMO administration to pregnant mouse females during the first three days of pregnancy (Lopez-Garcia, Lopez-Contreras et al. 2008). No previous reports are available in any species to demonstrate prolongation of the delay in embryo implantation by polyamine deprivation and the present study is the first demonstration of the role of polyamines in preimplantation embryonic development.

Ovarian progesterone support of the endometrium is essential for blastocysts reactivation following embryonic diapause in mink (Papke, Concannon et al. 1980), and polyamine deprivation induced by DFMO treatment has been reported to affect ovarian production of progesterone in mice (Bastida, Cremades et al. 2005). Our findings showed that progesterone synthesis was not disrupted by DFMO treatment in the mink. Thus, postponed embryo implantation associated with DFMO treatment during early reactivation does not result from failure of ovarian steroidogenesic, but rather from direct consequences of the lack of polyamines in the uterine environment during the preimplantation period.

Our results argue that the mechanism affected by polyamine deprivation leads to mitotic arrest, as cell proliferation was strikingly lower in embryos collected from DFMO-treated females compared to embryos from the control group. Embryo expansion, which we have previously shown to precede mitotic resumption in mink embryos (Desmarais, Bordignon et al. 2004), did not appear to be affected by the lack of polyamines. Trophoblast cells were more affected than cells from the inner cell mass, which displayed proliferative activity. It has been proposed that the cell cycle is arrested at G0/G1 in obligate diapause, a quiescent state of the mitotic cycle (Lopes, Desmarais et al. 2004), consistent with the proposed effect of ODC1 inhibition in inducing cell cycle arrest at G0/G1 (Hessels, Kingma et al. 1989; Broaddus, Xie et al. 2004; Deng, Jiang et al. 2008). Thus, our results support this concept and provide convincing evidence that polyamines are involved in blastocyst reactivation, specifically in the resumption of trophoblast cell proliferation. Postponed implantation events are a direct consequence of the arrest in embryo development following reactivation induced by the lack of polyamines at the time of emergence from embryonic diapause.

The *in vitro* results support the *in vivo* observations demonstrating that treatment of the dam with an inhibitor of polyamine synthesis arrests reactivation of the embryo. Indeed, mink trophoblast cells responded *in vitro* to polyamine deprivation by a precipitous decline in cell proliferation. Moreover, the fact that cell proliferation was rescued upon removal of the polyamine synthesis inhibitor is consistent with the resumption of embryonic development and successful pregnancies observed in DFMO-treated females, *in vivo*.

Changes in cell morphology are also consistent with an effect of polyamines on mitotic events. The treatment induced transformation of small and compact cells into enlarged multinucleate cells and there was translocation of ODC1 protein from perinuclear to nuclear subcellular sites in polyamine-deprived trophoblast cells. Similar changes in cell morphology and a decline in cell proliferation in response to the absence of polyamines have been reported in human epidermal keratinocytes (Pomidor, Ruhl et al. 1995). The subcellular localization of ODC1 protein appears to be tightly controlled during the cell cycle, with strong nuclear and a diffuse cytoplasmic localization during the M phase, specifically at cytokinesis, and perinuclear localization during the G1 and G2 phase human cervix carcinoma and human prostatic carcinoma cells (Schipper, Cuijpers et al. 2004). Perinuclear ODC1 and polyamines were reported to colocalize with the endoplasmic reticulum and polyribosomes, where they regulate protein synthesis in rat pancreatic acinar cells and neurons of the lateral reticular nucleus of rat medulla oblongata (Morisset, Sarfati et al. 1986; Fujiwara, Bai et al. 1998). In contrast, nuclear and cytoplasmic ODC1 localization suggests a role for polyamines in mitotic spindle formation, such as rearrangement of the cytoskeleton, and chromatin condensation (Heiskala, Zhang et al. 1999; Schipper, Cuijpers et al. 2004). Recently, ODC1 and polyamines were implicated in actin polymerization, which is indispensable for the process of cytokinesis (Pollard 2010), by regulating ras homolog gene family member A (RhoA), a member of the GTP-ase family (Makitie, Kanerva et al. 2009). Genetic disruption of the gene encoding for *RhoA* in Swiss 3T3 cells provoked inhibition of cell proliferation by retarding entry into the S phase of the cell cycle and

maintaining cells in G0/G1, and blocked successful completion of cytokinesis, resulting in an increase in binucleate cells (Morin, Flors et al. 2009). Together, these observations suggest that polyamine deprivation brings about cell cycle arrest at the G0/G1 in mink trophoblastic cells, as appear to be the case for mink embryos in diapause (Desmarais, Bordignon et al. 2004). Simultaneous treatment of cells with DFMO and putrescine prevented the induction of this quiescent-like state in mink trophoblast cells, thus reinforcing the fact that polyamines are indispensable for maintenance of the cell cycle in the embryo. Further experiments are required to provide better insight into molecular mechanisms underlying polyamine regulation of the cell cycle in trophoblast cells.

Our objective was to explore the involvement of polyamines in the resumption of embryonic development at the emergence of blastocysts from obligate embryonic diapause, using the mink as an animal model. The concomitant increase in uterine expression of *ODC1*, the rate limiting enzyme for polyamine biosynthesis and the increase of polyamine levels with emergence from embryonic diapause strongly support the view that polyamines are major factors supporting embryo reactivation in the mink. Our results showed that the lack of polyamines during reactivation of blastocysts from diapause extends or reinduces diapause, by maintaining trophoblast cells in a quiescent-state, as confirmed in our *in vitro* model. Since removal of the polyamine synthesis inhibitor resulted in postponed implantation of blastocysts but did not disrupt subsequent post-implantation pregnancy, we propose that polyamines are key factors of embryo reactivation that terminates obligate embryonic diapause in the mink.

E. Acknowledgements

The authors acknowledge the participation of Mira Dobias-Goff, Vickie Roussel, Debora Salmeron, Evelyn Llerena, Brïte Pauchet, Joelle Desmarais, Paul Carrière, Patrick Vincent and Catherine Charron for the technical support and sample collection, Anne-Marie Cadutal for ovarian progesterone measurement, Guy Beauchamp and Reza Kohan-Ghadr for help in statistical analysis.

F. References

(1986). Université René Descartes.

Adams, C. E. (1981). "Observations on the induction of ovulation and expulsion of uterine eggs in the mink, Mustela vison." J Reprod Fertil **63**(1): 241-248.

Aitken, R. J. (1977). "Changes in the protein content of mouse uterine flushings during normal pregnancy and delayed implantation, and after ovariectomy and oestradiol administration." J Reprod Fertil **50**(1): 29-36.

Aitken, R. J. (1977). "The culture of mouse blastocysts in the presence of uterine flushings collected during normal pregnancy, delayed implantation and pro-oestrus." J Embryol Exp Morphol **41**: 295-300.

Alcivar, A. A., L. E. Hake, et al. (1989). "Developmental and differential expression of the ornithine decarboxylase gene in rodent testis." Biol Reprod **41**(6): 1133-1142.

Alexandre, H. (1978). "[Effect of inhibitors of polyamine biosynthesis on primary differentiation of mouse egg]." C R Acad Sci Hebd Seances Acad Sci D **286**(16): 1215-1217.

Alexandre, H. (1979). "The utilization of an inhibitor of spermidine and spermine synthesis as a tool for the study of the determination of cavitation in the preimplantation mouse embryo." J Embryol Exp Morphol **53**: 145-162.

Allais, C. and L. Martinet (1978). "Relation between daylight ratio, plasma progesterone levels and timing of nidation in mink (Mustela vison)." J Reprod Fertil **54**(1): 133-136.

Alm, K. and S. Oredsson (2009). "Cells and polyamines do it cyclically." Essays Biochem **46**: 63-76.

Altschul, S. F., W. Gish, et al. (1990). "Basic local alignment search tool." J Mol Biol **215**(3): 403-410.

Ashworth, C. J., L. M. Toma, et al. (2009). "Nutritional effects on oocyte and embryo development in mammals: implications for reproductive efficiency and

environmental sustainability." Philos Trans R Soc Lond B Biol Sci **364**(1534): 3351-3361.

Bachrach, U. (2010). "The early history of polyamine research." Plant Physiol Biochem.

Bamberger, A. M., A. Makrigiannakis, et al. (2003). "Expression of the high-mobility group protein HMGI(Y) in human trophoblast: potential role in trophoblast invasion of maternal tissue." Virchows Arch **443**(5): 649-654.

Bardocz, S. (1993). "The role of dietary polyamines." Eur J Clin Nutr **47**(10): 683-690.

Barkai, U. and P. F. Kraicer (1978). "Definition of period of induction of deciduoma in the rat using ornithine decarboxylase as a marker of growth onset." Int J Fertil **23**(2): 106-111.

Bassez, T., J. Paris, et al. (1990). "Post-transcriptional regulation of ornithine decarboxylase in Xenopus laevis oocytes." Development **110**(3): 955-962.

Bastida, C. M., A. Cremades, et al. (2005). "Influence of ovarian ornithine decarboxylase in folliculogenesis and luteinization." Endocrinology **146**(2): 666-674.

Bastida, C. M., F. Tejada, et al. (2002). "The preovulatory rise of ovarian ornithine decarboxylase is required for progesterone secretion by the corpus luteum." Biochem Biophys Res Commun **293**(1): 106-111.

Belting, M., K. Mani, et al. (2003). "Glypican-1 is a vehicle for polyamine uptake in mammalian cells: a pivital role for nitrosothiol-derived nitric oxide." J Biol Chem **278**(47): 47181-47189.

Bengtsson, B. O., K. Wiberg, et al. (1994). "Ornithine decarboxylase activity and concentrations of polyamines in embryos of diabetic rats." Biol Neonate **66**(4): 230-237.

Berria, M., M. M. Joseph, et al. (1989). "Role of prolactin and luteinizing hormone in regulating timing of implantation in the spotted skunk." Biol Reprod **40**(2): 232-238.

Bininda-Emonds, O. R., J. L. Gittleman, et al. (1999). "Building large trees by combining phylogenetic information: a complete phylogeny of the extant Carnivora (Mammalia)." Biol Rev Camb Philos Soc **74**(2): 143-175.

Bistulfi, G., P. Diegelman, et al. (2009). "Polyamine biosynthesis impacts cellular folate requirements necessary to maintain S-adenosylmethionine and nucleotide pools." Faseb J.

Blackshear, P. J., J. M. Manzella, et al. (1989). "High level, cell-specific expression of ornithine decarboxylase transcripts in rat genitourinary tissues." Mol Endocrinol **3**(1): 68-78.

Blake, E. J., J. Schindler, et al. (1982). "Protein synthetic requirements for the outgrowth of trophoblast cells from mouse blastocysts." J Exp Zool **224**(3): 401-408.

Bloch, S. (1971). "Observations on the problem of delayed nidation in suckling mice." J Reprod Fertil **26**(2): 279-280.

Bolkenius, F. N. and N. Seiler (1981). "Acetylderivatives as intermediates in polyamine catabolism." Int J Biochem **13**(3): 287-292.

Bowness, E. R. (1968). "A survey of the gestation period and litter size in ranch mink." Can Vet J **9**(5): 103-106.

Broaddus, R. R., S. Xie, et al. (2004). "The chemopreventive agents 4-HPR and DFMO inhibit growth and induce apoptosis in uterine leiomyomas." Am J Obstet Gynecol **190**(3): 686-692.

Buchanan, T. A. and J. L. Kitzmiller (1994). "Metabolic interactions of diabetes and pregnancy." Annu Rev Med **45**: 245-260.

Bulger, W. H. and D. Kupfer (1976). "Induction of uterine ornithine decarboxylase (ODC) by antiestrogens. Inhibition of estradiol-mediated induction of ODC: a possible mechanism of action of antiestrogens." Endocr Res Commun **3**(3-4): 209-218.

Byers, T. L., J. R. Lakanen, et al. (1994). "The role of hypusine depletion in cytostasis induced by S-adenosyl-L-methionine decarboxylase inhibition: new evidence provided by 1-methylspermidine and 1,12-dimethylspermine." Biochem J **303 (Pt 2)**: 363-368.

Canivenc, R. and M. Bonnin (1979). "Delayed implantation is under environmental control in the badger (Meles meles L.)." Nature **278**(5707): 849-850.

Carpenter, J. R. and J. R. Fozard (1982). "Enhancement of ovulation in the rat by DL-alpha-difluoromethylornithine, an irreversible inhibitor of ornithine decarboxylase." Eur J Pharmacol **80**(2-3): 263-266.

Casero, R. A. and A. E. Pegg (2009). "Polyamine catabolism and disease." Biochem J **421**(3): 323-338.

Casero, R. A. and P. M. Woster (2009). "Recent Advances in the Development of Polyamine Analogues as Antitumor Agents (section sign)." J Med Chem.

Casillas, E. R., C. M. Elder, et al. (1980). "Adenylate cyclase activity of bovine spermatozoa during maturation in the epididymis and the activation of sperm particulate adenylate cyclase by GTP and polyamines." J Reprod Fertil **59**(2): 297-302.

Chan, J., Y. W. Kan, et al. (1997). "Cloning differentially expressed genes from small amounts of total RNA with the ClontechPCR-Select cDNA Subtraction Kit." Clontechniques **XII**((1)): 25–26.

Chang, M. C. (1968). "Reciprocal insemination and egg transfer between ferrets and mink." J Exp Zool **168**(1): 49-59.

Chen, G. G., G. Turecki, et al. (2009). "A quantitative GC-MS method for three major polyamines in postmortem brain cortex." J Mass Spectrom **44**(8): 1203-1210.

Chen, Y., Y. Zhang, et al. (2005). "SPD--a web-based secreted protein database." Nucleic Acids Res **33**(Database issue): D169-173.

Chirino-Galindo, G., L. A. Baiza-Gutman, et al. (2009). "Polyamines protect rat embryo in vitro from high glucose-induced developmental delay and dysmorphogenesis." Birth Defects Res B Dev Reprod Toxicol **86**(1): 58-64.

Christensen, H. N. (1990). "Role of amino acid transport and countertransport in nutrition and metabolism." Physiol Rev **70**(1): 43-77.

Cochrane, R. L. and R. K. Meyer (1957). "Delayed nidation in the rat induced by progesterone." Proc Soc Exp Biol Med **96**(1): 155-159.

Cochrane, R. L. and R. M. Shackelford (1962). "Effects of exogenous oestrogen alone and in combination with progestrone on pregnancy in the intact mink." J Endocrinol **25**: 101-106.

Corry, G. N., B. Tanasijevic, et al. (2009). "Epigenetic regulatory mechanisms during preimplantation development." Birth Defects Res C Embryo Today **87**(4): 297-313.

Cui, X. S. and N. H. Kim (2005). "Polyamines inhibit apoptosis in porcine parthenotes developing in vitro." Mol Reprod Dev **70**(4): 471-477.

Curlewis, J. D. (1992). "Seasonal prolactin secretion and its role in seasonal reproduction: a review." Reprod Fertil Dev **4**(1): 1-23.

Daniel, J. C., Jr. and R. S. Krishnan (1969). "Studies on the relationship between uterine fluid components and the diapausing state of blastocysts from mammals having delayed implantation." J Exp Zool **172**(3): 267-281.

Danzin, C., M. J. Jung, et al. (1979). "Effects of alpha-difluoromethylornithine, an enzyme-activated irreversible inhibitor or ornithine decarboxylase, on testosterone-induced regeneration of prostate and seminal vesicle in castrated rats." Biochem J **180**(3): 507-513.

Dass, C. M., S. Mohla, et al. (1969). "Time sequence of action of estrogen on nucleic acid and protein synthesis in the uterus and blastocyst during delayed implantation in the rat." Endocrinology **85**(3): 528-536.

Dassen, H., C. Punyadeera, et al. (2007). "Progesterone regulation of implantation-related genes: new insights into the role of oestrogen." Cell Mol Life Sci **64**(7-8): 1009-1032.

de las Heras, M. A. and R. S. Calandra (1987). "Androgen-dependence of ornithine decarboxylase in the rat epididymis." J Reprod Fertil **79**(1): 9-14.

de las Heras, M. A., M. O. Suescun, et al. (1988). "Ornithine decarboxylase activity as a marker of androgen and antiandrogen action in the rat epididymis." J Reprod Fertil **83**(1): 177-183.

Deng, W., X. Jiang, et al. (2008). "Role of ornithine decarboxylase in breast cancer." Acta Biochim Biophys Sin (Shanghai) **40**(3): 235-243.

Desmarais, J. A., V. Bordignon, et al. (2004). "The escape of the mink embryo from obligate diapause." Biol Reprod **70**(3): 662-670.

Desmarais, J. A., M. Cao, et al. (2008). "Spatiotemporal expression pattern of progranulin in embryo implantation and placenta formation suggests a role in cell proliferation, remodeling, and angiogenesis." Reproduction **136**(2): 247-257.

Desmarais, J. A., F. L. Lopes, et al. (2007). "The peroxisome proliferator-activated receptor gamma regulates trophoblast cell differentiation in mink (Mustela vison)." Biol Reprod **77**(5): 829-839.

Dey, S. K., H. Lim, et al. (2004). "Molecular cues to implantation." Endocr Rev **25**(3): 341-373.

Diatchenko, L., Y. F. Lau, et al. (1996). "Suppression subtractive hybridization: a method for generating differentially regulated or tissue-specific cDNA probes and libraries." Proc Natl Acad Sci U S A **93**(12): 6025-6030.

Douglas, D. A., A. Houde, et al. (1998). "Luteotropic hormone receptors in the ovary of the mink (Mustela vison) during delayed implantation and early-post-implantation gestation." Biol Reprod **59**(3): 571-578.

Douglas, D. A., R. A. Pierson, et al. (1994). "Ovarian follicular development in mink (Mustela vison)." J Reprod Fertil **100**(2): 583-590.

Douglas, D. A., J. H. Song, et al. (1997). "Luteal and placental characteristics of carnivore gestation: expression of genes for luteotrophic receptors and steroidogenic enzymes." J Reprod Fertil Suppl **51**: 153-166.

Dwivedi, A., G. Gupta, et al. (1999). "Changes in uterine ornithine decarboxylase activity and steroid receptor levels during decidualization in the rat induced by CDRI-85/287." Eur J Endocrinol **141**(4): 426-430.

Enders, A. C., R. K. Enders, et al. (1963). "AN ELECTRON MICROSCOPE STUDY OF THE GLAND CELLS OF THE MINK ENDOMETRIUM." J Cell Biol **18**: 405-418.

Enders, R. (1952). "Reproduction in the mink (Mustela vison). ." Proc Am Philos Soc **96**: 691-755.

Ferguson, S. H., J. A. Virgl, et al. (1996). "Evolution of delayed implantation and associated grade shifts in life history traits of North American carnivores." Ecoscience **3**: 7–17.

Ferkowicz, M. J. and M. C. Yoder (2005). "Blood island formation: longstanding observations and modern interpretations." Exp Hematol **33**(9): 1041-1047.

Fishel, S. B. (1979). "Analysis of mouse uterine proteins at pro-oestrus, during early pregnancy and after administration of exogenous steroids." J Reprod Fertil **55**(1): 91-100.

Fleming, A. D. and D. T. Armstrong (1985). "Effects of polyamines upon capacitation and fertilization in the guinea pig." J Exp Zool **233**(1): 93-100.

Fozard, J. R., M. L. Part, et al. (1980). "Inhibition of murine embryonic development by alpha-difluoromethylornithine, an irreversible inhibitor of ornithine decarboxylase." Eur J Pharmacol **65**(4): 379-391.

Fozard, J. R., M. L. Part, et al. (1980). "L-Ornithine decarboxylase:an essential role in early mammalian embryogenesis." Science **208**(4443): 505-508.

Francis, G. L., T. J. Triche, et al. (1981). "In Vitro Gonadotropin Stimulation of Bovine Sertoli

Cell Ornithine Decarboxylase Activity." J Androl **2**: 312-320.

Frostesjo, L., I. Holm, et al. (1997). "Interference with DNA methyltransferase activity and genome methylation during F9 teratocarcinoma stem cell differentiation induced by polyamine depletion." J Biol Chem **272**(7): 4359-4366.

Fujiwara, H., K. Tatsumi, et al. (2003). "Human blastocysts and endometrial epithelial cells express activated leukocyte cell adhesion molecule (ALCAM/CD166)." J Clin Endocrinol Metab **88**(7): 3437-3443.

Fujiwara, K., G. Bai, et al. (1998). "Immunoelectron microscopic study for polyamines." J Histochem Cytochem **46**(11): 1321-1328.

Galliani, G., G. Colombo, et al. (1983). "Contragestational effects of DL-alpha-difluoro-methylornithine, an irreversible inhibitor of ornithine decarboxylase, in the hamster." Contraception **28**(2): 159-170.

Gao, F., W. Lei, et al. (2007). "Differential expression and regulation of prostaglandin transporter and metabolic enzymes in mouse uterus during blastocyst implantation." Fertil Steril **88**(4 Suppl): 1256-1265.

Gao, H., G. Wu, et al. (2009). "Select Nutrients in the Ovine Uterine Lumen. V. Nitric Oxide Synthase, GTP Cyclohydrolase, and Ornithine Decarboxylase in Ovine Uteri and Periimplantation Conceptuses." Biol Reprod.

Gerlitz, G. (2010). "HMGNs, DNA repair and cancer." Biochim Biophys Acta **1799**(1-2): 80-85.

Given, R. L. and H. M. Weitlauf (1981). "Resumption of DNA synthesis during activation of delayed implanting mouse blastocysts." J Exp Zool **218**(2): 253-259.

Given, R. L. and H. M. Weitlauf (1982). "Resumption of DNA synthesis in delayed implanting mouse blastocysts during activation in vitro." J Exp Zool **224**(1): 111-114.

Graham, T. R. and J. C. Daniel, Jr. (1984). "The effect of accelerated lactation on fetal maintenance in the rat." Lab Anim **18**(2): 103-105.

Gray, C. A., C. A. Abbey, et al. (2006). "Identification of endometrial genes regulated by early pregnancy, progesterone, and interferon tau in the ovine uterus." Biol Reprod **74**(2): 383-394.

Green, M. L., L. L. Blaeser, et al. (1996). "Molecular cloning of spermidine/spermine N1-acetyltransferase from the periimplantation porcine uterus by messenger

ribonucleic acid differential display: temporal and conceptus-modulated gene expression." Endocrinology **137**(12): 5447-5455.

Gritli-Linde, A., J. Nilsson, et al. (2001). "Nuclear translocation of antizyme and expression of ornithine decarboxylase and antizyme are developmentally regulated." Dev Dyn **220**(3): 259-275.

Guha, S. K. and J. Janne (1976). "The synthesis and accumulation of polyamines in reproductive organs of the rat during pregnancy." Biochim Biophys Acta **437**(1): 244-252.

Gwatkin, R. B. (1966). "Defined media and development of mammalian eggs in vitro." Ann N Y Acad Sci **139**(1): 79-90.

Gwatkin, R. B. (1969). "Nutritional requirements for post-blastocyst development in the mouse. Amino acids and protein in the uterus during implantation." Int J Fertil **14**(2): 101-105.

Hakovirta, H., A. Keiski, et al. (1993). "Polyamines and regulation of spermatogenesis: selective stimulation of late spermatogonia in transgenic mice overexpressing the human ornithine decarboxylase gene." Mol Endocrinol **7**(11): 1430-1436.

Halmekyto, M., J. M. Hyttinen, et al. (1991). "Transgenic mice aberrantly expressing human ornithine decarboxylase gene." J Biol Chem **266**(29): 19746-19751.

Hamatani, T., M. G. Carter, et al. (2004). "Dynamics of global gene expression changes during mouse preimplantation development." Dev Cell **6**(1): 117-131.

Hansson, A. (1947). "The physiology of reproduction in mink (Mustela vison) with special reference to delayed implantation." Acta Zoologica **28**: 1–136.

Heald, P. J. (1979). "Changes in ornithine decarboxylase during early implantation in the rat." Biol Reprod **20**(5): 1195-1199.

Heby, O. (1995). "DNA methylation and polyamines in embryonic development and cancer." Int J Dev Biol **39**(5): 737-757.

Heby, O., L. Persson, et al. (1988). "Polyamines, DNA methylation and cell differentiation." Adv Exp Med Biol **250**: 291-299.

Hedlund, K., O. Nilsson, et al. (1972). "Attachment reaction of the uterine luminal epithelium at implantation: light and electron microscopy of the hamster, guinea-pig, rabbit and mink." J Reprod Fertil **29**(1): 131-132.

Heiskala, M., J. Zhang, et al. (1999). "Translocation of ornithine decarboxylase to the surface membrane during cell activation and transformation." Embo J **18**(5): 1214-1222.

Hessels, J., A. W. Kingma, et al. (1989). "Microbial flora in the gastrointestinal tract abolishes cytostatic effects of alpha-difluoromethylornithine in vivo." Int J Cancer **43**(6): 1155-1164.

Hickman-Smith, D., L. E. Bussmann, et al. (1982). "Ornithine decarboxylase as a monitor for luteal stimuli in the pregnant rat." J Reprod Fertil **66**(1): 265-272.

Hoffmann, R., Valencia, A. (2004). "A Gene Network for Navigating the Literature." Nature Genetics **36**: 664.

Holinka, C. F. and E. Gurpide (1985). "Ornithine decarboxylase activity in human endometrium and endometrial cancer cells." In Vitro Cell Dev Biol **21**(12): 697-706.

Holland, P. W., S. J. Harper, et al. (1987). "In vivo expression of mRNA for the Ca++-binding protein SPARC (osteonectin) revealed by in situ hybridization." J Cell Biol **105**(1): 473-482.

Hoshiai, H., Y. C. Lin, et al. (1981). "Ornithine decarboxylase activity and polyamine content of the placenta and decidual tissue in the rat." Placenta **2**(2): 105-116.

Hoshiai, H., S. Uehara, et al. (1982). "The variations of estrogen receptor, progesterone receptor, cAMP, ODC activity and RNA synthesis of deciduomata in pseudopregnant rats." Tohoku J Exp Med **137**(4): 349-360.

Hoversland, R. C. and H. M. Weitlauf (1981). "The volume of uterine fluid in 'implanting' and 'delayed implanting' mice." J Reprod Fertil **62**(1): 105-109.

Howe, C. C., G. C. Overton, et al. (1988). "Expression of SPARC/osteonectin transcript in murine embryos and gonads." Differentiation **37**(1): 20-25.

Huang, Y., L. J. Marton, et al. (2009). "Polyamine analogues targeting epigenetic gene regulation." Essays Biochem **46**: 95-110.

Icekson, I., A. M. Kaye, et al. (1974). "Stimulation by luteinizing hormone of ornithine decarboxylase in rat ovary: preferential response by follicular tissue." J Endocrinol **63**(2): 417-418.

Igarashi, K. and K. Kashiwagi (2009). "Modulation of cellular function by polyamines." Int J Biochem Cell Biol.

Illei, G. and D. M. Morgan (1979). "Polyamine oxidase activity in human pregnancy serum." Br J Obstet Gynaecol **86**(11): 878-881.

Ishida, M., Y. Hiramatsu, et al. (2002). "Inhibition of placental ornithine decarboxylase by DL-alpha-difluoro-methyl ornithine causes fetal growth restriction in rat." Life Sci **70**(12): 1395-1405.

Ivanov, I. P., J. F. Atkins, et al. (2010). "A profusion of upstream open reading frame mechanisms in polyamine-responsive translational regulation." Nucleic Acids Res **38**(2): 353-359.

Ivanov, I. P., A. Rohrwasser, et al. (2000). "Discovery of a spermatogenesis stage-specific ornithine decarboxylase antizyme: antizyme 3." Proc Natl Acad Sci U S A **97**(9): 4808-4813.

Jha, R. K., S. Titus, et al. (2006). "Profiling of E-cadherin, beta-catenin and Ca(2+) in embryo-uterine interactions at implantation." FEBS Lett **580**(24): 5653-5660.

Johnson, D. C. and T. Sashida (1977). "Temporal changes in ovarian ornithine decarboxylase and cyclic AMP in immature rats stimulated by exogenous or endogenous gonadotrophins." J Endocrinol **73**(3): 463-471.

Jones, R. L., C. Stoikos, et al. (2006). "TGF-beta superfamily expression and actions in the endometrium and placenta." Reproduction **132**(2): 217-232.

Juszczak, M. and M. Michalska (2006). "[The effect of melatonin on prolactin, luteinizing hormone (LH), and follicle-stimulating hormone (FSH) synthesis and secretion]." Postepy Hig Med Dosw (Online) **60**: 431-438.

Kabir-Salmani, M., S. Shiokawa, et al. (2005). "Tissue transglutaminase at embryo-maternal interface." J Clin Endocrinol Metab **90**(8): 4694-4702.

Kahana, C. (2009). "Antizyme and antizyme inhibitor, a regulatory tango." Cell Mol Life Sci **66**(15): 2479-2488.

Kaipia, A., J. Toppari, et al. (1990). "Stage- and cell-specific expression of the ornithine decarboxylase gene during rat and mouse spermatogenesis." Mol Cell Endocrinol **73**(1): 45-52.

Kaito, C., M. Kai, et al. (2001). "Activation of the maternally preset program of apoptosis by microinjection of 5-aza-2'-deoxycytidine and 5-methyl-2'-deoxycytidine-5'-triphosphate in Xenopus laevis embryos." Dev Growth Differ **43**(4): 383-390.

Kanerva, K., L. T. Makitie, et al. (2010). "Ornithine decarboxylase antizyme inhibitor 2 regulates intracellular vesicle trafficking." Exp Cell Res.

Kanerva, K., L. T. Makitie, et al. (2008). "Human ornithine decarboxylase paralogue (ODCp) is an antizyme inhibitor but not an arginine decarboxylase." Biochem J **409**(1): 187-192.

Kapyaho, K., A. Kallio, et al. (1984). "Differential effects of 2-difluoromethylornithine and methylglyoxal bis(guanylhydrazone) on the testosterone-induced growth of ventral prostate and seminal vesicles of castrated rats." Biochem J **219**(3): 811-817.

Kaye, A. M., I. Icekson, et al. (1971). "Stimulation by estrogens of ornithine and S-adenosylmethionine decarboxylases in the immature rat uterus." Biochim Biophys Acta **252**(1): 150-159.

Kilpelainen, P. T., J. Saarimies, et al. (2001). "Abnormal ornithine decarboxylase activity in transgenic mice increases tumor formation and infertility." Int J Biochem Cell Biol **33**(5): 507-520.

Kim, J., T. E. Spencer, et al. (2009). Arginine Stimulates Proliferation of Ovine Trophectoderm Cells Through FRAP1-RPS6K-RPS6 Signaling Cascade and Synthesis of Nitric Oxide and Polyamines. Science for the Public Good, SSR 42nd Annual Meeting, Pittsburgh, Pennsylvania, USA.

Kimball, S. R., L. M. Shantz, et al. (1999). "Leucine regulates translation of specific mRNAs in L6 myoblasts through mTOR-mediated changes in availability of eIF4E and phosphorylation of ribosomal protein S6." J Biol Chem **274**(17): 11647-11652.

Kirby, D. R. (1967). "Ectopic autografts of blastocysts in mice maintained in delayed implantation." J Reprod Fertil **14**(3): 515-517.

Kirchner, D. L., M. D. Mercieca, et al. (1999). "Developmental toxicity studies of 2-(difluoromethyl)-dl-ornithine (DFMO) in rats and rabbits." Toxicol Sci **50**(1): 127-135.

Kobayashi, Y., J. Kupelian, et al. (1971). "Ornithine decarboxylase stimulation in rat ovary by luteinizing hormone." Science **172**(981): 379-380.

Kolpovskii, V. M. (1976). "[Position of the embryos of American mink in the fetal chamber at different stages of development]." Arkh Anat Gistol Embriol **71**(10): 46-51.

Krebs, C., H. Winther, et al. (1997). "Vascular interrelationships of near-term mink placenta: light microscopy combined with scanning electron microscopy of corrosion casts." Microsc Res Tech **38**(1-2): 125-136.

Kusano, T., T. Berberich, et al. (2008). "Polyamines: essential factors for growth and survival." Planta **228**(3): 367-381.

Kwon, H., S. P. Ford, et al. (2004). "Maternal nutrient restriction reduces concentrations of amino acids and polyamines in ovine maternal and fetal plasma and fetal fluids." Biol Reprod **71**(3): 901-908.

Kwon, H., G. Wu, et al. (2003). "Developmental changes in polyamine levels and synthesis in the ovine conceptus." Biol Reprod **69**(5): 1626-1634.

Larque, E., M. Sabater-Molina, et al. (2007). "Biological significance of dietary polyamines." Nutrition **23**(1): 87-95.

Lavia, L. A., S. J. Stohs, et al. (1983). "Polyamine biosynthetic decarboxylase activities following estradiol-17 beta or estriol stimulation of the immature rat uterus." Steroids **42**(6): 609-618.

Lea, R. G., O. Porat, et al. (1991). "The detection of spermine and spermidine in human in vitro fertilization supernatants and their relation to early embryo-associated suppressor activity." Fertil Steril **56**(4): 771-775.

Lee, C. Y. and J. A. Dias (1988). "Cellular origin of prolonged induction of ornithine decarboxylase in the rat ovary." Proc Soc Exp Biol Med **187**(3): 350-354.

Lee, K. Y. and F. J. DeMayo (2004). "Animal models of implantation." Reproduction **128**(6): 679-695.

Lefevre, P. L. and B. D. Murphy (2009). Differential gene expression in the uterus and blastocyst during the reactivation of embryo development in a model of delayed implantation. Human Embryogenesis, Method and Protocols. J. Lafond and C. Vaillancourt. Montreal, Humana Press. **550:** 11-61.

Levine, A. J. and A. H. Brivanlou (2006). "GDF3, a BMP inhibitor, regulates cell fate in stem cells and early embryos." Development **133**(2): 209-216.

Lin, M. T. and C. V. Rao (1980). "Ornithine decarboxylase in bovine corpora lutea." J Endocrinol Invest **3**(2): 131-136.

Lopata, A., M. C. Sibson, et al. (2001). "Expression and localization of thioredoxin during early implantation in the marmoset monkey." Mol Hum Reprod **7**(12): 1159-1165.

Lopes, F. L., J. Desmarais, et al. (2006). "Transcriptional regulation of uterine vascular endothelial growth factor during early gestation in a carnivore model, Mustela vison." J Biol Chem **281**(34): 24602-24611.

Lopes, F. L., J. A. Desmarais, et al. (2004). "Embryonic diapause and its regulation." Reproduction **128**(6): 669-678.

Lopez-Contreras, A. J., C. Lopez-Garcia, et al. (2006). "Mouse ornithine decarboxylase-like gene encodes an antizyme inhibitor devoid of ornithine and arginine decarboxylating activity." J Biol Chem **281**(41): 30896-30906.

Lopez-Contreras, A. J., B. Ramos-Molina, et al. (2008). "Antizyme inhibitor 2 (AZIN2/ODCp) stimulates polyamine uptake in mammalian cells." J Biol Chem **283**(30): 20761-20769.

Lopez-Contreras, A. J., B. Ramos-Molina, et al. (2010). "Antizyme inhibitor 2: molecular, cellular and physiological aspects." Amino Acids **38**(2): 603-611.

Lopez-Contreras, A. J., B. Ramos-Molina, et al. (2009). "Expression of antizyme inhibitor 2 in male haploid germinal cells suggests a role in spermiogenesis." Int J Biochem Cell Biol **41**(5): 1070-1078.

Lopez-Garcia, C., A. J. Lopez-Contreras, et al. (2008). "Molecular and morphological changes in placenta and embryo development associated to the inhibition of polyamine synthesis during midpregnancy in mice." Endocrinology.

Lopez-Garcia, C., A. J. Lopez-Contreras, et al. (2008). "Molecular and morphological changes in placenta and embryo development associated with the inhibition of polyamine synthesis during midpregnancy in mice." Endocrinology **149**(10): 5012-5023.

Lopez-Garcia, C., A. J. Lopez-Contreras, et al. (2009). "Transcriptomic analysis of polyamine-related genes and polyamine levels in placenta, yolk sac and fetus during the second half of mouse pregnancy." Placenta **30**(3): 241-249.

Louie, D. F., K. K. Gloor, et al. (2000). "Phosphorylation and subcellular redistribution of high mobility group proteins 14 and 17, analyzed by mass spectrometry." Protein Sci **9**(1): 170-179.

Luzzani, F., G. Colombo, et al. (1982). "Evidence for a role of progesterone in the control of uterine ornithine decarboxylase in the pregnant hamster." Life Sci **31**(15): 1553-1558.

MacIndoe, J. H. and R. W. Turkington (1973). "Hormonal regulation of spermidine formation during spermatogenesis in the rat." Endocrinology **92**(2): 595-605.

Makitie, L. T., K. Kanerva, et al. (2009). "Ornithine decarboxylase regulates the activity and localization of rhoA via polyamination." Exp Cell Res **315**(6): 1008-1014.

Makitie, L. T., K. Kanerva, et al. (2009). "High expression of antizyme inhibitor 2, an activator of ornithine decarboxylase in steroidogenic cells of human gonads." Histochem Cell Biol.

Maneckjee, R. and N. R. Moudgal (1975). "Induction and inhibition of implantation in lactating rats." J Reprod Fertil **43**(1): 33-40.

Manen, C. A., R. D. Hood, et al. (1983). "Ornithine decarboxylase inhibitors and fetal growth retardation in mice." Teratology **28**(2): 237-242.

Mann, T. (1974). "Secretory function of the prostate, seminal vesicle and other male accessory organs of reproduction." J Reprod Fertil **37**(1): 179-188.

Mantalenakis, S. J. and M. M. Ketchel (1966). "Frequency and extent of delayed implantation in lactating rats and mice." J Reprod Fertil **12**(2): 391-394.

Martin, P. M. and A. E. Sutherland (2001). "Exogenous amino acids regulate trophectoderm differentiation in the mouse blastocyst through an mTOR-dependent pathway." Dev Biol **240**(1): 182-193.

Martin, P. M., A. E. Sutherland, et al. (2003). "Amino acid transport regulates blastocyst implantation." Biol Reprod **69**(4): 1101-1108.

Martinet, L. and D. Allain (1985). "Role of the pineal gland in the photoperiodic control of reproductive and non-reproductive functions in mink (Mustela vison)." Ciba Found Symp **117**: 170-187.

Mason, I. J., D. Murphy, et al. (1986). "Developmental and transformation-sensitive expression of the Sparc gene on mouse chromosome 11." Embo J **5**(8): 1831-1837.

Mateo, R. D., G. Wu, et al. (2007). "Dietary L-arginine supplementation enhances the reproductive performance of gilts." J Nutr **137**(3): 652-656.

Maudsley, D. V. and Y. Kobayashi (1974). "Induction of ornithine decarboxylase in rat ovary after administration of luteinizing hormone or human chorionic gonadotrophin." Biochem Pharmacol **23**(19): 2697-2703.

McNeilly, A. S. (1979). "Effects of lactation on fertility." Br Med Bull **35**(2): 151-154.

Mead, R. A. (1971). "Effects of light and blinding upon delayed implantation in the spotted skunk." Biol Reprod **5**(2): 214-220.

Mead, R. A. (1981). "Delayed implantation in mustelids, with special emphasis on the spotted skunk." J Reprod Fertil Suppl **29**: 11-24.

Mead, R. A. (1989). "The physiology and evolution of delayed implantation in carnivores." In Carnivore behavior, ecology, and evolution **1**: 437–464.

Mead, R. A. (1993). "Embryonic diapause in vertebrates." J Exp Zool **266**(6): 629-641.

Mead, R. A., A. W. Rourke, et al. (1979). "Changes in uterine protein synthesis during delayed implantation in the western spotted skunk and its regulation by hormones." Biol Reprod **21**(1): 39-46.

Mehrotra, P. K., S. Kitchlu, et al. (1998). "Effect of inhibitors of enzymes involved in polyamine biosynthesis pathway on pregnancy in mouse and hamster." Contraception **57**(1): 55-60.

Melendrez, C. S., J. L. Ruttle, et al. (1992). "Polyamines in ejaculated ram spermatozoa and their relationship with sperm motility." J Androl **13**(4): 293-296.

Mendez, J. D., M. Diaz-Flores, et al. (1983). "Inhibition of rat embryonic development by the intrauterine administration of alpha-difluoromethylornithine." Contraception **28**(1): 93-98.

Metcalf, B. W., C. Danzin, et al. (1978). "Catalytic irreversible inhibition of mammalian ornithine decarboxylase (E.C. 4.1.1.17) by substrate and product analogs." J Am Chem Soc **100**: 2551–2553

Meyuhas, O. (2000). "Synthesis of the translational apparatus is regulated at the translational level." Eur J Biochem **267**(21): 6321-6330.

Milovic, V. (2001). "Polyamines in the gut lumen: bioavailability and biodistribution." Eur J Gastroenterol Hepatol **13**(9): 1021-1025.

Milovic, V., D. Faust, et al. (2001). "Permeability characteristics of polyamines across intestinal epithelium using the Caco-2 monolayer system: comparison between transepithelial flux and mitogen-stimulated uptake into epithelial cells." Nutrition **17**(6): 462-466.

Min, S. H., R. C. Simmen, et al. (2002). "Altered levels of growth-related and novel gene transcripts in reproductive and other tissues of female mice overexpressing spermidine/spermine N1-acetyltransferase (SSAT)." J Biol Chem **277**(5): 3647-3657.

Mitchell, J. L., G. G. Judd, et al. (1994). "Feedback repression of polyamine transport is mediated by antizyme in mammalian tissue-culture cells." Biochem J **299 (Pt 1)**: 19-22.

Mitko, K., S. E. Ulbrich, et al. (2008). "Dynamic changes in messenger RNA profiles of bovine endometrium during the oestrous cycle." Reproduction **135**(2): 225-240.

Moinard, C., L. Cynober, et al. (2005). "Polyamines: metabolism and implications in human diseases." Clin Nutr **24**(2): 184-197.

Moller, O. M. (1973). "The progesterone concentrations in the peripheral plasma of the mink (Mustela vison) during pregnancy." J Endocrinol **56**(1): 121-132.

Moller, O. M. (1974). "Plasma progesterone before and after ovariectomy in unmated and pregnant mink, Mustela vison." J Reprod Fertil **37**(2): 367-372.

Morales, M. E., G. Rico, et al. (2003). "[Progressive motility increase caused by L-arginine and polyamines in sperm from patients with idiopathic and diabetic asthenozoospermia]." Ginecol Obstet Mex **71**: 297-303.

Moreau, G. M., A. Arslan, et al. (1995). "Development of immortalized endometrial epithelial and stromal cell lines from the mink (Mustela vison) uterus and their

effects on the survival in vitro of mink blastocysts in obligate diapause." Biol Reprod **53**(3): 511-518.

Morin, P., C. Flors, et al. (2009). "Constitutively active RhoA inhibits proliferation by retarding G(1) to S phase cell cycle progression and impairing cytokinesis." Eur J Cell Biol **88**(9): 495-507.

Morisset, J., P. Sarfati, et al. (1986). "Immunocytochemical demonstration of ornithine decarboxylase in the rat exocrine pancreas using the protein A-gold technique." Can J Physiol Pharmacol **64**(4): 444-448.

Moruzzi, M. S., G. Marverti, et al. (1993). "Effect of spermine on membrane-associated and membrane-inserted forms of protein kinase C." Mol Cell Biochem **124**(1): 1-9.

Murphy-Ullrich, J. E., T. F. Lane, et al. (1995). "SPARC mediates focal adhesion disassembly in endothelial cells through a follistatin-like region and the Ca(2+)-binding EF-hand." J Cell Biochem **57**(2): 341-350.

Murphy, B. D. (1983). "Precocious induction of luteal activation and termination of delayed implantation in mink with the dopamine antagonist pimozide." Biol Reprod **29**(3): 658-662.

Murphy, B. D., P. W. Concannon, et al. (1981). "Prolactin: the hypophyseal factor that terminates embryonic diapause in mink." Biol Reprod **25**(3): 487-491.

Murphy, B. D., G. B. DiGregorio, et al. (1990). "Interactions between melatonin and prolactin during gestation in mink (Mustela vison)." J Reprod Fertil **89**(2): 423-429.

Murphy, B. D. and D. A. James (1974). "The effects of light and sympathetic innervation to the head on nidation in mink." J Exp Zool **187**(2): 267-276.

Murphy, B. D., R. A. Mead, et al. (1983). "Luteal contribution to the termination of preimplantation delay in mink." Biol Reprod **28**(2): 497-503.

Murphy, B. D. and W. H. Moger (1977). "Progestins of mink gestation: the effects of hypophysectomy." Endocr Res Commun **4**(1): 45-60.

Murphy, B. D., K. Rajkumar, et al. (1993). "Control of luteal function in the mink (Mustela vison)." J Reprod Fertil Suppl **47**: 181-188.

Muzikova, E. and D. A. Clark (1995). "Polyamines may increase the percentage of in-vitro fertilized murine oocytes that develop into blastocysts." Hum Reprod **10**(5): 1172-1177.

Nicholson, S. A., M. Aslam, et al. (1988). "Effect of difluoromethylornithine on the LH surge and subsequent ovulation in the rat." J Endocrinol **117**(3): 447-453.

Nicholson, S. A. and G. A. Wynne-Jones (1989). "Differential effect of difluoromethylornithine on the increases in plasma concentrations of reproductive hormones on the afternoon of pro-oestrus in the rat." J Endocrinol **121**(3): 495-499.

Nieder, G. L. and H. M. Weitlauf (1985). "Effects of metabolic substrates and ionic environment on in-vitro activation of delayed implanting mouse blastocysts." J Reprod Fertil **73**(1): 151-157.

Nilsson, B. O. and L. Ljung (1985). "X-ray micro analyses of cations (Na, K, Ca) and anions (S, P, Cl) in uterine secretions during blastocyst implantation in the rat." J Exp Zool **234**(3): 415-421.

Nishimura, K., F. Nakatsu, et al. (2002). "Essential role of S-adenosylmethionine decarboxylase in mouse embryonic development." Genes Cells **7**(1): 41-47.

Nureddin, A. (1978). "Ovarian ornithine decarboxylase regulation in the immature, the pubescent, and the pseudopregnant rat." Proc Natl Acad Sci U S A **75**(5): 2530-2534.

O'Toole, B. A., K. W. Huffman, et al. (1989). "Effects of eflornithine hydrochloride (DFMO) on fetal development in rats and rabbits." Teratology **39**(2): 103-113.

Oda, M., K. Shiota, et al. (2006). "Trophoblast stem cells." Methods Enzymol **419**: 387-400.

Osborne, H. B., C. Duval, et al. (1991). "Expression and post-transcriptional regulation of ornithine decarboxylase during early Xenopus development." Eur J Biochem **202**(2): 575-581.

Osgerby, J. C., D. C. Wathes, et al. (2002). "The effect of maternal undernutrition on ovine fetal growth." J Endocrinol **173**(1): 131-141.

Osterman, J., E. P. Murono, et al. (1983). "Regulation of testicular ornithine decarboxylase in vitro. Effect of age, follicle-stimulating hormone, and luteinizing hormone." J Androl **4**(3): 175-182.

Oswald, C. and P. A. McClure (1987). "Energy allocation during concurrent pregnancy and lactation in Norway rats with delayed and undelayed implantation." J Exp Zool **241**(3): 343-357.

Palmer, A. J. and H. M. Wallace (2010). "The polyamine transport system as a target for anticancer drug development." Amino Acids **38**(2): 415-422.

Papke, R. L., P. W. Concannon, et al. (1980). "Control of luteal function and implantation in the mink by prolactin." J Anim Sci **50**(6): 1102-1107.

Paria, B. C., H. Lim, et al. (1998). "Coordination of differential effects of primary estrogen and catecholestrogen on two distinct targets mediates embryo implantation in the mouse." Endocrinology **139**(12): 5235-5246.

Park, M. H., K. Nishimura, et al. (2010). "Functional significance of eIF5A and its hypusine modification in eukaryotes." Amino Acids **38**(2): 491-500.

Pearson, O. P. and R. K. Enders (1944). "Duration of pregnancy in certain mustelids." Journal of Experimental Zoology: 9521–9535.

Pearson, O. P. and R. K. Enders (1944). "Duration of pregnancy in certain mustelids." J. Exp. Zool. **95**: 21-35.

Pegg, A. E., D. H. Lockwood, et al. (1970). "Concentrations of putrescine and polyamines and their enzymic synthesis during androgen-induced prostatic growth." Biochem J **117**(1): 17-31.

Pendeville, H., N. Carpino, et al. (2001). "The ornithine decarboxylase gene is essential for cell survival during early murine development." Mol Cell Biol **21**(19): 6549-6558.

Persson, L. (2009). "Polyamine homoeostasis." Essays Biochem **46**: 11-24.

Persson, L., K. Isaksson, et al. (1986). "Distribution of ornithine decarboxylase in ovaries of rat and hamster during pro-oestrus." Acta Endocrinol (Copenh) **113**(3): 403-409.

Persson, L., E. Rosengren, et al. (1982). "Immunohistochemical localization of ornithine decarboxylase in the rat ovary." Histochemistry **75**(2): 163-167.

Pfaffl, M. W. (2001). "A new mathematical model for relative quantification in real-time RT-PCR." Nucleic Acids Res **29**(9): e45.

Pfarrer, C., H. Winther, et al. (1999). "The development of the endotheliochorial mink placenta: light microscopy and scanning electron microscopical morphometry of maternal vascular casts." Anat Embryol (Berl) **199**(1): 63-74.

Pietila, M., L. Alhonen, et al. (1997). "Activation of polyamine catabolism profoundly alters tissue polyamine pools and affects hair growth and female fertility in transgenic mice overexpressing spermidine/spermine N1-acetyltransferase." J Biol Chem **272**(30): 18746-18751.

Pilbeam, T. E., P. W. Concannon, et al. (1979). "The annual reproductive cycle of mink (Mustela vison)." J Anim Sci **48**(3): 578-584.

Pitkanen, L. T., M. Heiskala, et al. (2001). "Expression of a novel human ornithine decarboxylase-like protein in the central nervous system and testes." Biochem Biophys Res Commun **287**(5): 1051-1057.

Pollard, T. D. (2010). "Mechanics of cytokinesis in eukaryotes." Curr Opin Cell Biol **22**(1): 50-56.

Pomidor, M. M., K. K. Ruhl, et al. (1995). "Relationship between ornithine decarboxylase and cytoskeletal organization in cultured human keratinocytes: cellular responses to phorbol esters, cytochalasins, and alpha-difluoromethylornithine." Exp Cell Res **221**(2): 426-437.

Pond, W. G., R. R. Maurer, et al. (1991). "Fetal organ response to maternal protein deprivation during pregnancy in swine." J Nutr **121**(4): 504-509.

Porat, O. and D. A. Clark (1990). "Analysis of immunosuppressive molecules associated with murine in vitro fertilized embryos." Fertil Steril **54**(6): 1154-1161.

Prasad, M. R., C. M. Dass, et al. (1968). "Action of oestrogen on the blastocyst and uterus in delayed implantation--an autoradiographic study." J Reprod Fertil **16**(1): 97-104.

Pulkkinen, P., R. Sinervirta, et al. (1975). "Modification of the metabolism of rat epididymal spermatozoa by spermine." Biochem Biophys Res Commun **67**(2): 714-722.

Qian, Z. U., Y. H. Tsai, et al. (1985). "Localization of ornithine decarboxylase in rat testicular cells and epididymal spermatozoa." Biol Reprod **33**(5): 1189-1195.

Quemener, V., Y. Blanchard, et al. (1992). "Depletion in nuclear spermine during human spermatogenesis, a natural process of cell differentiation." Am J Physiol **263**(2 Pt 1): C343-347.

Raught, B., A. C. Gingras, et al. (2000). "Serum-stimulated, rapamycin-sensitive phosphorylation sites in the eukaryotic translation initiation factor 4GI." Embo J **19**(3): 434-444.

Reddy, P. R. and V. Rukmini (1981). "Alpha-difluoromethylornithine as a postcoitally effective antifertility agent in female rats." Contraception **24**(2): 215-221.

Reese, J., S. K. Das, et al. (2001). "Global gene expression analysis to identify molecular markers of uterine receptivity and embryo implantation." J Biol Chem **276**(47): 44137-44145.

Renfree, M. B. (1981). "Embryonic diapause in marsupials." J Reprod Fertil Suppl **29**: 67-78.

Renfree, M. B. and G. Shaw (2000). "Diapause." Annu Rev Physiol **62**: 353-375.

Rijke, E. O. and R. E. Ballieux (1978). "Is thymus-derived lymphocyte inhibitor a polyamine?" Nature **274**(5673): 804-805.

Rodriguez-Sallaberry, C., F. A. Simmen, et al. (2001). "Polyamine- and insulin-like growth factor-I-mediated proliferation of porcine uterine endometrial cells: a potential role for spermidine/spermine N(1)-acetyltransferase during peri-implantation." Biol Reprod **65**(2): 587-594.

Rorke, E. A., K. L. Kendra, et al. (1984). "Relationships among uterine growth, ornithine decarboxylase activity and polyamine levels: studies with estradiol and antiestrogens." Mol Cell Endocrinol **38**(1): 31-38.

Rubinstein, S. and H. Breitbart (1991). "Role of spermine in mammalian sperm capacitation and acrosome reaction." Biochem J **278 (Pt 1)**: 25-28.

Rubinstein, S. and H. Breitbart (1994). "Cellular localization of polyamines: cytochemical and ultrastructural methods providing new clues to polyamine function in ram spermatozoa." Biol Cell **81**(2): 177-183.

Rubinstein, S., Y. Lax, et al. (1995). "Dual effect of spermine on acrosomal exocytosis in capacitated bovine spermatozoa." Biochim Biophys Acta **1266**(2): 196-200.

Ruijter, J. M., C. Ramakers, et al. (2009). "Amplification efficiency: linking baseline and bias in the analysis of quantitative PCR data." Nucleic Acids Res **37**(6): e45.

Russell, D. H. (1971). "Putrescine and spermidine biosynthesis in the development of normal and anucleolate mutants of Xenopus laevis." Proc Natl Acad Sci U S A **68**(3): 523-527.

Sage, H., C. Johnson, et al. (1984). "Characterization of a novel serum albumin-binding glycoprotein secreted by endothelial cells in culture." J Biol Chem **259**(6): 3993-4007.

Sandell, M. (1990). "The evolution of seasonal delayed implantation." Q Rev Biol **65**(1): 23-42.

Sanyal, M. K. and R. K. Meyer (1972). "Deoxyribonucleic acid synthesis in vitro in normal and delayed nidation preimplantation blastocysts of adult rats." J Reprod Fertil **29**(3): 439-442.

Saunderson, R. and P. J. Heald (1974). "Ornithine decarboxylase activity in the uterus of the rat during early pregnancy." J Reprod Fertil **39**(1): 141-143.

Schipper, R. G., V. M. Cuijpers, et al. (2004). "Intracellular localization of ornithine decarboxylase and its regulatory protein, antizyme-1." J Histochem Cytochem **52**(10): 1259-1266.

Schulz, L. C. and J. M. Bahr (2003). "Glucose-6-phosphate isomerase is necessary for embryo implantation in the domestic ferret." Proc Natl Acad Sci U S A **100**(14): 8561-8566.

Seiler, N. (2003). "Thirty years of polyamine-related approaches to cancer therapy. Retrospect and prospect. Part 2. Structural analogues and derivatives." Curr Drug Targets **4**(7): 565-585.

Seiler, N., J. G. Delcros, et al. (1996). "Polyamine transport in mammalian cells. An update." Int J Biochem Cell Biol **28**(8): 843-861.

Seiler, N. and F. Raul (2005). "Polyamines and apoptosis." J Cell Mol Med **9**(3): 623-642.

Shah, G. V., A. R. Sheth, et al. (1975). "Effect of spermine on adenyl cyclase activity of spermatozoa." Experientia **31**(6): 631-632.

Shaw, G. and M. B. Renfree (1986). "Uterine and embryonic metabolism after diapause in the tammar wallaby, Macropus eugenii." J Reprod Fertil **76**(1): 339-347.

Sheela Rani, C. S. and N. R. Moudgal (1979). "Effect of follicle-stimulating hormone and its antiserum on the activity of ornithine decarboxylase in the ovary of rat and hamster." Endocrinology **104**(5): 1480-1483.

Sherman, M. I. and P. W. Barlow (1972). "Deoxyribonucleic acid content in delayed mouse blastocysts." J Reprod Fertil **29**(1): 123-126.

Sheth, A. R. and S. B. Moodbidri (1977). "Significance of polyamines in reproduction." Adv Sex Horm Res **3**: 51-74.

Shi, L. and J. Wu (2009). "Epigenetic regulation in mammalian preimplantation embryo development." Reprod Biol Endocrinol **7**: 59.

Shibata, M., J. Shinga, et al. (1998). "Overexpression of S-adenosylmethionine decarboxylase (SAMDC) in early Xenopus embryos induces cell dissociation and

inhibits transition from the blastula to gastrula stage." Int J Dev Biol **42**(5): 675-686.

Shiokawa, K., M. Kai, et al. (2000). "Maternal program of apoptosis activated shortly after midblastula transition by overexpression of S-adenosylmethionine decarboxylase in Xenopus early embryos." Comp Biochem Physiol B Biochem Mol Biol **126**(2): 149-155.

Shubhada, S., S. N. Lin, et al. (1989). "Polyamine profiles in rat testis, germ cells and Sertoli cells during testicular maturation." J Androl **10**(2): 145-151.

Smith, M. S. (1980). "Role of prolactin in regulating gonadotropin secretion and gonad function in female rats." Fed Proc **39**(8): 2571-2576.

Song, H. and H. Lim (2006). "Evidence for heterodimeric association of leukemia inhibitory factor (LIF) receptor and gp130 in the mouse uterus for LIF signaling during blastocyst implantation." Reproduction **131**(2): 341-349.

Song, J. (1998). Implantation in the Mink (Mustela vison): Morphologic Progression of Trophoblast Invasion and Uterine Gene Expression. Faculté de Médecine Véterinaire. Montreal, CA, Université de Montreal.

Song, J. H., P. D. Carriere, et al. (1995). "Ultrasonographic analysis of gestation in mink (Mustela vison)." Theriogenology **43**(3): 585-594.

Song, J. H., A. Houde, et al. (1998). "Cloning of leukemia inhibitory factor (LIF) and its expression in the uterus during embryonic diapause and implantation in the mink (Mustela vison)." Mol Reprod Dev **51**(1): 13-21.

Song, J. H., J. Sirois, et al. (1998). "Cloning, developmental expression, and immunohistochemistry of cyclooxygenase 2 in the endometrium during embryo implantation and gestation in the mink (Mustela vison)." Endocrinology **139**(8): 3629-3636.

Soulet, D., L. Covassin, et al. (2002). "Role of endocytosis in the internalization of spermidine-C(2)-BODIPY, a highly fluorescent probe of polyamine transport." Biochem J **367**(Pt 2): 347-357.

Soulet, D., B. Gagnon, et al. (2004). "A fluorescent probe of polyamine transport accumulates into intracellular acidic vesicles via a two-step mechanism." J Biol Chem **279**(47): 49355-49366.

Spindler, R. E., M. B. Renfree, et al. (1996). "Carbohydrate uptake by quiescent and reactivated mouse blastocysts." J Exp Zool **276**(2): 132-137.

Stanger, J. D. and P. Quinn (1982). "Effect of polyamines on fertilization of mouse ova in vitro." J Exp Zool **220**(3): 377-380.

Stoufflet, I., M. Mondain-Monval, et al. (1989). "Patterns of plasma progesterone, androgen and oestrogen concentrations and in-vitro ovarian steroidogenesis during embryonic diapause and implantation in the mink (Mustela vison)." J Reprod Fertil **87**(1): 209-221.

Sundqvist, C., A. G. Amador, et al. (1989). "Reproduction and fertility in the mink (Mustela vision)." J Reprod Fertil **85**(2): 413-441.

Sunkara, P. S., D. A. Wright, et al. (1981). "An essential role for putrescine biosynthesis during meiotic maturation of amphibian oocytes." Dev Biol **87**(2): 351-355.

Surani, M. A. (1975). "Hormonal regulation of proteins in the uterine secretion of ovariectomized rats and the implications for implantation and embryonic diapause." J Reprod Fertil **43**(3): 411-417.

Surani, M. A. (1976). "Uterine luminal proteins at the time of implantation in rats." J Reprod Fertil **48**(1): 141-145.

Surani, M. A. (1977). "Response of preimplantation rat blastocysts in vitro to extracellular uterine luminal components, serum and hormones." J Cell Sci **25**: 265-277.

Swift, T. A. and J. A. Dias (1987). "Stimulation of polyamine biosynthesis by follicle-stimulating hormone in serum-free cultures of rat Sertoli cells." Endocrinology **120**(1): 394-400.

Swift, T. A. and J. A. Dias (1988). "Testosterone suppression of ornithine decarboxylase activity in rat Sertoli cells." Endocrinology **123**(2): 687-693.

Tabor, C. W. and H. Tabor (1984). "Methionine adenosyltransferase (S-adenosylmethionine synthetase) and S-adenosylmethionine decarboxylase." Adv Enzymol Relat Areas Mol Biol **56**: 251-282.

Tabor, C. W. and H. Tabor (1984). "Polyamines." Annu Rev Biochem **53**: 749-790.

Tabor, H. and C. W. Tabor (1964). "SPERMIDINE, SPERMINE, AND RELATED AMINES." Pharmacol Rev **16**: 245-300.

Takemura, Y., Y. Osuga, et al. (2006). "Expression of adiponectin receptors and its possible implication in the human endometrium." Endocrinology **147**(7): 3203-3210.

Tang, H., K. Ariki, et al. (2009). "Role of ornithine decarboxylase antizyme inhibitor in vivo." Genes Cells **14**(1): 79-87.

Thom, M. D., D. D. Johnson, et al. (2004). "The evolution and maintenance of delayed implantation in the mustelidae (mammalia: carnivora)." Evolution **58**(1): 175-183.

Thyssen, S. M., P. F. Hockl, et al. (2002). "Effects of polyamines on the release of gonadotropin-releasing hormone and gonadotropins in developing female rats." Exp Biol Med (Maywood) **227**(4): 276-281.

Tokuhiro, K., A. Isotani, et al. (2009). "OAZ-t/OAZ3 is essential for rigid connection of sperm tails to heads in mouse." PLoS Genet **5**(11): e1000712.

Torbit, C. A. and H. M. Weitlauf (1975). "Production of carbon dioxide in vitro by blastocysts from intact and ovariectomized mice." J Reprod Fertil **42**(1): 45-50.

Tosaka, Y., H. Tanaka, et al. (2000). "Identification and characterization of testis specific ornithine decarboxylase antizyme (OAZ-t) gene: expression in haploid germ cells and polyamine-induced frameshifting." Genes Cells **5**(4): 265-276.

Travis, H. F., T. E. Pilbeam, et al. (1978). "Relationship of vulvar swelling to estrus in mink." J Anim Sci **46**(1): 219-224.

Tsukamura, H. and K. Maeda (2001). "Non-metabolic and metabolic factors causing lactational anestrus: rat models uncovering the neuroendocrine mechanism underlying the suckling-induced changes in the mother." Prog Brain Res **133**: 187-205.

Uemura, T., H. F. Yerushalmi, et al. (2008). "Identification and characterization of a diamine exporter in colon epithelial cells." J Biol Chem **283**(39): 26428-26435.

van Leeuwenhoek, A. (1678). "Observationes D. Anthonii Leeuwenhoek, de Natis e semine genitali Animalculis." Philos. Trans. R. Soc. London **12**: 1040–1043.

Van Winkle, L. J. (1977). "Low Na+ concentration: a factor contributing to diminished uptake and incorporation of amino acids by diapausing mouse blastocysts?" J Exp Zool **202**(2): 275-281.

Van Winkle, L. J. (1981). "Activation of amino acid accumulation in delayed implantation mouse blastocysts." J Exp Zool **218**(2): 239-246.

Van Winkle, L. J. (2001). "Amino acid transport regulation and early embryo development." Biol Reprod **64**(1): 1-12.

Van Winkle, L. J. and A. L. Campione (1983). "Effect of inhibitors of polyamine synthesis on activation of diapausing mouse blastocysts in vitro." J Reprod Fertil **68**(2): 437-444.

Van Winkle, L. J., A. L. Campione, et al. (1983). "Sodium ion concentrations in uterine flushings from "implanting" and "delayed implanting" mice." J Exp Zool **226**(2): 321-324.

Van Winkle, L. J., J. K. Tesch, et al. (2006). "System B0,+ amino acid transport regulates the penetration stage of blastocyst implantation with possible long-term developmental consequences through adulthood." Hum Reprod Update **12**(2): 145-157.

Vanella, A., R. Pinturo, et al. (1978). "Polyamine levels in human semen of unfertile patients: effect of S-adenosylmethionine." Acta Eur Fertil **9**(2): 99-103.

Venge, O. (1973). "Reproduction in the mink." K. vet.-og Landbohojsk. Arsskr.: 95-146.

Vujcic, S., P. Liang, et al. (2003). "Genomic identification and biochemical characterization of the mammalian polyamine oxidase involved in polyamine back-conversion." Biochem J **370**(Pt 1): 19-28.

Wallace, H. M. (1987). "Polyamine catabolism in mammalian cells: excretion and acetylation." Med. Sci. Res. **15**: 1437–1440

Wallace, H. M. (2009). "The polyamines: past, present and future." Essays Biochem **46**: 1-9.

Wallace, H. M., A. V. Fraser, et al. (2003). "A perspective of polyamine metabolism." Biochem J **376**(Pt 1): 1-14.

Wallace, H. M. and A. J. Mackarel (1998). "Regulation of polyamine acetylation and efflux in human cancer cells." Biochem Soc Trans **26**(4): 571-575.

Wallace, H. M. and K. Niiranen (2007). "Polyamine analogues - an update." Amino Acids **33**(2): 261-265.

Wang, H. and S. K. Dey (2006). "Roadmap to embryo implantation: clues from mouse models." Nat Rev Genet **7**(3): 185-199.

Weiner, K. X. and J. A. Dias (1992). "Developmental regulation of ornithine decarboxylase (ODC) in rat testis: comparison of changes in ODC activity with changes in ODC mRNA levels during testicular maturation." Biol Reprod **46**(4): 617-622.

Weiner, K. X. and J. A. Dias (1993). "Regulation of ovarian ornithine decarboxylase activity and its mRNA by gonadotropins in the immature rat." Mol Cell Endocrinol **92**(2): 195-199.

Weiner, K. X., B. T. Pentecost, et al. (1990). "Testosterone decreases ornithine decarboxylase messenger RNA levels in primary cultures of rat Sertoli cells." Mol Endocrinol **4**(8): 1249-1256.

Weitlauf, H. M. (1969). "Temporal changes in protein synthesis by mouse blastocysts transferred to ovariectomized recipients." J Exp Zool **171**(4): 481-486.

Weitlauf, H. M. (1971). "Protein synthesis by blastocysts in the uteri and oviducts of intact and hypophysectomized mice." J Exp Zool **176**(1): 35-40.

Weitlauf, H. M. (1973). "In vitro uptake and incorporation of amino acids by blastocysts from intact and ovariectomized mice." J Exp Zool **183**(3): 303-308.

Weitlauf, H. M. (1974). "Metabolic changes in the blastocysts of mice and rats during delayed implantation." J Reprod Fertil **39**(1): 213-224.

Weitlauf, H. M. (1978). "Factors in mouse uterine fluid that inhibit the incorporation of [3H]uridine by blastocysts in vitro." J Reprod Fertil **52**(2): 321-325.

Weitlauf, H. M. and G. S. Greenwald (1965). "A comparison of 35-S methionine incorporation by the blastocysts of normal and delayed implanting mice." J Reprod Fertil **10**(2): 203-208.

Weitlauf, H. M. and A. A. Kiessling (1981). "Activation of 'delayed implanting' mouse embryos in vitro." J Reprod Fertil Suppl **29**: 191-202.

Wewer, U. M., R. Albrechtsen, et al. (1988). "Osteonectin/SPARC/BM-40 in human decidua and carcinoma, tissues characterized by de novo formation of basement membrane." Am J Pathol **132**(2): 345-355.

White, C. A., L. Robb, et al. (2004). "Uterine extracellular matrix components are altered during defective decidualization in interleukin-11 receptor alpha deficient mice." Reprod Biol Endocrinol **2**: 76.

White, S. S. and S. R. Ojeda (1981). "Changes in ovarian luteinizing hormone and follicle-stimulating hormone receptor content and in gonadotropin-induced ornithine decarboxylase activity during prepubertal and pubertal development of the female rat." Endocrinology **109**(1): 152-161.

Williams, K. (1997). "Interactions of polyamines with ion channels." Biochem J **325 (Pt 2)**: 289-297.

Wing, L. Y. (1988). "Effect of estradiol on the activities of ornithine decarboxylase and S-adenosyl-methionine decarboxylase in tissues of ovariectomized rats." Chin J Physiol **31**(2): 95-103.

Wu, G., F. W. Bazer, et al. (2004). "Maternal nutrition and fetal development." J Nutr **134**(9): 2169-2172.

Wu, G., F. W. Bazer, et al. (2008). "Proline metabolism in the conceptus: implications for fetal growth and development." Amino Acids **35**(4): 691-702.

Wu, G., F. W. Bazer, et al. (2009). "Arginine metabolism and nutrition in growth, health and disease." Amino Acids **37**(1): 153-168.

Wu, G., F. W. Bazer, et al. (2005). "Polyamine synthesis from proline in the developing porcine placenta." Biol Reprod **72**(4): 842-850.

Wu, G., F. W. Bazer, et al. (1995). "Developmental changes of free amino acid concentrations in fetal fluids of pigs." J Nutr **125**(11): 2859-2868.

Wu, G., F. W. Bazer, et al. (2006). "Board-invited review: intrauterine growth retardation: implications for the animal sciences." J Anim Sci **84**(9): 2316-2337.

Wu, G. and S. M. Morris, Jr. (1998). "Arginine metabolism: nitric oxide and beyond." Biochem J **336 (Pt 1)**: 1-17.

Wu, G., W. G. Pond, et al. (1998). "Maternal dietary protein deficiency decreases nitric oxide synthase and ornithine decarboxylase activities in placenta and endometrium of pigs during early gestation." J Nutr **128**(12): 2395-2402.

Wu, G., W. G. Pond, et al. (1998). "Maternal dietary protein deficiency decreases amino acid concentrations in fetal plasma and allantoic fluid of pigs." J Nutr **128**(5): 894-902.

Wynne-Jones, G. A. and A. M. Gurney (1993). "Pro-oestrous-specific role for polyamines in mediating the secretion of prolactin induced by thyrotrophin-releasing hormone in the rat." J Endocrinol **137**(1): 133-139.

Xiao, L. J., J. X. Yuan, et al. (2006). "Expression and regulation of stanniocalcin 1 and 2 in rat uterus during embryo implantation and decidualization." Reproduction **131**(6): 1137-1149.

Yoshinaga, K. and C. E. Adams (1966). "Delayed implantation in the spayed, progesterone treated adult mouse." J Reprod Fertil **12**(3): 593-595.

YoungLai, E. V. and A. G. Byskov (1983). "Relationship of meiotic prophase and ornithine decarboxylase in the neonatal rabbit ovary." Cell Tissue Res **231**(3): 565-570.

Younglai, E. V., F. Godeau, et al. (1980). "Increased ornithine decarboxylase activity during meiotic maturation in Xenopus laevis oocytes." Biochem Biophys Res Commun **96**(3): 1274-1281.

Zanelli, C. F. and S. R. Valentini (2007). "Is there a role for eIF5A in translation?" Amino Acids **33**(2): 351-358.

Zeng, X., F. Wang, et al. (2008). "Dietary arginine supplementation during early pregnancy enhances embryonic survival in rats." J Nutr **138**(8): 1421-1425.

Zhao, Y. C., Y. J. Chi, et al. (2008). "Polyamines are essential in embryo implantation: expression and function of polyamine-related genes in mouse uterus during peri-implantation period." Endocrinology **149**(5): 2325-2332.

Zhou, Y., C. Ma, et al. (2009). "Antiapoptotic role for ornithine decarboxylase during oocyte maturation." Mol Cell Biol **29**(7): 1786-1795.

Zwierzchowski, L., M. Czlonkowska, et al. (1986). "Effect of polyamine limitation on DNA synthesis and development of mouse preimplantation embryos in vitro." J Reprod Fertil **76**(1): 115-121.

G. Figures

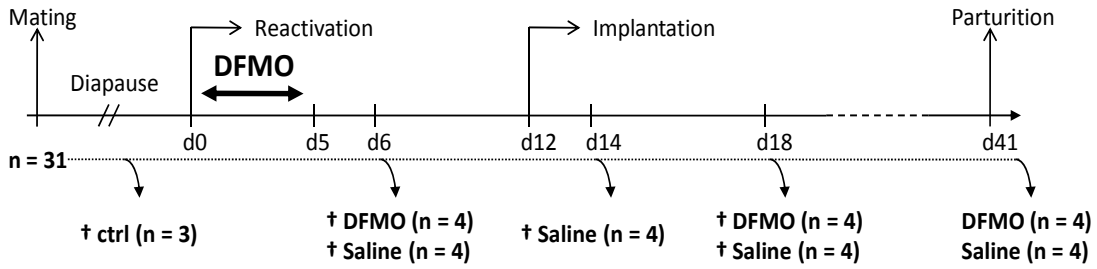

Figure 39. Experimental design for DFMO treatment of mated mink females.

Thirty-one females were mated to fertile males according to standard farming condition procedures. Injections of α-difluoromethylornithine (DFMO) or saline were administered twice a day to 12 and 16 mated females, respectively, during the first five days following prolactin-induced reactivation of blastocysts at day (d) 0. At days 6 and 18 after reactivation, four mated females subjected to DFMO and saline treatment at each stage were sacrificed (†) to investigate the consequences of polyamine deprivation on early embryo reactivation and post-implantation embryonic development. To assess whether polyamine deprivation was detrimental to subsequent fetal-placental (conceptus) development, four mated females treated or not with DFMO were left to complete gestation and parturition. As a control group, three and four mated females were sacrificed during diapause and at day 14 after reactivation of blastocysts (or 2 days after implantation).

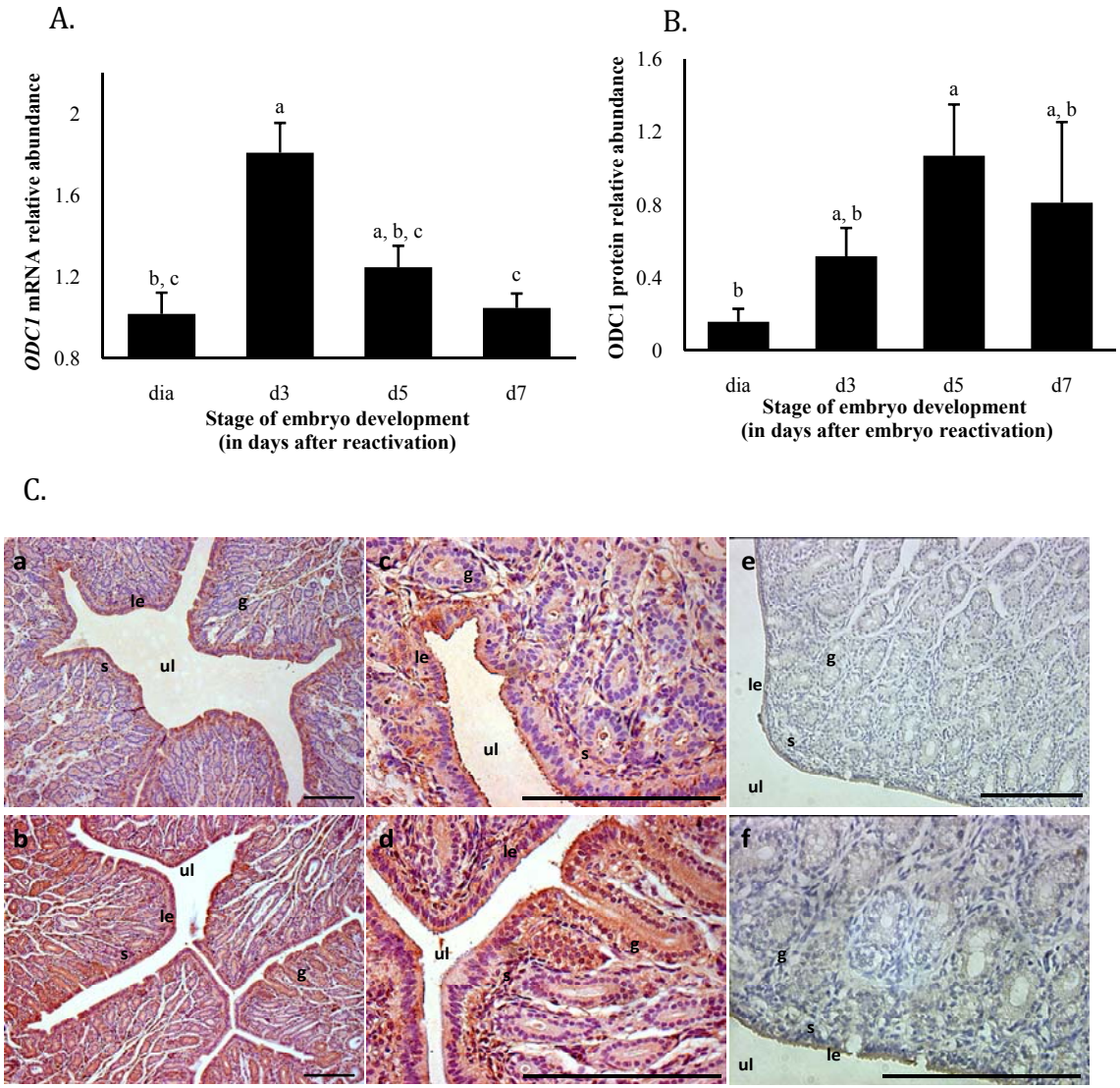
A.
ODC1 mRNA relative abundance
2
1.6
1.2
0.8
a
b, c
a, b, c
c
dia
d3
d5
d7
Stage of embryo development
(in days after reactivation)
B.
ODC1 protein relative abundance
1.6
1.2
0.8
0.4
0
a
a, b
b
a, b
dia
d3
d5
d7
Stage of embryo development
(in days after embryo reactivation)
C.
a
le
g
s
ul
c
g
le
ul
s
e
g
le
s
ul
b
ul
le
s
g
d
le
ul
g
s
f
g
s
le
ul

Figure 40. *Ornithine decarboxylase 1* gene expression in the mink uterus at embryo reactivation.

A. Temporal expression pattern of *ornithine decarboxylase 1* (*ODC1*) in the mink uterus at reactivation. The abundance of *ODC1* mRNA was measured by real time PCR (in triplicate) in whole uterine samples that were collected from three individuals during diapause (dia) and on each of days (d) 3, 5 or 7 after reactivation. Data represents mean ratios ± SEM relative to *GAPDH* and diapause. Significant differences ($P < 0.05$) are represented by different letters. **B**. Semi-quantification of the abundance ODC1 protein relative to β-actin was measured in triplicate during diapause, at d3, d5 and d7 after reactivation in mink uterine protein extracts. Significant differences ($P < 0.05$) are represented by different letters. **C.** Ornithine decarboxylase 1 (ODC1) immunolocalization in mink uteri during diapause and at embryo reactivation. Immunolocalization of ODC1 was performed in mink uterine cross-sections during diapause (**a, c**) and on day 1 (**b, d**) after embryo reactivation. Weak staining for ODC1 was detected in the luminal epithelium and subepithelial stroma during diapause (**a**) while the intensity of ODC1 signal was substantially increased in the luminal and glandular epithelia and, subepithelial stroma on day 1 after embryo reactivation (**b**). The expression of ODC1 was precisely localized in the cytoplasmic subcellular compartment, as revealed by observations at higher magnification (**c**, **d**). No staining could be detected in negative control tissues (**e, f)**. Bars correspond to 200 μm. g: gland; le: luminal epithelium; s:stroma; ul: uterine lumen.

A.

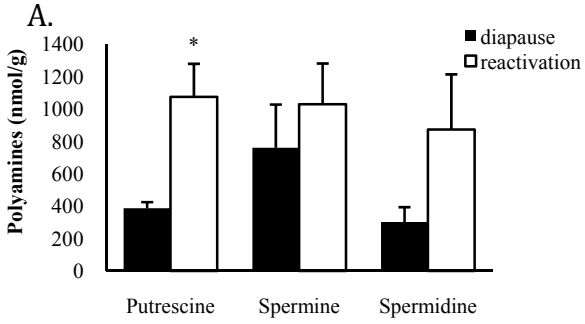
Polyamines (nmol/g)
1400
1200
1000
800
600
400
200
0
*
diapause
reactivation
Putrescine
Spermine
Spermidine

B.

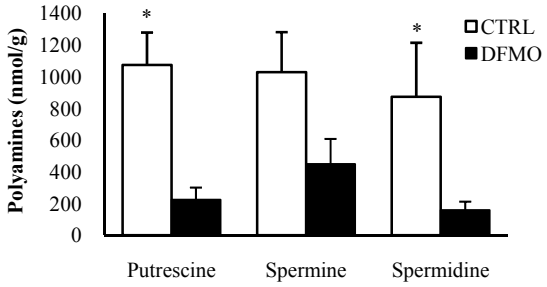
Polyamines (nmol/g)
1400
1200
1000
800
600
400
200
0
*
*
CTRL
DFMO
Putrescine
Spermine
Spermidine

Figure 41. Quantification of polyamine content in uterine samples collected during diapause and at embryo reactivation in control and DFMO-treated mated mink females.

Putrescine, spermine and spermidine were quantified by GC-MS in uterine samples (n=3 in each experimental group). **A**. Putrescine levels were significantly increased in uterine samples between diapause (black bars) and d6 after embryo reactivation (open bars). **B**. Levels of putrescine, spermine and spermidine in uterine samples from mated females treated with 0.5 mg/kg of α-difluoromethylornithine (DFMO) or saline two times per day during the first five days of embryo reactivation were quantified. In uterine samples collected from DFMO treated females (black bars), putrescine, spermine and spermidine levels were significantly reduced in comparison with values for the control (CTRL) group (open bars) on day 6 after embryo reactivation. Data are presented as mean (nmol/g) ± SEM. Statistically significant differences with a $P < 0.05$ (*) between means are represented.

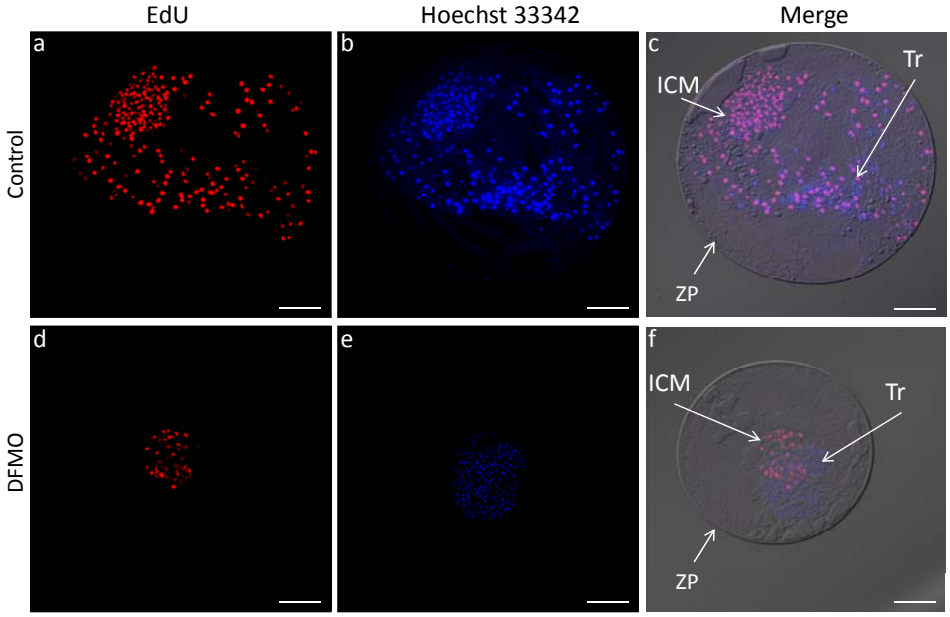
EdU
Hoechst 33342
Merge
Control
DFMO
a
b
c
d
e
f
ICM
Tr
ZP
ICM
Tr
ZP

Figure 42. Effects of polyamine deprivation during blastocyst reactivation on DNA synthesis in mink blastocysts.

Proliferating cells in embryos collected from DFMO-treated (**d**, **e** and **f**) and non-treated females (**a**, **b** and **c**) on day 6 after embryo reactivation were labeled with modified nucleoside 5-ethynyl-2'-deoxyuridine (EdU) which is detected with Alexa 594 (red) (**a** and **d**). All nuclei were counterstained by Hoechst 33342 (**b** and **e**). Whole blastocysts were visualized using differential interference contrast microscopy and merges of the EdU and Hoechst staining are represented (**c** and **f**). In embryos from the control group, nearly all nuclei from the inner cell mass (ICM) and trophoblast displayed proliferation activity (**a**) and were dispersed over the entire blastocyst (**c**). In contrast, blastocysts from the DFMO treated-group exhibited a limited amount of proliferating cells (**d**) located in the ICM, rather than in trophoblast cells, and the distribution among cells was not as extensive as observed in embryos from the control group (**c**). Bars represent 100 μm. ICM: intern cell mass; Tr: trophectoderm; ZP: zona pellucida.

A.

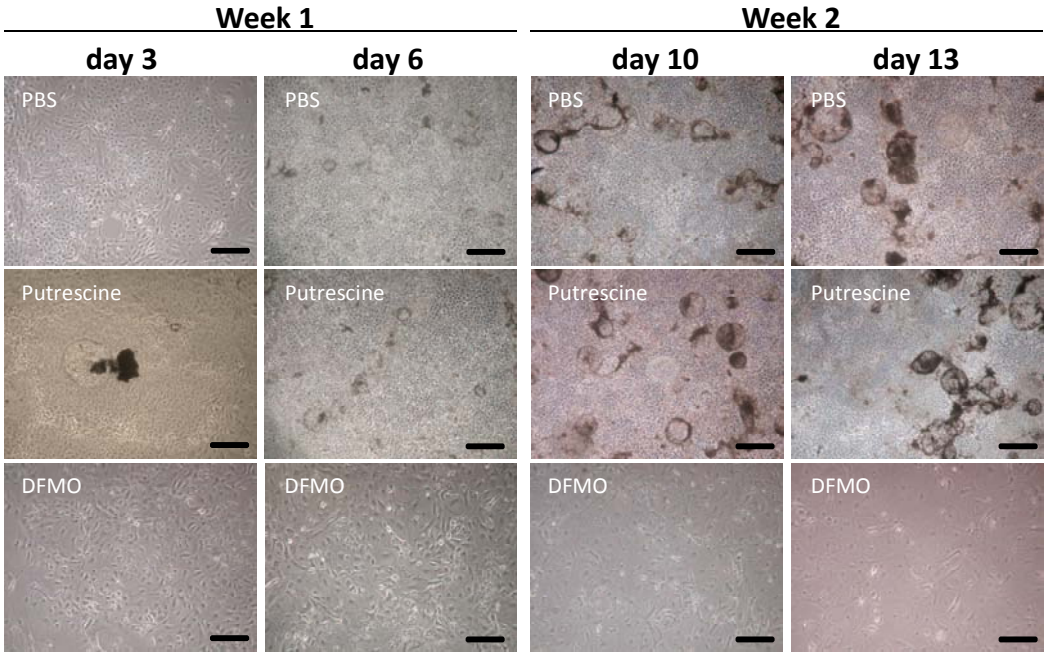
Week 1
Week 2
day 3
day 6
day 10
day 13
PBS
PBS
PBS
PBS
Putrescine
Putrescine
Putrescine
Putrescine
DFMO
DFMO
DFMO
DFMO

B.

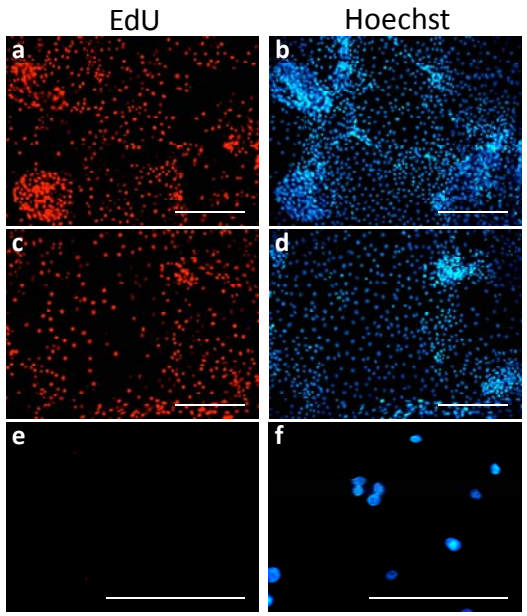
EdU
Hoechst
a
b
c
d
e
f

Figure 43. *In vitro* effects of polyamine deprivation on cultured mink trophoblast cells

A. Trophoblast cells were plated with either PBS 1X as a control (upper panel), putrescine 1 mM (middle panel) or DFMO 10 mM (lower panel) for two weeks. Medium and treatment were renewed every two days and pictures of trophoblast cell colonies were taken every three to four days. In the control, as in the putrescine treated groups (upper and middle panels), trophoblast cells actively proliferated to form well-defined compact colonies of small cells which were visible starting after three days of treatment and thereafter, formed trophoblast vesicles which floated in the medium above the colonies attached at the bottom of the Petri dish. In contrast, no colony growth was observed in cells treated with DFMO and these cells displayed enlarged nuclei and expanded cytoplasm and were highly dispersed (lower panel). **B.** After two weeks of putrescine or DFMO treatment, trophoblast cells were submitted to Click-iT reaction with EdU and Alexa 959 to evaluate the rate of cell proliferation (**a**, **c** and **e**). Hoechst 33342 was used to counterstain all nuclei (**b**, **d** and **f**). Cell proliferation was evident in the control (**a**, **b**) and putrescine treated group (**c**, **d**). Strikingly, none of the DFMO treated cells exhibited proliferative activity (**e**), and they had enlarged nuclei and sharply reduced cell density (**f**) as compared to control and / or the putrescine-treated cells (**b**, **d**). Binucleate cells were also detected in the DFMO-treated cell culture (**f**). Bars represent 200 μm.

A.

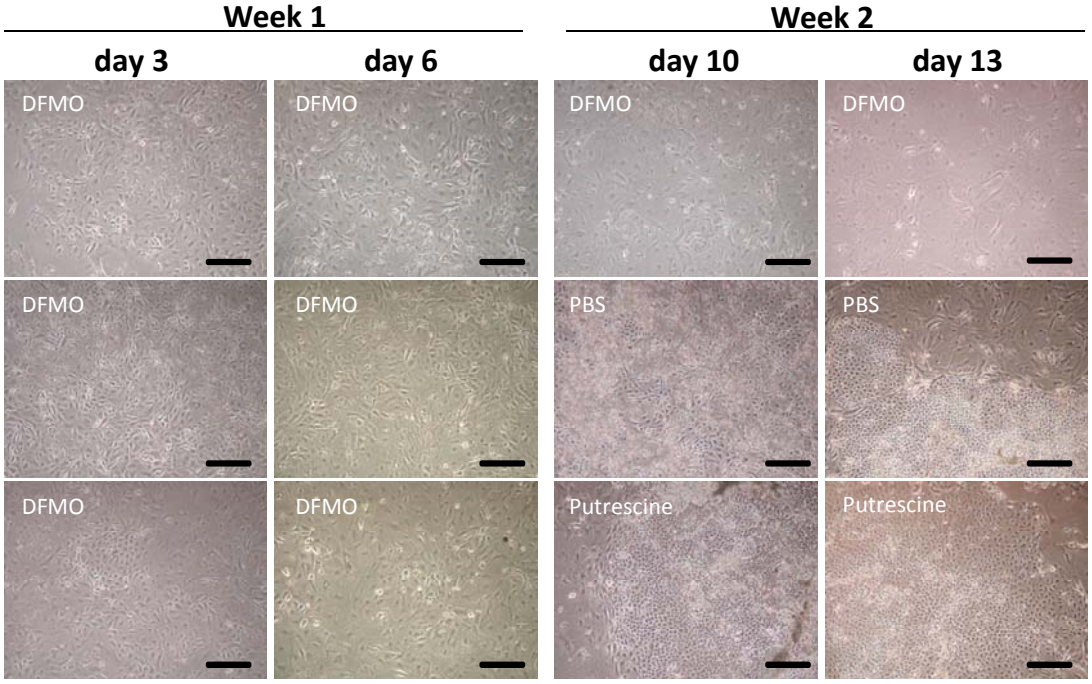
Week 1
Week 2
day 3
day 6
day 10
day 13
DFMO
DFMO
DFMO
DFMO
DFMO
DFMO
PBS
PBS
DFMO
DFMO
Putrescine
Putrescine

B.

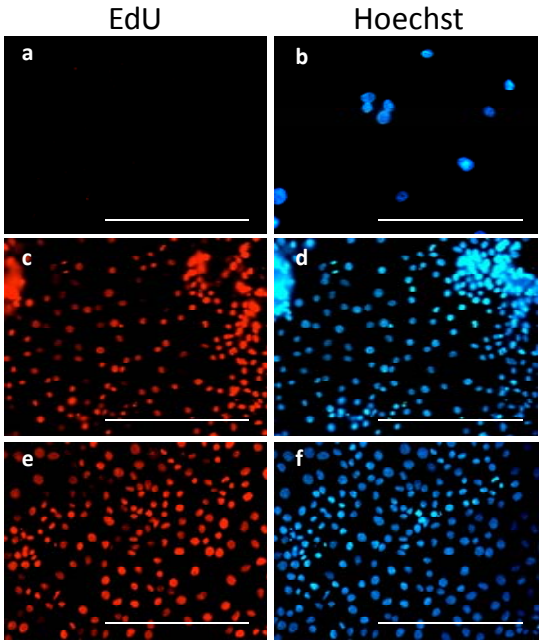
EdU
Hoechst
a
b
c
d
e
f

Figure 44. ***In vitro*** **effects of DFMO removal on cultured mink trophoblast cells.**

A. Trophoblast cells were plated with DFMO 10 mM for two weeks (upper panel), or for one week, and replaced by PBS, as a control (middle panel) or by putrescine 1 mM (lower panel) for the second week of treatment. Medium and treatments were renewed every two days and photos of trophoblast cell colonies taken every three days. During the first week of DFMO treatment, similar changes in cell morphology as previously described were observed (**Figure 43** A (p 292)). When DFMO treatment was removed and replaced by either PBS or putrescine, trophoblast cells actively proliferated to form well-defined compact colonies of small cells after three days of treatment. **B.** After two weeks of DFMO treatment or replacement of DFMO by PBS or putrescine treatment during the second week, trophoblast cells were submitted to Click-iT reaction with EdU and Alexa 959 to evaluate the cell proliferation rate (**a**, **c** and **e**). Hoechst 33342 was used to counterstain all nuclei (**b**, **d** and **f**). Cell proliferation and high cell density were clearly detected in PBS (**c**, **d**) and putrescine treated cell cultures (**e**, **f**) during the second week of treatment, in comparison to the complete absence of proliferating cells and highly dispersed distribution of cells in the DFMO treated group over two weeks of treatment (**a**, **b**). Bars represent 200 μm.

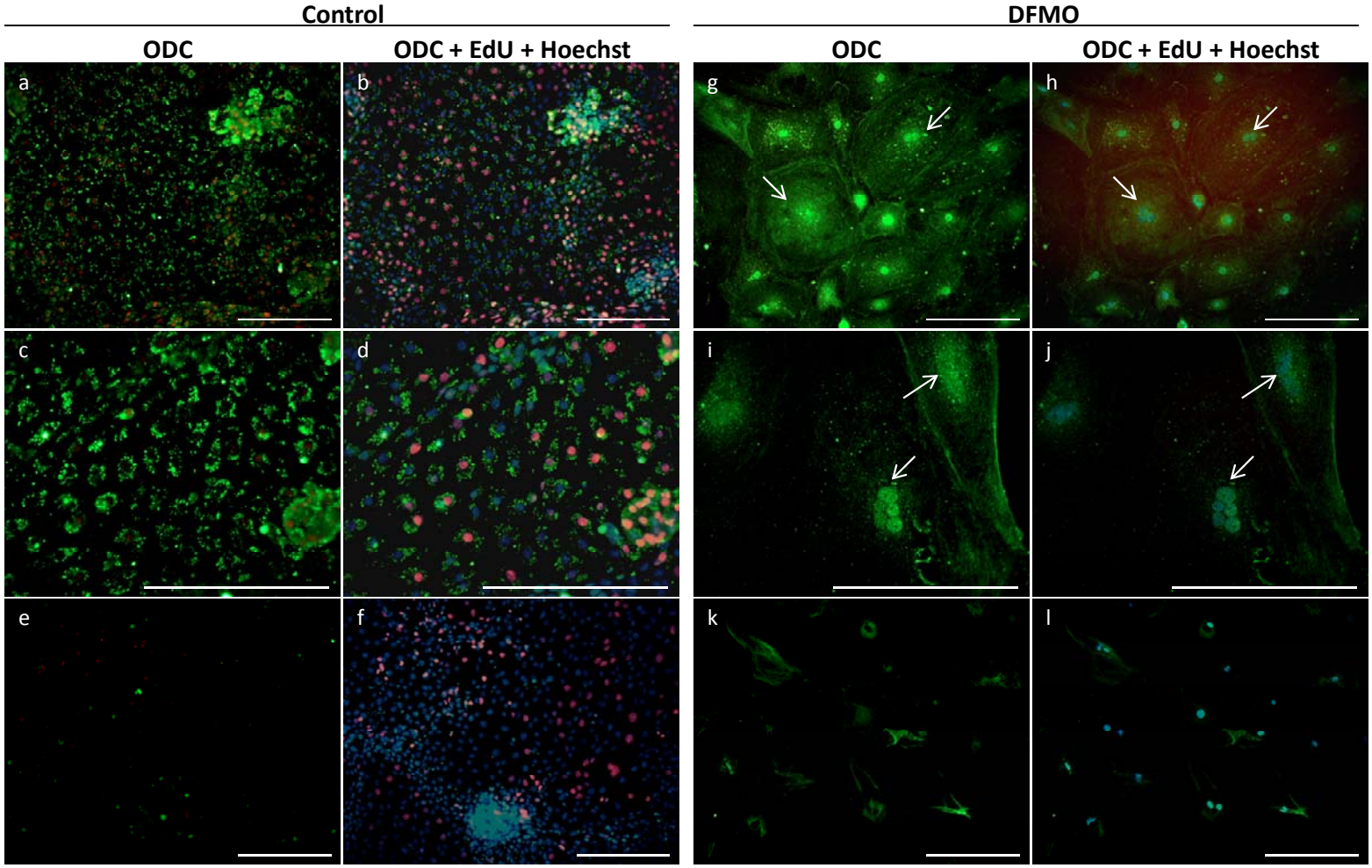
Control
DFMO
ODC
ODC + EdU + Hoechst
ODC
ODC + EdU + Hoechst
a
b
g
h
c
d
i
j
e
f
k
l

Figure 45. Immunolocalization of ODC1 in DFMO-treated mink trophoblastic cells.

Immunolocalization of ODC1 in mink trophoblastic cells treated with DFMO (**g**-**l**) or not (**a**-**f**) for two weeks revealed that ODC1 was abundant in the control trophoblastic cells (**a**). Merge of ODC staining with proliferating cells (EdU) and all cells (Hoechst) (**b**) revealed that ODC1 expression was not specific to proliferating cells. Observations at higher magnification revealed a perinuclear localization of ODC1 and that ODC1 appeared to be contained in vesicle-like organelles, in both proliferating and non proliferating cells (**c**, **d**). In contrast, in DFMO-treated trophoblastic cells, ODC1 exhibited diffuse nuclear, cytoplasmic and plasma membrane immunostaining (**g**, **i**), colocalizing with all nuclei (**h**, **j**). ODC1 was also found in nuclei from multinucleate cells, as indicated by white arrows (**h**-**j**). No staining for ODC1 was observed in cells of the negative control group (**e**, **f**) or DFMO-treated group (**k**, **l**). Bars correspond to 200 μm

.

A.

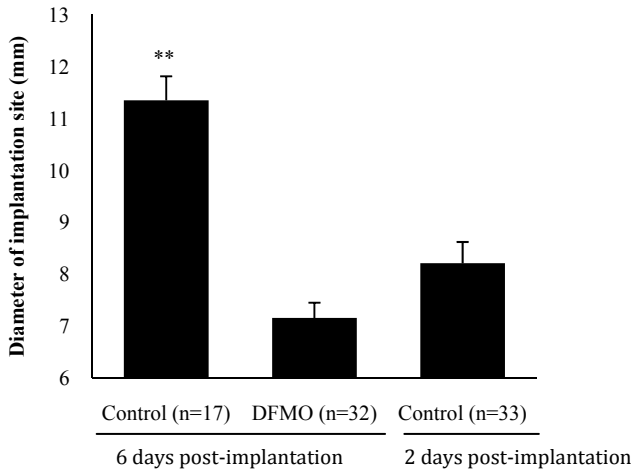
Diameter of implantation site (mm)
13
12
11
10
9
8
7
6
**
Control (n=17)
DFMO (n=32)
Control (n=33)
6 days post-implantation
2 days post-implantation

B.

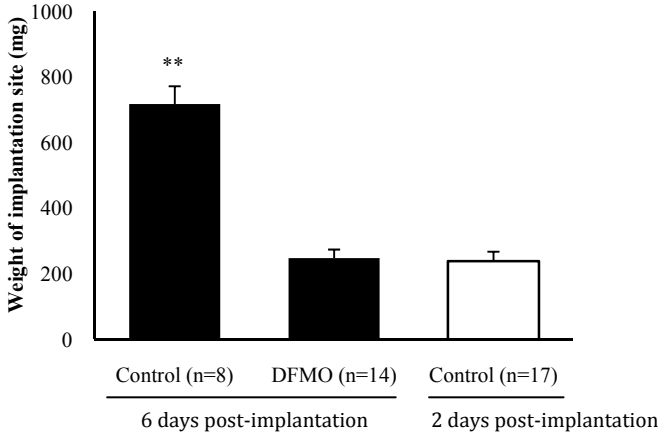
Weight of implantation site (mg)
1000
800
600
400
200
0
**
Control (n=8)
DFMO (n=14)
Control (n=17)
6 days post-implantation
2 days post-implantation

Figure 46. Effects of polyamine deprivation during blastocyst reactivation on consequent implantation and post-implantation development of blastocysts.

Mean diameter (A) and weight (B) of implantation sites collected from DFMO-treated and control females at day (d) 14 or day 18 after reactivation (day 2 or day 6 days post implantation). In the DFMO-treated group, mean weight and diameter of implantation sites were significantly lower than for implantation sites from control mink at day 18 after implantation (black bars) and the latter were reduced to levels similar to those for implantation sites collected at day 14 after blastocyst reactivation, or two days after implantation (open bar). Data represent mean weight ± SEM and mean diameter ± SEM. Statistical significance with a $P<0.01$ (**) between means is represented.

VII. DISCUSSION GÉNÉRALE

Si les mécanismes physiologiques qui contrôlent la diapause embryonnaire obligatoire et facultative, impliquant une fine régulation de l'axe hypothalamo-gonado-hypophysaire, ont été relativement bien élucidés, le rôle utérin provoquant l'émergence de la diapause embryonnaire constitue depuis longtemps une zone d'ombre dans la compréhension de ce phénomène.

L'objectif initial de ce projet de doctorat était donc d'explorer les modifications de l'environnement utérin associées à la réactivation du développement embryonnaire chez le vison américain et ce, afin d'identifier le(s) voie(s) de signalisation utérine(s) responsable(s) de l'émergence de la diapause embryonnaire, durant la période de préimplantation.

Les principaux résultats obtenus sont les suivants :

- Analyse du transcriptome utérin à l'émergence de la diapause embryonnaire (Chapitre IV) :

- Nous avons construit une librairie de 211 séquences utérines de cDNA différentiellement exprimées à l'émergence de la diapause embryonnaire, dont 58 % des séquences sont homologues à des séquences de gènes connues.
- Ces gènes connus sont impliqués dans la régulation du métabolisme (25 %), de l'expression génique (21 %), de la transduction de signal (15 %), du cycle

cellulaire (15 %), de la régulation du transport (10 %) et de la structure cellulaire (9 %).

- Nous avons validé l'expression utérine différentielle de dix gènes à la réactivation du développement embryonnaire, tels que *GDF3*, *ALCAM*, *ADIPOR1*, *HMGN1*, *TXNL1*, *TGM2*, *SPARC*, et trois gènes codant pour *AZI1*, *ODC1* et *SAT1*, des enzymes impliquées dans la biosynthèse des polyamines.
- Nous avons décrit le patron spatio-temporel de l'expression utérine des gènes *SPARC* et *HMGN1* qui illustre d'importants changements utérins, notamment un remodelage tissulaire et de la chromatine à la sortie de la diapause embryonnaire et de l'implantation de l'embryon.
- Codant pour des produits sécrétés, les gènes *GDF3*, *ALCAM*, *TXNL1*, *TGM2*, ainsi que les polyamines, constituent des candidats utérins considérables pour leur participation à l'émergence de la diapause embryonnaire.

- Étude du rôle des polyamines dans la réactivation du développement embryonnaire (Chapitre VI) :

- Nous avons mesuré une augmentation des concentrations utérines en polyamines à l'émergence de la diapause embryonnaire.
- L'inhibition de la biosynthèse des polyamines par l'utilisation du DFMO a provoqué une diminution significative de la prolifération cellulaire dans les embryons supposés être en réactivation et un retard de l'implantation, sans pour autant affecter le succès de la reproduction.

- Un état de dormance dans les cellules de trophoblast *in vitro* a été induit par l'inhibition de la biosynthèse des polyamines par le DFMO. Cet état se manifeste par une réduction de la prolifération cellulaire, une différenciation morphologique, et le changement de la distribution subcellulaire d'ODC1. Ces effets sont réversibles lors de l'arrêt du traitement au DFMO.

A. Analyse du transcriptome utérin à l'émergence de la diapause embryonnaire

1. Technique de la SSH et design expérimental

Pour répondre à notre objectif initial, nous avons entrepris une analyse du transcriptome utérin à la réactivation du développement embryonnaire chez le vison. Tel que décrit dans le Chapitre III de ce manuscript, nous avons eu recours à la technique de la SSH qui permet une comparaison de deux transcriptomes extraits dans deux conditions différentes et, la construction d'une librairie de séquences d'ADNc différentiellement exprimées entre ces deux conditions. Cette technique ne nécessite pas de connaissances préalables du génome de l'espèce étudiée, ce qui représente un avantage considérable dans le cadre de notre étude, basée sur le vison (Diatchenko, Lau et al. 1996).

Les principaux signes de réactivation de l'embryon en diapause chez le vison ayant été observés durant les sept jours suivant la fin de la diapause embryonnaire (Desmarais, Bordignon et al. 2004), le transcriptome utérin de vison en diapause a été comparé aux transcriptomes utérins prélevés à 3, 5 et 7 jours suivant la

réactivation du développement embryonnaire et regroupés ensemble. Dans le but d'obtenir une vue globale du transcriptome utérin à l'émergence de la diapause embryonnaire, nous avons délibérément choisi de conserver les échantillons d'utérus intacts, non dénués du myomètre, et de travailler sur une large fenêtre temporelle. Cependant, ce design expérimental peut être source de perte d'informations. La réactivation du développement embryonnaire chez le vison, a été corrélé à un accroissement de l'activité de sécrétion vers la lumière utérine suggérant la libération de facteurs utérins impliqués dans la réactivation de l'embryon (Enders 1952). L'expression de ces derniers est donc probablement spécifique à l'épithélium luminal et glandulaire utérin qui borde la lumière utérine. Par conséquent, il serait probant d'approfondir cette première approche par une analyse du transcriptome endométrial et ce, sur des échantillons prélevés dans une fenêtre de temps plus courte.

2. Analyse de la librairie SSH

Une librairie comprenant 211 séquences d'ADNc spécifiquement exprimées dans l'utérus chez le vison à la sortie de la diapause a été générée. Ces séquences ont été enregistrées dans la banque de données GenBank et permettent ainsi d'élargir le nombre de séquences connues du génome de vison.

L'analyse des séquences d'ADNc homologues à des séquences de gènes connues, en grande partie d'origines canines (*Canis familiaris*) (78% des séquences), a démontré l'expression de gènes utérins impliqués dans la régulation du métabolisme, de l'expression génique, des signaux de transduction, du cycle

cellulaire, du transport et de la structure cellulaire au moment de l'émergence de la diapause embryonnaire. Cela reflète ainsi des modifications cellulaires et moléculaires importantes de l'environnement utérin chez le vison à la réactivation du développement embryonnaire et ce, en vue de la préparation à l'implantation. Une distribution similaire de la fonction biologique des gènes impliqués dans l'émergence de la diapause facultative a été décrite chez la souris (Reese, Das et al. 2001).

Afin de valider la SSH et d'approfondir cette étude, dix gènes ont été spécifiquement choisi dans la librairie utérine selon leur implication dans le développement embryonnaire en période de préimplantation et/ou implantation chez d'autres espèces, rapportées dans la littérature. Leur rôle éventuel dans le remodelage utérin associé à la réactivation du développement embryonnaire (*SPARC*, *HMGN1*, *ADIPOR1*), mais également leur potentiel à constituer des facteurs utérins induisant la réactivation de l'embryon (*GDF3*, *ALCAM*, *TXNL1*, *TGM2*, *ODC1*, *SAT1* et *AZI1*) sont des critères qui ont également été pris en compte. L'expression utérine de ces dix gènes était significativement augmentée à la reprise du développement embryonnaire, validant ainsi l'efficacité de la SSH.

3. Gènes-candidats impliqués dans les changements de l'environnement utérin à la réactivation de l'embryon

L'augmentation de l'expression utérine du gène codant pour HMGN1, une protéine nucléaire différente des histones (Gerlitz 2010), illustre particulièrement un remodelage intensif de la chromatine dans l'utérus de vison à l'émergence de la

diapause, pouvant ainsi être à l'origine de l'expression de gènes importants dans ce processus. Par ailleurs, HMGN1 semble témoigner d'une localisation cytoplasmique pendant la mitose tandis qu'une localisation nucléaire pour HMGN1 est observée pendant la phase S du cycle cellulaire (Louie, Gloor et al. 2000). Par conséquent, nous avons supposé que la régulation de la proliferation cellulaire au niveau utérin dépendait de HMGN1, à la réactivation du développement embyonnaire.

La protéine SPARC appartient à la superfamille des protéines matricellulaires qui sont secrétées dans la matrice extracellulaire et joue un rôle anti-adhésif et inhibiteur de la prolifération cellulaire (Sage, Johnson et al. 1984). L'accroissement de l'expression utérine de *SPARC* chez le vison au moment de la reprise du développement embryonnaire a été observé et pourrait témoigner d'un remodelage tissulaire important au moment de la réactivation. En se basant sur le patron d'expression spatio-temporelle de *SPARC*, nous avons supposé que SPARC, de part son caractère anti-adhésif, participerait à l'orientation de l'embryon vers son site d'implantation.

Au niveau des sites d'implantation et inter-implantation, *HMGN1* et *SPARC* ont témoigné d'un patron d'expression subcellulaire spécifique, suggérant ainsi la participation de ces deux facteurs utérins dans le processus d'implantation, chez le vison. La protéine HMGN1 était detectée dans les parties extraembryonnaires, tels que dans le noyau des cellules des plaques trophoblastiques et des cellules mesenchymateuses des capillaires fœtaux. Une localisation cytoplasmique de HMGN1 était également observée dans le syncythiotrophoblaste et les

compartiments maternels uterins, à savoir, l'epithelium luminal et glandulaire et, le stroma. Cette distribution spécifique de HMGN1 au niveau des sites d'implantation pourrait témoigner d'un rôle spécifique de ce regulateur de la structure chromatinienne dans le développement du placenta, chez le vison. Quant à SPARC, le patron d'expression génique et la localisation de la protéine de SPARC démontre clairement que SPARC est specifiquement exprimés au pôle apical de l'epithelium luminal des sites d'inter-implantation et au pôle mésometrial des sites d'implantation. Cette distribution spécifique suggére que SPARC, de part son caractére anti-adhesif, serait important pour orienter l'embryon vers son site d'implantation. De plus, la détection de la protéine SPARC dans le compartiment utérin maternel, tels que dans le noyau des cellules de l'épithelium gandulaire, du stroma et du symplasma maternel suggérent que SPARC serait impliqué dans l'inhibition de la proliferation cellulaire utérin au niveau du site d'invasion trophobloblastique dans l'endométre utérin.

4. Gènes candidats potentiellement impliqués dans la réactivation du développement embryonnaire

Le facteur de croissance et de différentiation 3 (growth and differentiation 3, GDF3) figurait également dans la librairie SSH. Ce dernier est un membre de la famille des facteurs de transformation de croissance β (transforming growth factor β, TGFβ) et a été décrit comme un facteur sécrété et marqueur de la pluripotence ou de la différenciation des cellules souches embryonnaires humaines ou murines, respectivement (Levine and Brivanlou 2006). La présence de GDF3 a de plus été

détectée chez des blastocystes de souris (Levine and Brivanlou 2006). Les TGFβ participent activement au remodelage tissulaire associé à l'implantation. Ces facteurs seraient aussi secrétés dans la lumière utérine ou ils agiraient sur le développement embryonnaire (revue par (Jones, Stoikos et al. 2006)). Des embryons de visons collectés pendant la période de diapause et des cellules de trophoblastes de vison ont été soumis à un traitement *in vitro* avec une protéine recombinante GDF3. Nous n'avons pu observer aucun signe de réactivation des embryons, ni d'effet sur la prolifération et/ou la différenciation des cellules de trophoblastes *in vitro*. La protéine recombinante GDF3 utilisée dans le cadre de ces expériences a été construite a partir de la séquence protéique correspondant à celle de la protéine humaine de GDF3. Il se pourrait par conséquent qu'elle ne soit pas reconnue par les récepteurs de GDF3 exprimés chez le vison. Néanmoins, GDF3 demeure cependant un candidat potentiellement impliqué dans l'émergence de la diapause embryonnaire.

D'autres gènes identifiés dans la librairie SSH ont attiré notre attention de part leur fonction dans la régulation de la prolifération cellulaire, leur potentiel à être secrétés et/ou leur implication dans le processus de l'implantation rapportée dans la littérature chez d'autres espèces. Ces gènes codent pour *ALCAM*, *ADIPOR1*, *TXLN1* et pour *TGM2*. Toutes les tentatives de localisation de ces protéines par immunohistochimie ayant échouées, en raison probablement de l'absence de spécificité des anticorps utilisés pour ces protéines exprimées chez le vison, nous avons décidé de ne pas poursuivre l'étude du rôle de ces gènes dans la réactivation

de l'embryon. Ces gènes représentent néanmoins des candidats utérins ayant un rôle potentiel dans l'émergence de la diapause embryonnaire. L'analyse de leur expression tissulaire par d'autres techniques, telle que l'hybridation *in situ*, ouvrirait probablement de nouvelles portes sur la compréhension des voies de signalisation utérines impliquées dans la sortie de la diapause embryonnaire.

Finalement, trois genes codant pour des facteurs de la biosynthèse des polyamines, l'*ODC1*, la *SAT1* et *AZI1*, ont été répértoriés dans la librairie SSH. Les polyamines, à savoir la putrescine, la spermidine et la spermine, sont des polycations capables d'interagir avec les acides nucléiques et d'induire une condensation de la chromatine (revue par (Wallace, Fraser et al. 2003)). Ces molécules sont par conséquent d'importants régulateurs de la prolifération cellulaire, mais aussi de l'expression génique. De plus, les polyamines sont soumises à une forte activité de sécrétion reflétant une régulation fine des contenu intracellulaire en polyamines (revue par (Wallace, Fraser et al. 2003)). L'étude bibliographique que nous avons entreprise recense les divers rôles des polyamines dans la reproduction (chapitre V), que ce soit dans le processus de la gamétogénèse, de la fertilisation, du développement embryonnaire, de l'implantation et de la placentation. Plus spécifiquement, des études réalisées chez les rongeurs et les ruminants ont démontré l'implication des polyamines dans le développement embryonnaire et durant la placentation (Fozard, Part et al. 1980; Wu, Pond et al. 1998; Kwon, Ford et al. 2004; Wu, Bazer et al. 2005; Lopez-Garcia, Lopez-Contreras et al. 2008; Zhao, Chi et al. 2008; Gao, Wu et al. 2009; Kim, Spencer et al. 2009; Wu,

Bazer et al. 2009). Aussi, la présence de l'inhibiteur de l'ODC1, le DFMO, dans le milieu de culture d'embryons de souris en diapause a été associée à l'inhibition de la réactivation de ces derniers et ce, de manière réversible (Van Winkle and Campione 1983).

Par conséquent, nous avons suggéré que l'expression différentielle d'*ODC1*, *SAT1* et *AZIN1* pourrait refléter une synthèse utérine accrue des polyamines potentiellement impliquées dans la réactivation du développement embryonnaire chez le vison. L'augmentation du contenu utérin en polyamines, principalement de la putrescine, concomitante avec l'émergence de la diapause embryonnaire a renforcé cette hypothèse et nous avons par conséquent décidé de poursuivre dans cette direction.

B. Rôle des polyamines à l'émergence de la diapause embryonnaire

1. Validation du modèle expérimental

Afin de tester notre hypothèse concernant le rôle des polyamines produites au niveau utérin dans la sortie de la diapause embryonnaire chez le vison, des femelles visonnes accouplées à des mâles fertiles ont été soumises à une injection sous-cutanée de DFMO à raison de deux fois par jour, afin de bloquer la biosynthèse de polyamines durant les cinq premiers jours de la réactivation embryonnaire supposément induite par la prolactine.

La période de reproduction chez le vison étant saisonnière, nous n'avons pas été en mesure d'effectuer une étude préliminaire qui nous aurait permis d'optimiser la dose, la fréquence et le mode d'administration du DFMO chez cette espèce. Pour déterminer les conditions expérimentales, nous nous sommes donc basés sur des études réalisées chez la souris et le rat (Fozard, Part et al. 1980; Lopez-Garcia, Lopez-Contreras et al. 2008; Zhao, Chi et al. 2008).

En se basant sur l'utilisation du DFMO pour bloquer l'activité de l'ODC1, des études ont de plus démontré un lien entre les polyamines et la biosynthèse et la sécrétion de prolactine par la glande pituitaire (Wynne-Jones and Gurney 1993), et également entre les polyamines et la production ovarienne de progestérone (Bastida, Tejada et al. 2002). Étant donné que la prolactine et la progestérone sont des hormones-clés de la reprise du développement embryonnaire chez le vison (Lopes, Desmarais et al. 2004), nous voulions être certains que les effets du traitement au DFMO n'affecteraient pas la production de ces hormones. Dans notre expérience, la réactivation du développement embryonnaire chez les femelles constituant nos groupes expérimentaux, est synchronisée par une injection quotidienne de prolactine, à compter du 21 mars, ce qui contrecarre un éventuel effet du DFMO sur la production de prolactine. Par ailleurs, la concentration ovarienne de progestérone a été mesurée dans les ovaires de femelles traitées au DFMO ou pas et la concentration ovarienne en progestérone ne s'est pas avérée être affectée par le traitement. Nous avons de plus dosé les quantités de polyamines

dans des échantillons utérins : celles-ci étaient considérablement diminuées par l'inhibition de l'ODC1, ce qui nous a permis de valider notre modèle expérimental.

2. Effets de l'inhibition de la synthèse des polyamines à l'émergence de la diapause embryonnaire :

a. Sur la réactivation du développement embryonnaire

Afin de mesurer les effets directs de la réduction des contenus utérins de polyamines sur la reprise du développement embryonnaire, des blastocystes ont été flushés de l'utérus de femelles un jour suivant la fin du traitement de DFMO. Le nombre moyen d'embryons par femelles traitées et la viabilité de ces derniers n'étaient pas affecté par la réduction des taux de polyamines. Les signes de réactivation de l'embryon, tels que l'expansion des embryons, la prolifération cellulaire et la synthèse protéique ont été mesurés. Pour des raisons inconnues, la quantification de la synthèse protéique dans les embryons n'a pas fonctionné. L'augmentation du diamètre à la réactivation, résultant de l'incorporation de fluides intra-utérins dans les embryons (Desmarais, Bordignon et al. 2004), n'était pas perturbée par l'inhibition de la biosynthèse des polyamines.

Par contre, la prolifération cellulaire s'est avérée nettement réduite au sein des embryons issus des femelles traitées au DFMO en comparaison au groupe contrôle, suggérant que la réduction de polyamines affecte de manière considérable la reprise de la prolifération cellulaire. Les cellules du trophoblaste étaient visiblement plus ciblées par le traitement au DFMO que les cellules de l'ICM. Pour confirmer cette observation, un marquage différentiel des cellules du trophoblaste

et de l'ICM aurait été nécessaire. Cependant, une telle expérience est délicate du fait qu'elle nécessite une étape de digestion de la zone pellucide entourant l'embryon et, que les embryons de visons se désagrègent lorsque la zone pellucide est retirée.

En présence de DFMO dans le milieu de culture, la croissance trophoblastique associée à la réactivation d'embryons de souris en diapause est inhibée (Van Winkle and Campione 1983). Nos données confortent ces résultats dans l'hypothèse que les polyamines sont indispensables à la reprise de la prolifération cellulaire dans les cellules du trophoblaste. Un arrêt du cycle cellulaire en phase G0/G1 a été associé à l'état de diapause chez les embryons de souris (Sanyal and Meyer 1972; Sherman and Barlow 1972) et de visons (Desmarais, Bordignon et al. 2004). Parallèlement, l'inhibition de l'ODC1 par le DFMO a été corrélée à un arrêt du cycle cellulaire en phase G0/G1 dans plusieurs lignées de cellules (revue par (Wallace, Fraser et al. 2003)). De ce fait, la carence en polyamines pourrait être à l'origine de la réduction de la prolifération cellulaire dans les cellules du trophoblaste de l'embryon, maintenu ou replongé ainsi en diapause.

Afin d'évaluer les effets directs des polyamines sur l'émergence de la diapause embryonnaire, des embryons de visons en diapause ont été mis en présence de putrescine sur une période allant de 24 heures à deux semaines (résultats non publiés). Nous n'avons pu détecter aucun signe de réactivation des embryons traités. Néanmoins, la proportion d'embryons présentant des noyaux cellulaires fragmentés semblaient être diminuée dans les embryons en présence de putrescine après trois jours de traitement (0 sur 3 embryons) en comparaison avec

les embryons non-traités (3 sur 3 embryons). Cela suggère un rôle antiapoptotique des polyamines sur les embryons de visons en diapause. Une étude a souligné que la présence de putrescine, spermidine et spermine dans le milieu de culture d'embryons porcins favorisait le développement de l'embryon du stade deux cellules au stade de blastocyste, et ce en réduisant les taux d'apoptose (Cui and Kim 2005). Bien que des études plus approfondies soient nécessaires et ce, en faisant appel une technique de marquage de l'apoptose, telle qu'un marquage TUNEL, il serait probable que les polyamines favorisent la survie des embryons à l'émergence de la diapause. Il serait aussi pertinent, d'examiner un éventuel effet dose-dépendant de la putrescine dans le milieu de culture, l'effet d'autres polyamines, tels que la spermidine ou spermine, ou encore la combinaison de ces dernières sur la survie et la réactivation *in vitro* d'embryons de visons collectés pendant la diapause.

b. Sur l'implantation et le développement post-implantation

Le diamètre et le poids moyens des sites d'implantation à six jours après l'implantation étaient réduits à des valeurs comparables à celles mesurées pour des sites d'implantation à deux jours suivant l'implantation chez les femelles traitées au DFMO durant la période de réactivation. Ces résultats démontrent que, suite à la réduction de la prolifération cellulaire induite par une carence en polyamines à l'émergence de la diapause, l'implantation s'effectue de manière normale, mais avec un retard dans le temps, comparativement à la normale. Cela suggère fortement une réinduction ou un maintien des embryons en diapause soumis à une carence en

polyamines, ayant pour conséquence un décalage du moment de l'implantation dans le temps.

Le fait que le succès reproducteur ne soit pas affecté par le traitement de DFMO durant l'émergence de la diapause embryonnaire conforte ces résultats. Cela confirme aussi que l'inhibition de la synthèse des polyamines durant l'émergence de la diapause embryonnaire provoque un retard de l'implantation et non une résorption embryonnaire au niveau des sites d'implantation.

La durée de la gestation chez les femelles soumises au traitement n'était cependant pas différente de celle observée chez les femelles contrôles. L'effectif des animaux utilisés dans cette expérience était relativement faible (n=4 par groupe), ce qui n'est peut être pas suffisant pour que les résultats soient représentatifs de ceux attendus, à savoir une durée de gestation plus longue et ce, de manière proportionnelle à la durée du traitement au DFMO. La répétition de cette expérience, mais en utilisant un plus grand nombre d'individus, serait par conséquent nécessaire pour la validation de ce résultat. Il serait aussi pertinent de mesurer les effets de différentes durées de traitement au DFMO, durant l'émergence de la diapause embryonnaire sur la durée totale de la gestation.

La majorité des études répertoriées dans la littérature traitent davantage du rôle des polyamines dans le processus de l'implantation chez les rongeurs. L'inhibition de la synthèse des polyamines au moment de l'implantation a été corrélée à un échec de la gestation chez les rongeurs, qui se manifeste par une résorption des sites d'implantation et un arrêt du développement embryonnaire

(Fozard, Part et al. 1980; Lopez-Garcia, Lopez-Contreras et al. 2008; Zhao, Chi et al. 2008). Par conséquent, notre étude est innovatrice, dans le sens où elle démontre, pour la première fois, le rôle des polyamines dans le développement embryonnaire pendant la période de préimplantation, notamment à la sortie de la diapause embryonnaire.

L'inhibition de la biosynthèse des polyamines par un traitement au DFMO durant les quatres jours suivants l'implantation chez le vison a également provoqué une diminution significative du diamètre et du poids des sites d'implantation et un échec complet de la gestation (résultats non publiés). L'analyse des cicatrices placentaires chez les femelles traitées au DFMO pendant l'implantation (résultats non publiés) démontre un fort taux de résorption fœtale au niveau des sites d'implantation, mais aussi, une distribution anormale de ces derniers le long des cornes utérines (résultats non publiés). Ces données soulignent que les polyamines sont indispensables à l'implantation de l'embryon chez le vison et ouvrent de nouvelles portes sur la compréhension des mécanismes sous-jacents de la placentation endotheliochoriale chez les carnivores.

Globalement, notre étude réalisée *in vivo* valide l'hypothèse selon laquelle les polyamines sont indispensables à la réactivation du développement embryonnaire puisque une carence en polyamines est à l'origine non seulement, de l'induction ou du maintien des embryons dans un état de dormance, mais également d'un retard de l'implantation, sans conséquences néfastes sur le succès reproducteur.

3. Effet de l'inhibition de la biosynthèse des polyamines sur des cellules trophoblastique

Étant donné l'accès limité à la collecte d'embryons de visons qui ne peut être effectuée qu'une fois par année, et la fragilité de ces derniers, l'utilisation d'une lignée de cellules trophoblastiques de vison nous a semblé être une bonne alternative pour approfondir notre étude.

La croissance des cellules trophoblastiques s'est trouvée inchangée en présence de putrescine dans le milieu de culture en comparaison au groupe contrôle. En revanche, le traitement des cellules avec du DFMO a provoqué d'importantes modifications morphologiques se manifestant par un arrêt complet de la prolifération cellulaire, un élargissement de la taille des cellules et des noyaux, ainsi que l'apparition de cellules multinucléées. Ces modifications liées à l'inhibition de la synthèse des polyamines étaient de plus réversibles : l'arrêt du traitement de DFMO était en effet corrélé à une reprise rapide de la croissance cellulaire et un retour à une morphologie similaire à celle des colonies observées dans le groupe contrôle. La translocation d'ODC1 d'une localisation péri- nucléaire à nucléaire et cytoplasmique a également pu être observée sous l'effet du traitement au DFMO. Une corrélation entre la localisation subcellulaire de l'ODC1 et le cycle cellulaire a été établie par des études antérieures (Schipper, Cuijpers et al. 2004). Il a de plus été démontré que l'ODC1 cytoplasmique est impliquée dans la polymérisation de l'actine au moment de la cytokinèse lors de la mitose (Pomidor, Ruhl et al. 1995), impliquant la polyamination de la GTP-ase RhoA, un régulateur important de la

polymérisation de l'actine (Makitie, Kanerva et al. 2009). La délétion du gène codant pour *RhoA* dans des cellules Swiss 3T3 a provoqué un arrêt du cycle cellulaire en phase G0/G1 résultant d'une cytokinèse défaillante et de la formation de cellules binucléées (Morin, Flors et al. 2009). Par comparaison, l'arrêt de la prolifération cellulaire, la translocation de l'ODC1 et la formation de cellules multinucléées en réponse à l'inhibition de l'ODC1 dans les cellules de trophoblaste de vison suggèrent sensiblement que ces cellules sont arrêtées en phase G0/G1 du cycle cellulaire, ou dans un état similaire à celui suggéré dans les cellules de l'embryon en diapause. Une étude complémentaire basée sur l'utilisation de la technique de cytométrie de flux permettrait de tester cette hypothèse.

Aussi, l'ajout de putrescine, en plus du DFMO, dans le milieu de culture de cellules de trophoblastes de vison contrecarre les effets du DFMO sur les cellules de trophoblaste, qui démontrent alors une morphologie et une prolifération cellulaire comparables à celles observées dans les cellules contrôles (données non publiées). De manière similaire, des embryons de souris en diapause soumis à un traitement simultané de DFMO et de putrescine ne répondent pas à l'inhibition induite par le DFMO et démontrent une croissance trophoblastique comparable à celle observée chez les embryons contrôles (Van Winkle and Campione 1983). Par conséquent, la présence de polyamines exogènes semble n'avoir d'effet que si la biosynthèse de ces dernières est réprimée, suggérant un mécanisme de régulation précis des concentrations intracellulaires en polyamines.

Ces expériences confortent par conséquent nos résultats obtenus *in vivo* et renforcent l'hypothèse que les polyamines sont indispensables à la prolifération cellulaire des cellules du trophoblaste à l'émergence de la diapause embryonnaire chez le vison.

C. Perspectives et directions futures

1. Polyamines d'origine utérines ou embryonnaires ?

Nos expériences ont démontré que l'inhibition de la biosynthèse des polyamines durant la période de réactivation de l'embryon induit ou maintient les embryons de vison dans un état de diapause, en bloquant la reprise de la prolifération cellulaire au niveau du trophoblaste et ce, de manière réversible. Nous avons observé que le prolongement de la période de la diapause provoqué par une carence en polyamines se répercute sur le processus de l'implantation qui est alors retardé, mais n'affecte pas le succès de la reproduction.

Par contre, nos résultats soulèvent d'importantes questions : L'émergence de la diapause embryonnaire résulte-t'elle de l'incorporation de polyamines d'origine utérine par l'embryon ? Ou bien de la stimulation de la synthèse des polyamines intraembryonnaire ? D'un coté, la présence de polyamines exogènes augmenterait la survie des embryons en diminuant les taux d'apoptose, comme le suggèrent nos données (non publiées) et celles rapportées chez les embryons porcins (Cui and Kim 2005). Dans nos expériences, nous avons observé qu'une carence utérine en polyamines n'affecte pourtant pas la survie des embryons à l'émergence de la

diapause embryonnaire. De plus, l'étude de Van Winkle (Van Winkle and Campione 1983) démontre un effet direct du DFMO sur les embryons de souris et, les cellules de trophoblaste de visons se sont avérées réceptives au traitement de DFMO. Il est donc fort probable que la réactivation de l'embryon soit davantage induite par la reprise de la biosynthèse des polyamines intraembryonnaire.

Cette hypothèse entraine deux autres questions fondamentales, à savoir : quels sont les stimuli utérins à l'origine de la synthèse intraembryonnaire des polyamines ? Et, par quels mécanismes moléculaires et cellulaires les polyamines participent-elles à la réactivation de l'embryon ?

2. Quels sont les stimuli utérins induisant la synthèse intraembryonnaire des polyamines ?

Le modèle proposé par Van Winkle et al. décrit dans le chapitre II de cet ouvrage (partie II. C. 2.) suggère que la réactivation embryonnaire, chez la souris, serait provoquée par un changement de la concentration en Na^+ dans les fluides utérins (Van Winkle 1977; Van Winkle, Campione et al. 1983), duquel résulterait l'activation des transporteurs spécifique de la leucine et l'arginine (systèmes $B^{0,+}$ et $b^{0,+}$) (Van Winkle 1981; Martin, Sutherland et al. 2003). Dans le milieu intraembryonnaire, la leucine stimulerait la voie de signalisation mTOR qui induirait l'expression et l'activation de l'ODC1 permettant alors la synthèse de polyamines, à partir de l'arginine incorporée, de s'effectuer (Kimball, Shantz et al. 1999; Martin, Sutherland et al. 2003). Cette synthèse intraembryonnaire en polyamines serait

alors à l'origine de la reprise de la croissance trophoblastique, associée à la réactivation de l'embryon et son implantation.

En se basant sur ce modèle, il serait pertinent de poursuivre notre étude chez le vison en explorant les mécanismes utérins et embryonnaires qui sont en amont de la reprise de la biosynthèse des polyamines intraembryonnaire, et ce en explorant :

- les facteurs utérins, à savoir l'évolution de la concentration de Na^+ dans les fluides utérins entre la diapause et la réactivation, ou encore l'effet d'un milieu de culture hypersodique sur la réactivation *in vitro* d'embryons de vison en diapause.
- les facteurs embryonnaires, tels l'expression des systèmes de transports $B^{0,+}$ et $b^{0,+}$ de la leucine et de l'arginine, les acteurs de la voie de signalisation mTOR, et l'expression et l'activité d'ODC1 dans les embryons de vison à la réactivation.

3. Par quels mécanismes moléculaires et cellulaires les polyamines participent-elles à la réactivation de l'embryon ?

Nos résultats démontrent clairement que les polyamines régulent le cycle cellulaire de l'embryon à la sortie de la diapause embryonnaire et des cellules de trophoblaste de vison. À la lumière d'études antécédentes, nous avons suggéré que les polyamines participeraient spécifiquement à la cytokinèse (Pomidor, Ruhl et al. 1995; Schipper, Cuijpers et al. 2004), en impliquant la GTP-ase Rho, un facteur

important de la polymérisation de l'actine (Makitie, Kanerva et al. 2009), dans les cellules trophoblastiques à la réactivation du développement embryonnaire.

Cette hypothèse représente par conséquent un point qu'il serait intéressant d'approfondir afin d'explorer le mécanisme moléculaire par lequel les polyamines régulent le cycle cellulaire, et plus précisément la cytokinèse et le passage de la phase G0/G1 à la réactivation de l'embryon.

VIII. CONCLUSION GÉNÉRALE

Dans un but de réaliser une analyse globale du transcriptome utérin à l'émergence de la diapause embryonnaire, nous avons construit une librairie SSH contenant 211 séquences utérines de cDNA différentiellement exprimées à l'émergence de la diapause embryonnaire, dont 58 % des séquences sont homologues à des séquences de gènes connues.

L'analyse de la distribution des fonctions biologiques parmi ces gènes a montré une modulation importante dans la régulation du métabolisme, de l'expression génique, de la transduction de signal, du cycle cellulaire, du transport ainsi que de la structure cellulaire. Cela reflète des modifications de l'environnement utérin considérables, associées à l'émergence de la diapause embryonnaire. De plus, le patron spatio-temporel de l'expression utérine des gènes *SPARC* et *HMGN1* illustre des changements importants au niveau du remodelage tissulaire et de la chromatine au moment de la sortie de la diapause embryonnaire et de l'implantation de l'embryon.

Le produit d'expression des gènes *GDF3*, *ALCAM*, *TXNL1*, *TGM2*, différentiellement exprimés dans l'utérus de vison au moment de la reprise du développement embryonnaire, sont des facteurs utérins qui pourraient être directement impliqué dans la réactivation de l'embryon.

L'expression différentielle de trois gènes codant pour des enzymes impliquées dans la biosynthèse des polyamines, *AZI1*, *ODC1* et *SAT1*, ont suggéré une

augmentation du contenu utérin en polyamines, concomitante avec la sortie de la diapause embryonnaire. Les concentrations utérines en polyamines étaient de plus augmentées au moment de l'émergence de la diapause embryonnaire. Nous avons par conséquent fait l'hypothèse que les polyamines jouaient un rôle important dans la réactivation du développement embryonnaire, chez le vison.

Nous avons montré qu'une carence en polyamines, résultat d'un inhibiteur de l'ODC1, ré-induit ou maintient les embryons dans un état de diapause embryonnaire, qui se traduit par une diminution de la prolifération cellulaire dans les embryons supposés être en réactivation. Ce rallongement de la diapause a pour conséquence un retard de l'implantation dans le temps, mais n'affecte pas le succès de la reproduction.

De plus, un état de dormance dans les cellules de trophoblaste de vison *in vitro* a été provoqué par l'inhibition de la biosynthèse des polyamines par le DFMO. Cet état s'est manifesté par une réduction de la prolifération cellulaire, une différenciation de la morphologie cellulaire, et le changement de la distribution subcellulaire d'ODC1. Ces effets se sont avérés réversibles lors de l'arrêt du traitement au DFMO, confortant ainsi nos résultats obtenus *in vivo*.

En conclusion, notre étude place les polyamines comme facteurs-clés de l'émergence de la diapause embryonnaire chez le vison et, cela constitue une avancée majeure dans la compréhension des mécanismes utéro-embryonnaires qui contrôlent la diapause et la réactivation embryonnaire.

IX. RÉFÈRENCES

Adams, C. E. (1981). "Observations on the induction of ovulation and expulsion of uterine eggs in the mink, Mustela vison." J Reprod Fertil **63**(1): 241-248.

Aitken, R. J. (1977a). "Changes in the protein content of mouse uterine flushings during normal pregnancy and delayed implantation, and after ovariectomy and oestradiol administration." J Reprod Fertil **50**(1): 29-36.

Aitken, R. J. (1977b). "The culture of mouse blastocysts in the presence of uterine flushings collected during normal pregnancy, delayed implantation and pro-oestrus." J Embryol Exp Morphol **41**: 295-300.

Allais, C. and L. Martinet (1978). "Relation between daylight ratio, plasma progesterone levels and timing of nidation in mink (Mustela vison)." J Reprod Fertil **54**(1): 133-136.

Ashworth, C. J., L. M. Toma, et al. (2009). "Nutritional effects on oocyte and embryo development in mammals: implications for reproductive efficiency and environmental sustainability." Philos Trans R Soc Lond B Biol Sci **364**(1534): 3351-3361.

Bastida, C. M., F. Tejada, et al. (2002). "The preovulatory rise of ovarian ornithine decarboxylase is required for progesterone secretion by the corpus luteum." Biochem Biophys Res Commun **293**(1): 106-111.

Berria, M., M. M. Joseph, et al. (1989). "Role of prolactin and luteinizing hormone in regulating timing of implantation in the spotted skunk." Biol Reprod **40**(2): 232-238.

Blake, E. J., J. Schindler, et al. (1982). "Protein synthetic requirements for the outgrowth of trophoblast cells from mouse blastocysts." J Exp Zool **224**(3): 401-408.

Bloch, S. (1971). "Observations on the problem of delayed nidation in suckling mice." J Reprod Fertil **26**(2): 279-280.

Bowness, E. R. (1968). "A survey of the gestation period and litter size in ranch mink." Can Vet J **9**(5): 103-106.

Canivenc, R. and M. Bonnin (1979). "Delayed implantation is under environmental control in the badger (Meles meles L.)." Nature **278**(5707): 849-850.

Chang, M. C. (1968). "Reciprocal insemination and egg transfer between ferrets and mink." J Exp Zool **168**(1): 49-59.

Christensen, H. N. (1990). "Role of amino acid transport and countertransport in nutrition and metabolism." Physiol Rev **70**(1): 43-77.

Cochrane, R. L. and R. K. Meyer (1957). "Delayed nidation in the rat induced by progesterone." Proc Soc Exp Biol Med **96**(1): 155-159.

Cochrane, R. L. and R. M. Shackelford (1962). "Effects of exogenous oestrogen alone and in combination with progestrone on pregnancy in the intact mink." J Endocrinol **25**: 101-106.

Cui, X. S. and N. H. Kim (2005). "Polyamines inhibit apoptosis in porcine parthenotes developing in vitro." Mol Reprod Dev **70**(4): 471-477.

Curlewis, J. D. (1992). "Seasonal prolactin secretion and its role in seasonal reproduction: a review." Reprod Fertil Dev **4**(1): 1-23.

Daniel, J. C., Jr. and R. S. Krishnan (1969). "Studies on the relationship between uterine fluid components and the diapausing state of blastocysts from mammals having delayed implantation." J Exp Zool **172**(3): 267-281.

Dass, C. M., S. Mohla, et al. (1969). "Time sequence of action of estrogen on nucleic acid and protein synthesis in the uterus and blastocyst during delayed implantation in the rat." Endocrinology **85**(3): 528-536.

Desmarais, J. A., V. Bordignon, et al. (2004). "The escape of the mink embryo from obligate diapause." Biol Reprod **70**(3): 662-670.

Desmarais, J. A., M. Cao, et al. (2008). "Spatiotemporal expression pattern of progranulin in embryo implantation and placenta formation suggests a role in cell proliferation, remodeling, and angiogenesis." Reproduction **136**(2): 247-257.

Desmarais, J. A., F. L. Lopes, et al. (2007). "The peroxisome proliferator-activated receptor gamma regulates trophoblast cell differentiation in mink (Mustela vison)." Biol Reprod **77**(5): 829-839.

Dey, S. K., H. Lim, et al. (2004). "Molecular cues to implantation." Endocr Rev **25**(3): 341-373.

Diatchenko, L., Y. F. Lau, et al. (1996). "Suppression subtractive hybridization: a method for generating differentially regulated or tissue-specific cDNA probes and libraries." Proc Natl Acad Sci U S A **93**(12): 6025-6030.

Douglas, D. A., A. Houde, et al. (1998). "Luteotropic hormone receptors in the ovary of the mink (Mustela vison) during delayed implantation and early-post-implantation gestation." Biol Reprod **59**(3): 571-578.

Douglas, D. A., R. A. Pierson, et al. (1994). "Ovarian follicular development in mink (Mustela vison)." J Reprod Fertil **100**(2): 583-590.

Douglas, D. A., J. H. Song, et al. (1997). "Luteal and placental characteristics of carnivore gestation: expression of genes for luteotrophic receptors and steroidogenic enzymes." J Reprod Fertil Suppl **51**: 153-166.

Enders, A. C., R. K. Enders, et al. (1963). "AN ELECTRON MICROSCOPE STUDY OF THE GLAND CELLS OF THE MINK ENDOMETRIUM." J Cell Biol **18**: 405-418.

Enders, R. (1952). "Reproduction in the mink (Mustela vison). ." Proc Am Philos Soc **96**: 691-755.

Ferguson, S. H., J. A. Virgl, et al. (1996). "Evolution of delayed implantation and associated grade shifts in life history traits of North American carnivores." Ecoscience **3**: 7–17.

Fishel, S. B. (1979). "Analysis of mouse uterine proteins at pro-oestrus, during early pregnancy and after administration of exogenous steroids." J Reprod Fertil **55**(1): 91-100.

Fozard, J. R., M. L. Part, et al. (1980). "Inhibition of murine embryonic development by alpha-difluoromethylornithine, an irreversible inhibitor of ornithine decarboxylase." Eur J Pharmacol **65**(4): 379-391.

Fozard, J. R., M. L. Part, et al. (1980). "L-Ornithine decarboxylase:an essential role in early mammalian embryogenesis." Science **208**(4443): 505-508.

Gao, H., G. Wu, et al. (2009). "Select Nutrients in the Ovine Uterine Lumen. V. Nitric Oxide Synthase, GTP Cyclohydrolase, and Ornithine Decarboxylase in Ovine Uteri and Periimplantation Conceptuses." Biol Reprod.

Gerlitz, G. (2010). "HMGNs, DNA repair and cancer." Biochim Biophys Acta **1799**(1-2): 80-85.

Given, R. L. and H. M. Weitlauf (1981). "Resumption of DNA synthesis during activation of delayed implanting mouse blastocysts." J Exp Zool **218**(2): 253-259.

Given, R. L. and H. M. Weitlauf (1982). "Resumption of DNA synthesis in delayed implanting mouse blastocysts during activation in vitro." J Exp Zool **224**(1): 111-114.

Graham, T. R. and J. C. Daniel, Jr. (1984). "The effect of accelerated lactation on fetal maintenance in the rat." Lab Anim **18**(2): 103-105.

Gwatkin, R. B. (1966). "Defined media and development of mammalian eggs in vitro." Ann N Y Acad Sci **139**(1): 79-90.

Gwatkin, R. B. (1969). "Nutritional requirements for post-blastocyst development in the mouse. Amino acids and protein in the uterus during implantation." Int J Fertil **14**(2): 101-105.

Hamatani, T., M. G. Carter, et al. (2004). "Dynamics of global gene expression changes during mouse preimplantation development." Dev Cell **6**(1): 117-131.

Hansson, A. (1947). "The physiology of reproduction in mink (Mustela vison) with special reference to delayed implantation." Acta Zoologica **28**: 1–136.

Hedlund, K., O. Nilsson, et al. (1972). "Attachment reaction of the uterine luminal epithelium at implantation: light and electron microscopy of the hamster, guinea-pig, rabbit and mink." J Reprod Fertil **29**(1): 131-132.

Hoversland, R. C. and H. M. Weitlauf (1981). "The volume of uterine fluid in 'implanting' and 'delayed implanting' mice." J Reprod Fertil **62**(1): 105-109.

Jones, R. L., C. Stoikos, et al. (2006). "TGF-beta superfamily expression and actions in the endometrium and placenta." Reproduction **132**(2): 217-232.

Juszczak, M. and M. Michalska (2006). "[The effect of melatonin on prolactin, luteinizing hormone (LH), and follicle-stimulating hormone (FSH) synthesis and secretion]." Postepy Hig Med Dosw (Online) **60**: 431-438.

Kim, J., T. E. Spencer, et al. (2009). Arginine Stimulates Proliferation of Ovine Trophectoderm Cells Through FRAP1-RPS6K-RPS6 Signaling Cascade and Synthesis of Nitric Oxide and Polyamines. Science for the Public Good, SSR 42nd Annual Meeting, Pittsburgh, Pennsylvania, USA.

Kimball, S. R., L. M. Shantz, et al. (1999). "Leucine regulates translation of specific mRNAs in L6 myoblasts through mTOR-mediated changes in availability of eIF4E and phosphorylation of ribosomal protein S6." J Biol Chem **274**(17): 11647-11652.

Kirby, D. R. (1967). "Ectopic autografts of blastocysts in mice maintained in delayed implantation." J Reprod Fertil **14**(3): 515-517.

Kolpovskii, V. M. (1976). "[Position of the embryos of American mink in the fetal chamber at different stages of development]." Arkh Anat Gistol Embriol **71**(10): 46-51.

Kwon, H., S. P. Ford, et al. (2004). "Maternal nutrient restriction reduces concentrations of amino acids and polyamines in ovine maternal and fetal plasma and fetal fluids." Biol Reprod **71**(3): 901-908.

Levine, A. J. and A. H. Brivanlou (2006). "GDF3, a BMP inhibitor, regulates cell fate in stem cells and early embryos." Development **133**(2): 209-216.

Lopes, F. L., J. Desmarais, et al. (2006). "Transcriptional regulation of uterine vascular endothelial growth factor during early gestation in a carnivore model, Mustela vison." J Biol Chem **281**(34): 24602-24611.

Lopes, F. L., J. A. Desmarais, et al. (2004). "Embryonic diapause and its regulation." Reproduction **128**(6): 669-678.

Lopez-Garcia, C., A. J. Lopez-Contreras, et al. (2008). "Molecular and morphological changes in placenta and embryo development associated with the inhibition of polyamine synthesis during midpregnancy in mice." Endocrinology **149**(10): 5012-5023.

Makitie, L. T., K. Kanerva, et al. (2009). "Ornithine decarboxylase regulates the activity and localization of rhoA via polyamination." Exp Cell Res **315**(6): 1008-1014.

Maneckjee, R. and N. R. Moudgal (1975). "Induction and inhibition of implantation in lactating rats." J Reprod Fertil **43**(1): 33-40.

Mantalenakis, S. J. and M. M. Ketchel (1966). "Frequency and extent of delayed implantation in lactating rats and mice." J Reprod Fertil **12**(2): 391-394.

Martin, P. M. and A. E. Sutherland (2001). "Exogenous amino acids regulate trophectoderm differentiation in the mouse blastocyst through an mTOR-dependent pathway." Dev Biol **240**(1): 182-193.

Martin, P. M., A. E. Sutherland, et al. (2003). "Amino acid transport regulates blastocyst implantation." Biol Reprod **69**(4): 1101-1108.

Martinet, L. and D. Allain (1985). "Role of the pineal gland in the photoperiodic control of reproductive and non-reproductive functions in mink (Mustela vison)." Ciba Found Symp **117**: 170-187.

McNeilly, A. S. (1979). "Effects of lactation on fertility." Br Med Bull **35**(2): 151-154.

Mead, R. A. (1971). "Effects of light and blinding upon delayed implantation in the spotted skunk." Biol Reprod **5**(2): 214-220.

Mead, R. A. (1981). "Delayed implantation in mustelids, with special emphasis on the spotted skunk." J Reprod Fertil Suppl **29**: 11-24.

Mead, R. A. (1993). "Embryonic diapause in vertebrates." J Exp Zool **266**(6): 629-641.

Mead, R. A., A. W. Rourke, et al. (1979). "Changes in uterine protein synthesis during delayed implantation in the western spotted skunk and its regulation by hormones." Biol Reprod **21**(1): 39-46.

Metcalf, B. W., C. Danzin, et al. (1978). "Catalytic irreversible inhibition of mammalian ornithine decarboxylase (E.C. 4.1.1.17) by substrate and product analogs." J Am Chem Soc **100**: 2551–2553

Meyuhas, O. (2000). "Synthesis of the translational apparatus is regulated at the translational level." Eur J Biochem **267**(21): 6321-6330.

Moller, O. M. (1973). "The progesterone concentrations in the peripheral plasma of the mink (Mustela vison) during pregnancy." J Endocrinol **56**(1): 121-132.

Moller, O. M. (1974). "Plasma progesterone before and after ovariectomy in unmated and pregnant mink, Mustela vison." J Reprod Fertil **37**(2): 367-372.

Moreau, G. M., A. Arslan, et al. (1995). "Development of immortalized endometrial epithelial and stromal cell lines from the mink (Mustela vison) uterus and their effects on the survival in vitro of mink blastocysts in obligate diapause." Biol Reprod **53**(3): 511-518.

Morin, P., C. Flors, et al. (2009). "Constitutively active RhoA inhibits proliferation by retarding G(1) to S phase cell cycle progression and impairing cytokinesis." Eur J Cell Biol **88**(9): 495-507.

Murphy, B. D. (1983). "Precocious induction of luteal activation and termination of delayed implantation in mink with the dopamine antagonist pimozide." Biol Reprod **29**(3): 658-662.

Murphy, B. D., P. W. Concannon, et al. (1981). "Prolactin: the hypophyseal factor that terminates embryonic diapause in mink." Biol Reprod **25**(3): 487-491.

Murphy, B. D., G. B. DiGregorio, et al. (1990). "Interactions between melatonin and prolactin during gestation in mink (Mustela vison)." J Reprod Fertil **89**(2): 423-429.

Murphy, B. D. and D. A. James (1974). "The effects of light and sympathetic innervation to the head on nidation in mink." J Exp Zool **187**(2): 267-276.

Murphy, B. D., R. A. Mead, et al. (1983). "Luteal contribution to the termination of preimplantation delay in mink." Biol Reprod **28**(2): 497-503.

Murphy, B. D. and W. H. Moger (1977). "Progestins of mink gestation: the effects of hypophysectomy." Endocr Res Commun **4**(1): 45-60.

Murphy, B. D., K. Rajkumar, et al. (1993). "Control of luteal function in the mink (Mustela vison)." J Reprod Fertil Suppl **47**: 181-188.

Nieder, G. L. and H. M. Weitlauf (1985). "Effects of metabolic substrates and ionic environment on in-vitro activation of delayed implanting mouse blastocysts." J Reprod Fertil **73**(1): 151-157.

Nilsson, B. O. and L. Ljung (1985). "X-ray micro analyses of cations (Na, K, Ca) and anions (S, P, Cl) in uterine secretions during blastocyst implantation in the rat." J Exp Zool **234**(3): 415-421.

Oswald, C. and P. A. McClure (1987). "Energy allocation during concurrent pregnancy and lactation in Norway rats with delayed and undelayed implantation." J Exp Zool **241**(3): 343-357.

Papke, R. L., P. W. Concannon, et al. (1980). "Control of luteal function and implantation in the mink by prolactin." J Anim Sci **50**(6): 1102-1107.

Paria, B. C., H. Lim, et al. (1998). "Coordination of differential effects of primary estrogen and catecholestrogen on two distinct targets mediates embryo implantation in the mouse." Endocrinology **139**(12): 5235-5246.

Pearson, O. P. and R. K. Enders (1944). "Duration of pregnancy in certain mustelids." J. Exp. Zool. **95**: 21-35.

Pfarrer, C., H. Winther, et al. (1999). "The development of the endotheliochorial mink placenta: light microscopy and scanning electron microscopical morphometry of maternal vascular casts." Anat Embryol (Berl) **199**(1): 63-74.

Pilbeam, T. E., P. W. Concannon, et al. (1979). "The annual reproductive cycle of mink (Mustela vison)." J Anim Sci **48**(3): 578-584.

Pomidor, M. M., K. K. Ruhl, et al. (1995). "Relationship between ornithine decarboxylase and cytoskeletal organization in cultured human keratinocytes: cellular responses to phorbol esters, cytochalasins, and alpha-difluoromethylornithine." Exp Cell Res **221**(2): 426-437.

Prasad, M. R., C. M. Dass, et al. (1968). "Action of oestrogen on the blastocyst and uterus in delayed implantation--an autoradiographic study." J Reprod Fertil **16**(1): 97-104.

Raught, B., A. C. Gingras, et al. (2000). "Serum-stimulated, rapamycin-sensitive phosphorylation sites in the eukaryotic translation initiation factor 4GI." Embo J **19**(3): 434-444.

Reese, J., S. K. Das, et al. (2001). "Global gene expression analysis to identify molecular markers of uterine receptivity and embryo implantation." J Biol Chem **276**(47): 44137-44145.

Renfree, M. B. (1981). "Embryonic diapause in marsupials." J Reprod Fertil Suppl **29**: 67-78.

Renfree, M. B. and G. Shaw (2000). "Diapause." Annu Rev Physiol **62**: 353-375.

Sage, H., C. Johnson, et al. (1984). "Characterization of a novel serum albumin-binding glycoprotein secreted by endothelial cells in culture." J Biol Chem **259**(6): 3993-4007.

Sandell, M. (1990). "The evolution of seasonal delayed implantation." Q Rev Biol **65**(1): 23-42.

Sanyal, M. K. and R. K. Meyer (1972). "Deoxyribonucleic acid synthesis in vitro in normal and delayed nidation preimplantation blastocysts of adult rats." J Reprod Fertil **29**(3): 439-442.

Schipper, R. G., V. M. Cuijpers, et al. (2004). "Intracellular localization of ornithine decarboxylase and its regulatory protein, antizyme-1." J Histochem Cytochem **52**(10): 1259-1266.

Schulz, L. C. and J. M. Bahr (2003). "Glucose-6-phosphate isomerase is necessary for embryo implantation in the domestic ferret." Proc Natl Acad Sci U S A **100**(14): 8561-8566.

Sherman, M. I. and P. W. Barlow (1972). "Deoxyribonucleic acid content in delayed mouse blastocysts." J Reprod Fertil **29**(1): 123-126.

Smith, M. S. (1980). "Role of prolactin in regulating gonadotropin secretion and gonad function in female rats." Fed Proc **39**(8): 2571-2576.

Song, J. (1998). Implantation in the Mink (Mustela vison): Morphologic Progression of Trophoblast Invasion and Uterine Gene Expression. Faculté de Médecine Véterinaire. Montreal, CA, Université de Montreal.

Song, J. H., P. D. Carriere, et al. (1995). "Ultrasonographic analysis of gestation in mink (Mustela vison)." Theriogenology **43**(3): 585-594.

Song, J. H., A. Houde, et al. (1998). "Cloning of leukemia inhibitory factor (LIF) and its expression in the uterus during embryonic diapause and implantation in the mink (Mustela vison)." Mol Reprod Dev **51**(1): 13-21.

Song, J. H., J. Sirois, et al. (1998). "Cloning, developmental expression, and immunohistochemistry of cyclooxygenase 2 in the endometrium during embryo implantation and gestation in the mink (Mustela vison)." Endocrinology **139**(8): 3629-3636.

Spindler, R. E., M. B. Renfree, et al. (1996). "Carbohydrate uptake by quiescent and reactivated mouse blastocysts." J Exp Zool **276**(2): 132-137.

Stoufflet, I., M. Mondain-Monval, et al. (1989). "Patterns of plasma progesterone, androgen and oestrogen concentrations and in-vitro ovarian steroidogenesis during embryonic diapause and implantation in the mink (Mustela vison)." J Reprod Fertil **87**(1): 209-221.

Sundqvist, C., A. G. Amador, et al. (1989). "Reproduction and fertility in the mink (Mustela vision)." J Reprod Fertil **85**(2): 413-441.

Surani, M. A. (1975). "Hormonal regulation of proteins in the uterine secretion of ovariectomized rats and the implications for implantation and embryonic diapause." J Reprod Fertil **43**(3): 411-417.

Surani, M. A. (1976). "Uterine luminal proteins at the time of implantation in rats." J Reprod Fertil **48**(1): 141-145.

Surani, M. A. (1977). "Response of preimplantation rat blastocysts in vitro to extracellular uterine luminal components, serum and hormones." J Cell Sci **25**: 265-277.

Thom, M. D., D. D. Johnson, et al. (2004). "The evolution and maintenance of delayed implantation in the mustelidae (mammalia: carnivora)." Evolution **58**(1): 175-183.

Torbit, C. A. and H. M. Weitlauf (1975). "Production of carbon dioxide in vitro by blastocysts from intact and ovariectomized mice." J Reprod Fertil **42**(1): 45-50.

Travis, H. F., T. E. Pilbeam, et al. (1978). "Relationship of vulvar swelling to estrus in mink." J Anim Sci **46**(1): 219-224.

Tsukamura, H. and K. Maeda (2001). "Non-metabolic and metabolic factors causing lactational anestrus: rat models uncovering the neuroendocrine mechanism underlying the suckling-induced changes in the mother." Prog Brain Res **133**: 187-205.

Van Winkle, L. J. (1977). "Low Na+ concentration: a factor contributing to diminished uptake and incorporation of amino acids by diapausing mouse blastocysts?" J Exp Zool **202**(2): 275-281.

Van Winkle, L. J. (1981). "Activation of amino acid accumulation in delayed implantation mouse blastocysts." J Exp Zool **218**(2): 239-246.

Van Winkle, L. J. (2001). "Amino acid transport regulation and early embryo development." Biol Reprod **64**(1): 1-12.

Van Winkle, L. J. and A. L. Campione (1983). "Effect of inhibitors of polyamine synthesis on activation of diapausing mouse blastocysts in vitro." J Reprod Fertil **68**(2): 437-444.

Van Winkle, L. J., A. L. Campione, et al. (1983). "Sodium ion concentrations in uterine flushings from "implanting" and "delayed implanting" mice." J Exp Zool **226**(2): 321-324.

Van Winkle, L. J., J. K. Tesch, et al. (2006). "System B0,+ amino acid transport regulates the penetration stage of blastocyst implantation with possible long-term developmental consequences through adulthood." Hum Reprod Update **12**(2): 145-157.

Venge, O. (1973). "Reproduction in the mink." K. vet.-og Landbohojsk. Arsskr.: 95-146.

Wallace, H. M., A. V. Fraser, et al. (2003). "A perspective of polyamine metabolism." Biochem J **376**(Pt 1): 1-14.

Weitlauf, H. M. (1969). "Temporal changes in protein synthesis by mouse blastocysts transferred to ovariectomized recipients." J Exp Zool **171**(4): 481-486.

Weitlauf, H. M. (1971). "Protein synthesis by blastocysts in the uteri and oviducts of intact and hypophysectomized mice." J Exp Zool **176**(1): 35-40.

Weitlauf, H. M. (1973). "In vitro uptake and incorporation of amino acids by blastocysts from intact and ovariectomized mice." J Exp Zool **183**(3): 303-308.

Weitlauf, H. M. (1974). "Metabolic changes in the blastocysts of mice and rats during delayed implantation." J Reprod Fertil **39**(1): 213-224.

Weitlauf, H. M. (1978). "Factors in mouse uterine fluid that inhibit the incorporation of [3H]uridine by blastocysts in vitro." J Reprod Fertil **52**(2): 321-325.

Weitlauf, H. M. and G. S. Greenwald (1965). "A comparison of 35-S methionine incorporation by the blastocysts of normal and delayed implanting mice." J Reprod Fertil **10**(2): 203-208.

Weitlauf, H. M. and A. A. Kiessling (1981). "Activation of 'delayed implanting' mouse embryos in vitro." J Reprod Fertil Suppl **29**: 191-202.

Wu, G., F. W. Bazer, et al. (2004). "Maternal nutrition and fetal development." J Nutr **134**(9): 2169-2172.

Wu, G., F. W. Bazer, et al. (2009). "Arginine metabolism and nutrition in growth, health and disease." Amino Acids **37**(1): 153-168.

Wu, G., F. W. Bazer, et al. (2005). "Polyamine synthesis from proline in the developing porcine placenta." Biol Reprod **72**(4): 842-850.

Wu, G., W. G. Pond, et al. (1998). "Maternal dietary protein deficiency decreases nitric oxide synthase and ornithine decarboxylase activities in placenta and endometrium of pigs during early gestation." J Nutr **128**(12): 2395-2402.

Wynne-Jones, G. A. and A. M. Gurney (1993). "Pro-oestrous-specific role for polyamines in mediating the secretion of prolactin induced by thyrotrophin-releasing hormone in the rat." J Endocrinol **137**(1): 133-139.

Zhao, Y. C., Y. J. Chi, et al. (2008). "Polyamines are essential in embryo implantation: expression and function of polyamine-related genes in mouse uterus during peri-implantation period." Endocrinology **149**(5): 2325